Simple models of district heating systems for load and demand side management and operational optimisation

Bøhm, B.; Larsen, Helge V.

Publication date:
2005

Document Version
Publisher's PDF, also known as Version of record

Simple models of district heating systems

for load and demand side management and operational optimisation

Benny Bøhm
Helge V. Larsen

Department of Mechanical Engineering
Technical University of Denmark

Risø National Laboratory
Systems Analysis Department

December 2004

Simple models of district heating systems

for load and demand side management

and operational optimisation

Simple modeller for fjernvarmesystemer

med henblik på belastningsudjævning og driftsoptimering

Benny Bøhm
Helge V. Larsen

Department of Mechanical Engineering
Technical University of Denmark

Risø National Laboratory
Systems Analysis Department

Energiforskningsprogrammet EFP
ENS J.nr. 1373/01-0041

December 2004

Simple models of district heating systems

for load and demand side management and operational optimisation

Department of Mechanical Engineering,
Technical University of Denmark,
and
RISØ National Laboratory,
Systems Analysis Department.

ISBN 87-7475-323-1

Preface

The research project ”Simple models of district heating systems for load and demand side management and operational optimisation” has been supported by the Energy Research Programme of the Danish Energy Agency, J.no. 1373/01-0041.

The work has been carried out in co-operation between Energy Engineering, Department of Mechanical Engineering (MEK), Technical University of Denmark, and Systems Analysis Department, Risoe National Laboratory, and Roedovre District Heating (DH) company, Vestegnens Kraftvarmeselskab I/S (VEKS) and Danfoss A/S. Until 2002 Ishoej Varmeværk also participated in the work. Additional support has been obtained from the Energy Flexible Thermal Systems Programme, Nordic Energy Research, through a Ph.D. scholarship to Frank Pedersen, BYG DTU. The support is very much appreciated.

The project group consisted of:

Benny Bøhm, MEK DTU (Project leader)
Helge V. Larsen, Risoe
Frank Pedersen, DTU
Jens Munk Pedersen and Steen Cloos, Roedovre DH company
Jørgen Jensen, VEKS
Niels Andersen and Atli Benonysson, Danfoss A/S.

In 2001 Leif Ptak, Steen Fangel and Erling Harlev, Ishoej DH company, participated in the work.

The project benefited from important contributions from our support group:

Flemming Andersen, VEKS
Leif Andersson, Hoeje Taastrup Fjernvarme
Jan Elleriis, CTR
Steffen Moe, Soenderborg Fjernvarmeselskab
Jan Eric Thorsen, Danfoss A/S.

The work has been co-ordinated with two IEA projects, Programme of Research, Development and Demonstration on District Heating and Cooling, including the integration of CHP: “Simple Models for Operational Optimisation” (Annex VI) and “Dynamic Heat Storage Optimisation and Demand Side Management” (Annex VII). The co-operation has been very fruitful and we would like to thank the IEA partners UMSICHT, Germany, VTT, Finland and Korea District Heating Corporation.

Many individuals, not mentioned here, supplied information in various ways. All help is very much appreciated.

Lyngby, December 2004

Benny Bøhm
Project Leader

Contents

Resumé og konklusioner (in Danish)

Projektets formål har været at videreudvikle og afprøve simple (aggregerede) modeller for fjernvarmesystemer med henblik på simulering og driftsoptimering, samt at undersøge belastningsfordelingens betydning for de samlede driftsomkostninger.

Arbejdet er baseret på fysisk-matematisk modellering og simulering af fjernvarmesystemer, og er en fortsættelse af et tidligere EFP 96-projekt, Pálsson et al. (1999). Arbejdet har været koordineret med to IEA-projekter: "Simple Models for Operational Optimisation" (Annex VI) og "Dynamic Heat Storage Optimisation and Demand Side Management" (Annex VII, i gangværende).

I nærværende projekt har målene været at forbedre den danske aggregeringsmetode ved at tage hensyn til tryktab ved aggregeringen, og at afprøve metoderne på et større datagrundlag end i EFP 96-projektet.

For at kunne verificere modellerne er det af afgørende betydning at have gode data til rådighed. Fuld information om varmebehov og temperaturer ikke kun på fjernvarmecentralen, men i hver enkelt tilsluttet bygning er nødvendig, og derfor findes der ikke mange fjernvarmesystemer i Danmark, der kan levere disse oplysninger. Oprindeligt var det planlagt at gennemføre projektet på Ishøj Varmeværk, men på grund af problemer med dataopsamlingen blev det tidligt nødvendigt at skifte til Rødovre Fjernvarmeforsyning.

I *kapitel 1* findes en kort beskrivelse af de fjernvarmesystemer, der har leveret data. 6-minutters værdier fra oktober 2002 til september 2003 fra R01 Madumvej og R02 Broparken i Rødovre er blevet indsamlet, og fra dette store datasæt er udvalgt 3 uger fra hvert delsystem. Disse uger repræsenterer en vinter-, en forårs- og en sommerperiode. For brugerinstallationerne blev varmeeffekt og primære temperaturer benyttet. Sekundære temperaturer og varmevekslerstørrelser var ikke tilgængelige, og derfor blev en ny udgave af vort simuleringsprogram DHSim udviklet til at håndtere dette tilfælde.

5-minutters værdier fra Ishøj Varmeværk fra perioden 19-24 december 2000 blev også anvendt. I dette tilfælde kendes både primære og sekundære temperaturer hos brugerne, samt varmevekslerstørrelserne.

Fra Hvalsø Kraftvarmeværk benyttedes 2-minutters værdier fra værket for januar 1998. Data fra bygningerne (varmebehov og varmeanlæg) var ikke tilgængelige.

De udvalgte systemer repræsenterer et bredt spektrum af fjernvarmesystemer med hensyn til liniebelastning, fjernvarmenettets nyttevirkning, samt til brændselsprisforhold.

I *kapitel 2* beskrives aggregeringen af de tre fjernvarmesystemer R01 Madumvej, R02 Broparken og Ishøj Varmeværk. Kvaliteten af de aggregerede modeller blev testet ved simuleringer i de udvalgte uger.

For den termiske model fastlægges fejlen pga. aggregeringen ved varmeproduktionen og returtemperaturen på fjernvarmecentralen (eller rettere vekslerstationen). For tryktabsmodellen udtrykkes fejlen ved fjernvarmecentralens differenstryk.

I *afsnit 2.2* beskrives aggregeringen af Madumvej og Broparken for en vinter-, en forårs- og en sommeruge. For hver uge gennemføres aggregeringen ved at der dannes aggregerede modeller med færre og færre ledninger, indtil kun én ledning er tilbage.

Aggregeringen af Ishøj beskrives i *afsnit 2.3*. Her benyttedes 5-minuttersværdier fra 19. til 24. december 2000. Da der manglede data for nogle af varmecentralerne, var det nødvendigt at danne de manglende data ud fra data fra tilsvarende varmecentraler. På denne både forelå der varmeeffekt, samt primære og sekundære temperaturer for samtlige 23 varmecentraler på 5-minutters basis.

De aggregerede modellers nøjagtighed er blevet udtrykt ved fejlen i varmeproduktion, returtemperatur og differenstryk på fjernvarmecentralen mellem det fysiske netværk og den aggregerede model.

I Bøhm et al. (2002) og Larsen et al. (2004) er foretaget en sammenligning mellem den her behandlede aggregeringsmetode og en metode udviklet ved UMSICHT, Tyskland, jvf. Loewen (2001). Begge metoder fungerer godt.

Med hensyn til effekt og returtemperatur kan det konkluderes, at antallet af ledninger kan reduceres til 3 for Madumvej og til 5 for Broparken uden at fejlen vokser meget. For Ishøj Varmeværk må antallet af ledninger ikke reduceres til under 3. Selv aggregerede ledningsnet med kun 1 ledning reproducerer informationen om det fysiske net i et vist omfang, som det kan ses på figur 2.4 og 2.6. Afhængig af formålet med at anvende modellen, så vil selv en 1-rørs model være brugelig.

Med hensyn til aggregerede modeller for tryktab er situationen lidt mere uklar, når metoden testes på Rødovre. For vinterperioden fungerer aggregeringen fint, men for forårs- og sommerperioden, hvor belastningen er meget mindre, kan der opstå betragtelige fejl. Dette skyldes hovedsageligt on/off-regulering af flere af varmeinstallationerne, hvilket resulterer i store ”trykspidser”, der måske kun varer i ét tidstrin (6 minutter).

Simple modeller for tilslutningsanlæg og vekslerstationer behandles i *kapitel 3*. Formålet med disse modeller er ikke en eksakt modellering, men at separere varmeeffekten i en graddageafhængig del og i en tidsfunktion, der kun afhænger af klokkeslættet, idet det formodes, at tidsfunktionen i vid udstrækning kan ændres med DSM (Demand Side Management). Tidsfunktionerne findes vha. lineær regressionsanalyse (i parametrene) i Matlab. Tidsfunktioner på timebasis (Vanløse) og på 6-minutters basis (Rødovre) blev bestemt for bygninger og vekslerstationer. Modeller med 480 og 1680 parametre blev afprøvet, svarende til tidsfunktioner på ugedag/weekend og på døgnbasis (ti parametre per time).

Blandt de udvalgte bygninger var en etageejendom i Vanløse. Det er karakteristisk for denne bygning, at der ikke anvendtes natsænkning, og at varmekredsens effekt er kendt. Her er tidsfunktionen lille i forhold til graddageafhængigheden. Bygninger tilsluttet R01 Madumvej blev også analyseret. Tidsfunktionerne for skolen L1-08 og rækkehusbebyggelsen L1-01 er meget forskellige, hvilket selvfølgelig hænger sammen med deres forskellige anvendelsesmåde.

Tilsvarende modeller blev konstrueret for Madumvej vekslerstation. Her er belastnings-variationerne mindre end variationerne i nogle af de tilsluttede bygninger.

Kapitel 4 og 5 behandler driftsoptimering af fjernvarmesystemer. I *kapitel 4* betragtes kun varmetabsomkostning og pumpeomkostning, medens en incitamentstarif medtages i *kapitel 5*. Incitamentstariffen anvendes i VEKS's transmissionssystem, og er en del af afregnings-grundlaget mellem VEKS og de enkelte fjernvarmeselskaber. Der pålægges en straf, når retur-temperaturen i vekslerstationerne (Rødovre eller Ishøj) er for høj eller de daglige lastvariationer er for store. Modsat modtager fjernvarmeselskabet en belønning, når returtemperaturen er lav, eller belastningsvariationerne små.

Den optimale fremløbstemperaturkurve findes for de kommende to døgn vha. funktionen fmincon i Matlab 6. Fmincon minimerer de samlede omkostninger under hensyntagen til givne bibetingelser. En set-up funktion i Matlab er blevet programmeret til at kalde simuleringsprogrammet DHSim og sende den nødvendige information til fmincon. Ved at gennemføre simuleringer med DHSim overføres driftsomkostningerne til en "object"-funktion, og trykforhold (pumpekurven) og eventuelle krav om begrænsninger i ændringen af fremløbstemperaturen per time overføres til en bibetingelsesfunktion ("constraints").

Følgende tilfælde (cases) blev betragtet: A: Ishøj Varmeværk (5-rørs model), B: Hvalsø (fysisk model), C: Hvalsø (12-rørs model), D: Rødovre R01 Madumvej uge 2 (fysisk model), E: Rødovre R01 Madumvej uge 13 (fysisk model), F: Rødovre R01 Madumvej uge 13 (5-rørs termisk og 5-rørs tryktabsmodel), G: Rødovre R02 Broparken uge 33 (fysisk model).

Formålet med de udførte optimeringer var at undersøge betydningen af liniebelastning, varmelast og omkostningsrelationer på det optimale fremløbstemperaturniveau, snarere end det var at finde en præcis løsning for de pågældende fjernvarmesystemer med en præcis beskrivelse af systemet, nyttevirkninger og prisstruktur.

For fjernvarmesystemer som Ishøj og Rødovre R01 Madumvej og R02 Broparken med høj liniebelastning (lave procentiske varmetab) og dyr pumpeomkostning i forhold til varmeomkostningen, er det optimale temperaturniveau i vinterperioden højt, 105 ˚C for Ishøj og 90-100 ˚C for R01 Madumvej.

I forårsugen er det optimale temperaturniveau for R01 Madumvej 75-85 ˚C, medens det om sommeren for R02 Broparken er 70-75 ˚C.

Disse resultater gælder, når det kun er varmetab og pumpeomkostning, der betragtes, og resultaterne kan ikke direkte overføres til andre fjernvarmesystemer, hvor liniebelastning og prisstruktur er anderledes, og hvor nettet kan være udnyttet i større udstrækning end i Rødovre (dvs. større pumpeomkostning). Det skal også understreges, at returtemperaturens ændring ved andre fremløbstemperaturer er baseret på en model, der endnu ikke er verificeret.

For fjernvarmesystemerne i Ishøj og Rødovre findes der som tidligere nævnt en incitamentstarif. Incitamentet hidrører fra daglige belastningsvariationer og returtemperaturens niveau i vekslerstationen (til transmissionssystemet). For andre fjernvarmesystemer kan der gælde andre incitamenter/straffunktioner, f.eks. for at overskride et aftalt maksimalt gasforbrug eller en tilladt emissionskvote (CO_2 eller andre forureningskomponenter).

For Ishøj og R01 Madumvej har incitamentstariffen stor indflydelse på den optimale fremløbstemperaturkurve. I den optimale løsning ændres temperaturkurven for at reducere f-faktoren (belastningsvariationen), men dette er kun muligt i et begrænset omfang, da varmebehovene i bygningerne ikke kan ændres.

For Hvalsø Kraftvarmeværk er situationen ganske anderledes end i Ishøj og Rødovre, fordi varmetabene er store og brændslet er dyrere end i fjernvarmesystemer tilsluttet VEKS. For januar måned er det optimale temperaturniveau omkring 75 ˚C, når det kun er varmetab og pumpeomkostninger, der minimeres.

For Hvalsø fandt vi, at simuleringstiden for at finde den optimale løsning med en fysisk model er ca. 5 timer, medens 12-rørs-modellen tager 0,3 time. Dette resultat hænger blandt andet sammen med løsningen af de 535 varmevekslerligninger i den fysiske model i hvert tidsskridt.

Kapitel 6 til 8 omhandler driftsoptimering med belastningsudjævning (Demand Side Management, DSM). Da vi ikke har detaljerede oplysninger om bygningerne og deres varmeanlæg, har vi benyttet en meget simpel form for DSM, nemlig at udglatte spidser og "dale" i belastningen hos samtlige forbrugere. I *kapitel 6* anvendes 20% belastningsudjævning i fjernvarmesystemerne Ishøj og Rødovre. Ved at reducere belastningsvariationerne (f-faktoren) reduceres driftsomkostningerne, og faktisk kan Ishøj få penge tilbage fra VEKS pga. lav f-faktor. For R01 Madumvej uge 13 vedbliver f-faktoren at være større end 1, når der anvendes 20% udjævning.

I *kapitel 7 og 8* forøges lastudjævningen til henholdsvis 50% og 80%. I sidstnævnte tilfælde vil R01 Madumvej modtage penge fra VEKS, da f-faktoren nu bliver mindre end 1.

En anden måde at behandle bygningernes belastning på er undersøgt i *kapitel 9*. Formålet er at finde en enklere måde at danne input-filerne på til simuleringsprogrammet med henblik på en on-line applikation. To fremgangsmåder er afprøvet. Ved den første metode dannes en matrice, der forbinder varmeeffekten i hver bygning med vekslerstationens belastning i hvert tidstrin. Dette giver det korrekte resultat, når alle belastninger er kendte, men tanken er, at matricen ikke behøver at blive opdateret hele tiden. Her er matricen for uge 13 anvendt i uge 2 for R01 Madumvej.

Ved den anden fremgangsmåde antages det, at alle belastninger i bygningerne varierer proportionalt med vekslerstationens belastning. Der ses her bort fra tidsforsinkelsen mellem belastningsvariationer i bygninger og i vekslerstationen.

Ved begge fremgangsmåder fandt vi, at den optimale fremløbstemperaturkurve ændres i nogen grad sammenlignet med løsningen med de sande belastninger, og at belastningsvariationerne i vekslerstationen bliver lidt større. I *case 9D* skyldes det, at belastningerne i uge 13 varierer mere end i uge 2, og i *case 9E* skyldes det, at bygningernes belastning varierer proportionalt under simuleringen, medens de i virkeligheden ikke er i fase. Case 9E giver bedre resultat end case 9D. Resultaterne er lovende i den betydning, at metoderne vil kunne videreudvikles, så der kan opnås en bedre overensstemmelse, når der benyttes ækvivalente belastninger.

Appendiks A indeholder oplysninger om fjernvarmenettene i Rødovre, medens *Appendiks B* viser de målte tidsserier.

Appendiks C og D indeholder oplysninger om fjernvarmenettet og belastningerne i Ishøj.

Projektets hovedkonklusioner er følgende:

Fysisk-matematisk modellering af fjernvarmesystemer kan - i modsætning til "black box" modellering (f.eks. tidsserieanalyse) – håndtere komplekse fjernvarmenet og fjernvarmesystemer med flere produktionsenheder. En ulempe ved fysisk-matematisk modellering er, at der må foreligge information (viden eller antagelser) om fjernvarmenettets fysiske struktur, om varmebehovene i bygningerne og om varmeanlæggenes afkøling (samt om andre størrelser) for at en simulering kan gennemføres.

Selv med dagens hurtige computere er det at finde en optimal fremløbstemperaturkurve for den kommende periode (1-2 døgn), samt fordelingen af produktionen på flere produktionsenheder, en stor udfordring.

For at reducere beregningstiden er aggregerede modeller af fjernvarmenet og forbrugere (bygninger) et attraktivt alternativ til at anvende en fuldstændig fysisk beskrivelse af fjernvarmesystemet. I dette arbejde er vores termiske aggregerede model, udviklet i Pálsson et

al. (1999), yderligere valideret på nye fjernvarmesystemer og på større datasæt. En ny metode til tryktabsaggregering er endvidere udviklet i projektet.

For både den termiske model og for tryktabsaggregeringen har vi vist, at antallet af ledninger og forbrugere kan reduceres til 3-5 uden at det forøger simuleringsunøjagtigheden væsentligt. Ved en on-line applikation vil usikkerheden hidrørende fra vejr- og belastningsprognoser være langt større end den unøjagtighed, der kommer fra aggregeringen.

Aggregerede såvel som fuldstændige beskrivelser af fjernvarmesystemer er blevet anvendt til at bestemme det optimale temperaturniveau. For Hvalsø Kraftvarmeværk med 535 forbrugere opnåede vi ved at benytte en 12-rørs aggregeret model at beregningstiden til at finde den optimale løsning kunne reduceres fra 5 timer til 0,3 time. Reduktionen hænger sammen med løsningen af varmevekslerligningen, og derfor påvirker den model, der benyttes for bygningernes afkølingsevne, den reduktion af regnetiden, der kan opnås. For DHSim option –e (uden varmevekslermodel) er reduktionen mindre. For R01 Madumvej uge 13 fandt vi en reduktion fra 50 minutter for den fysiske model til 7 minutter for en 5-rørs model.

Det optimale temperaturniveau for et fjernvarmesystem afhænger af en lang række størrelser, f.eks. rørdesign (rørdiametrene påvirker pumpeomkostningen), geografisk udbredelse (ledningslængden påvirker varmetabet), liniebelastning (varmetæthed) og prisstruktur (dyrt eller billigt brændsel sammenlignet med elektricitet til pumper). Hvert fjernvarmesystem har derfor sin egen optimale løsning. Selv om pumpeomkostningen typisk er lille i forhold til totalomkostningen, så afhænger bibetingelserne af pumpekurven. Den optimale løsning ved gratis elektricitet til pumpen, er ikke den optimale løsning, når pumpeomkostningen medtages i optimeringen.

For fjernvarmesystemer med høj liniebelastning og lavt brændselspris/elektricitetspris-forhold som i Ishøj og Rødovre, er det optimale temperaturniveau højt (90-105 ˚C om vinteren). For fjernvarmesystemer med store (procentiske) varmetab er temperaturniveauet lavere.

Driftsoptimering af fjernvarmesystemer må formodes at blive mere kompliceret i fremtiden, ikke kun for elektricitetsproducerende enheder, men også ved ren varmedistribution. Emissionskvoter (CO2) og variable gas- og elektricitetspriser må medtages ved en fremtidig optimering. I dette arbejde betragtes fjernvarmesystemer forsynet fra VEKS, og incitaments-tariffen (der indgår i afregningsgrundlaget mellem VEKS og fjernvarmeselskaberne) vedr. daglige belastningsvariationer og returtemperaturen i vekslerstationen skal medtages ved en optimering. Incitamentstariffen har stor indflydelse på den optimale fremløbstemperaturkurve.

Demand Side Management bør også medtages, når det optimale temperaturniveau fastlægges.

Forbrugerne og fjernvarmeselskabet bør udarbejde en strategi for DSM til fælles gavn, således at fjernvarmeselskabet kan reducere belastningsspidserne, når det er hensigtsmæssigt. Vi har vist, at DSM i Ishøj og R01 Madumvej kan reducere driftsomkostningerne ved at reducere de daglige belastningsvariationer.

Summary and Conclusions

The purpose of this research project has been to further develop and test simple (aggregated) models of district heating (DH) systems for simulation and operational optimisation, and to investigate the influence of Load Management and Demand Side Management (DSM) on the total operational costs.

The work is based on physical-mathematical modelling and simulation of DH systems, and is a continuation of previous EFP 96-work, Pálsson et al. (1999). The work has been co-ordinated with two IEA projects, Programme of Research, Development and Demonstration on District Heating and Cooling, including the integration of CHP: "Simple Models for Operational Optimisation" (Annex VI) and "Dynamic Heat Storage Optimisation and Demand Side Management" (Annex VII, on-going).

In the present EFP 2001-project the goals have been to improve the Danish method of aggregation by addressing the problem of aggregation of pressure losses, and to test the methods on a much larger data set than in the EFP 96-work.

In order to verify the models it is crucial to have good data at disposal. Full information on the heat loads and temperatures not only at the DH plant but also at every consumer (building) is needed, and therefore only a few DH systems in Denmark can supply such data. Initially the work was planned to be carried out at Ishoej DH system, but due to technical problems with the data collection system it was soon necessary to change to Roedovre DH system.

In *Chapter 1* the DH systems supplying data to the work are described. At Roedovre subsystems R01 Madumvej and R02 Broparken 6-minutes values were available from October 2002 until September 2003, and from this huge data set three weeks were selected for each subsystem. The selected weeks represent a winter, a spring and a summer period. In the analysis, heat load and primary temperatures at the consumers were used. Secondary temperatures and the size of the heat exchangers were not available and therefore a new option in our simulation programme DHSim was developed to handle this situation.

5-minutes data from Ishoej DH system was used from the period December 19-24, 2000. In this case not only information from the primary side of the heat exchanger was available but also secondary temperatures and the size of the heat exchangers.

From the Hvalsoe DH system 2-minutes data measured at the plant for January 1998 were utilized. Data from the buildings (heat loads and heating installations) was not available.

The selected systems represent a broad range of DH systems with respect to line heat demands and efficiencies of the networks as well as to price relationships.

Aggregation of three DH systems R01 Madumvej and R02 Broparken in Roedovre, and Ishoej is described in *Chapter 2*. Simulations for selected weeks with time steps 5 or 6 minutes have been carried out to assess the quality of the aggregated models.

For the thermal model, errors caused by aggregation are evaluated by the heat production and the return temperature at the DH plant (or substation) delivering heat to the grid. Likewise, for the pressure model the error is evaluated by calculating the differential pressure at the DH plant.

In *Section 2.2* the aggregation of R01 Madumvej and R02 Broparken is described. A winter, spring and summer week have been selected. For each of these weeks aggregation has been carried out ending up with a series of aggregated systems with a number of branches as small as just one.

The work on the Ishoej DH system is described in *Section 2.3*. Here 5-minutes values from December 19-24, 2000 are used. Because data was not available for all house stations, a realistic data set had to be created from those house stations where data existed. Thus for the 23 house stations in Ishoej, heat loads and primary and secondary supply and return temperatures were available every 5 minutes.

The accuracy of the aggregation models has been documented as the errors in heat production, return temperature, and differential pressure at the DH plant between the physical network and the aggregated model.

Furthermore, in Bøhm et al. (2002) and Larsen et al. (2004) a comparison has been made between the aggregation method described here and a German method, Loewen (2001). Both aggregation methods work well.

Regarding the thermal model it is concluded that the number of branches can be reduced to 3 for Madumvej and to 5 for Broparken without increasing the error very much. For the Ishoej system the number of branches should not be reduced below 3. Even aggregated systems with only one branch still hold some of the information on the full physical system as can be seen in e.g. Figure 2.4 and Figure 2.6. Depending on to what purpose the model is to be used, even a one-branch grid could be useful.

When turning to aggregated models for calculation of pressure losses, the situation does not seem that clear as tests on the Roedovre systems show. For the winter week the aggregation method functions well, but in spring and summer when the heat load is much smaller, then a considerable error might arise. This is mainly due to the on/off operation of several heat loads that results in large pressure 'spikes' with a duration of perhaps only one time step (6 minutes).

Modelling the DH house stations (consumer installations) and the substations with simple heat load models is described in *Chapter 3*. The purpose of these models is not an exact modelling but to separate the heat load into a degree-day dependent part and a clock function only dependent on the time of the day, assuming that DSM can modify the clock function to a great extent. The clock functions are found from linear (in the parameters) regression analysis in Matlab. Clock functions on an hourly basis (Vanloese) as well as on 6-minutes basis (Roedovre) were determined for buildings and substations. Models with 480 and 1680 parameters were tested, representing a weekday/weekend and a daily clock function (ten parameters per hour).

One of the single buildings selected was an apartment building in Vanloese. A particular characteristic of this building is that night set back was not applied and that heat load data for the space heating system alone is available. Its clock function is small compared with the degree-day dependent part. Buildings in R01 Madumvej subsystem were also analysed. The clock function for a school (L1-08) and semi-detached houses (L1-01) look very different, which of course reflects the different use of the buildings.

Similar models were constructed for R01 Madumvej substation. Here the load variations were smaller than the load variations in some of the buildings connected to the network.

Chapters 4 and 5 deal with operational optimisation of DH systems. In *Chapter 4* only heat losses and pumping costs are considered, while in *Chapter 5* an incentive tariff is included. The incentive tariff is part of the contract between VEKS and the distribution companies. If the return temperature at the substations in Roedovre and Ishoej DH systems is too high or the daily load variations are too big a penalty must be paid. On the other hand the DH company receives a bonus if the return temperature is low or the load variations small.

The optimum supply temperature curve is found for a two-day period by the fmincon function in Matlab 6. Fmincon minimises the total costs while taking the constraints into account. A set-up function in Matlab has been programmed to call DHSim and send the necessary information to fmincon. By performing simulation with the DHSim programme, the object function (the operational costs) can be calculated as well as the constraint function (pumping curve and maximum permitted change of supply temperature per hour).

The following cases are considered: A: Ishoej DH system (5-pipe model), B: Hvalsoe DH system (physical model), C: Hvalsoe DH system (12-pipe model), D: Roedovre R01 Madumvej week 2 (physical model), E: Roedovre R01 Madumvej week 13 (physical model), F: Roedovre R01 Madumvej week 13 (5-pipe model), G: Roedovre R02 Broparken week 33 (physical model).

The goal of these optimisations being to document the significance of line heat demand, heat loads and costs relationships on the optimum supply temperature level rather than to find a very exact solution in a specific case (with a very precise description of the DH system, efficiencies and the cost elements).

We found that for DH systems like Ishoej and Roedovre R01 and R02 with high line heat demands (low heat losses) and expensive electricity cost compared with the fuel cost, the optimum supply temperature in the winter week is high, 105 ˚C for Ishoej and 90-100 ˚C for R01 Madumvej.

In the spring period the optimum supply temperature in R01 Madumvej is 75-85 ˚C, while in the summer for R02 Broparken the optimum temperature is 70-75 ˚C.

These result apply when only heat losses and pumping costs are considered, and the results cannot directly be used for other DH systems, where the line heat demands and price structure are different and where the network is utilized to a higher degree (i.e. higher pumping costs). It should also be pointed out that the return temperature response at a modified supply temperature level is based on a model that has not been verified yet.

As previously mentioned we consider in this work an incentive tariff that applies for the Ishoej and Roedovre DH companies. The incentive relates to daily load variations and to the return temperature at the substation (to the transmission system). In other DH systems there could be other incentives/penalties to consider, for instance a penalty for exceeding a maximum gas consumption or exceeding a quota for emissions (CO2 and other pollutants).

In the Ishoej and R01 Madumvej cases, we found that the incentive tariff has a big influence on the optimum supply temperature curve. In the optimum solution the temperature curve is changed in order to reduce the f-factor (load variations) but this is only possible to a limited extent, as the heat demands in the buildings cannot be changed.

For Hvalsoe DH system the situation is quite different than in Ishoej and Roedovre, i.e. the heat losses are high and the fuel is more expensive compared with systems connected to VEKS. In

January we found an optimum temperature level of approximately 75 ˚C when only heat losses and pumping costs are considered.

In the Hvalsoe case we found that by using a full description of the DH system the simulation time to reach the optimum solution increases from 0.3 h to 5 hours compared with a 12-pipe model. This result is influenced by the time to solve the heat exchanger equation at each of the 535 consumers in every time step.

Chapters 6-8 deal with operational optimisation with DSM (Demand Side Management) measures. As we have no detailed information about the building structures and the heating system, a very simple form of DSM was applied, i.e. the peaks and the valleys were evened out in the same way for all consumers. In Chapter 6, 20% peak reduction is applied in Ishoej and Roedovre. By reducing the load variations (f-factor) the operational costs are reduced, and in fact Ishoej DH company can receive money from VEKS due to a low load factor. In R01 Madumvej week 13, the f-factor (load variations) remains bigger than one with only 20% peak shaving.

In *Chapter 7 and 8* the peak shaving is increased to 50 and 80%, respectively. In the latter case, R01 Madumvej will now receive money from VEKS due to a f-factor below one.

A different way of finding the building heat loads is tested in *Chapter 9*. The incentive is to make it easier to make the input files for the simulation programme in an on-line application. Two approaches have been tested. In the first one a matrix is created that relates the heat load in every building in every time step to the heat load at the substation (the plant). This will give an exact match if all heat loads are available, but the idea is that the matrix does not need to be updated very often. Here the matrix for week 13 has been applied in week 2 for R01 Madumvej.

In the second approach, it is assumed that the heat load in all house stations varies proportionally to the heat load at the substation (DH plant). The time delay between the load variation in the buildings and in the substation is not taken into account.

For both approaches we found that the optimum supply temperature curve is slightly affected from the optimum curve for the true heat loads, and that the load variations (f-factor) at the substation are slightly exaggerated. In the first *case 9D* it is caused by bigger variations in week 13 than in week 2, and in the second *case 9E* it is caused by the proportional variation in all buildings while with the real heat loads the buildings are “counteracting” each other. The results in case 9E are better than in case 9D. The results are promising in the sense that these methods can no doubt be further developed to ensure a better match when the equivalent heat loads are used.

Appendix A contains information on the DH grids in Roedovre, while *Appendix B* contains the measured time series.

Appendices C and D contains information on the grid and the measured time series in Ishoej, respectively.

The main conclusions of the project are the following:

Physical-mathematical modelling of DH systems can - in contrast to black box models (for instance time-series models) - treat complex DH networks and DH systems with several production units. As a drawback of physical-mathematical modelling, information on the physical network structure, on the heat loads in the buildings and on the cooling of the heating system (among other things) is required to run a simulation.

Despite the capability of modern computers, it is still a challenging job to reach an optimum solution for the supply temperature and the load distribution on different production units for the coming period (1-2 days).

To reduce the simulation time, aggregated models of the network and consumers are an attractive alternative to a full description of the DH system. In this work our thermal aggregated model developed in Pálsson et al. (1999) has been further validated on new DH systems and on large data sets. Moreover, a new aggregated model for pressure losses has been developed in the present project.

For both the thermal and the pressure aggregated models we found that the number of pipes and consumers can be reduced to three to five pipes without seriously affecting the accuracy of the simulation. In an on-line application, the uncertainty associated with the weather and heat load forecasts is expected to be much greater than the inaccuracy from aggregation of the DH system.

Aggregated models as well as full descriptions of the DH systems have been applied to find the optimum temperature level. For the Hvalsoe DH system with 535 consumers we found that by using an aggregated 12-pipe model the simulation time to reach the optimum solution was reduced from 5 hours to 0.3 hour. The reduction of simulation time partly depends on solving the heat exchanger equation, and therefore the applied model for the cooling of the DH water affects the reduction of the simulation time. For DHSim option –e (with no heat exchanger model) the reduction is less. For R01 Madumvej week 13 we found a reduction from 50 minutes for the physical model to 7 minutes for a 5-pipe model.

The optimum temperature level is specific for each and every DH system, depending on its design (pipe sizes affecting pumping costs), geographical structure (pipe lengths affecting heat losses), line heat demand (heat demand per meter pipe) and its cost structure (cheap or expensive fuel compared with electricity for pumping). Although the pumping cost often is a small part of the total costs, the pumping influences the constraints during the optimisation. The optimum solution in case of no pumping costs (zero electricity price) is not the optimum solution when the pumping cost is included in the optimisation.

For DH systems with high line heat demands and low fuel/electricity cost ratio like in Ishoej and Roedovre R01 Madumvej, the optimum temperature level is high (90-105 ˚C in the winter period). For DH systems with large heat losses (in percentage) the temperature level is lower.

Operational optimisation of DH systems is expected to be more complicated in the future, not only for electricity producing plants but also with respect to heat distribution only. Emission taxes (CO2) and variable gas and electricity prices need to be taking into account to find an optimum solution. In this work, DH systems connected to the VEKS transmission company are considered, and here an incentive tariff between VEKS and the distribution companies applies. An incentive for daily load variations and the return temperature level at the substation must be

taken into account. This incentive has a big influence on the optimum supply temperature curve.

Demand Side Management should be taken into account to find the optimum temperature level. The consumers and the DH company should work out a strategy for DSM in the interest of both parties, so that the DH company can reduce the peaks when it is required. We have shown how DSM in Ishoej and Roedovre R01 Madumvej can reduce the operational costs by reducing the daily load variations.

Other publications in this project:

Bøhm, B. (2002): Simple models for operational optimisation. DBDH News 3/2002, pp.10-15.

Bøhm, B., Ha, S., Kim, W., Kim, B., Koljonen, T., Larsen, H.V., Lucht, M., Park, Y., Sipilä, K., Wigbels, M. and Wistbacka, M. (2002): "Simple models for operational optimisation", IEA Annex VI, NOVEM, 2002. ISBN 90-5748-021-2.*

Bøhm, B., Ha, S., Kim, W., Kim, B., Koljonen, T., Larsen, H.V., Lucht, M., Park, Y., Sipilä, K., Wigbels, M. and Wistbacka, M. (2002): "Simple models for operational optimisation", Proceedings of the 8th. Int. Symp. on District Heating and Cooling, Trondheim, August 14-16, 2002. ISBN 82-594-2341-3.

Larsen, H.V., Bøhm, B. and Wigbels, M. (2004): "A Comparison of Aggregated Models for Simulation and Operational Optimisation of District Heating Networks". Energy Conversion and Management (2004) 45/7-8, pp. 1119-1139.

* This work contains a comparison of the Danish and German aggregation methods.

Introduction

The liberalisation of the energy market (electricity, gas and to some extent heat) is already well under way. This means that a more complex price structure as well as a more complex production system can be foreseen, if not already in place compared to "the old days". As a result modelling, simulation and optimisation will have a growing importance for the energy companies in order to minimise the operational costs.

Although computers get faster and faster, it can still be a very challenging task to optimise large energy networks and systems. In this connection our work on aggregation of District Heating (DH) systems falls well within this framework. The first project "Equivalent models of district heating systems, for on-line minimization of operational costs of the complete district heating system" was carried out from 1996 until 1999, Pálsson et al. (1999), Larsen et al. (2002). Here the method of aggregation was developed by Helge Larsen and co-workers and the method was tested on a limited data set from VEKS / Ishoej and Hvalsoe DH systems. The method could handle thermal networks without loops.

At the same time in Germany, the Fraunhofer Institut für Umwelt-, Sicherheits- und Energietechnik UMSICHT also developed a method of aggregation, Loewen (2001). In the IEA Annex VI project "Simple models for operational optimisation" it became possible to compare these two approaches on the Ishoej DH system, Bøhm et al. (2002), Larsen et al. (2004).

In the present EFP 2001-project the goals have been to improve the Danish method of aggregation by addressing the problem of aggregation of pressure losses, and to test the methods on a much larger data set. Furthermore the questions of Load Management and Demand Side Management have been addressed.

In order to test the aggregation methods, it is crucial to have good data. Very few DH systems can supply adequate data for a whole DH system and often these systems will be of the "transmission" type with a limited number of consumers. In this way it is necessary to test the methods on DH systems that cannot be regarded as typical Danish DH systems. However, we feel confident that our models also work on more typical DH systems. In fact, in an on-going IEA Annex VII project data from a typical Danish system will be used, Bøhm et al. (2004).

In the present work we use data from the following DH systems:

Subsystems R01 Madumvej and R02 Broparken in Roedovre. Data is available on a 6-minutes basis from all consumers and the plant (from the Supervision, Control And Data Acquisition system, SCADA), period from October 2002 until September 2003.

Ishoej DH system. Data on 5-minutes basis from the consumers and the plant, period December 19-24, 2000. Additional data are supplied from the VEKS SCADA system, if necessary.

Hvalsoe DH system. Data on a 2-minutes basis from the SCADA system, period 1998. Data from the consumers not available, except for the yearly consumption.

The line heat demand and the efficiency of the network are very different in these systems, ranging from a heat loss of approximately 3% in Ishoej to 20% in Hvalsoe. The price relationship between fuel and electricity is also very different from the DH systems Ishoej and Roedovre connected to VEKS, and the Hvalsoe DH system with decentralised CHP production. The optimum temperature level will, among other things, depend on these parameters. In this way the work covers a broad range of DH systems.

The report is structured in the following way:

In *Chapter 2* the algorithms for aggregation of DH grids are presented and the Roedovre and Ishoej DH systems are used as case studies.

Chapter 3 describes modelling of DH house stations (consumer installations) and the substations with the purpose of separating the heat load in a degree-day dependent part and a part dependent on the clock. This clock function could be a measure of the possibility to modify the heat load by Demand Side Management (DSM).

Chapter 4 deals with operational optimisation when only heat losses and pumping costs are part of the object function, while *Chapter 5* treats the cases when an incentive tariff is included in the optimisation.

Chapters 6, 7 and 8 treat operational optimisation with different degrees of DSM measures (peak reductions).

Finally, in *Chapter 9* a different way of finding the building heat loads is discussed in order to ease the data treatment.

Chapter 1 The District Heating Systems

In this chapter we will briefly describe the district heating systems from which data was collected for this work.

1.1 The Roedovre District Heating System

Roedovre is a suburb of Copenhagen, located 9 km west of the city center. The supply area consists mainly of blocks of flats, semidetached houses, institutions and shops.

Roedovre DH Company consists of five separate networks, all supplied from VEKS. The distribution systems were constructed in 1986-1989. The connection to the transmission system as well the connection to the consumer installations are made by heat exchangers. There are no peak load boilers. In 2001, 99% of the planned total amount of consumers was connected to the Roedovre DH system. With 12.9 km distribution pipes and 11.1 km service pipes to the consumers (for all five systems), the line heat demand is approximately 20.5 GJ/m and the heat loss approximately 7%.

1.1.2 House stations (consumer installations)

Most consumers have one heat exchanger for the radiator system and one for the hot water system, however, in some buildings the hot water system is connected to the radiator circuit.

There are different types of hot water systems in use: Hot water tanks with built-in heating coils, or storage tanks connected to a heat exchanger with a loading circuit. There are also heat exchangers without storage tanks, often with a heat exchanger for preheating of the cold tap water. One consumer uses electricity to produce hot water in the summer period.

Most radiator systems are 2-string systems, but there are a few 1-string systems. Most radiators are equipped with radiator thermostats.

Many up-risers (radiator supply strings) are equipped with adjustment valves but the internal adjustment (balance) is often a problem. Nearly all new circulation pumps have variable speed control.

The heat consumption of the building is measured by an energy meter. This heating cost is distributed to the tenants according to tariffs established by each housing company.

1.1.3 Substations and the distribution system

The connection to VEKS are made by two heat exchangers, each with a capacity of 75% of the maximum heat load. There are two main circulation pumps, each with a capacity of 100% of the maximum load. The pumps are controlled according to the differential pressure at the most remote consumer installation. The differential pressure here is 0.5 bar. The static pressure is maximum 10 bar and usually approximately 3.5 bar.

All pipes are preinsulated steel pipes with standard insulation thickness. There are compensators and expansion bendings (in concrete chambers). The design temperatures are 90 and 55 ºC for the supply and return temperatures, respectively. Usually a lower supply temperature is applied, according to the outdoor temperature.

1.1.4 Heat accounting

The variable cost paid to VEKS is approximately 60% of the total costs, while the rest is a fixed cost. The tariff includes two extra incentives: An extra charge/bonus for cooling when the secondary return temperature is above or below 55 ºC, and an extra charge/bonus for load

variations. Both charges are based on daily hourly values and weighed with the daily consumption, cf. Section 4.2.

1.1.5 Measurements

A SCADA system collects data from the substations and the house stations with an interval of 6 minutes. The following data are available for the **house stations** (consumers):

- instantaneous heat load and flow (as well as accumulated heat meter readings)
- primary supply and return temperatures
- secondary temperatures for some, but not all consumers.

For the **substations** information on the differential pressure and the power consumption of the pumps (see later) is available as well as the differential pressure at the critical consumer. Finally, the outdoor air temperature is measured.

After some initial tests, data was collected from medio October 2002 until medio September 2003. From this large data set, three one-week periods were selected, representing a winter, a spring and a summer situation. In the selection process, erroneous and missing data had to be considered. Finally the following periods were selected:

Period 1: Week 2, 6 January, 2003, 00:00 – 12 January, 2003 23:54 for Subsystems R01 and R02

Period 2: Week 13, 24 March, 2003 00:00 – 30 March, 2003, 23:54 for Subsystem R01
Week 19, 5 May, 2003 00:00 – 11 May, 2003, 23:54 for Subsystems R02

Period 3: Week 23, 2 June, 2003, 00:00 – 9 June, 2003, 23:54 for Subsystem R01
Week 33, 11 August 2003, 00:00 – 17 August, 2003, 23:54 for Subsystem R02.

In Appendix B, operational data can be found for the substations and the consumer installations. The variations in heat loads noticeable are caused by the local control system, for example with regard to night set back of the secondary supply temperature during the night. There is no failure in the heat supply from the VEKS substations in the selected periods.

Subsystem R01 Madumvej

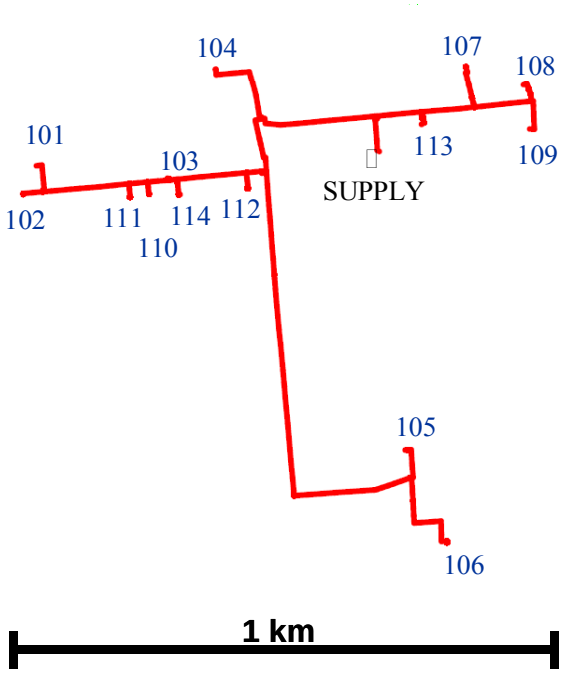

Figure 1.1. The distribution network R01 Madumvej in Roedovre with 14 house stations.

Subsystem R01 consists of 14 consumers as shown in the following table.

Table 1.1. Design heat loads, consumer categories and measurements 2003.

#	Design heat load			Category			Heat meters 2003	
	Heating	Hot water	Total				Consumption	Cooling
	kW	kW	kW		# Flats	Area m^2	MWh	ºC
1-01	370	189	559	Semidetached	60	5,280	662	26.6
1-02	570	0	570	Trade, workshops		3,730	692	27.5
1-03	300	87	387	Semidetached	35	3,415	549	35.3
1-04	650	0	650	Institution		6,571	1,304	24.6
1-05	1,200	465	1,665	Semidetached	198	16,493	2,833	32.6
1-06	630	120	750	Semidetached	90	8,313	1,137	26.8
1-07	1,000	0	1,000	School		4,990	934	25.4
1-08	1,200	0	1,200	School		12,232	1,559	26.0
1-09	370	0	370	Semidetached	56	5,220	607	35.1
1-10	200	32	232	Trade, offices		4,101	330	29.8
1-11	150	50	200	Trade, offices, store		1,283	133	33.5
1-12	230	35	265	Trade, offices, store		3,007	400	33.9
1-13	150	70	220	Flats	31	2,348	245	41.1
1-14	87	30	117	Trade, store		1,638	139	29.0
Total			8,185			78,621	11,524	

When the design hot water load is equal to zero, it means that the hot water system is connected to the secondary side of the radiator heat exchanger.

The magnitude of the heat consumption for the different consumers as well as the cooling should be observed. The annual cooling varies from 25 to 41 ºC.

It should be noted, that as shown in Appendix A, the outdoor temperature in January 2003 was below –12 ºC, the design temperature in Denmark. Nevertheless, the measured heat loads were lower than the design values in Table 1.1.

In Subsystem R01, the total length of the network is 2.708 m. With a total measured consumption of 11.524 MWh in 2003, the line heat demand is approximately 15 GJ/m.

Subsystem R02 Broparken

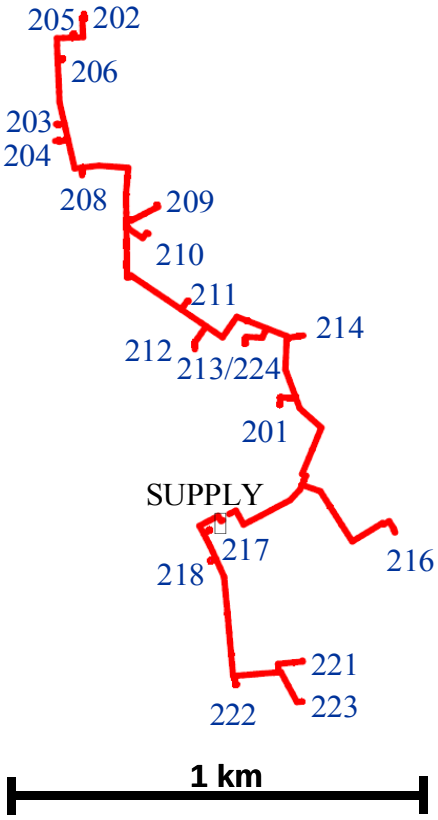

Figure 1.2. The distribution network R02 Broparken in Roedovre with 20 house stations.

Subsystem R02 consists of 20 consumers as shown in the following table. Building 2-24 was connected during 2003.

Table 1.2. Design heat loads, consumer categories and measurements 2003.

#	Design heat load			Category			Heat meters 2003	
	Heating	Hot water	Total				Consumption	Cooling
	kW	kW	kW		# Flats	Area m^2	MWh	ºC
2-01	1,800	0	1800	Institutions		21,388	2,647	25.2
2-02	500	283	783	Flats	82	5,440	862	36.6
2-03	87	30	117	Flats	15	1,116	128	34.4
2-04	130	50	180	Flats	42	1,820	278	40.4
2-05	500	357	857	Flats	104	5,760	966	37.5
2-06	500	344	844	Flats	98	7,039	939	36.9
2-08	185	90	275	Flats	48	2,676	402	20.2
2-09	500	170	670	Flats	57	3,838	660	33.0
2-10	118	0	118	Offices		916	187	25.9
2-11	150	66	216	Workshop, offices		9,389	271	31.2
2-12	964	160	1124	Flats	168	10,692	1,634	31.3
2-13	600	32	632	Flats, institution	59	4,389	1,036	30.3
2-14	150	60	210	Flats	34	2,390	294	39.9
2-16	482	210	692	Sport arena		2,621	629	30.8
2-17	500	200	700	Flats	173	12,303	791	33.9
2-18	1,400	535	1935	Flats, semidetached	226	18,909	2,772	36.5
2-21	821	300	1121	Flats, institution, shops	132	16,038	1,910	33.5
2-22	218	68	286	Semidetached	23	2,645	447	32.5
2-23	500	200	700	Flats	97	6,321	990	32.2
2-24	600	0	600	Semidetached	100	9,177	842	33.4
Total			13,860			144,867	18,685	

In Subsystem R02, the total length of the network is 3.503 m. With a total measured consumption of 18.685 MWh in 2003, the line heat demand is approximately 19 GJ/m in Subsystem R02.

The annual cooling in 2003 varies from 20 to 40 ºC.

For both subsystems, the heat load variations shown in Appendix B should be observed. For the schools, a clear pattern can be observed with a lower heat demand in the weekends.

Some block of flats apply a night setback of the temperature and an increased heating in the morning while other consumers do not show this behaviour.

For some consumers the heat load variations change during the measurement period. This could either be caused by manual control adjustments or by a defective control system.

1.1.6 Modelling R01 and R02 DH systems

In the modelling of the Roedovre DH systems the collected time series were used as input files to the general simulation programme DHsim. Time series for the heat load have been used for each house station, but because secondary forward and return temperatures are not available, DHSim was used with option –e, cf. Section 4.3.1.

1.2 The Ishoej District Heating System

Ishoej is a suburb of Copenhagen, located 17 km south-west of the city centre. The built-up area consists mainly of blocks of flats, semidetached houses, institutions and shopping centres. Many of the buildings were erected in the 1970s.

The DH system was built in 1982. Today, 8000 dwellings, five schools and the city centre with many shops and institutions are supplied from the DH system. All consumer installations are indirectly connected through 23 substations (each substation consists of one or two plate heat exchangers).

The distribution network is shown in Figure 1.3. It is made of preinsulated pipes, mostly with "standard" insulation thickness, and in pipe dimensions from 48 to 356 mm. The total length of the network is approximately 8.3 km. As all connected buildings are situated within a small area, the line heat demand is high, approximately 42 GJ/m, and the annual heat loss (from the primary network) is only approximately 3%.

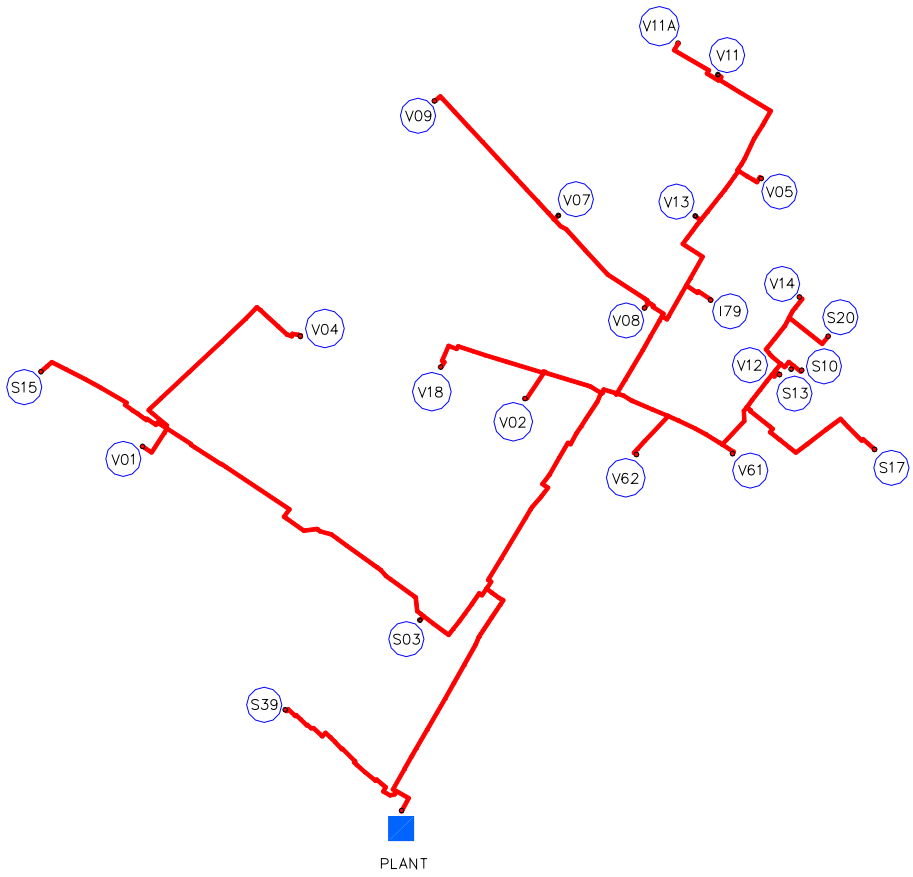

Figure 1.3. The distribution network in Ishoej with 23 house stations.

In the beginning the heat was produced by three coal-fired boilers, each with a nominal capacity of 17 MW, and by a smaller gas-fired peak load boiler. Today the Ishoej DH system is connected to the West Copenhagen Heating Transmission Company, VEKS. The boilers have been modified for bio fuel and the plant can supply heat both locally and to the transmission grid.

The Ishoej DH company has installed an advanced control and supervision system, which, among other tasks, stores data from the substations and the plant at a five-minute interval.

At a typical house station the following data is available:

- Primary and secondary supply temperature
- Primary and secondary return temperature
- Pressures in the supply and return line
- Accumulated heat meter readings (energy and volume).

At the Ishoej plant the production by the boilers and the amount of heat delivered from the VEKS system is available, as well as flow, temperature and pressure measurements.

Due to reconstruction and connection of new house stations, as well as the installation of a new computer system at the plant, the data collection was not effective for all house stations in year 2000.

1.2.1 Measurements

In this work 5-minutes data from December 19-24, 2000, is used. The heat loads at the substations were obtained by filtering the heat meter data. Heat production data at the Ishoej plant was obtained from VEKS. In this period the boilers were used only a couple of hours.

Manual reading of the heat meters had taken place on December 11 and 18, and the associated heat consumption is shown in Table 1.3. For those substations where no data was available, a heat load series was constructed from other substations with data, taking into account the type of building (block of flats, school, etc.) and the heat consumption according to Table 1.3. To distinguish between these two kinds of substations, substations with real measurements are called Vxx or Ixx, while substations with simulated time series are called Sxx. Despite the uncertainty associated with this way of generating the missing data, the result is quite good as is shown in Figure 1.4. Here the measured heat production at the Ishoej plant is compared with the sum of the heat loads in the house stations.

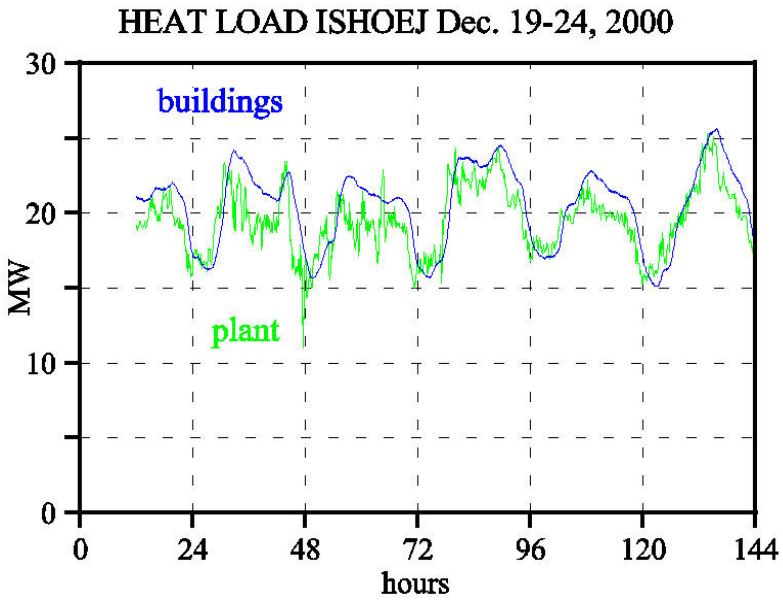

Figure 1.4. Measured heat production at the plant and the sum of the (filtered) heat loads in the house stations.

Table 1.3 shows the heat consumption at the house stations the week before the time series start, as well as the average heat load in the time series for the period December 19, 12:00 - December 24, 24:00.

Table 1.3. The house stations in the Ishoej DH system.

House station	Heat meters Dec. 11-18, 2000 GJ	Average load Dec. 19-24 MW	Category
V01	655	1.404	Apartments
V02	524	1.112	Shopping centre
S03	3191	6.736	Apartments
V04	1036	2.205	Apartments
V05	260	0.611	Apartments
V61	153	0.335	Shopping centre
V62	201	0.441	Shopping centre
V07	1,245	2.628	Apartments
V08	849	1.787	Apartments
V09	94	0.203	Apartments
S10	144	0.315	Apartments
V11	22	0.045	Apartments
V11A	35	0.075	Apartments
V12	142	0.309	Apartments
S13	130	0.378	Public school
I13	4	0.008	Kindergarten
V14	188	0.416	Public school
S15	132	0.378	Public school
S17	47	0.100	Youth hostel
V18	16	0.039	Church
S20	53	0.113	Institution
S39	251	0.556	Public school
I79	104	0.298	Technical school
Total		20.491	

To give an impression of the type of consumers in Ishoej, the heat consumption and the primary and secondary supply and return temperatures for the 23 house stations are shown in Appendix D. Several interesting things can be observed: The size and time variation of the heat loads are very different, varying from 8 kW to 6.7 MW on the average, cf. Table 1.3, and from almost constant consumption to substations with distinct time variations (night set back). Due to the Christmas holidays at the end of the period, the consumers behave very differently, as for instance some of the institutions are closed down for the holidays.

1.2.2 Modelling the Ishoej DH system

In the modelling of the Ishoej system the generated data set has been used as input files to the general simulation program DHsim. Time series for heat load as well as for secondary forward and return temperatures have been used for each substation. All substations were modelled as one plate heat exchanger, and the kA-values were estimated from the measured heat load, and the measured primary and secondary supply and return temperatures.

1.3 The Hvalsoe district heating system

Hvalsoe is a small town of approximately 2500 inhabitants, situated on Zealand about 40 km West of Copenhagen. Due to its location outside the transmission system of the Greater Copenhagen area, Hvalsoe has its own district heating system. The heat is produced by a gas engine with auxiliary boilers, and with an accumulator tank for storing heat. In the accounting period 1997/1998, the total heat production was 14.95 GWh, with a maximum production of 6 MW (3.6 MW by the engine).

In Figure 1.5 the distribution network in Hvalsoe can be seen. The maximum dimensions of the grid are 1400 m x 1600 m approximately (the town is slowly but continuously expanding). The figure also shows the location of the heat and power production plant and of the pressure transducer used for controlling the distribution pumps. The total length of the distribution network is 20.2 km, consisting of 1079 pipes with 32 different pipe diameters. Approximately 30 thermostatic bypasses are in use in the outskirts of the network.

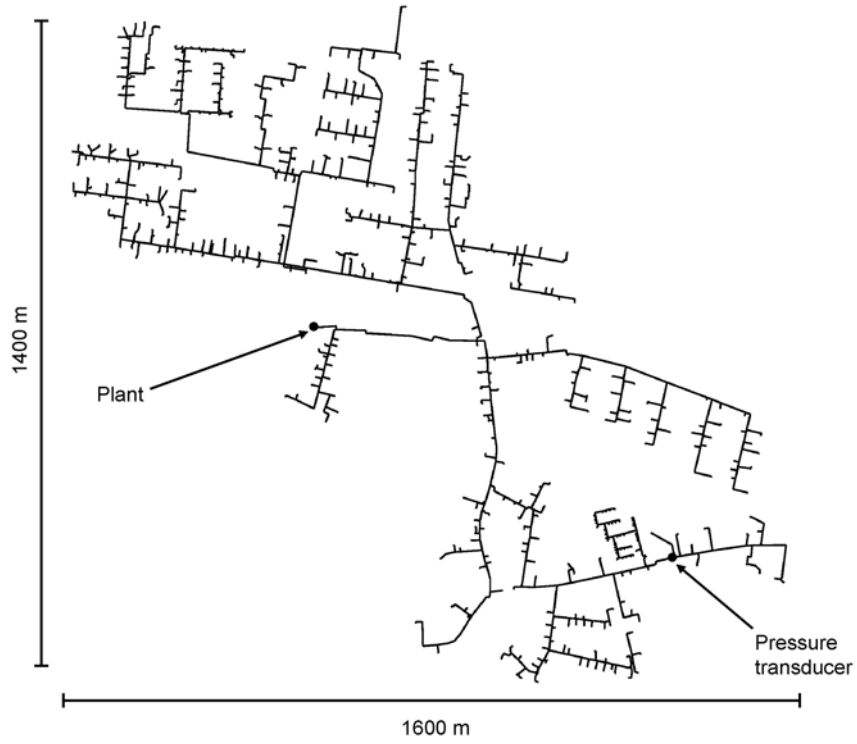

Figure 1.5. The distribution network in Hvalsoe, Pálsson et al. (1999).

1.3.1 Consumers

The network of Hvalsoe supplies heat to the great majority of the buildings of the town, for a total of 535 dwellings (loads) in the year 1997/1998. The distribution of the yearly heat demands of the consumers in Hvalsoe is shown in Figure 1.6. It appears that most consumers live in single-family houses, but some large consumers like apartment blocks and institutions also exist.

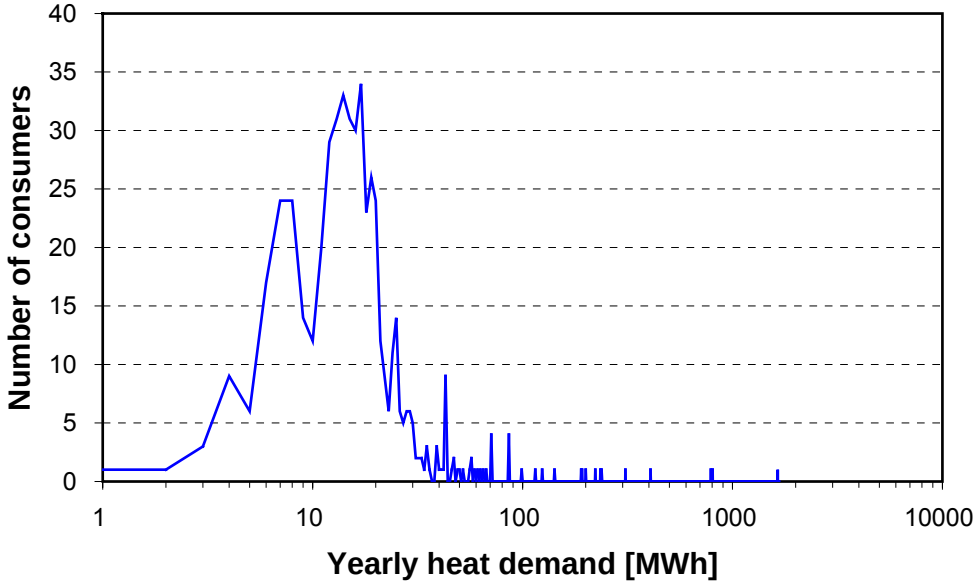

Figure 1.6. Distribution of yearly heat demand of the consumers in Hvalsoe in 1997/98, Pálsson et al. (1999).

All consumers use district heating for both space heating and for hot tap water. It is known that most buildings are directly connected to the distribution system, but the larger buildings are connected through a heat exchanger. The heating systems can differ in many ways, such as:

- Type of connection (direct or indirect)
- Type of heating system (one or two string radiator systems, radiator size, floor heating)
- Devices for the tap water heating (storage tank with or without a built-in heating coil, heat exchanger)
- Ratio between the thermal energy required for space heating and for the tap water
- Amount and time profile of the daily consumption.

1.3.2 Measurements

Data were collected from the plant from July 1997 until 1999 as two minutes values. In this project data from 1998 will be used. Figure 1.7 shows the supply and returns temperatures from the DH plant as well as the heat load at the plant.

1.3.3 Modelling the Hvalsoe DH system

In Tryggvason (1999) simulations of the Hvalsoe system were carried out with different types of consumer installations, i.e. direct connections with two string radiators (with or without a bypass at the service line), or indirect connections with heat exchangers. Even though it is known that most consumers in Hvalsoe have radiator systems, Tryggvason found that the assumption of indirect connections gave the best simulated return temperatures at the plant when compared with the measurements.

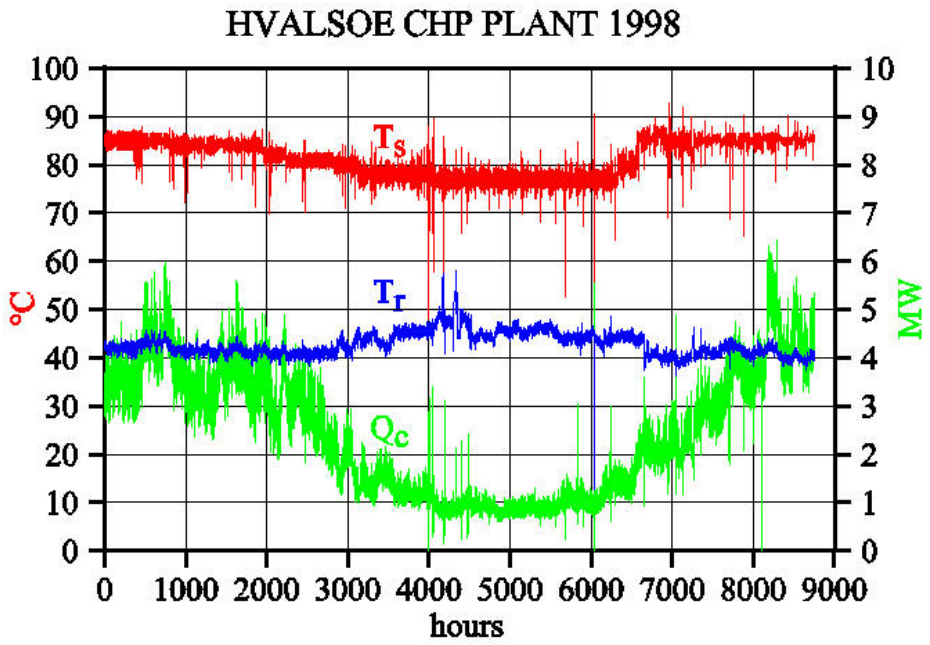

Figure 1.7. Heat production and supply and return temperatures from the plant in Hvalsoe in 1998.

Consequently, in the following modelling of the Hvalsoe system an indirect heating system at the consumers will be assumed. Based on the measured annual heat and volume consumptions in 1997/1998, the annual cooling of the DH water can be calculated. Heat transfer areas (kA) for the individual heat exchangers were then calculated which fitted the measured cooling of the DH water. It was further assumed that the secondary temperatures of the heat exchangers of all consumers were 60 and 40 °C, respectively.

No account was taken of the hot water systems in the buildings or of bypasses in the network in the modelling. However, it should be remembered that detailed information of the 535 consumer installations is not available, and that the goal of this work is to verify the aggregated models with realistic assumptions, but not to achieve an exact match with the real system.

Based on a thorough analysis of the measurements three periods in 1998 were selected for further analysis. These represent a winter, a spring and a summer situation. Based on several test simulations, the heat load at the consumers was obtained from the load at the DH plant reduced by the heat loss of the network, cf. Bøhm et al. (2002). No account was taken of the time delay in the system. The heat load at the consumers was distributed according to the measured annual consumption in 1997/1998.

In Bøhm et al. (2002) the work on network aggregation is described. Here we will focus on operational optimisation and only the winter situation January 22-23, 1998 will be considered in Section 4.4.

Chapter 2 Aggregation of district heating systems

2.1 Algorithms for aggregation of DH grids

Simulations and especially optimizations of the operation of DH systems with tens or hundreds of pipes and consumers will take a considerable time. For each time step the simulations take into account flow, temperature, heat loss and differential pressure loss in each branch of the grid. To improve the situation various ways of simplifying the grid can be used. In the utmost situation a whole DH grid can be reduced to one pipe and one consumer, but then it must be accepted that all details of the system are lost, e.g. the delay from the DH plant to each consumer cannot be represented.

Here a systematic way of gradually reducing the complexity of a large DH system is considered. The phrase 'physical' will be used to identify the actual DH system whereas phrases 'aggregated', 'simplified' and 'equivalent' will be used for various model grids that are defined by reducing the complexity of the physical system. Starting out from the physical DH system, two aggregated systems are defined. One system is used to calculate temperatures and heat loss, and another system is used to calculate differential pressure.

The symbols used in the formulas are defined in Table 2.1 and Table 2.2.

Table 2.1. Symbol definitions.

Variable	Unit	Definition
m	*kg/s*	Mass flow to load
μ	*kg/s*	Mass flow in pipe
v	*m/s*	Velocity (temp. front)
τ	*s*	Time delay
L	*m*	Pipe length
d	*m*	Steel pipe inner diameter
D	*m*	Steel pipe outer diameter
V	m^3	Water volume
h	*W/(m·°C)*	Specific heat conductivity
H	*W/°C*	Heat conductivity
c	*kJ/(kg·°C)*	Specific heat capacity
C	*kJ/(m·°C)*	Heat capacity per meter
ρ	kg/m^3	Density
Π	*m* H_2O	Pressure head

Subscript	Definition
1	Branch or node 1
2	Branch or node 2
A	Branch or node A
B	Branch or node B

Superscript	Definition
s	Supply
r	Return
w	Water
p	Steel pipe

Table 2.2. Auxiliary variables.

Symbol	Definition	Condition
α	m_2/m_1	$\alpha > 0$
β	$1-\alpha$	$\beta > 1$
φ	$C^w/\left(C^w + C^p\right)$	$0 < \varphi < 1$
ψ	φ_2/φ_1	$\psi > 0$
γ	$\left(V_1/V_2\right)\cdot\left(m_2/m_1\right) = \left(V_1/V_2\right)\cdot\alpha$	$0 < \gamma \le 1/\psi$
X	$\dfrac{\rho^p \cdot c^p}{\rho^w \cdot c^w}$	$X > 0$

2.1.1 Temperature and heat loss

The aggregation algorithms are in detail described in Pálsson et al. (1999) and Larsen et al. (2002). Here a short discussion of the method will be given together with the resulting formulas.

An aggregation process is started by collecting data on all pipe branches of the DH grid (length, inner and outer diameter of the steel pipes, insulation thickness). Then representative flow values (kg/s) for all branches must be chosen. These flows should be as close as possible to the average flows for the time period for which the aggregated grid is to be used.

The aggregation consists of two separate processes:

- Changing a tree structure into a line structure.
- Removing pipes in a line structure.

2.1.1.1 Changing a tree structure into a line structure

The process of changing the tree structure of an entire DH grid into a line structure can be considered as a succession of simple reductions as shown in Figure 2.1.

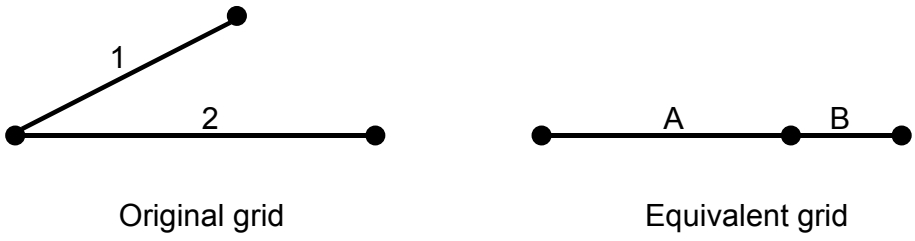

Figure 2.1. Changing basic tree structure into line structure.

In the development of the algorithms some quantities are conserved (e.g. mass flow) whereas others are not. Table 2.3 shows the physical properties that are conserved by the aggregation.

Table 2.3. Changing tree structure into line structure.

	Conserved
Pipe length	No
Pipe inner diameter	DB = D2
Water volume	Yes
Delay	Yes
Mass flow	Yes
Heat load	Yes
Heat loss from supply pipe	Yes
Heat loss from return pipe	Yes

The algorithm for changing a tree structure into a line structure is shown below. The symbols used in the formulas are defined in Table 2.1 and Table 2.2.

First the formulas that give the dimensions (except for the insulation) of the equivalent branches are given:

$$m_A = m_1$$

$$L_A = L_1 \cdot \frac{1 + \alpha^2 \cdot \psi \cdot A_1 / A_2}{\beta}$$

$$d_A = 2 \cdot \sqrt{\frac{\beta \cdot (1 + \alpha \cdot \psi) \cdot A_1 \cdot A_2}{(A_2 + A_1 \cdot \alpha^2 \cdot \psi) \cdot \pi}}$$

$$\varphi_A = \frac{\varphi_1 + \alpha \cdot \varphi_2}{1 + \alpha}$$

$$D_A = d_A \cdot \sqrt{1 + \frac{1 - \varphi_A}{X \cdot \varphi_A}}$$

$$m_B = m_2$$

$$d_B = d_2$$

$$D_B = D_2$$

$$L_B = L_2 \cdot (1 - \gamma \cdot \psi)$$

In the development of the algorithms for aggregating a DH grid all variables are considered constant in time. To take care of heat loss it is furthermore necessary to assume that all return temperatures at the loads are equal. Of cause these assumptions are never fulfilled but

nevertheless the resulting aggregated DH systems are very useful when simulating the operation of the DH system.

The supply side heat conductivities of the equivalent branches A and B are given by the following formulas:

$$
\begin{aligned}
&\textit{If } H_2^s / H_1^s \geq m_2 / m_1 : \\
&\quad H_A^s = (1+\alpha) \cdot H_1^s \\
&\quad H_B^s = H_2^s - \alpha \cdot H_1^s
\end{aligned}
$$

$$
\begin{aligned}
&\textit{If } H_2^s / H_1^s < m_2 / m_1 : \\
&\quad H_A^s = H_1^s + \gamma \cdot \psi \cdot H_2^s \\
&\quad H_B^s = H_2^s \cdot (1 - \gamma \cdot \psi)
\end{aligned}
$$

$$h_A^s = H_A^s / L_A$$

$$h_B^s = H_B^s / L_B$$

For the return side the formulas are similar:

$$
\begin{aligned}
&\textit{If } H_2^r / H_1^r \geq m_2 / m_1 : \\
&\quad H_A^r = (1+\alpha) \cdot H_1^r \\
&\quad H_B^r = H_2^r - \alpha \cdot H_1^r
\end{aligned}
$$

$$
\begin{aligned}
&\textit{If } H_2^r / H_1^r < m_2 / m_1 : \\
&\quad H_A^r = H_1^r + \gamma \cdot \psi \cdot H_2^r \\
&\quad H_B^r = H_2^r \cdot (1 - \gamma \cdot \psi)
\end{aligned}
$$

$$h_A^r = H_A^r / L_A$$

$$h_B^r = H_B^r / L_B$$

2.1.1.2 Removing pipes in a line structure

When a DH network consisting of many branches is converted into a line structure as described above, many nodes in the equivalent network will be positioned close to each other separated by relatively short pipes. Such nearby nodes can be collapsed to further simplify the equivalent network, c.f. Figure 2.2. If the method is also used for longer pipes, the equivalent network can be reduced to only a few or just one branch. This will of course reduce the quality of the resulting network model.

Figure 2.2. Removing a short branch in a line structure.

Table 2.4 shows the physical properties conserved by removing a branch.

Table 2.4. Removing pipes in a line structure.

	Conserved
Pipe length	Yes
Pipe inner diameter	No
Water volume	Yes
Delay	Yes
Mass flow	Yes
Heat load	Yes
Heat loss from supply pipe	Yes
Heat loss from return pipe	Yes

Figure 2.3 shows in detail how a short branch (branch 2) in-between branches 1 and 3 is removed. Loads may be present at both ends of branch 2 as indicated by m_1 and m_2 in the figure. During this process the two loads are also transformed as described in the following.

Let indices 1, 2, and 3 describe the three branches in the original DH network while indices A and B describe the slightly changed replacements for branches 1 and 3. Branch 2 is divided in two parts as indicated in the figure. Branch A represents branch 1 and the first part of branch 2 while branch B represents the other part of branch 2 and branch 3.

Below the formulas for removing this short branch and at the same time changing branches 1 and 3 is given. A detailed description of the algorithm can be found in Pálsson et al. (1999) and Larsen et al. (2002).

The symbol μ is used to indicate flow in branches while m as in the previous sections indicates flow to loads. Branch 2 is split between branches A and B according to factors f_A and f_B that are calculated from the flows as indicated below. The loads at the two ends of branch 2 are split between three loads as shown in Figure 2.3. This split is given by the factors g_{AA}, g_{AB}, g_{BA} and g_{BB} that are calculated from the time delays in the branches.

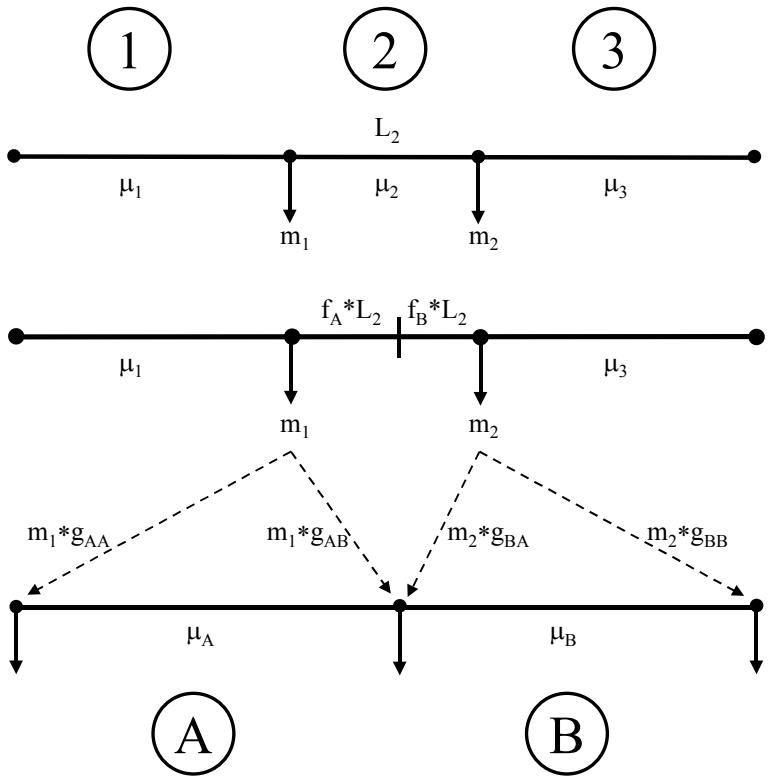

Figure 2.3. Removing a branch in a line structure.

The algorithm for changing branches 1, 2 and 3 into branches A and B is as follows:

$$m_1 = \mu_1 - \mu_2 \qquad m_2 = \mu_2 - \mu_3$$

$$f_A = \frac{m_2}{m_1 + m_2} \qquad f_B = \frac{m_1}{m_1 + m_2} = 1 - f_A$$

$$L_A = L_1 + f_A \cdot L_2 \qquad L_B = L_3 + f_B \cdot L_2$$

$$\varphi_A = \left(1 + X \cdot \frac{V_1^p + f_A \cdot V_2^p}{V_1 + f_A \cdot V_2}\right)^{-1} \qquad \varphi_B = \left(1 + X \cdot \frac{V_3^p + f_B \cdot V_2^p}{V_3 + f_B \cdot V_2}\right)^{-1}$$

$$V_A = V_1 \cdot \frac{\mu_A}{\mu_1} \cdot \frac{\varphi_A}{\varphi_1} + f_A \cdot V_2 \cdot \frac{\mu_A}{\mu_2} \cdot \frac{\varphi_A}{\varphi_2} \qquad V_B = V_3 \cdot \frac{\mu_B}{\mu_3} \cdot \frac{\varphi_B}{\varphi_3} + f_B \cdot V_2 \cdot \frac{\mu_B}{\mu_2} \cdot \frac{\varphi_B}{\varphi_2}$$

$$V_A^p = V_A \cdot \frac{1 - \varphi_A}{\varphi_A \cdot X} \qquad V_B^p = V_B \cdot \frac{1 - \varphi_B}{\varphi_B \cdot X}$$

$$d_A = 2 \cdot \sqrt{\frac{V_A}{\pi \cdot L_A}} \qquad d_B = 2 \cdot \sqrt{\frac{V_B}{\pi \cdot L_B}}$$

$$D_A = 2 \cdot \sqrt{\frac{V_A + V_A^p}{\pi \cdot L_A}} \qquad D_B = 2 \cdot \sqrt{\frac{V_B + V_B^p}{\pi \cdot L_B}}$$

$$h_A = \frac{h_1 \cdot L_1 + f_A \cdot h_2 \cdot L_2}{L_A} \qquad h_B = \frac{h_3 \cdot L_3 + f_B \cdot h_2 \cdot L_2}{L_B}$$

$$\tau_1 = \frac{\rho^w \cdot V_1}{\mu \cdot \varphi_1} \qquad \tau_2 = \frac{\rho^w \cdot V_2}{\mu \cdot \varphi_2}$$

$$g_{AA} = \frac{f_A \cdot \tau_2}{\tau_1 + f_A \cdot \tau_2} \qquad g_{BA} = \frac{\tau_3}{\tau_3 + f_B \cdot \tau_2}$$

$$g_{AB} = \frac{\tau_1}{\tau_1 + f_A \cdot \tau_2} \qquad g_{BB} = \frac{f_B \cdot \tau_2}{\tau_3 + f_B \cdot \tau_2}$$

2.1.2 Differential pressure

Differential pressure cannot be calculated from the aggregated grids considered in the previous section. This can be explained by looking at the basic transformation shown in Figure 2.1.

Let us as above assume that *delay* in branch 1 is *less* than delay in branch 2. Then the load at the right end of branch A is equivalent to the load at the right end of branch1, and the load at the right end of branch B is equivalent to the load at the right end of branch 2. Delay in branch A equals delay in branch 1, and delay in branch B equals delay in branch 2 minus delay in branch 1.

Furthermore, let us assume that *pressure loss* in branch 1 is *greater* than pressure loss in branch 2. Then pressure loss in branch A equals pressure loss in branch 1, and pressure loss in branch B equals pressure loss in branch 2 minus pressure loss in branch 1. This is however a negative pressure loss which cannot easily be interpreted or handled in simulations. Therefore a separate aggregation procedure for differential pressure is needed.

A procedure quite similar to the one used for aggregating the DH system with regard to temperature and heat loss is implemented when aggregating with regard to differential pressure. In the basic transformation in Figure 2.1, we now focus on pressure loss instead of delay. Let us assume that *pressure loss* in branch 1 is *less* than pressure loss in branch 2. Then the load at the right end of branch A is equivalent to the load at the right end of branch1, and the load at the right end of branch B is equivalent to the load at the right end of branch 2. Except for the fundamental difference (that we are using pressure loss and not delay when deciding which load (1 or 2) to move to the right end of branch A) the procedure is rather similar to the one used for calculating temperatures and heat loss.

In the algorithms shown below the symbol Π represents pressure loss. The connection between pressure loss and surface roughness is handled by Darcy-Weisbach's equation.

2.1.2.1 Changing a tree structure into a line structure

Material constant *X*:

$$X = \frac{\rho^p \cdot c^p}{\rho^w \cdot c^w}$$

φ is the ratio between velocity of a temperature front (assuming the same temperature in any cross-section of water and steel pipe) and water velocity:

$$\varphi_1 = \frac{1}{1 + X \cdot \left(\left(D_1 / d_1 \right)^2 - 1 \right)}$$

$$\varphi_2 = \frac{1}{1 + X \cdot \left(\left(D_2 / d_2 \right)^2 - 1 \right)}$$

Velocity of a temperature front *v:*

$$v_1 = \frac{4 \cdot \varphi_1 \cdot m_1}{\rho^w \cdot \pi \cdot \left(d_1 \right)^2}$$

$$v_2 = \frac{4 \cdot \varphi_2 \cdot m_2}{\rho^w \cdot \pi \cdot \left(d_2 \right)^2}$$

First, we look at branch B:

$$m_B = m_2$$

$$\Pi_B = \Pi_2 - \Pi_1$$

We choose to let branch B be equal to branch 2 – except for the length:

$$d_B = d_2$$

$$D_B = D_2$$

$$\chi_B = \chi_2$$

Then pressure loss per meter of branch B equals that of branch 2:

$$L_B = L_2 \cdot \left(1 - \Pi_1 / \Pi_2 \right)$$

Next, consider branch A:

$$m_A = m_1$$

$$\Pi_A = \Pi_1$$

It is chosen to let φ_A equal φ_1:

$$\varphi_A = \varphi_1$$

Volume is conserved by demanding:

$$V_A = V_1 + V_2 \cdot \Pi_1 / \Pi_2$$

It is assumed that the velocity of a temperature front in branch A is a weighted average of the values for branches 1 and 2:

$$v_A = \left(v_1 + \alpha \cdot v_2\right) / \beta$$

Then

$$L_A = \frac{\rho^w \cdot v_A \cdot V_A}{\beta \cdot m_1 \cdot \varphi_A}$$

$$d_A = 2 \cdot \sqrt{\frac{\beta \cdot m_1 \cdot \varphi_A}{\pi \cdot \rho^w \cdot v_A}}$$

$$D_A = d_A \cdot \sqrt{1 + \frac{1 - \varphi_A}{X \cdot \varphi_A}}$$

A rather simple model is used for heat loss since we are focussing on pressure loss:

$$h_A^s = h_B^s = \frac{h_1^s \cdot L_1 + h_2^s \cdot L_2}{L_A + L_B}$$

$$h_A^r = h_B^r = \frac{h_1^r \cdot L_1 + h_2^r \cdot L_2}{L_A + L_B}$$

Due to this simple heat loss model, temperature and heat loss should not be calculated by the differential pressure model. Instead the temperature and heat loss model should be used.

2.1.2.2 Removing pipes in a line structure

The algorithm discussed in *Section 2.1.1.2* is valid here, too. It only needs an extension for calculating pressure loss and surface roughness for branches A and B.

Differential pressure loss is given by:

$$\Pi_A = \Pi_1 + f_A \cdot \Pi_2$$

$$\Pi_B = \Pi_3 + f_B \cdot \Pi_2$$

Surface roughness is handled by Darcy-Weisbach's equation.

2.2 Aggregation of the Roedovre DH system

The aggregation algorithms developed above are tested on two areas (R01 Madumvej and R02 Broparken) of the Roedovre DH system described in *Section 1.1*. Each of the areas is connected to the central VEKS transmission system by a heat exchanger. In R01 Madumvej there are 14 consumers and 30 branches, and in R02 Broparken 18-20 consumers and 40-44 branches. Data for the two areas have been recorded with a time step of 6 minutes from mid-October 2002 until mid-September 2003.

For each of these areas three weeks have been selected: A winter, a spring and a summer week. Due to lack of data for shorter time periods and due to general data quality aspects weeks 2, 13 and 23 have been chosen for R01 Madumvej, and weeks 2, 19 and 33 for R02 Broparken. All weeks are in 2003. That is, we have six DH systems to aggregate. The data used in the aggregation is shown in *Appendix A.*

Appendix B shows measured time series for primary supply and return temperatures and heat consumption at each of the loads. Supply and return temperature at the secondary side of the VEKS heat exchangers supplying R02 Broparken and R01 Madumvej are also shown in *Appendix B* together with power delivered to the DH grid and differential pressure loss from the heat exchanger and out to the critical consumer.

All 6 systems have been aggregated to various degrees of simplification – ending up with very simple systems with only one branch. The standard method of aggregation is used:

- The total area (R01 Madumvej or R02 Broparken) with its full tree structure is modelled.
- The tree structure is changed into a line structure.
- Branches with no loads in-between are combined to one branch. The physical loads are still unchanged.
- Branches are removed one after another, starting with the shortest one. The loads near this branch are changed.

It has been chosen to use the standard procedure of aggregation on the total area in question. Alternatively the area could have been divided into a few sub-areas that subsequently are aggregated independently.

To test the quality of the aggregated systems the 6 weeks have been simulated, first by using the physical system (i.e. with a full description of the grid) and then by using the various aggregated models of the grid. During these simulations measured time series for supply temperature from the main VEKS heat exchanger (*see Appendix B*) and measured time series for the load at the individual consumers are used.

Due to lack of data on secondary temperatures at the consumers, and due to the fact that some consumers have separate heat exchangers for heating and for hot tap water, it has not been possible to model the consumers by using a heat exchanger model. Therefore the cooling dT at the consumers is calculated using the following model.

$$dT = dT^0 + \left(T_S - T_S^0\right) - \left(\left[\frac{T_S}{T_S^0}\right]^a - 1\right) \cdot b$$

where dT : Cooling (primary side)

T_S : Primary supply temperature

^{0} : Standard situation

a : Constant

b : Constant

The value of a depends of the situation:

$$If\ T_S > T_S^0 : a = -1$$

$$If\ T_S \leq T_S^0 : a = -3$$

A value of 5 is used for b.

Measured time series are used as standard situation when simulating the physical system. When the system is aggregated, information is recorded on how the physical loads are split between the aggregated loads. This information is then used to calculate a standard situation for each of the aggregated loads.

The quality of an aggregated system is estimated by calculating the standard deviation of the difference between the simulation result for the aggregated system and for the physical system. Three time series are considered:

- Power delivered from the central DH heat exchanger.
- Secondary return temperature at the central DH heat exchanger.
- Necessary differential pressure at the central DH heat exchanger to ensure a certain minimum differential pressure at all consumers.

2.2.1 Power and return temperature

An example of the simulations is given in Figure 2.4 that shows the heat power supplied by the central DH heat exchanger in R01 Madumvej in week 2 for the physical system and for an aggregated system with only 1 branch left. Figure 2.5 shows the difference between these two time series. In Figure 2.6 and Figure 2.7 the same situation is shown, but now with focus on the return temperature to the central heat exchanger.

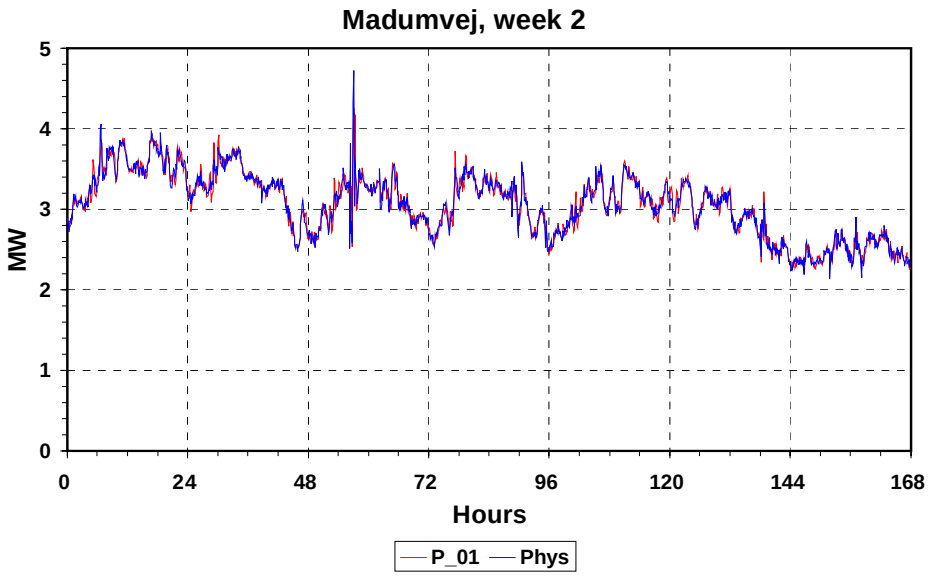

Figure 2.4. R01 Madumvej week 2. Heat power from the central heat exchanger for the physical system and for an aggregated system with 1 branch.

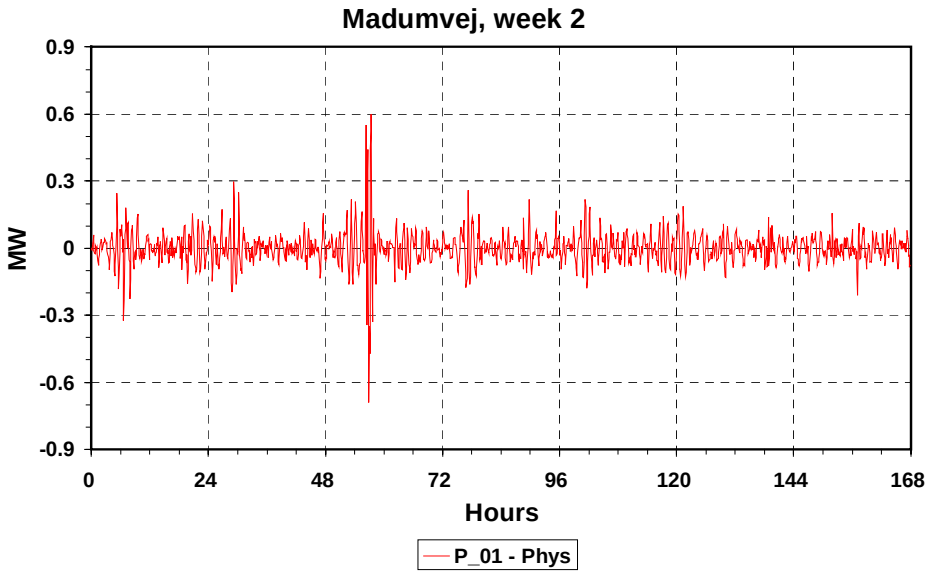

Figure 2.5. R01 Madumvej week 2. Error in heat power from the central heat exchanger for an aggregated system with 1 branch.

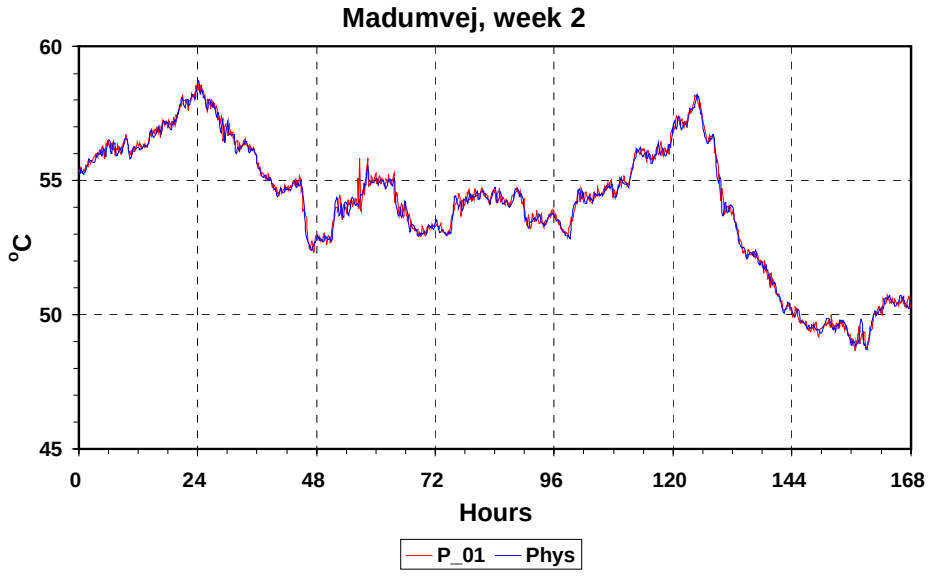

Figure 2.6. R01 Madumvej week 2. Return temperature at the central heat exchanger for the physical system and for an aggregated system with 1 branch.

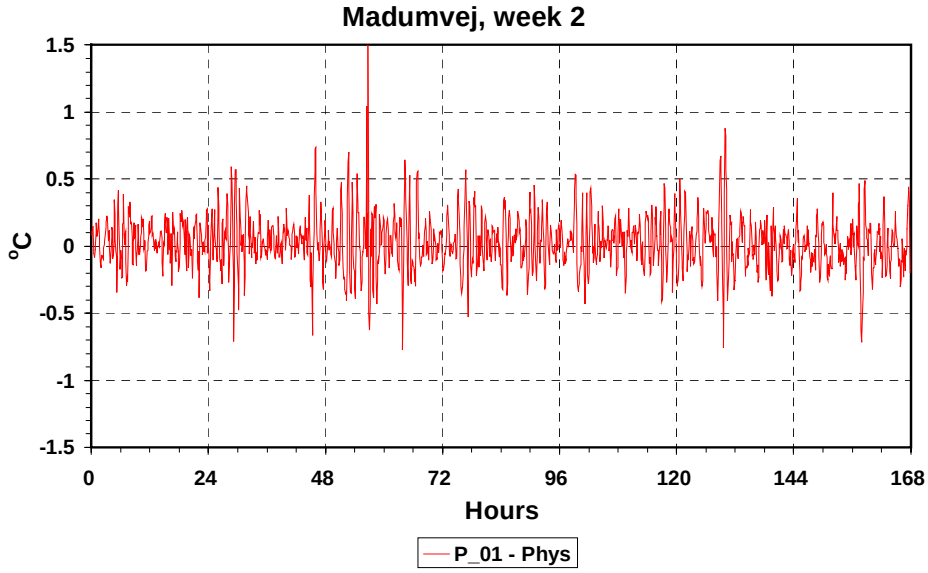

Figure 2.7. R01 Madumvej week 2. Error in return temperature at the central heat exchanger for an aggregated system with 1 branch.

The results of all simulations are given in a condensed form in Figure 2.8 and Figure 2.9 that show error in power at the central DH heat exchanger for R01 Madumvej and R02 Broparken, and in Figure 2.10 and Figure 2.11 showing error in return temperature at the central DH heat exchanger.

To estimate the importance of the values of (constant) flows used when aggregating the grids, the R01 Madumvej summer grid with 5 branches has been used for the winter situation, and vice versa. These situations are indicated with blue dots in Figure 2.8 and Figure 2.10.

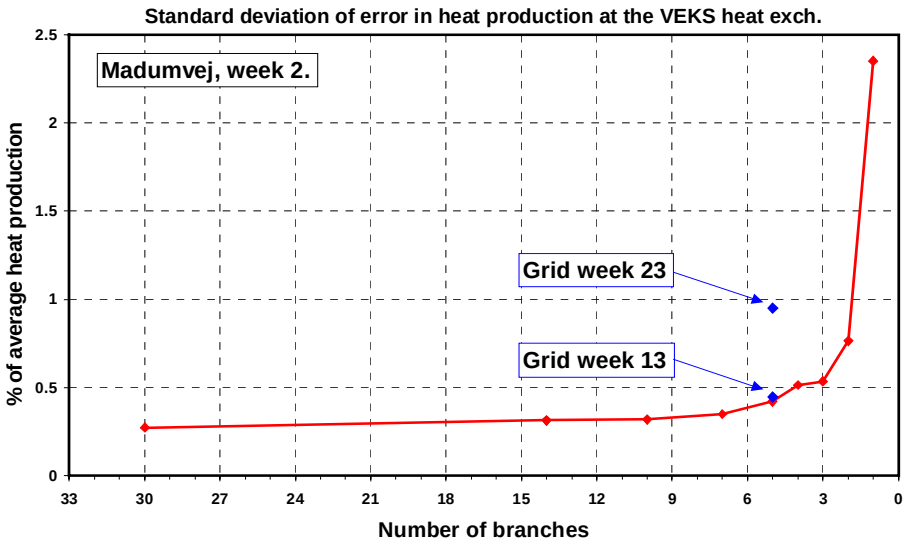

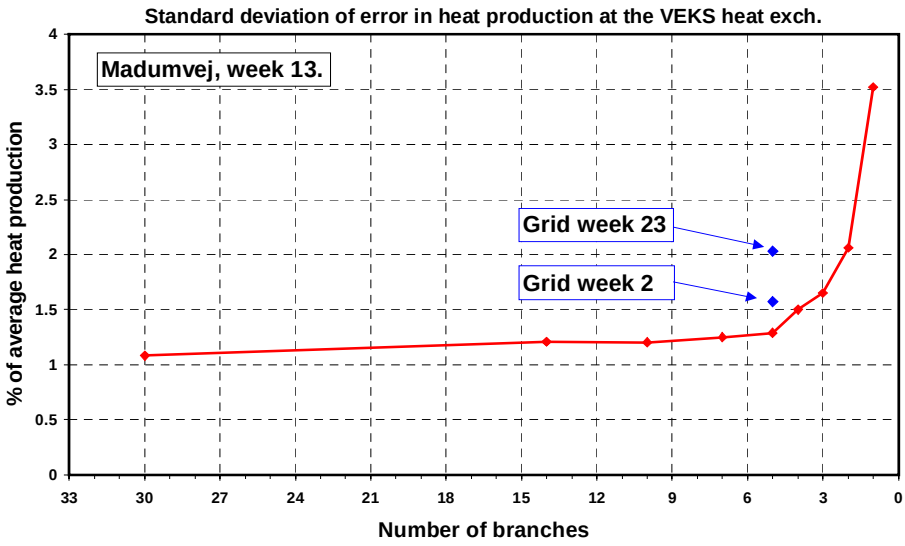

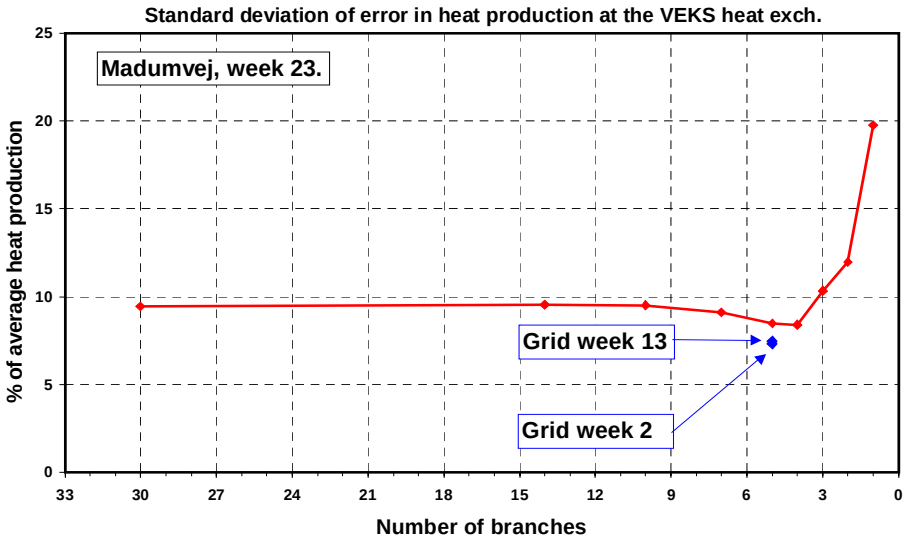

Figure 2.8. R01 Madumvej. Standard deviation of error in power at the central DH heat exchanger.

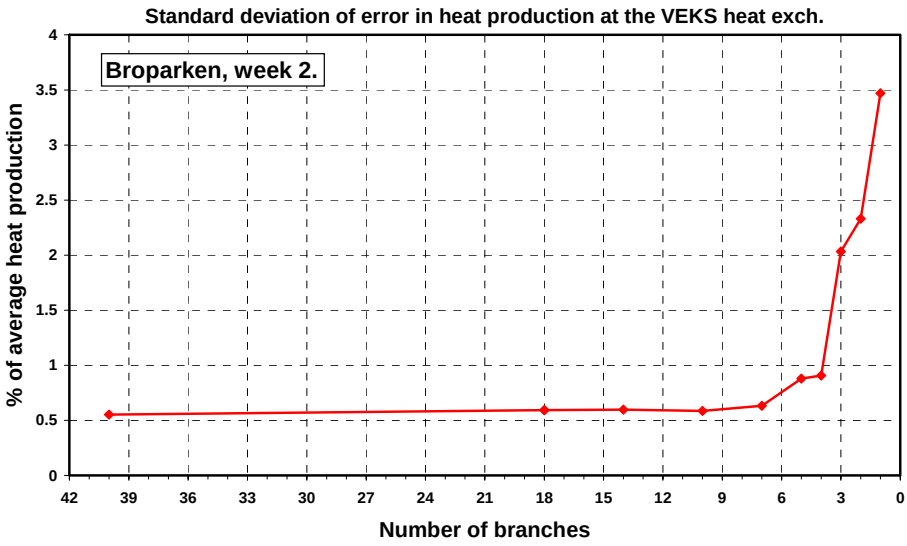

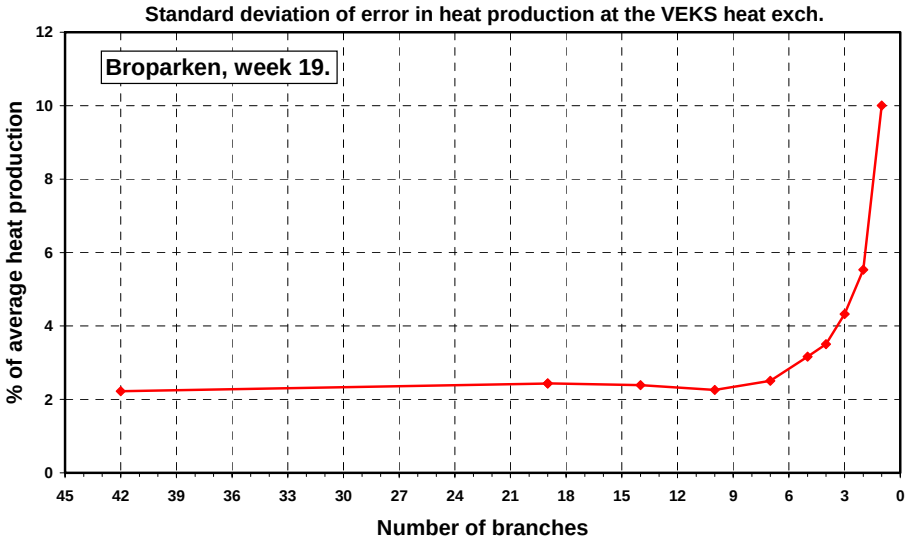

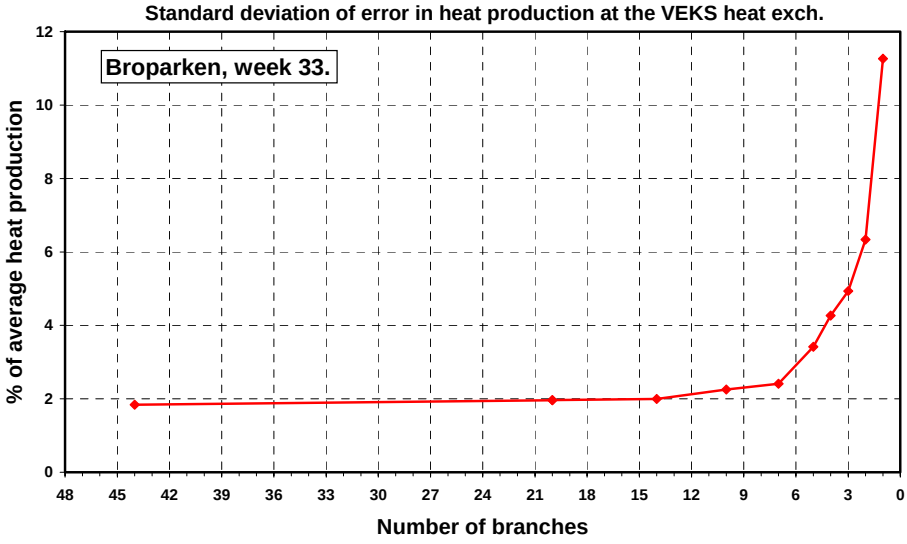

Figure 2.9. R02 Broparken. Standard deviation of error in power at the central DH heat exchanger.

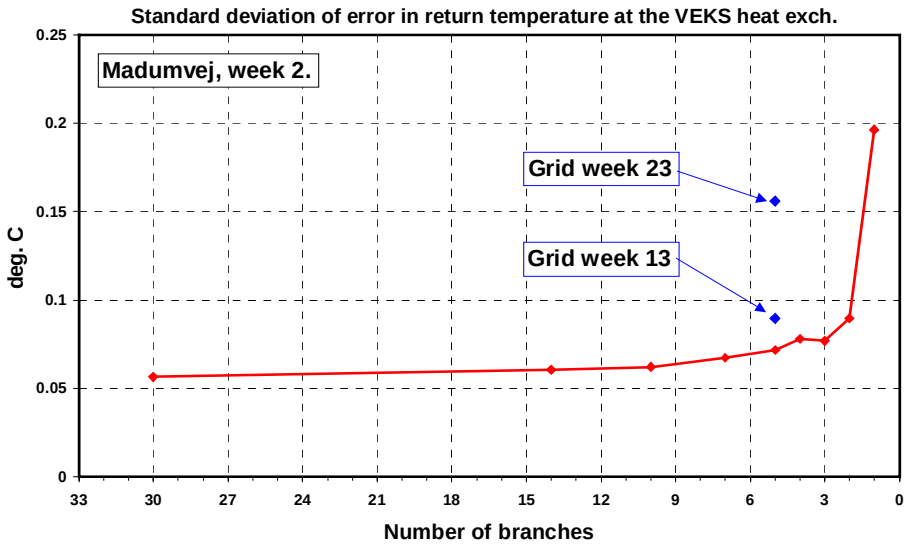

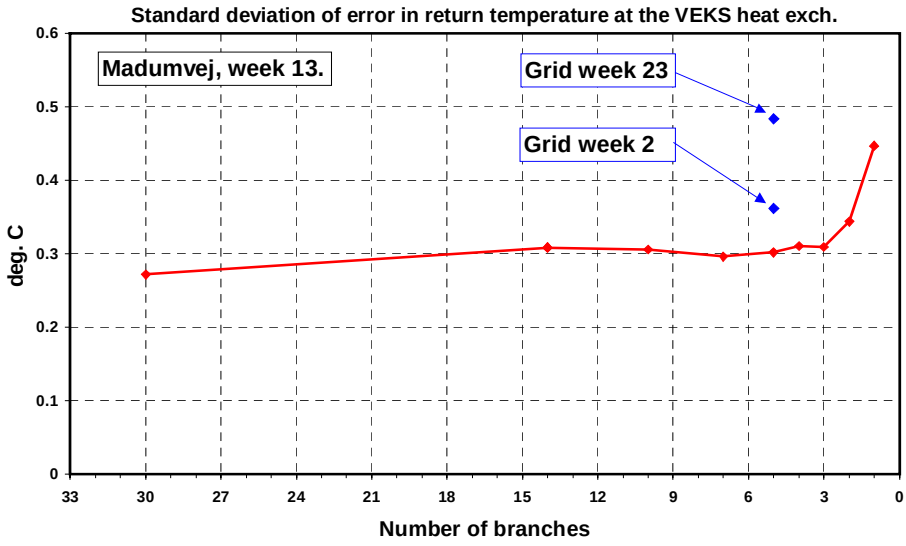

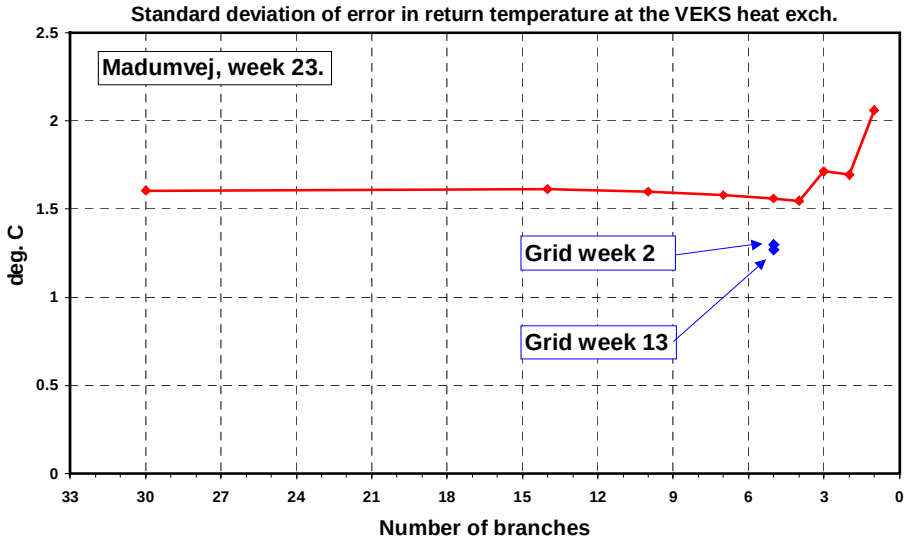

Figure 2.10. R01 Madumvej. Standard deviation of error in return temperature at the central DH heat exchanger.

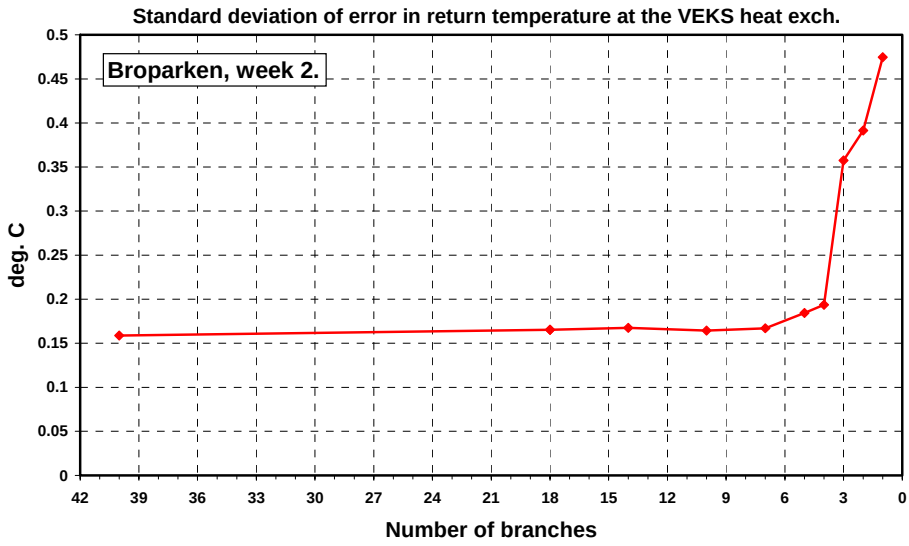

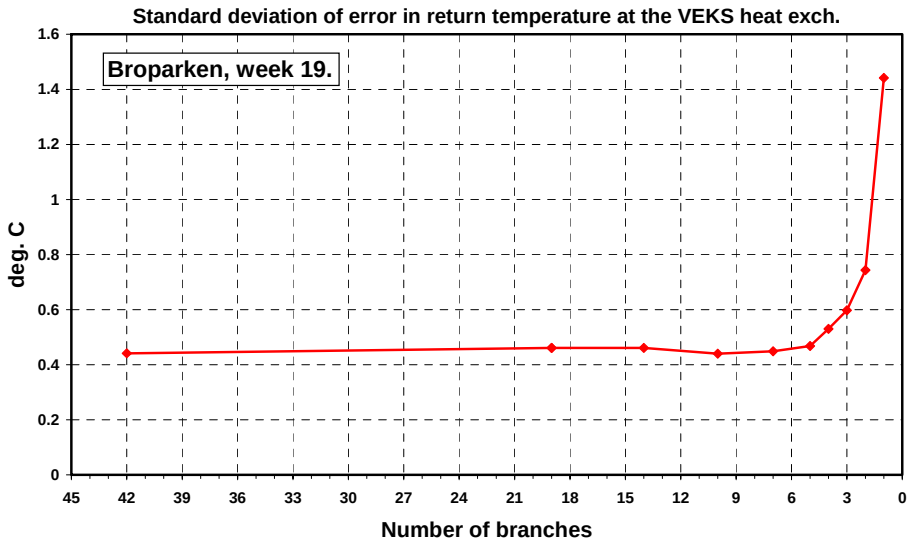

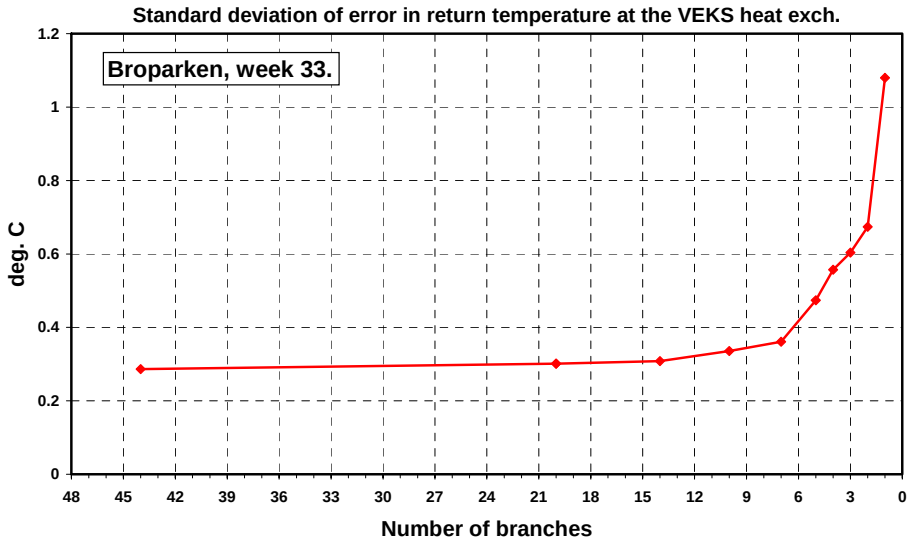

Figure 2.11. R02 Broparken. Standard deviation of error in return temperature at the central DH heat exchanger.

It is seen that the number of branches can be reduced to 3 for R01 Madumvej and to 5 for R02 Broparken without increasing the error very much.

In the two figures for R01 Madumvej week 23 it is seen that even the aggregated system with 30 branches causes considerable errors. This is due to the fact that some of the loads are extremely fluctuating. For these loads the flow seems to be regulated on/off instead of being reduced to some small value. Therefore it could not be expected that any model would be able to predict exactly when such abrupt changes will return to the VEKS heat exchanger. In Figure 2.12 the average error instead of standard deviation of error is shown for R01 Madumvej week 23. It is seen that the average error in heat production is less than 0.3 % of average heat production as long as the number of branches is not reduced below 3. The average error in return temperature is approx. 0.1 °C when the number of branches is greater than one.

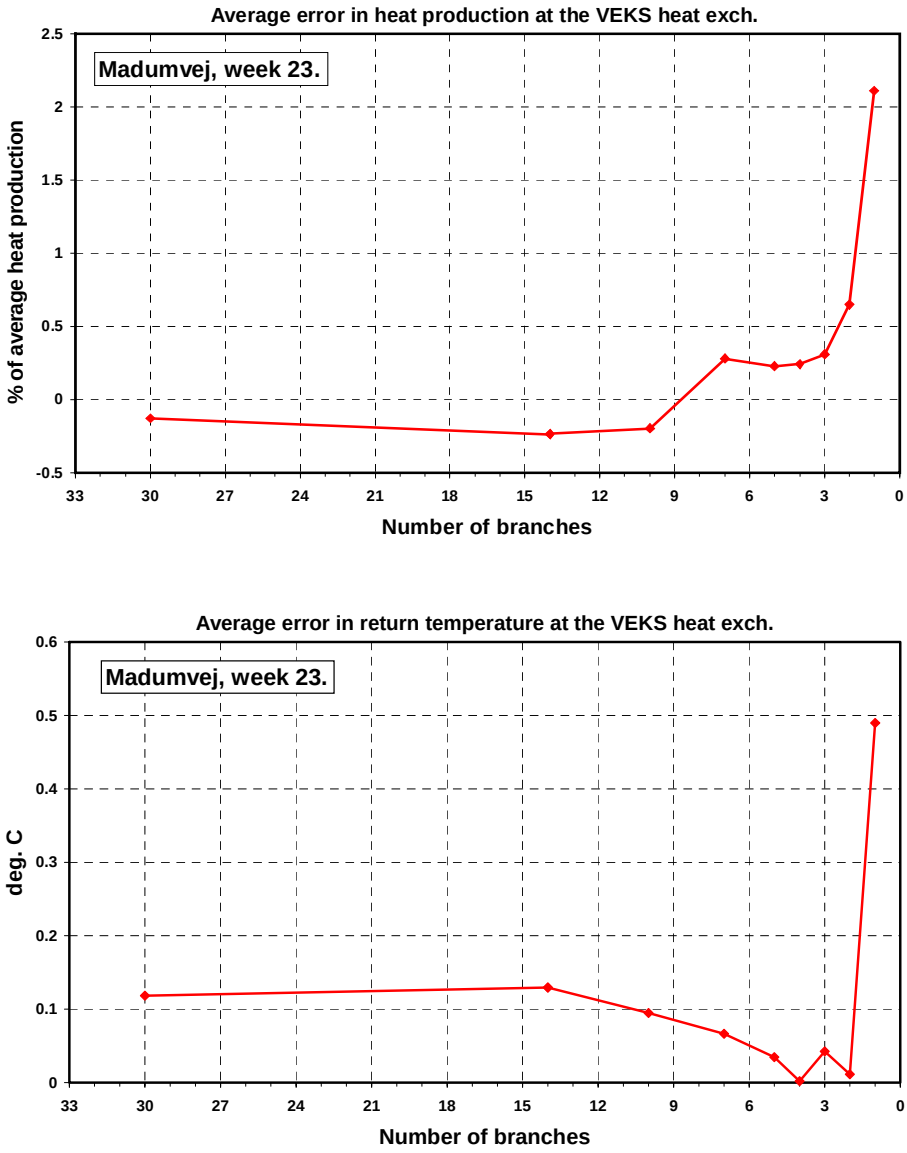

Figure 2.12. R01 Madumvej. Average error in power and return temperature at the central DH heat exchanger.

For R01 Madumvej each of the three grids (winter, spring and summer grid) with 5 branches has been tested for the other two seasons. For instance the winter grid has been tested for the spring and summer situations (loads etc.). The results of these 'cross-over' tests are shown as blue dots in Figure 2.8 and Figure 2.10. For R02 Broparken it has not been possible to make this sort of test because data on load L2-23 is missing in week 2 and data on load L2-01 is missing in week 19. It is seen that replacing a 'correct' aggregated grid by a 'cross-over' grid will increase the error by only approx. ½ % of average heat production and less than 0.2 °C. For R01 Madumvej week 23 the situation is slightly improved when a 'cross-over' grid is used. This can again be explained by the very fluctuating nature of the load in R01 Madumvej week 23 that causes some rather unpredictable simulation errors.

To test the importance of the many fluctuations in power demand in R01 Madumvej week 23, the measured time series for each consumer (heat load and primary supply and return temperatures) and for the supply temperature from the central VEKS heat exchanger have been smoothed by calculating a moving average. In mathematically terms this is done by folding each time series by the weight function shown in Figure 2.13. The sum of the weight function is one. Each column in Figure 2.13 corresponds to a time step of 6 minutes.

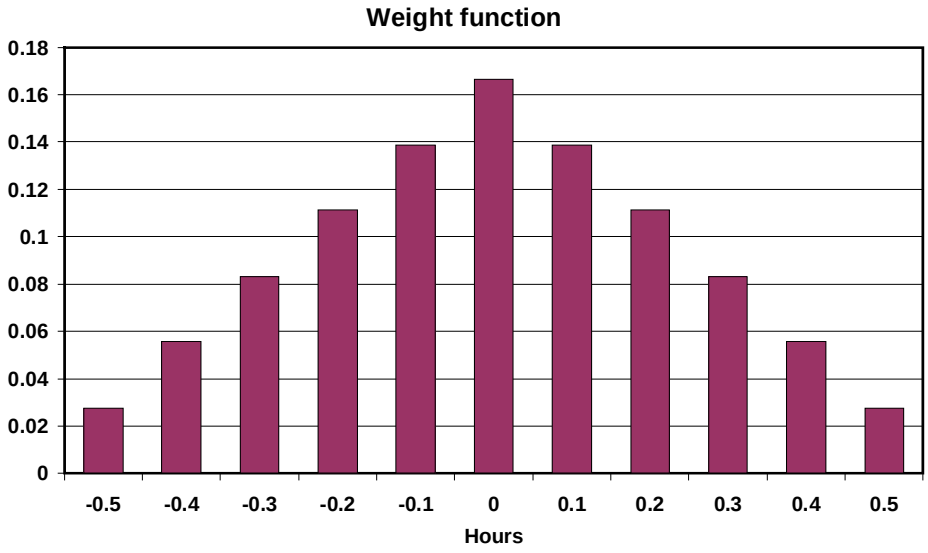

Figure 2.13. Weight function used in smoothing time series.

Figure 2.14 gives an example of smoothing. The measured values for the heat load at user L1-04 (indicated by "Normal") is shown together with the smoothed time series. It is seen that most of the fluctuations have been removed.

The result of aggregating R01 Madumvej in week 23 when using the smoothed time functions is shown in Figure 2.15. The figure shows that the error in heat production is almost halved by the smoothing whereas only a minor reduction of the error in return temperature is obtained.

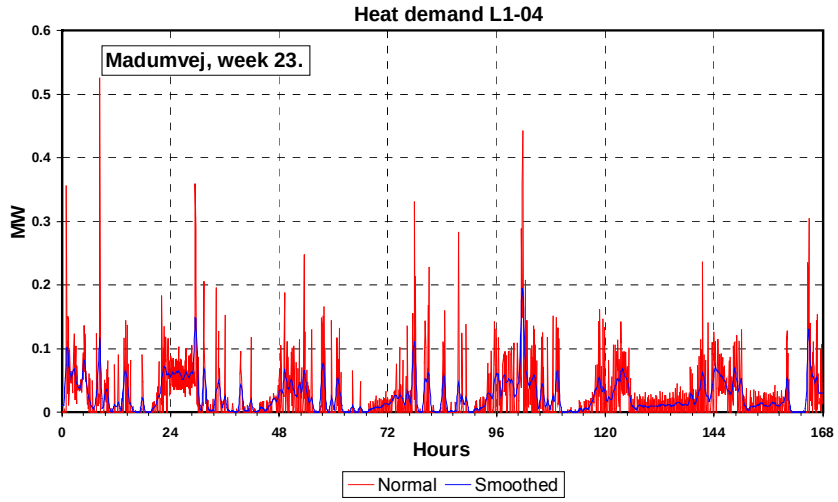

Figure 2.14. Heat demand in L1-04. Measured and smoothed time series.

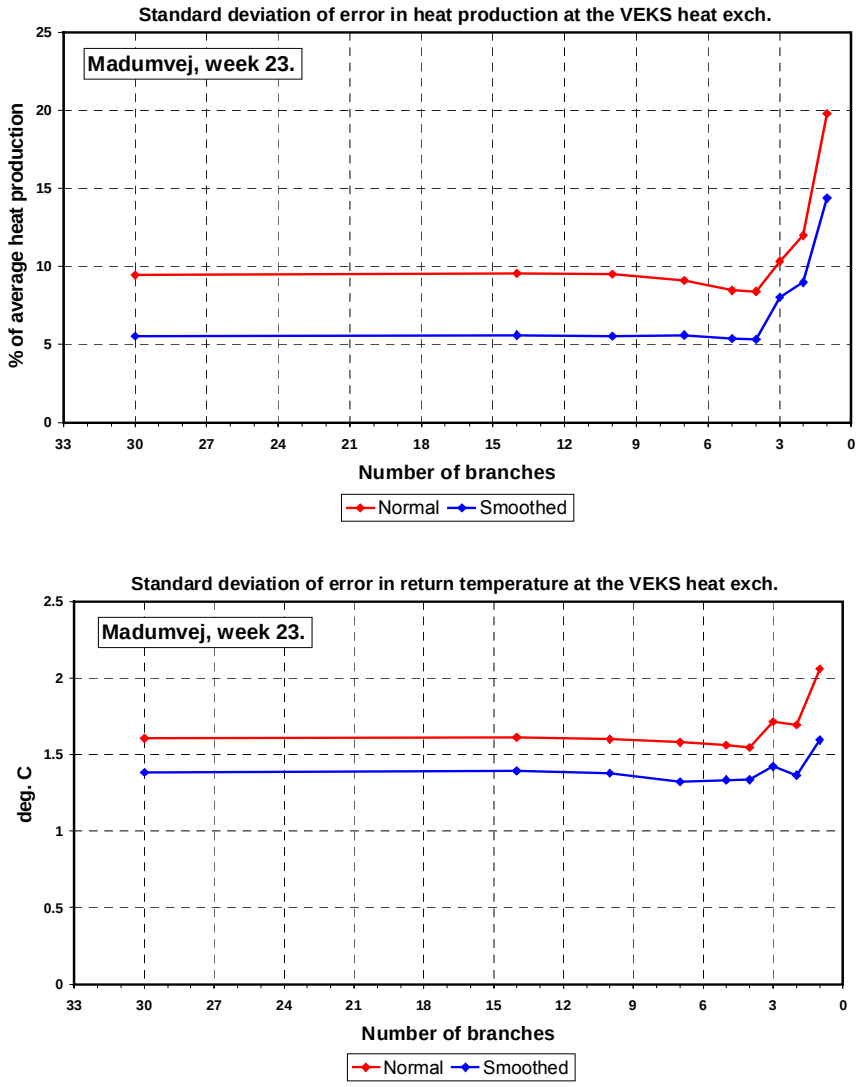

Figure 2.15. Standard deviation of error when using smoothed time series. R01 Madumvej week 23.

2.2.2 Differential pressure

Condensed results of the simulations are given in Figure 2.16 and Figure 2.17 showing standard deviation of error in differential pressure at the central DH heat exchanger.

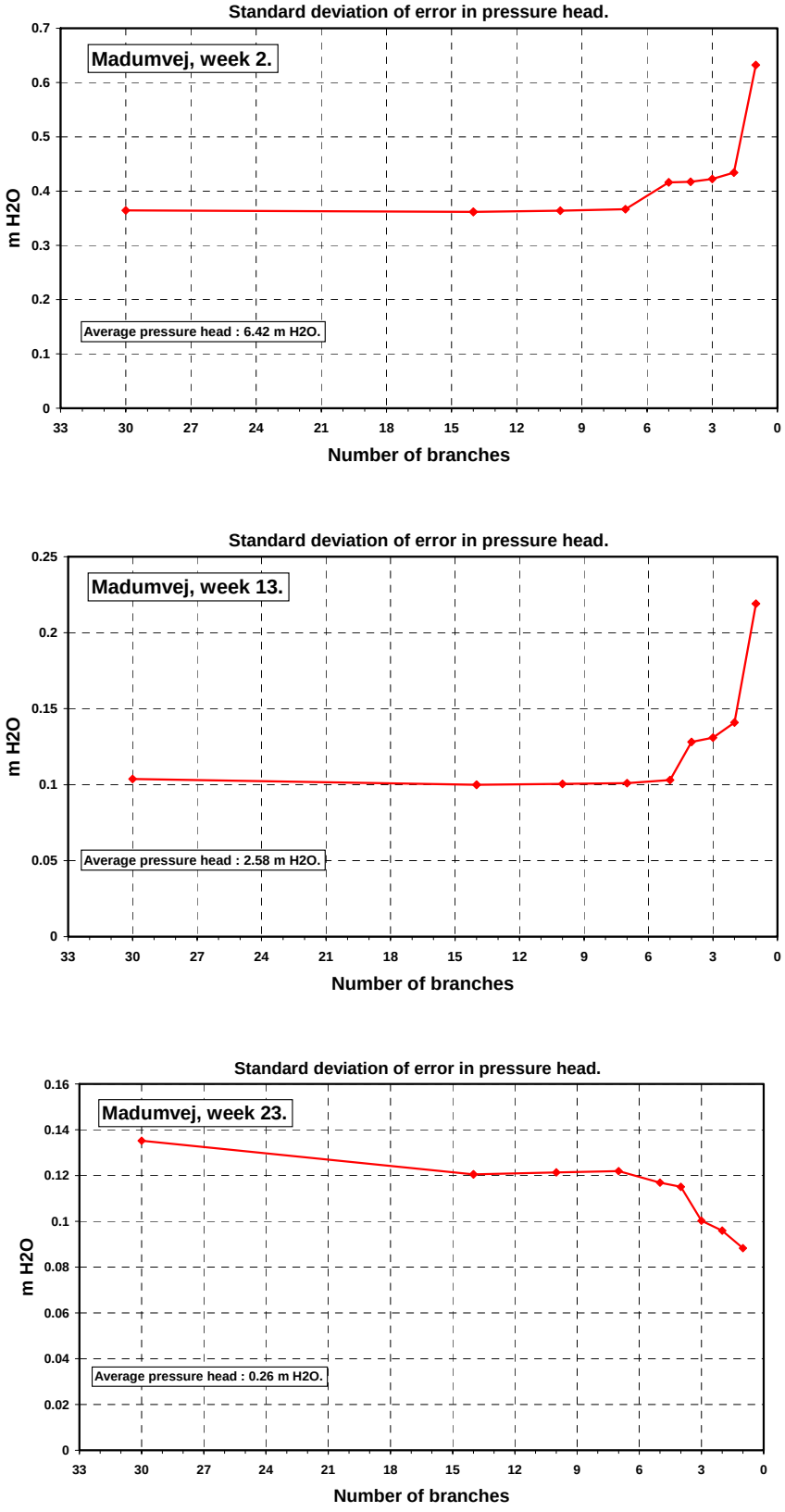

Figure 2.16. R01 Madumvej. Standard deviation of error in differential pressure at the central DH heat exchanger.

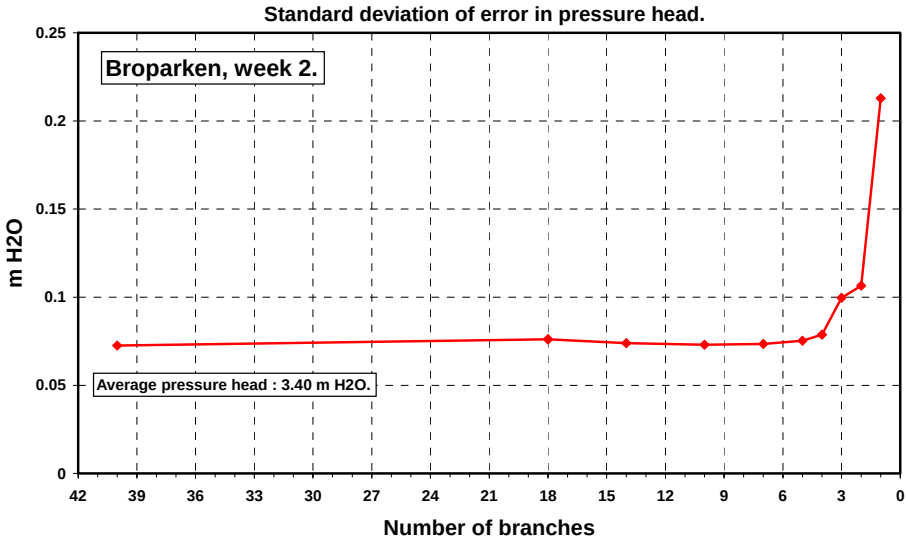

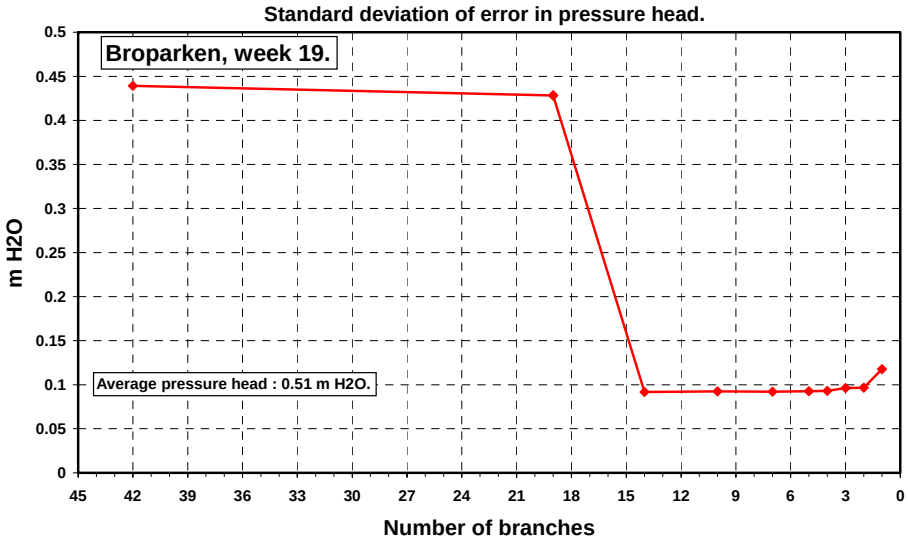

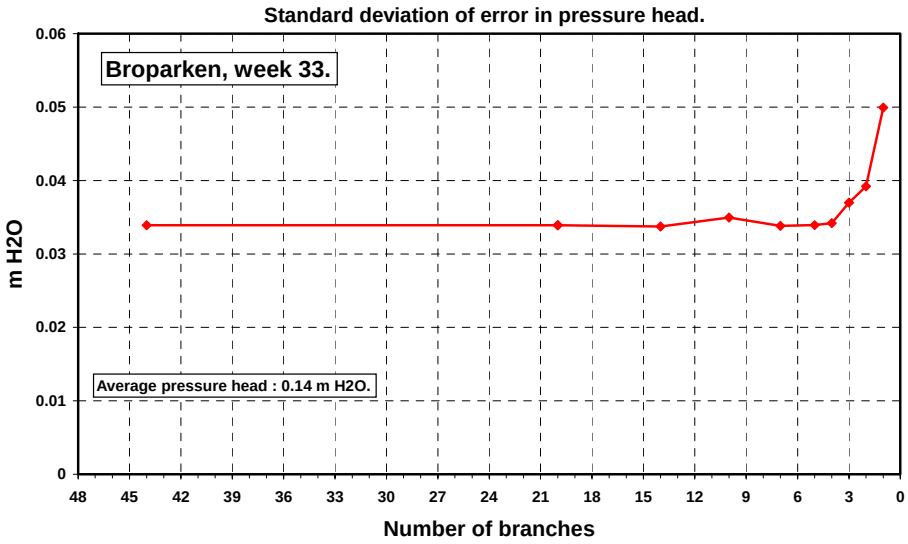

Figure 2.17. R02 Broparken. Standard deviation of error in differential pressure at the central DH heat exchanger.

For some of the situations in Figure 2.16 and Figure 2.17 the result seems rather good, e.g. R01 Madumvej weeks 2 and 19 and R02 Broparken week 2. The results for the other three weeks are not that good (standard deviation above 20 %). The reason for this poor result, which is mainly seen in the summer weeks, is that loads and hence flows for many consumers during the summer are regulated in an almost on-off way. This causes very fast flow variations as seen in Figure 2.18 that shows simulated flow from the central heat exchanger and differential pressure loss from the heat exchanger and out to the critical consumer. The figure applies to the physical model of R01 Madumvej week 23, i.e. the full model with no reduction in the number of branches and with the tree structure still present.

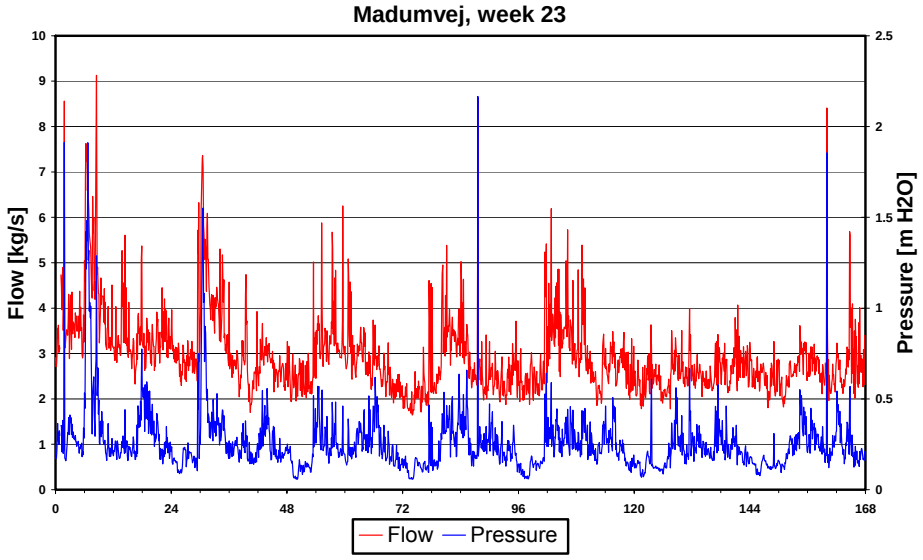

Figure 2.18. Simulation results for the physical system. Flow and differential pressure.

Many spikes in the curves in Figure 2.18 have duration of only one time step. Hence it is clear that even a very small simulation error with regard to time delay will result in considerable errors expressed by standard deviation. If instead the error is expressed by average difference as shown in Figure 2.19, then it is seen that the error is acceptable.

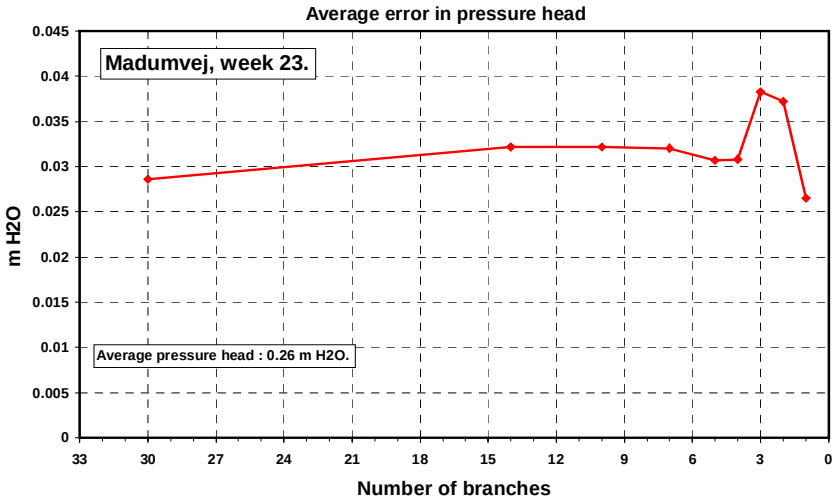

Figure 2.19. R01 Madumvej week 23. Average error in differential pressure at the central DH heat exchanger.

Until now all aggregations have been carried out on the full DH grid (R01 Madumvej or R02 Broparken). To maintain some of the geographical information in the physical grid it can alternatively be split up in some sub-areas before aggregation. The aggregated sub-grids are then joined together to make a full aggregated grid. Figure 2.20 shows how R01 Madumvej is split into 5 sub-areas.

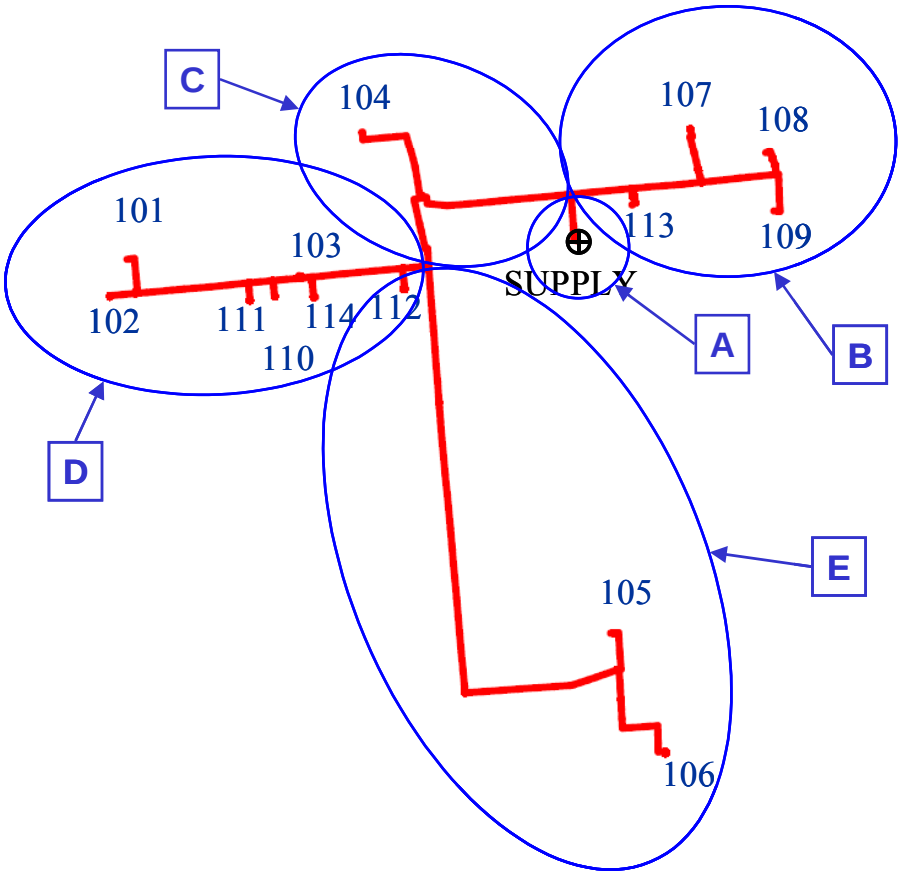

Figure 2.20. R01 Madumvej split into 5 sub-areas.

Three aggregated sub-grids have been made for each of the five sub-areas:

- The tree-structure is changed to a line structure.
- Branches with no load in-between are replaced by one branch.
- The number of branches is reduced to one (except for the sub-area C).

The blue curves in Figure 2.21 and Figure 2.22 show simulation results for aggregated grids found by splitting R01 Madumvej in 5 sub-areas. The red curves correspond to the situation where no sub-areas are defined. As could be expected the error for the same number of branches is reduced when some of the geographical information is maintained.

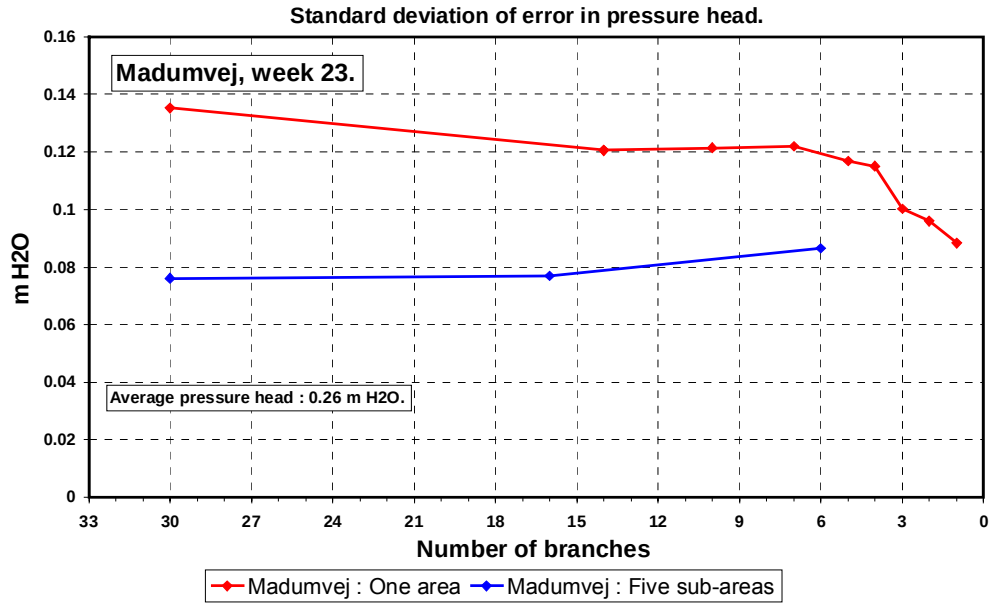

Figure 2.21. R01 Madumvej week 23. The area is split into 5 sub-areas before aggregation. Standard deviation of error in differential pressure at the central DH heat exchanger.

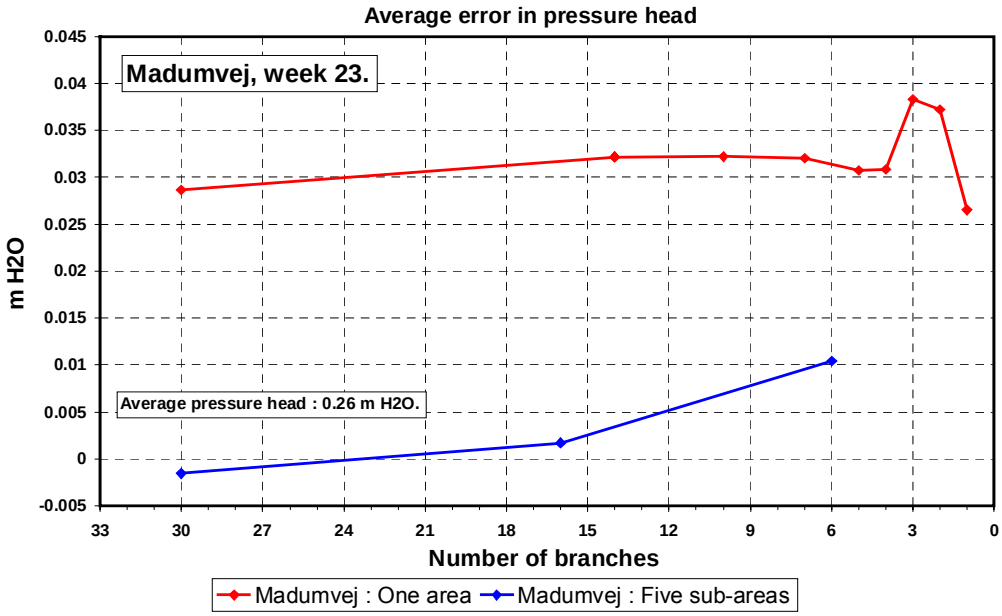

Figure 2.22. R01 Madumvej week 23. The area is split into 5 sub-areas before aggregation. Average error in differential pressure at the central DH heat exchanger.

2.3 Aggregation of the Ishoej DH system

The Ishoej DH system is described in Section 1.2. The physical grid consists of 44 branches and 23 loads, cf. Appendix C.

Measured time series covering the period from December 19, 2000 12:00 until December 24, 2000 24:00 with time steps of 5 minutes are used in the simulations. These time series are shown in Appendix D. Average loads for the period are shown in Table 1.3.

Time series for heat load as well as for secondary forward and return temperatures have been used for each substation. All substations were modelled as one plate heat exchanger, and kA values were estimated from measured heat load and measured primary and secondary supply and return temperatures.

For aggregated systems, where substations have been combined, heat loads are modelled by using weighted sums of measured time series (heat load and secondary forward and return temperatures).

For the Ishoej system, network aggregation has only been carried out with regard to power and temperatures and not with regard to differential pressure. Aggregated grids with 44, 23, 20, 15, 10, 5, 4, 3, 2, and 1 branch have been modelled. A detailed description of the aggregation can be found in Bøhm et al. (2002) and Larsen et al. (2004).

The definition of aggregated systems identified by D_nn can be found in Appendix C.

Regarding supply temperature from the plant two situations are considered:

- The supply temperature is as measured (i.e. varying around 105 ^{o}C). See Appendix D.
- The supply temperature is 100 ^{o}C for a period and then suddenly increased to 110 ^{o}C.

In Bøhm et al. (2002) and Larsen et al. (2004) the aggregation method considered here has been compared to a German method, cf. Loewen (2001) and Loewen et al. (2001). In the comparison of aggregation methods Ishoej DH system is used as example.

2.3.1 Aggregation results

Figure 2.23 shows the amount of heat supplied by the DH plant for the physical system and for an aggregated system with 5 branches. In Figure 2.24 the difference between the two time series in Figure 2.23 is shown.

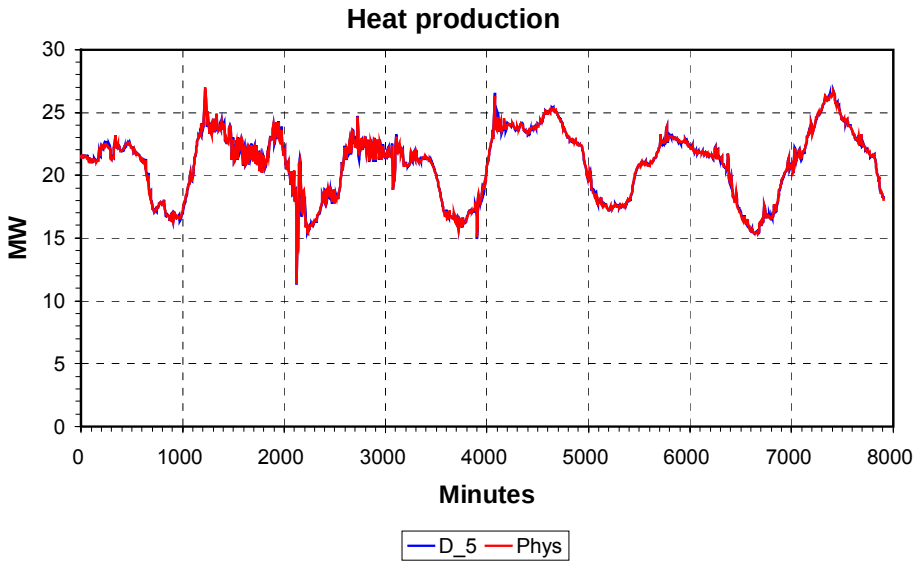

Figure 2.23. Heat production supplied by the plant for the physical system and for an aggregated system with 5 branches. The measured time series is used as supply temperature from the plant.

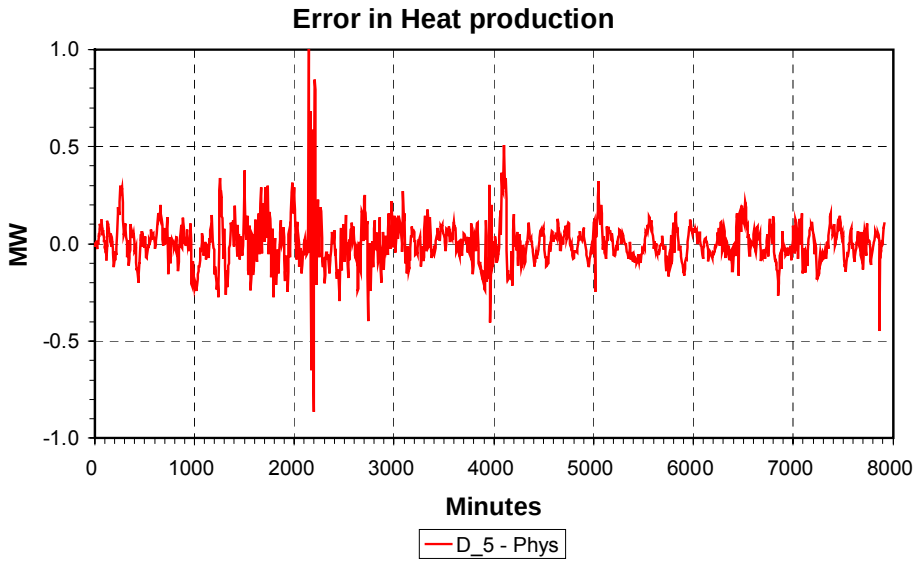

Figure 2.24. Error in heat production for an aggregated system with 5 branches as compared to the physical system. The measured time series is used as supply temperature from the plant.

To assess the quality of a specific aggregated model, time series for the amount of heat supplied by the plant are found by simulating the aggregated system as well as the physical system. The standard deviation of the error between these two time series is then used as a criterion for the quality of the aggregation.

Another criterion is also introduced. It is based on the standard deviation of the error between the return temperature to the plant calculated for the physical system and for the aggregated system.

The following figures show how the standard deviation of error increases as the number of branches is reduced.

For the physical system all loads and secondary forward and return temperatures are represented by measured time series. For aggregated systems, however, time series for loads and secondary temperatures are calculated as weighted averages of measured series.

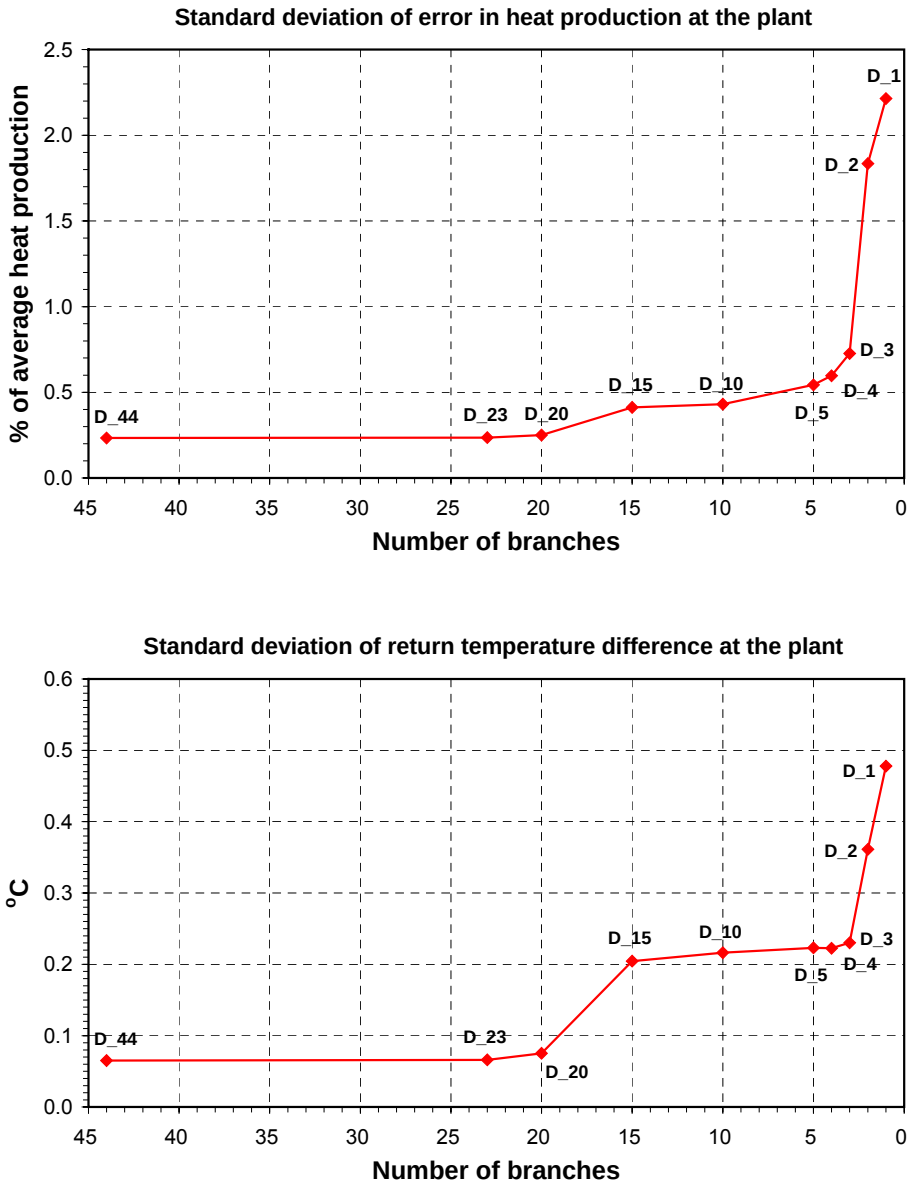

Figure 2.25. Standard deviation of error. The measured time series is used as supply temperature from the plant.

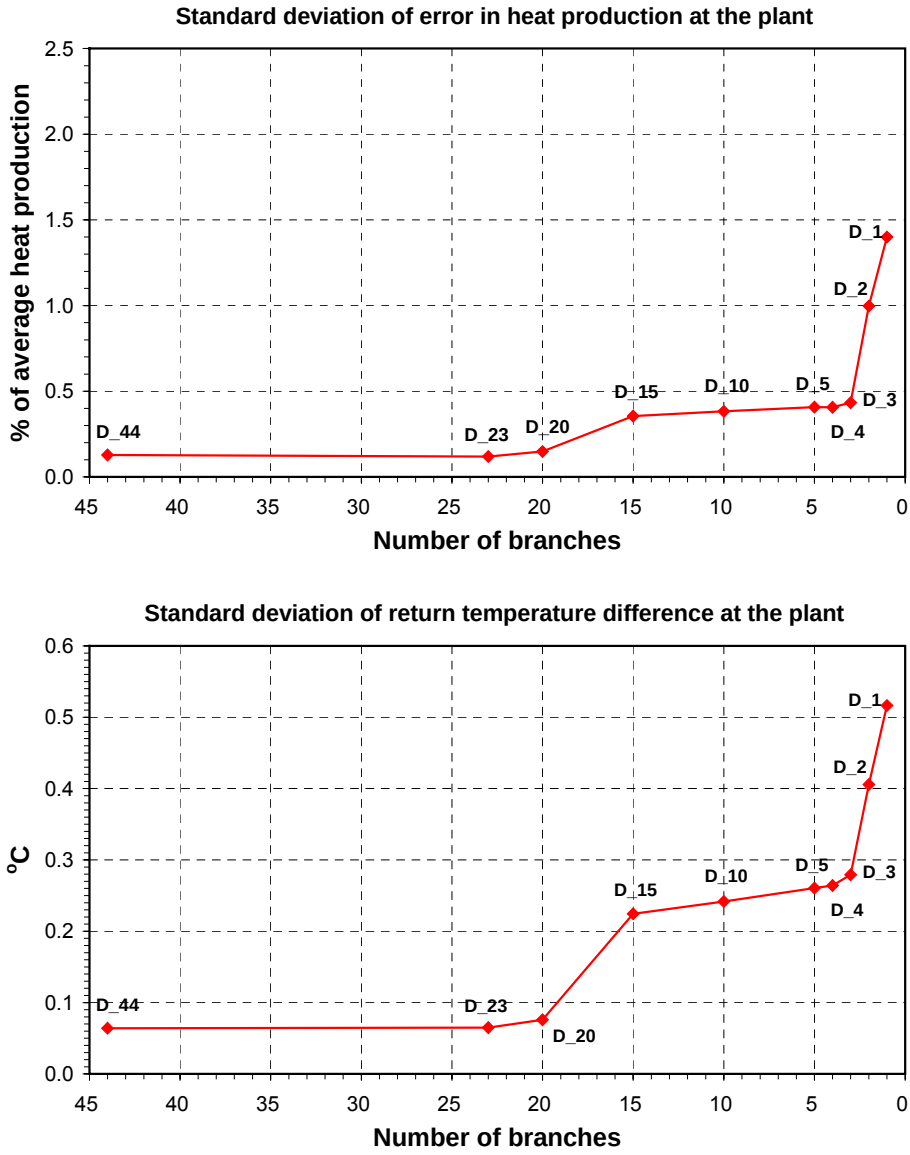

Figure 2.26. Standard deviation of error. A step function is used as supply temperature from the plant.

It is seen that the number of branches can be reduced from 44 to 3 without significantly increasing the error. Model D_1 with only one branch and two loads has a standard deviation of the error (defined on basis of heat production at the plant) of approximately 2 %, but the average error over the simulated time period is as small as 0.01 %.

2.4 Aggregation summary

The goal of the present work has been to further verify aggregated power and temperature models of DH systems with the purpose of making simulations and optimisations of DH systems based on mathematical-physical models of the components. Moreover, a new method for aggregating DH systems when focussing on differential pressure is developed and tested.

Aggregation of three Danish DH systems R01 Madumvej and R02 Broparken in Roedovre, and Ishoej is described. Simulations for selected weeks with time steps 5 or 6 minutes have been carried out to assess the quality of the aggregated models.

For the power and temperature models, errors caused by aggregation are evaluated by the heat production and the return temperature at the DH plant delivering heat to the grid. Likewise, for the pressure model the error is evaluated by looking at the differential pressure as seen from the DH plant.

In Section 2.2 the aggregation of R01 Madumvej and R02 Broparken is described. A winter, spring and summer week have been selected. For each of these weeks aggregation has been carried out ending up with a series of aggregated systems with a number of branches as small as just one.

The work on the Ishoej DH system is described in Section 2.3. Here 5 minutes values from December 19-24, 2000 are used. Because data was not available for all substations, a realistic data set had to be created from those heat exchanger stations where data existed. Thus for the 23 substations in Ishoej, heat loads and primary and secondary supply and return temperatures were available every 5 minutes.

The accuracy of the aggregation models has been documented as the errors in heat production, return temperature, and differential pressure at the DH plant between the physical network and the aggregated model.

Furthermore, in Bøhm et al. (2002) and Larsen et al. (2004) a comparison has been made between the aggregation method described here and a German method. Both aggregation methods work well.

Regarding power and temperature models it is concluded that the number of branches can be reduced to 3 for R01 Madumvej and to 5 for R02 Broparken without increasing the error very much. For the Ishoej system the number of branches should not be reduced below 3. Even aggregated systems with only one branch still hold some of the information on the full physical system as can be seen in e.g. Figure 2.4 and Figure 2.6. Depending on to what purpose the model is to be used, even a one branch grid could be useful.

When turning to aggregated models for calculation of differential pressure, the situation does not seem that clear. For the winter week the aggregation method functions well, but in spring and summer when the heat load is much smaller, then a considerable error might arise. This is mainly due to the on/off operation of several heat loads that results in large pressure ‘spikes’ with a duration of perhaps only one time step (6 minutes).

By using the three aggregated grids (winter, spring and summer grid) for R01 Madumvej for the two other seasons, it has been tested whether the same aggregated model could be used for not only a shorter period but for a whole year (c.f. Figure 2.8 and Figure 2.10). It is seen that replacing a ‘correct’ aggregated grid by a ‘cross-over’ grid could increase the error by only approx. ½ % of average heat production and less than 0.2 °C. When using the aggregated winter or spring grids for the summer week the situation is slightly improved compared to using the summer grid. This is however only an accidental result caused by the very fluctuating nature of the load in R01 Madumvej week 23.

Finally, work is required to further automate the aggregation process, which today still requires decisions taken by an experienced researcher. Here the goal will be to make the process fully automatic or at least so simple that the operator can update the aggregated network when it is required, for instance due to a changed load distribution or to an expansion of the DH network.

Chapter 3 Modelling the DH house stations (consumer installations) and the substations

Many different kind of models can be made for the heat consumption and the return temperature from the heat exchangers in the buildings or the heat exchangers in the substations in the transmission system. For example Benonysson (1991) constructed models that were based on physical relationships and with parameters estimated from time series of measurements. The models included for instance present and past values for the outdoor air temperature, solar radiation, wind speed, and sinusoidal terms for the daily and weekly variations.

In the present work we want to investigate the influence of the load profile on the operational costs of the DH system and thus a very exact modelling of the actual system is not required.

Larsson (1999, 2003) applied a simple model based on hourly values of heat demand and air temperature to model some Swedish systems. The models furthermore included a term that depended on the time of the day and the day in the week (working day/weekend). A similar approach will be taken here, but in the case of the Roedovre DH system 6-minutes data are available.

3.1 Single Buildings

3.1.1 Apartment building in Vanloese

We will first consider an apartment building in Vanloese, Copenhagen, Bøhm and Danig (2004). A diagram of the heating system is shown in Figure 3.1.

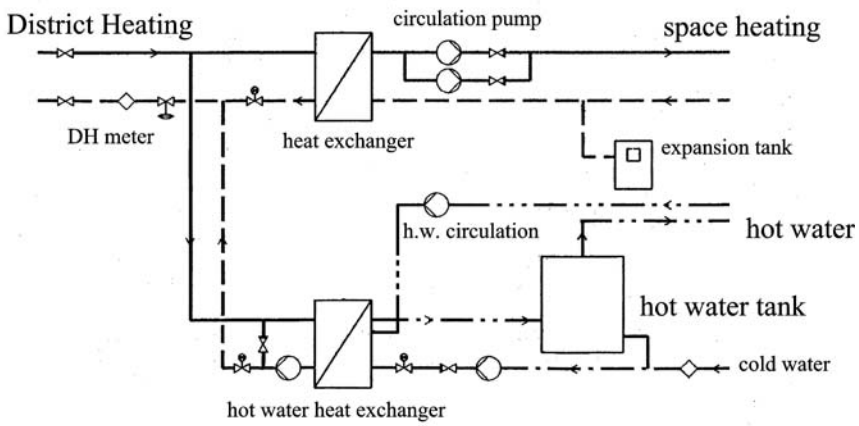

Figure 3.1. Diagram of heating system in apartment building in Vanloese, Bøhm and Danig (2004).

In Vanloese, 1-hour mean values are available for the period June 2001 – May 2002. Measurements were made on the radiator circuit separately, which mean that the load is not affected by the hot water consumption. The supply temperature is controlled according to the outdoor temperature as shown in Figure 3.2. When the outdoor temperature is higher than 18 °C in the summer, the pump stops. The caretaker can shift the set point curve upwards or downwards, if necessary. Thus, in this building, night set back is not applied.

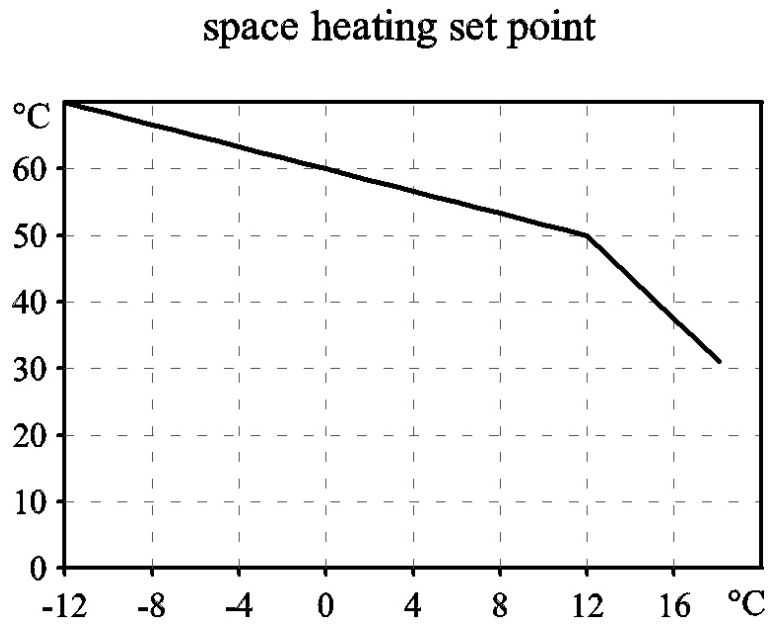

Figure 3.2. Set point as a function of outdoor temperature, Bøhm and Danig (2004).

The first heat load model to be applied assumes that the heat load depends on the number of degree-days and on the time of the day:

$q = A \cdot (tu - 17) + \text{clock function}$,

where tu is the outdoor temperature and the clock function is different for every day in the week, i.e. 168 parameters are to be determined. If the outdoor temperature is higher than 17 ˚C, A = 0. The clock function is found from linear (in the parameters) regression in Matlab by fitting the heat load model to the data. Matlab estimates the 169 parameters as shown in Figure 3.3, and the model is $q = -2.289 \cdot (tu - 17) + \text{clock function}$. In this case the clock function is small compared to the degree-day dependent part.

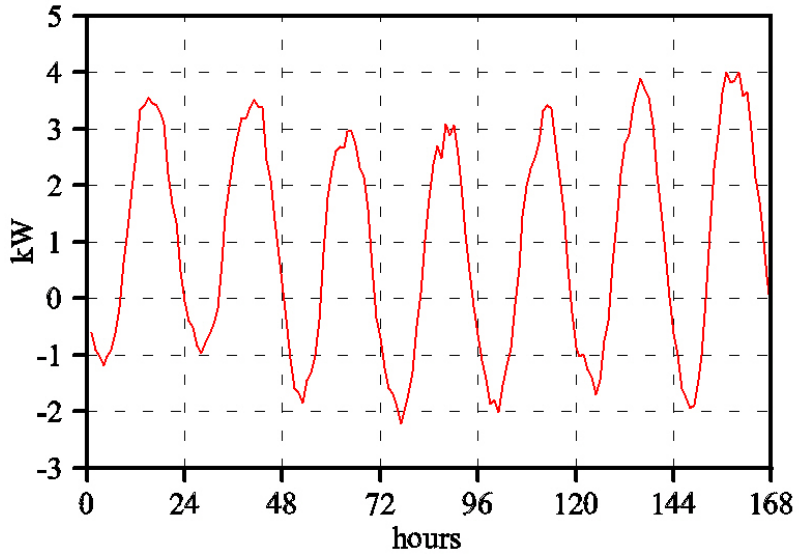

Figure 3.3. The 168 parameters describing the clock function (from Monday to Sunday) for the apartment building in Vanloese. Space heating load only. A = -2.289 kW/ºC.

Figure 3.4 shows the measured (blue) and simulated (green) heat loads as a function of outdoor temperature, while Figure 3.5 shows the heat loads as a function of time and the associated errors (red).

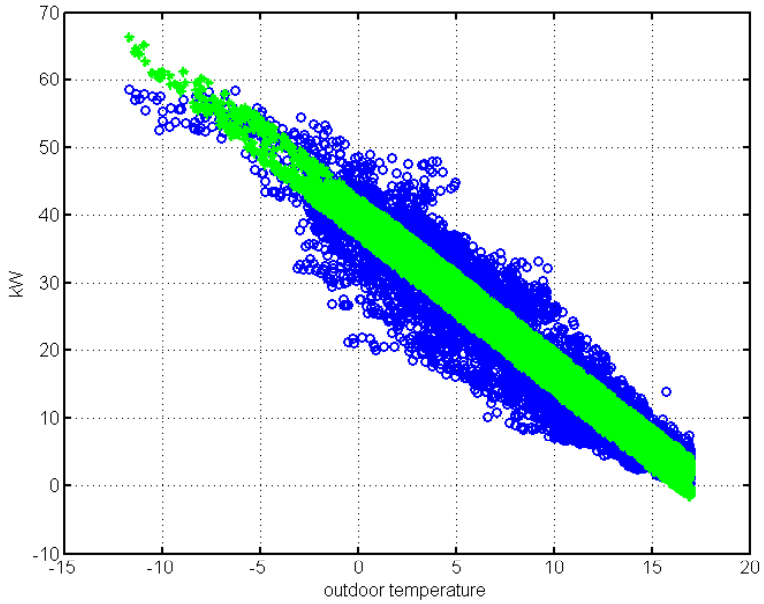

Figure 3.4. Measured (blue) and simulated (green) heat loads in kW, as a function of outdoor temperature.

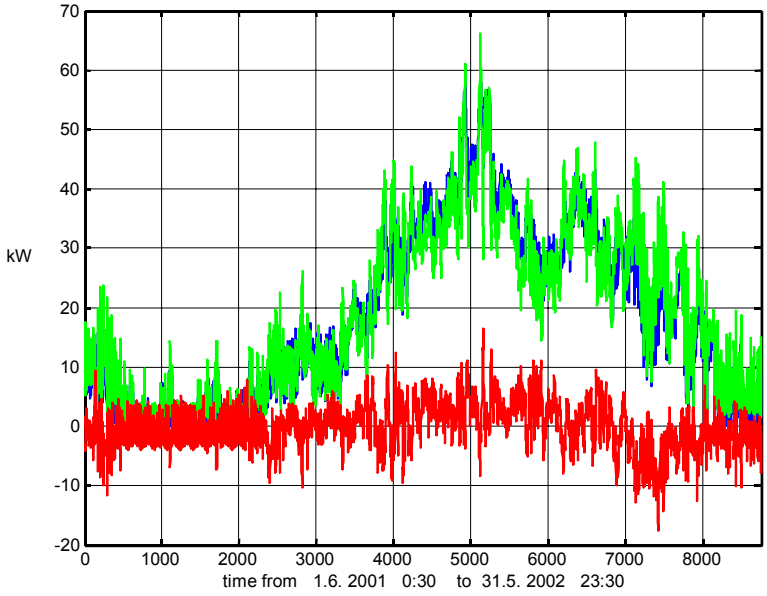

Figure 3.5. Measured (blue) and simulated (green) heat loads in apartment building, and the error (red). Space heating only.

In the apartment building the hot domestic water is produced by a so-called loading circuit, i.e. a plate heat exchanger connected to a hot water tank, cf. Figure 3.1. The advantage of this system design is fairly low heat loads on the heat exchanger. From the period October 1, 2001

to May 31, 2001, hourly data for the total district heating load is available and these data have been used to find the parameters in a model with 169 parameters.

Figure 3.6 shows the clock function. Compared with the pure space heating model, the daily variations now oscillate 10-15 kW, compared with 5 kW for the pure space heating model.

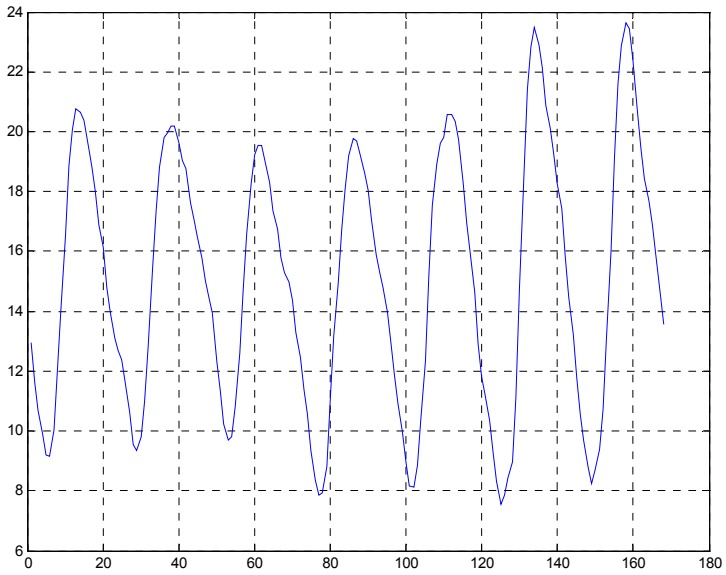

Figure 3.6. The 168 parameters describing the clock function (from Monday to Sunday, in kW) for the apartment building in Vanloese. Total district heating load. A = -2.603 kW/C.

Figure 3.7 shows the measured (blue) and simulated (green) heat loads as a function of outdoor temperature.

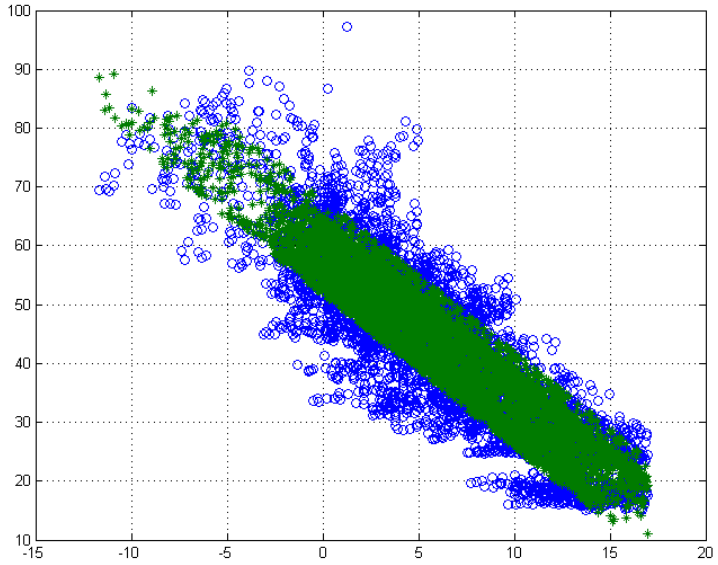

Figure 3.7. Measured (blue) and simulated (green) total heat loads in kW, as a function of outdoor temperature.

In summary, we found that for space heating only, the clock function covers a variation of ±3 kW or ±5 % of the design load (at –12 ˚C), while for the total heat load, the variation is ±8 kW or ±10 % of the design load. The biggest variations occur in the weekend.

Buildings in Roedovre

Next we will analyse some of the buildings in Roedovre in DH system R01 Madumvej.

3.1.2 Building L1-08, a public school

We will first consider building L1-08, which is a public school, supplied from the Madumvej heat exchanger station. Data for the winter period week 01 and 02 (December 30, 2002 – January 12, 2003) will first be used. We will examine different models for this particular consumer. The first heat load model to be applied is: $q = A \cdot (tu - 17)$ + clock function, where we will use one clock function for week days, and another for week ends, i.e. 10 parameters per hour, in all 480 parameters. The two clock functions are shown in Figure 3.8. It appears that the morning peaks in weekdays are not present during the weekends, where the school is not in use.

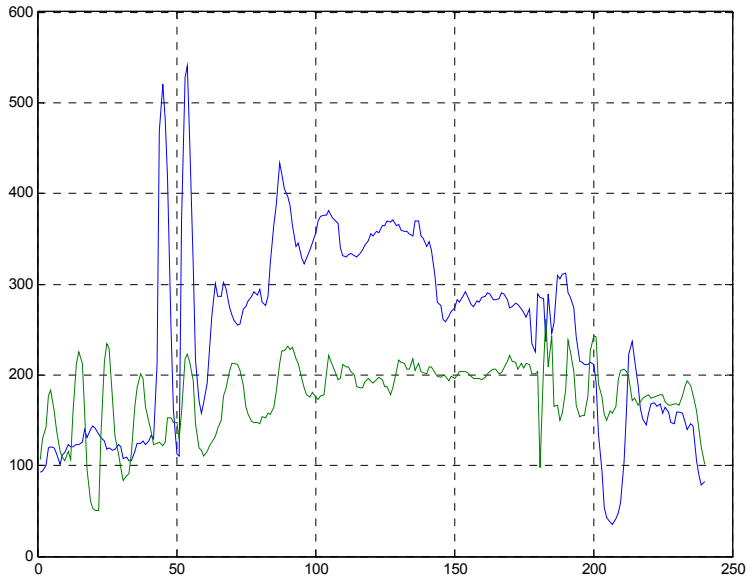

Figure 3.8. L1-08. Week 01 + 02. Clock function (in kW) with 480 parameters, weekdays (blue) and weekends (green). A = -7.4021 kW/˚C.

Figure 3.9 shows the heat load in kW as a function of the outdoor temperature.

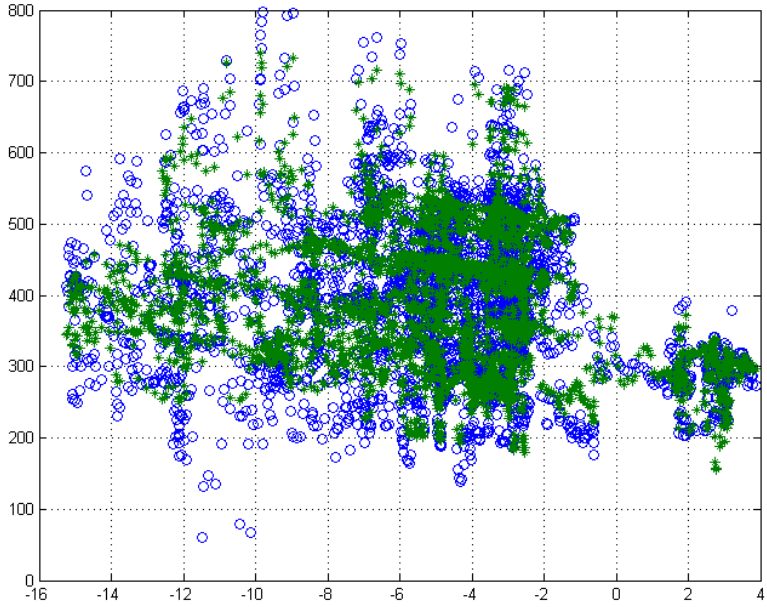

Figure 3.9. L1-08. Week 01 + 02. Model with 481 parameters. Measured (blue) and simulated (green) heat load in kW as a function of outdoor temperature.

The following figure shows the measured (blue) and simulated (green) heat loads as well as the difference (red).

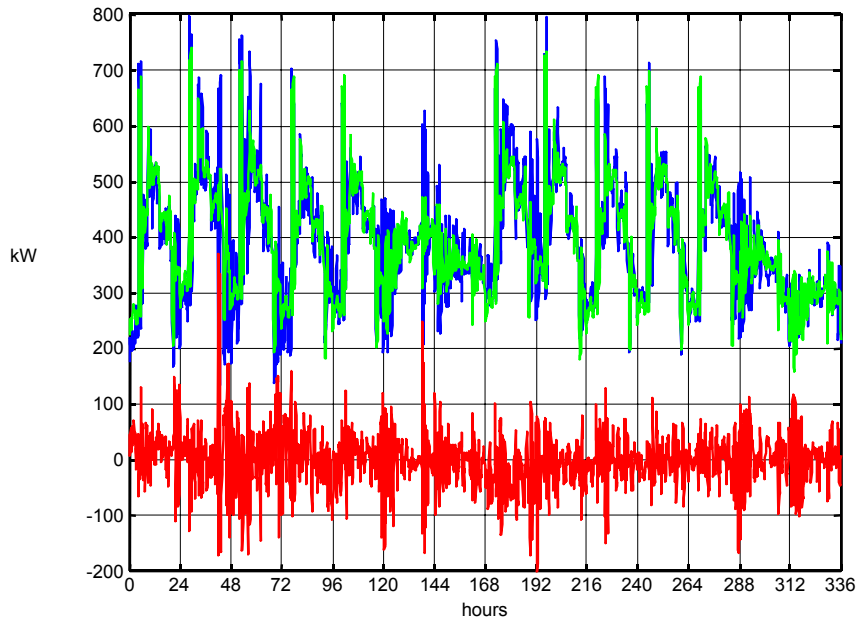

Figure 3.10. L1-08.Week 01 + 02. Model with 481 parameters. Measured (blue) and simulated (green) heat loads in kW as well as the difference (red). Standard deviation of error 47.4 kW.

Next we will apply a model with different parameters for each day, i.e. 1681 parameters. The result is shown in Figure 3.11.

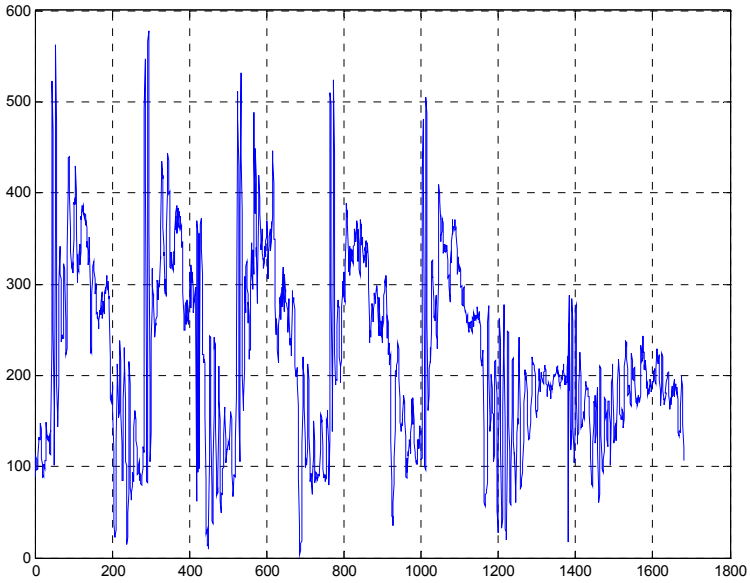

Figure 3.11. L1-08. Week 01 + 02. Clock function (in kW) with 1680 parameters. A = -7.6488 kW/˚C.

The next figure shows the heat load in kW as a function of the outdoor temperature. It should be observed that the nominal design heat load at –12 ˚C is 1200 kW, cf. Table 1.1, far from the observations.

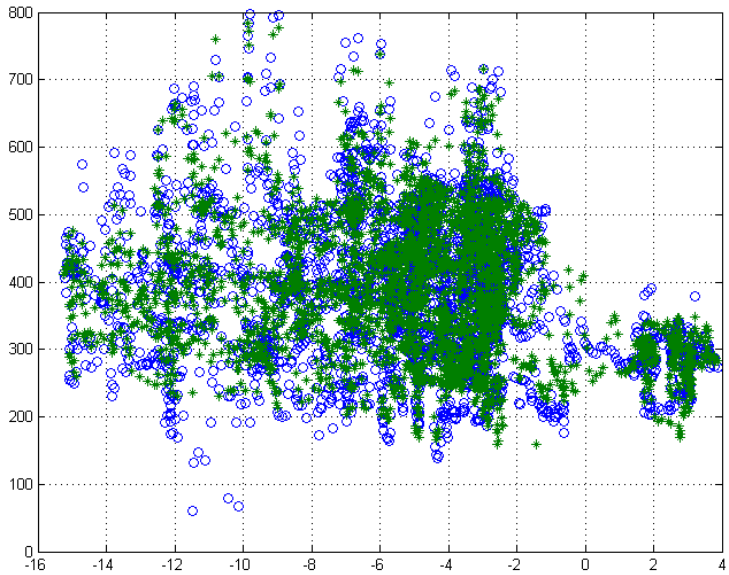

Figure 3.12. L1-08. Week 01 + 02. Model with 1681 parameters. Measured (blue) and simulated (green) heat load in kW as a function of outdoor temperature.

The following figure shows the measured (blue) and simulated (green) heat loads as well as the difference (red).

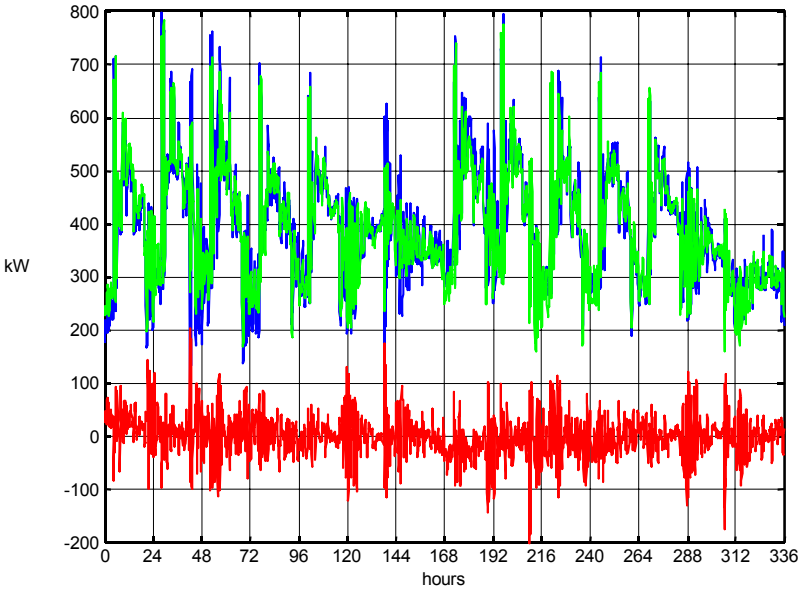

Figure 3.13. L1-08. Week 01 + 02. Model with 1681 parameters. Measured (blue) and simulated (green) heat loads in kW as well as the difference (red). Standard deviation of error 37.7 kW.

It appears that the standard diviation has decreased when the number of model parameters were increased from 481 to 1681.

Figure 3.14 shows the measured heat load compared with the degree day dependent part, according to the model with 1681 parameters. This heat load follows the instantaneous outdoor temperature without a delay.

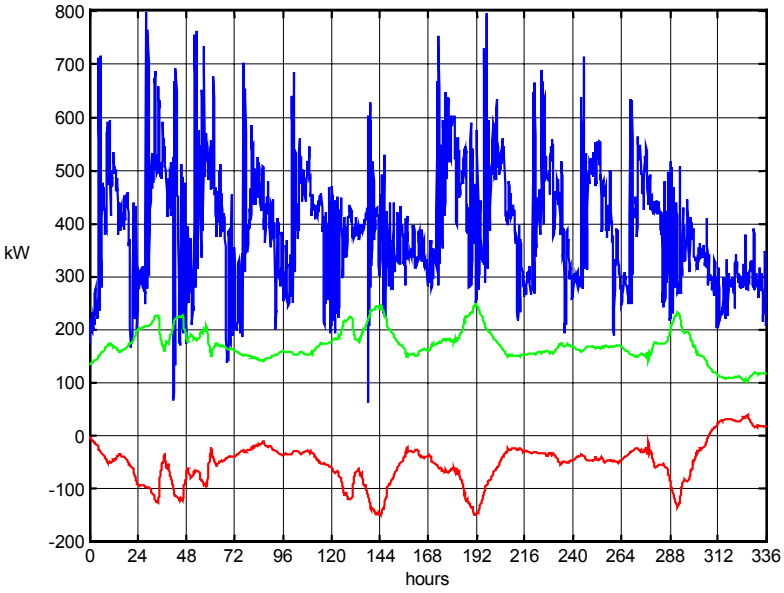

Figure 3.14. L1-08. Week 01 + 02. Model with 1681 parameters. Measured (blue) and simulated degree day dependent part of the heat load (green) in kW. The red curve is the outdoor temperature in ˚C multiplied by 10.

The models so far have been based on data from the two winter weeks. For comparison 10 weeks of data prior to the winter period (from October 2002) will be used. Figure 3.15 shows the result for the clock function with 1680 parameters.

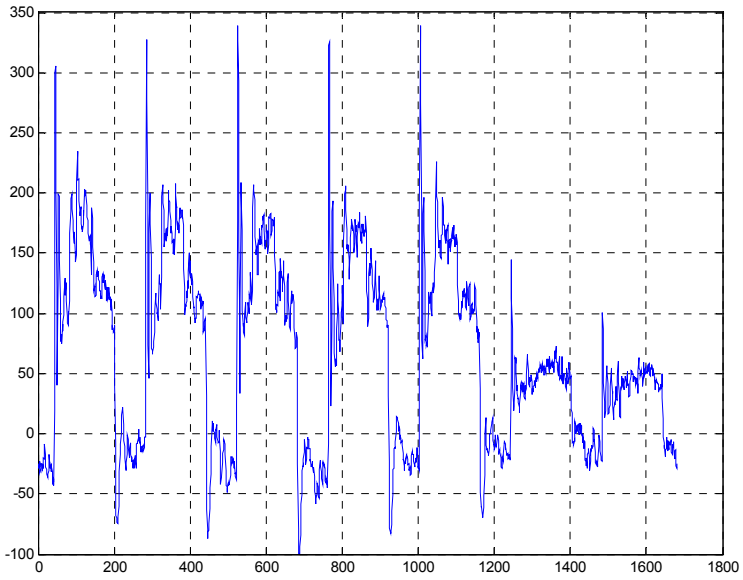

Figure 3.15. L1-08. 10 weeks in autumn 2002. Clock function (in kW) with 1680 parameters.
A = -14.0168 kW/°C.

Although the absolute values are different, the patterns in Figures 3.11 and 3.15 are similar, with a clear difference between weekdays and weekends.

For the three weeks we used for aggregation of the networks, the heat load variations can be found in Appendix B. For building L1-08 the normalized heat loads and the outdoor temperature are shown in Figure 3.16.

The absolute values are different between the weeks, but the patterns are similar, and we see again a clear difference between weekdays and weekends.

To sum up, we have applied a model where the heat load is separated in a degree day dependent part - utilising the instant outdoor temperature - and a clock function. Different clock functions have been tested. One clock function has 480 parameters, i.e. 240 parameters for a week day and 240 parameters for weekends (10 data points per hour). Another clock function has 1680 parameters (10 data points foe every hour of the week). The performance increases with the number of parameters.

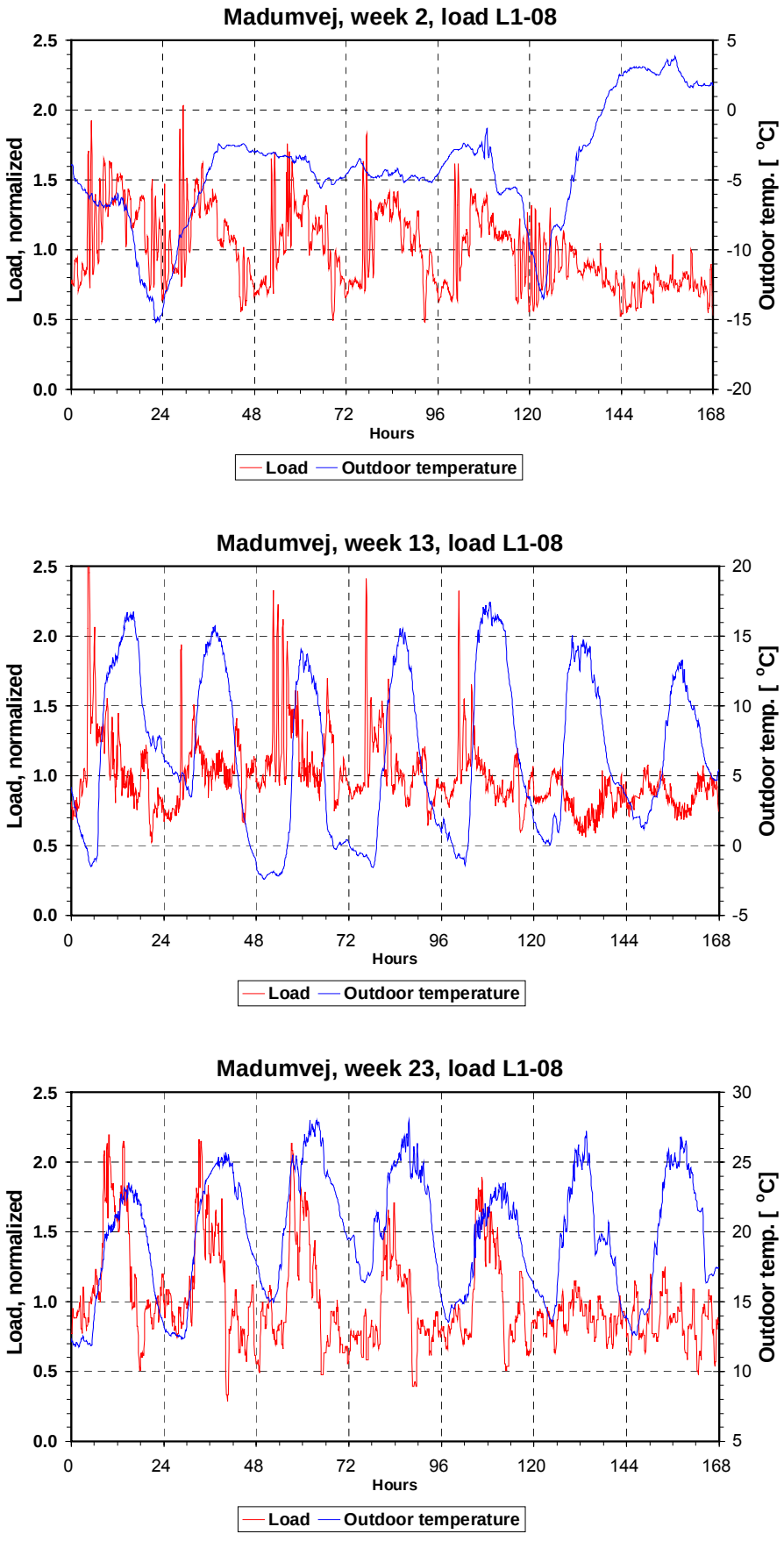

Figure 3.16. Normalized heat loads in weeks 2, 13 and 23 for building L1-08, and the outdoor temperature.

3.1.3 Building L1-01, semidetached houses

For comparison with building L1-08 the load variations in a few other buildings will be examined in the following. First we will consider building L1-01, semidetached houses with a nominal heat load of 559 kW. Figure 3.17 shows the clock function with 1680 parameters.

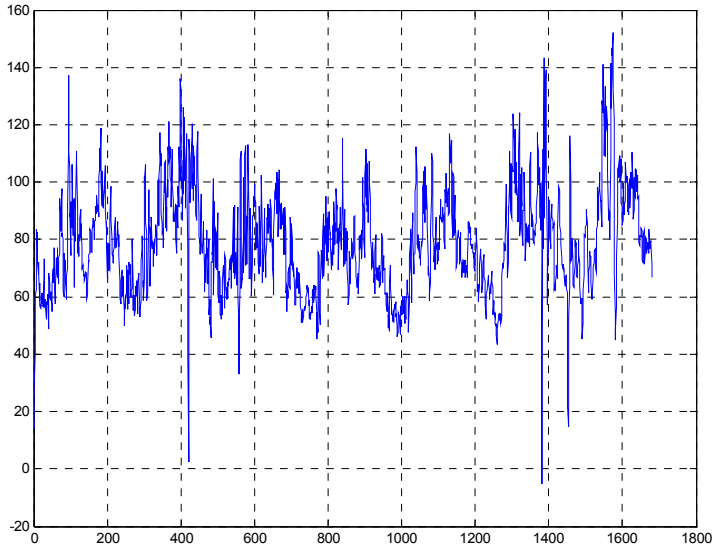

Figure 3.17. L1-01. Week 01 + 02. Clock function in kW with 1680 parameters. A = -4.050 kW/˚C.

For L1-01 we see a more uniform load variation during the week than for L1-08. The following figure shows the heat load a as function of outdoor temperature, while Figure 3.19 shows the measured and simulated heat loads as well as the difference.

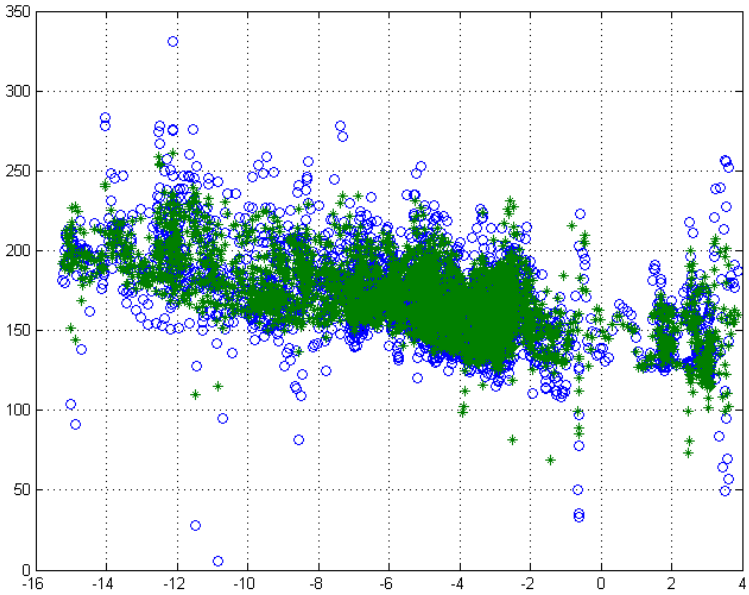

Figure 3.18. L1-01. Week 01 + 02. Model with 1681 parameters. Measured (blue) and simulated (green) heat load in kW as a function of outdoor temperature.

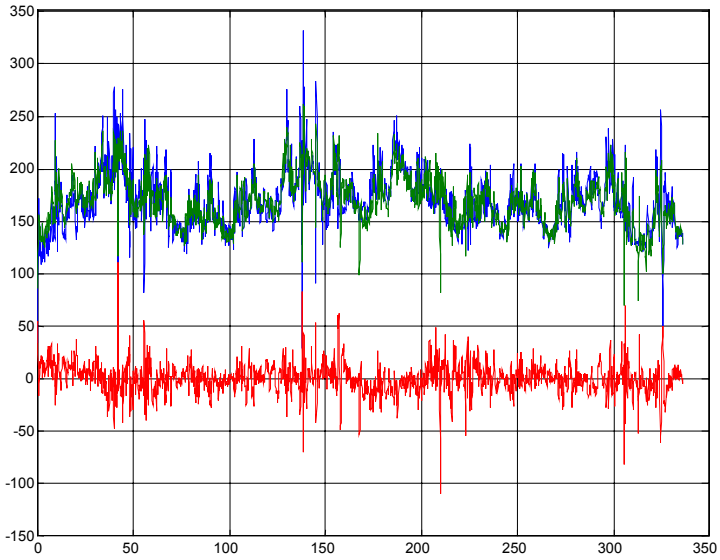

Figure 3.19. L1-01. Week 01 + 02. Model with 1681 parameters. Measured (blue) and simulated (green) heat loads in kW as well as the difference (red). Standard deviation of error 13.8 kW.

Figure 3.20 shows the outdoor temperature and the normalized heat load variations in the three weeks used in the aggregation work. The load variations in week 23 differ from the two other weeks.

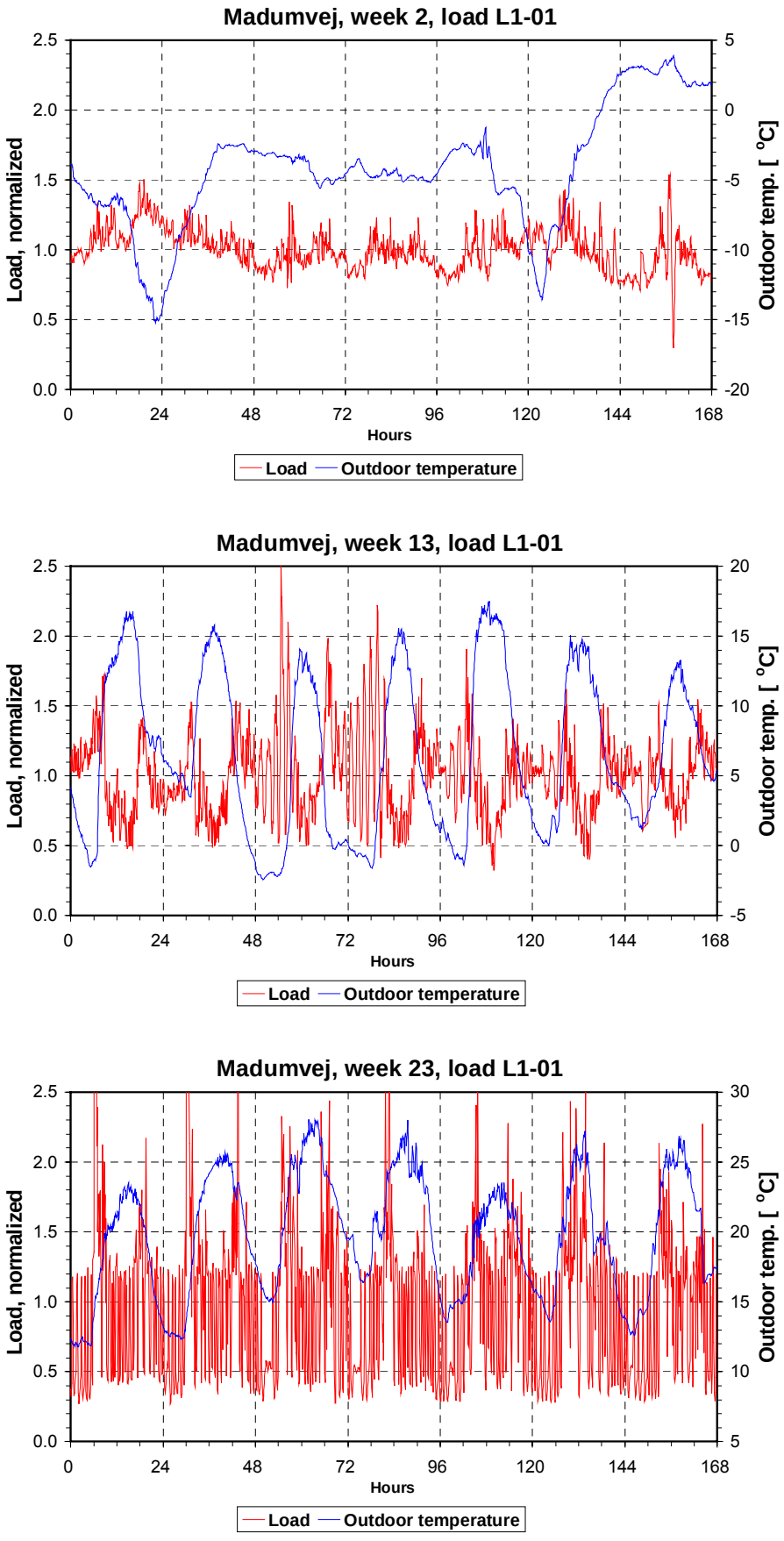

Figure 3.20. Normalized heat loads in weeks 2, 13 and 23 for building L1-01, and the outdoor temperature.

In the following, the clock functions will be shown for the buildings L1-04, L1-05 and L1-07.

3.1.4 L1-04, an institution

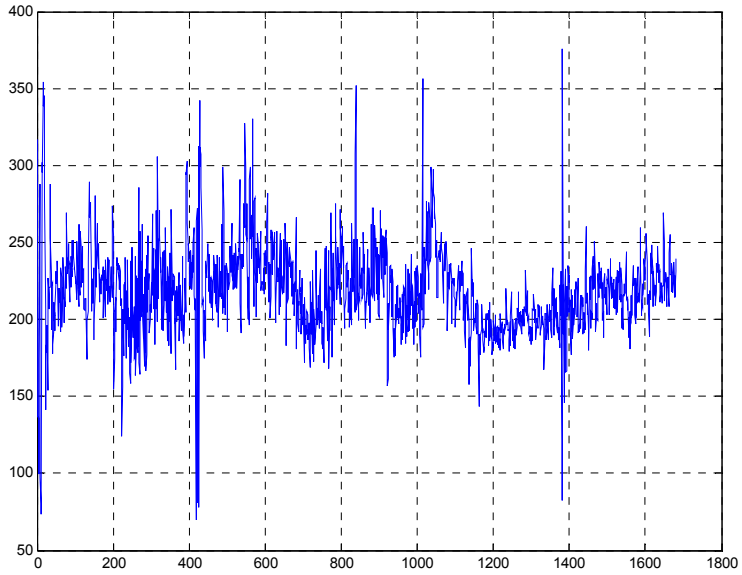

Figure 3.21. L1-04. Week 01 + 02. Clock function in kW with 1680 parameters. A = -4.614 kW/˚C.

3.1.5 L1-05, semidetached houses

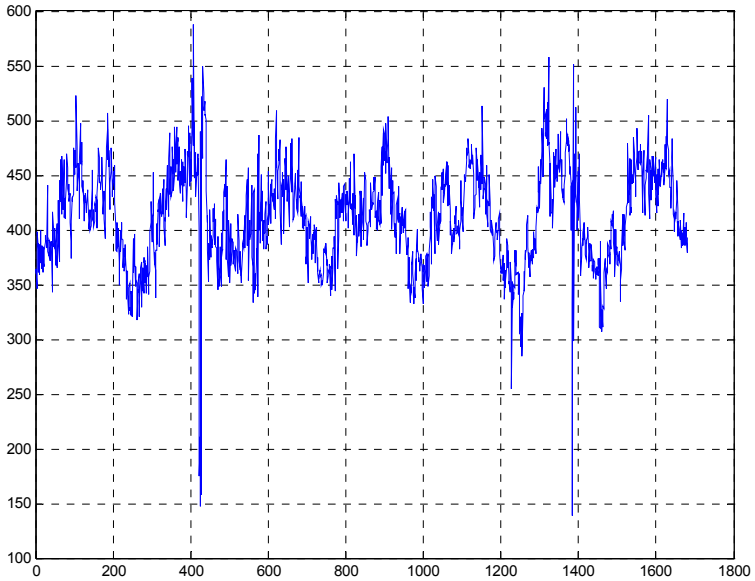

Figure 3.22. L1-05. Week 01 + 02. Clock function in kW with 1680 parameters. A = -11.139 kW/˚C.

3.1.6 L1-07, a public school

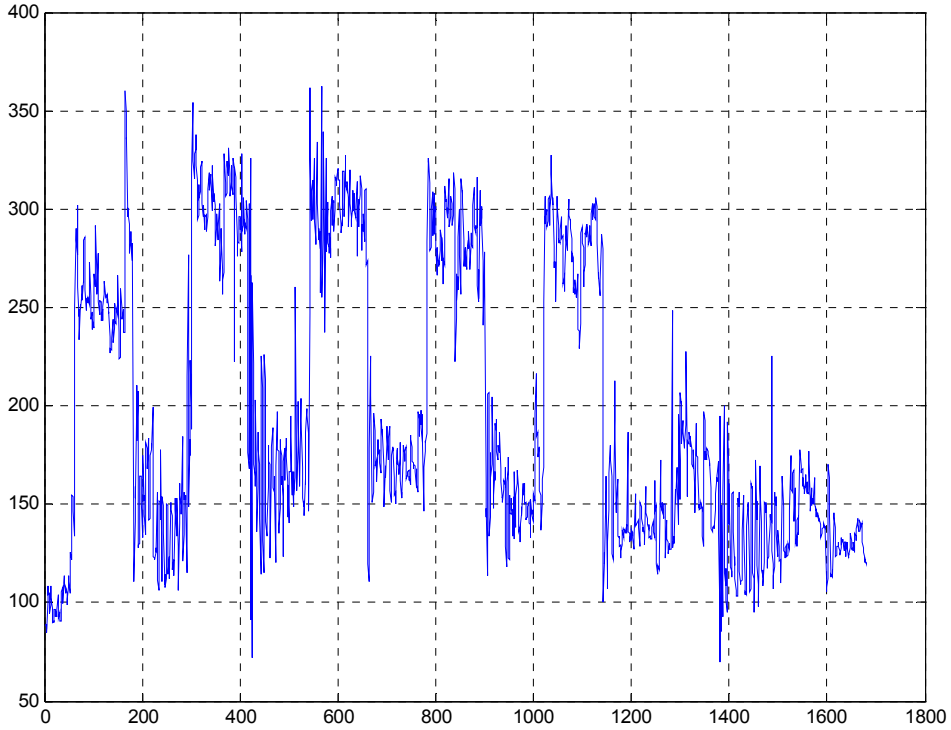

Figure 3.23. L1-07. Week 01 + 02. Clock function in kW with 1680 parameters. A = -2.166 kW/˚C.

3.2 Madumvej Substation

All buildings considered so far are supplied from the Madumvej substation. In the following we will examine the load variations at Madumvej. The first heat load model to be applied is: q = A · (tu –17) + clock function, where the clock function is different for weekdays and for weekends. Figure 3.24 shows the two clock functions.

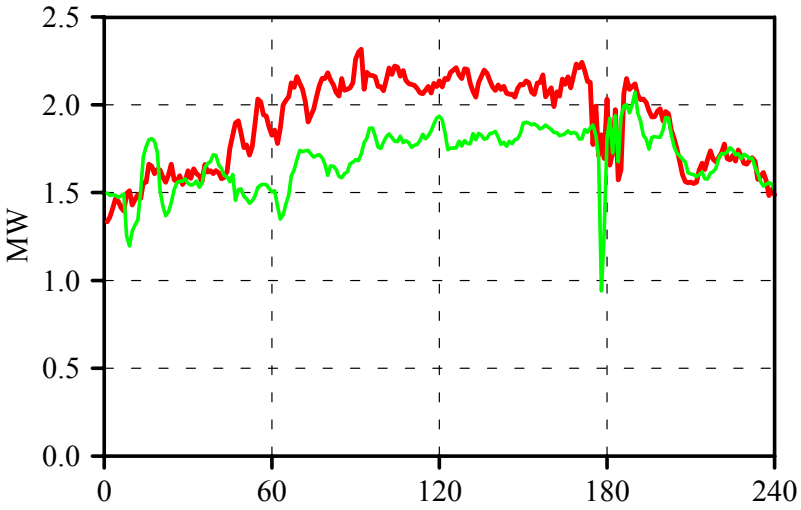

Figure 3.24. Madumvej. Week 01 + 02. Clock function with 480 parameters, 240 for weekdays (red) and 240 for weekends (green). A = -0.059 MW/˚C.

Compared to Building L1-08, the two clock functions for Madumvej are similar and do not vary so much during the day.

Figure 3.25 shows the measured (blue) and simulated (green) heat loads as well as the difference (red).

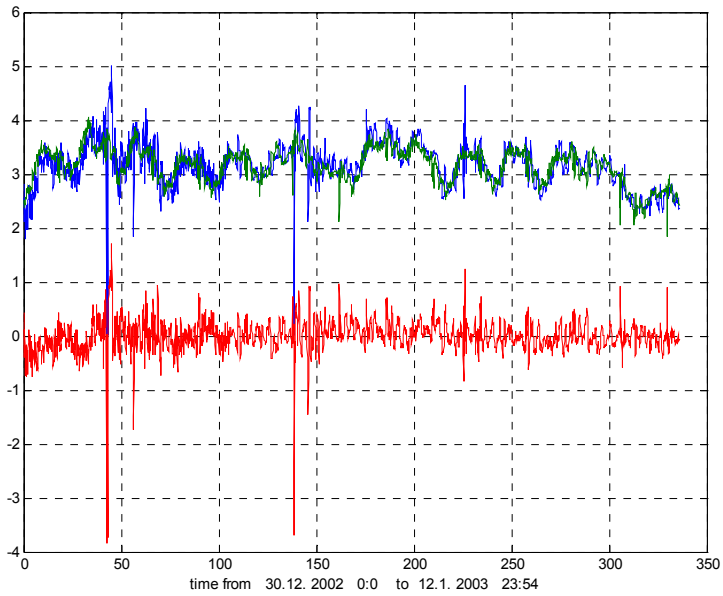

Figure 3.25. Madumvej. Week 01 + 02. Model with 481 parameters. Measured (blue) and simulated (green) heat loads in MW as well as the difference (red). Standard deviation of error 0.2634 MW.

Next we will apply a model with 1681 parameters. Figure 3.26 shows the clock function.

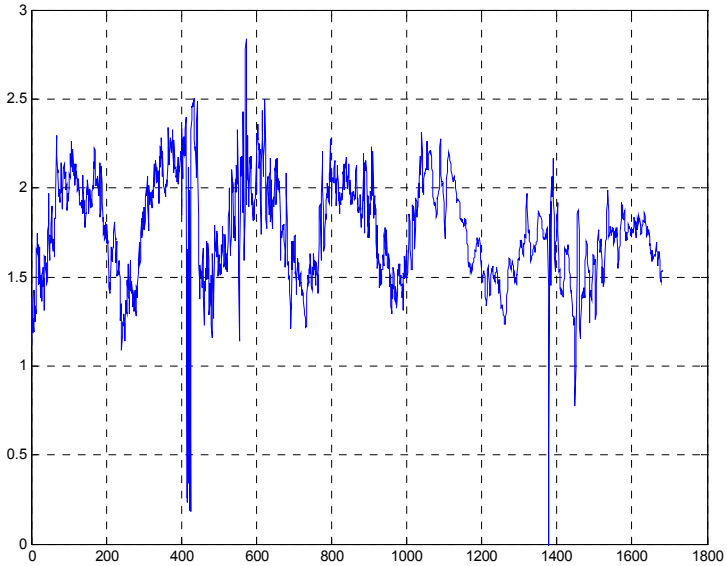

Figure 3.26. Madumvej. Week 01 + 02. Clock function in MW with 1680 parameters.
A = -0.0634 MW/˚C.

Figure 3.27 shows the heat load in MW as a function of the outdoor temperature.

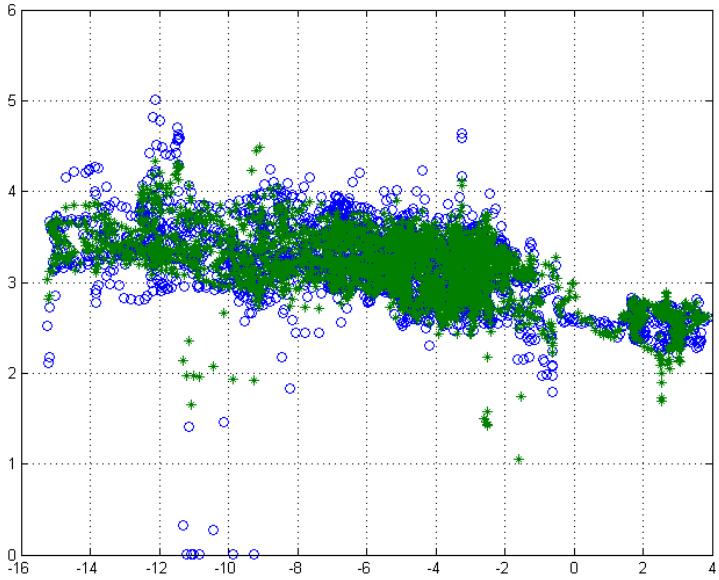

Figure 3.27. Madumvej. Week 01 + 02. Model with 1681 parameters. Measured (blue) and simulated (green) heat load in MW as a function of outdoor temperature.

The next figure shows the heat load as a function of time, measured (blue) and simulated (green) as well as the error (red).

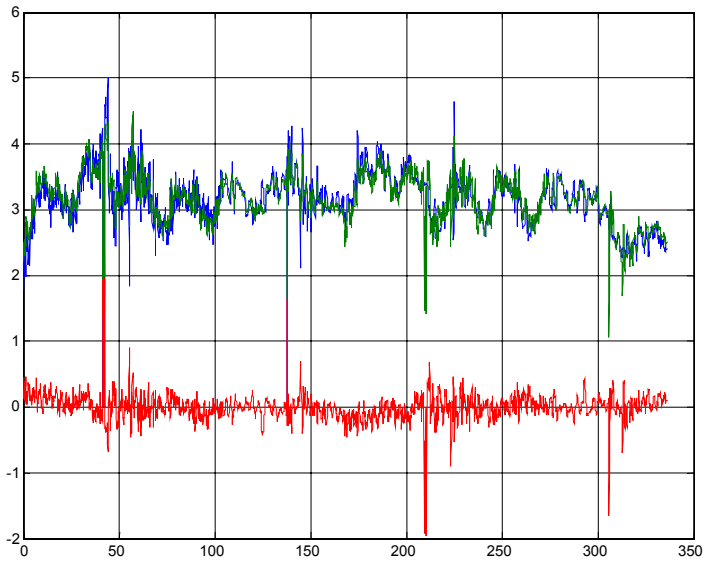

Figure 3.28. Madumvej, week 01 + 02. Model with 1681 parameters. Measured (blue) and simulated (green) heat loads in MW as well as the difference (red). Standard deviation of error 0.2062 MW.

For comparison we will also use data from the period of 10 weeks in the autumn 2002, just prior to the winter period.

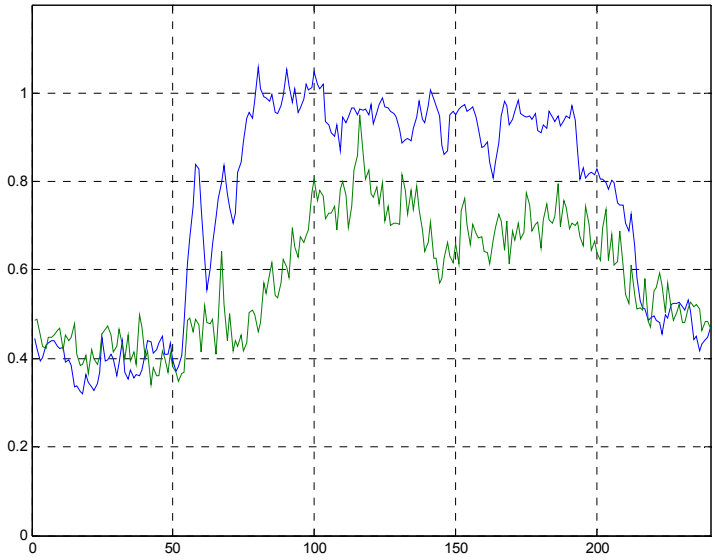

Figure 3.29. Madumvej. 10 weeks in autumn 2002. Clock function (in MW) with 480 parameters, 240 for weekdays (red) and 240 for weekends (green).

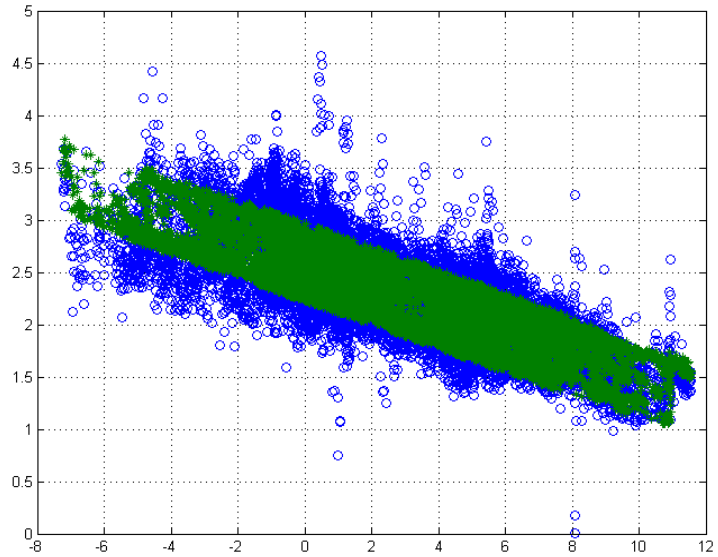

Figure 3.30. Madumvej. 10 weeks in autumn 2002. Model with 481 parameters. Measured (blue) and simulated (green) heat load in MW as a function of outdoor temperature.

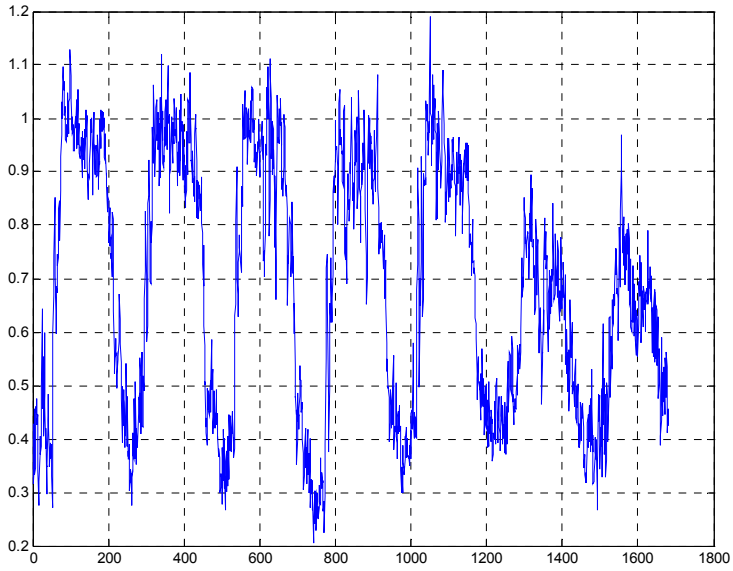

Figure 3.31. Madumvej. 10 weeks in autumn 2002. Clock function (in MW) with 1680 parameters.
A = -0.1128 MW/˚C.

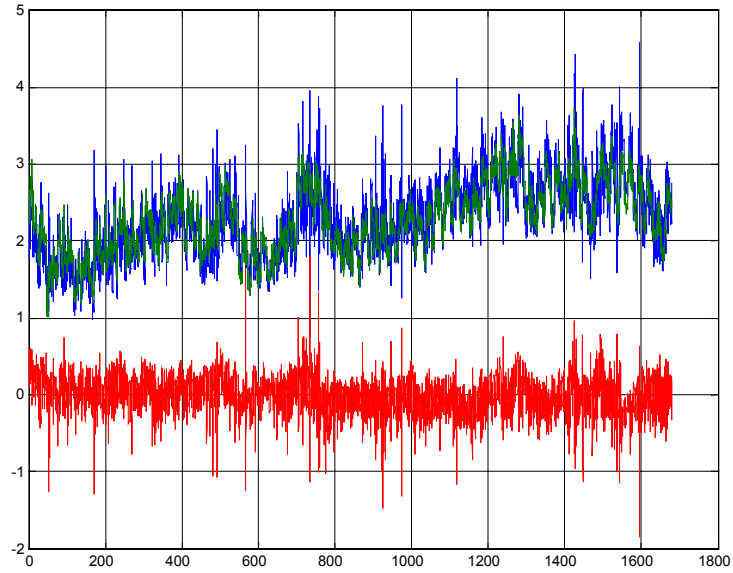

Figure 3.32. Madumvej, 10 weeks in autumn 2002. Model with 1681 parameters. Measured (blue) and simulated (green) heat loads in MW as well as the difference (red).
Standard deviation of error 0.2096 MW.

For the three weeks we used for aggregation of the networks, the heat load variations can be found in Appendix B. For Madumvej substation the normalized heat loads and the outdoor temperature are shown in Figure 3.33.

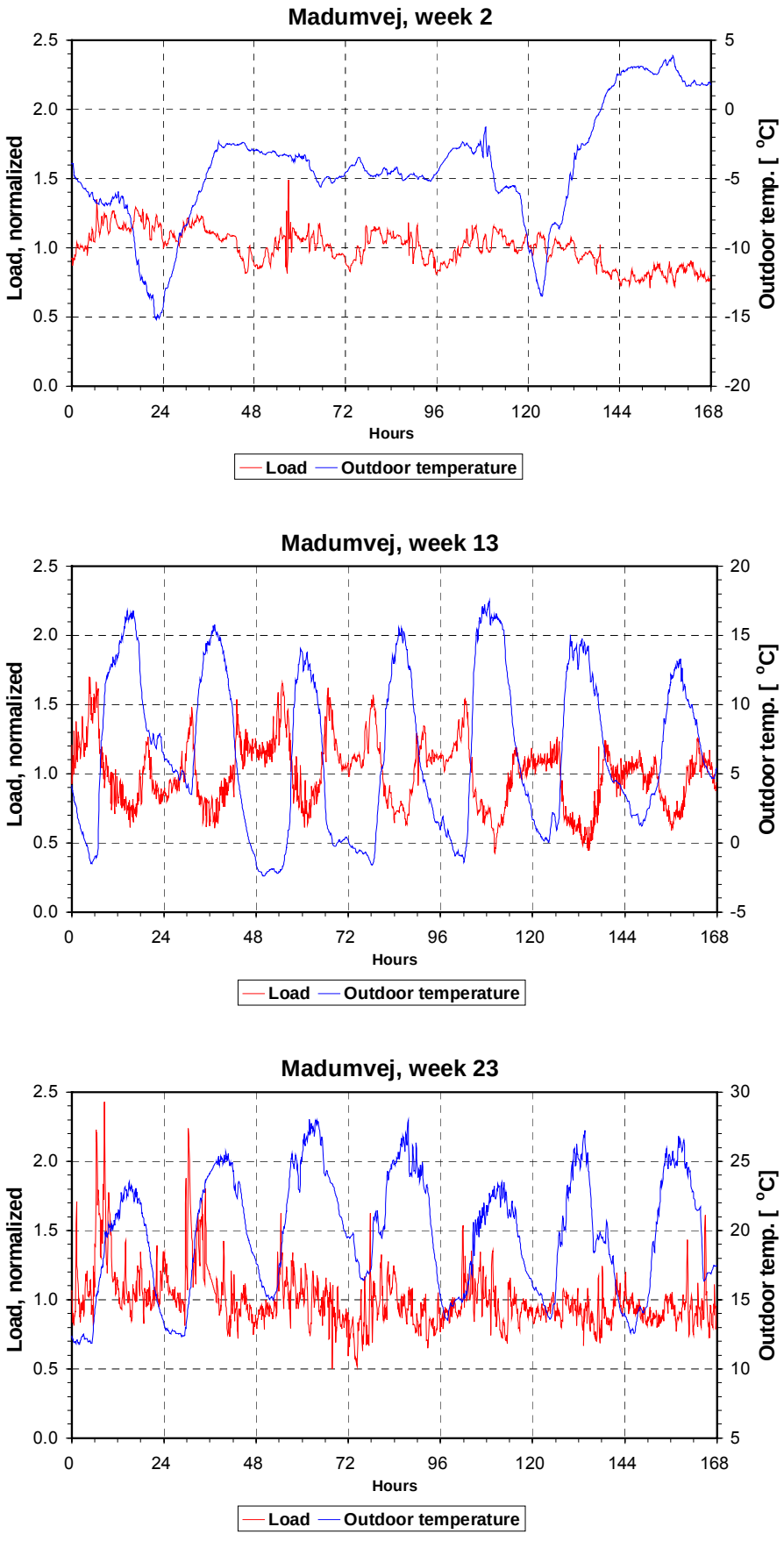

Figure 3.33. Normalized heat loads in weeks 2, 13 and 23 for Madumvej substation, and the outdoor temperature.

3.3 Summary

The heat load variations in R01 Madumvej DH system have been examined for some of the buildings and the substation.

Whether we look at the measured data directly or we model the data by a degree-day dependent model and a clock function, we see clear differences from building to building. Some buildings like the public schools exhibit a clear difference between week days and weekends, where the load in the weekends are much smaller when the schools are not in use.

Other buildings like the apartment building in Vanloese has small variations in general and exhibits the highest (hot water) loads in the weekends.

As expected we found that the load variations at Madumvej substation were smaller than the load variations in some of the buildings connected to the network.

The load variations described here by the clock function are likely to be associated with the control equipment and the control strategy of the building owner. As we have seen, these variations differ from building to building and it is likely that the buildings with the largest variations can reduce the load variations by applying some form of peak shaving.

In Chapters 6-8, we will discuss the effect of Demand Side Management on the operational costs.

Chapter 4 Operational optimisation

In this chapter some results on the operational optimisation of DH systems will be discussed.

The price information will be based on information from Roedovre DH company who buys heat from the VEKS transmission company. This price is low compared to DH companies producing heat on natural gas or fuel oil. So in addition to the Ishoej and Roedovre systems we will also examine a more typical DH system with higher heat losses (in percentage) and more expensive fuel.

In order to make the conclusions more generally applicable, the price information will be of a simple structure. For example only a mean value for the price of electricity for the circulation pumps will be used although the actual price could depend on the time of the day. We will also disregard all costs, which do not have an influence on the optimisation problem, for example all fixed costs.

4.1 DH Systems

The DH systems to be examined are:

IV_1: Aggregated model of Ishoej DH system with 1 pipe in the thermal network and 5 pipes in the pressure network.

IV_5: Aggregated model of Ishoej DH system with 5 pipes in the thermal network and 5 pipes in the pressure network.

R01 Madumvej: Physical model of Roedovre subsystem 1.

R02 Broparken: Physical model of Roedovre subsystem 2.

R01 Madumvej week13_5 (P05-K05). Aggregated model of Roedovre subsystem 1 for week 13 with 5 pipes in both the thermal and the pressure network.

Hvalsoe: Physical model of Hvalsoe DH system.

Hvalsoe_12: Aggregated model of Hvalsoe DH system with 12 pipes in the thermal network The calculated differential pressure in the 12 pipe model is scaled to obtain the differential pressure in the physical network.

4.2 Cost assumptions

In the reference case we will use the following prices:

Fuel (VEKS - CHP and incineration): 48.91 kr/GJ.

Fuel (Decentralised production): 81.66 kr/GJ.

Electricity for pumps: 1.18 kr/kWh (327.78 kr/GJ).

An incentive tariff applies between the VEKS transmission company and the DH distribution companies. If either the return temperature is too high or the daily load variations are too big, a penalty must be paid. On the other hand the distribution companies receive money from VEKS if the return temperature level or the load variations are low, cf. Chapter 5. These costs are

based on hourly mean values, weighed by the daily consumption, and paid on an annual basis. In order to include these costs in the object function, the costs are changed to a daily basis.

Load factor:

q_i is the hourly heat production,

q_m is the mean daily heat production.

If the hourly heat production q_i is higher than q_m, a load factor is calculated from:

$$Td = \sqrt{\sum_{i=1}^{24} \left(\frac{qi}{qm} - 1 \right)^2} \qquad \text{for } q_i > q_m$$

$$f = 0.90 + 0.23 \cdot Td$$

Cost1 = (f-1) · (24·qm) · K, where K = 46.5 DKK/GJ for Madum substation, K = 45.7 DKK/GJ for Broparken substation, and K = 61.66 DKK/GJ for Ishoej DH plant.

Return temperature level:

Tr is the average return temperature on the secondary side of the heat exchanger, weighed by the hourly heat production.

Cost2 = (Tr- 55) · (24·qm) · 0.19 [kr/GJ/K]

Both Cost1 and Cost2 can be negative or positive. Usually the load factor f is below 1, and the DH company thus receives money from VEKS. However, it should be kept in mind that the fixed charge paid to VEKS is not included in the optimisation.

4.3 Technical considerations

4.3.1 DH Sim

Risoe and MEK DTU have developed a simulation programme called DH Sim, which was used in previous work, including the EFP 96 and the IEA Annex VI work, Pálsson et al. (1999), Bøhm et al. (2002). DH Sim has been developed to treat heat loads as time series – in contrast to many commercial programmes that treat the heat loads in the connected buildings in a simple way (for instance as annual values and a time factor to get the instantaneous load, and often with the same cooling in all buildings).

DH Sim has a facility to use different models for the house stations, for example the equations for a plate heat exchanger is solved to give realistic return temperatures from the heat exchanger. A 2-string radiator system and a hot water system can also be modeled. In the optimisation of the DH system, the supply temperature is often changed from the actual value to higher or lower values. In this respect it is important that the thermal response of the house station is modeled correctly. As an example, Figure 4.1 shows the primary return temperature from a specific heat exchanger as a function of supply temperature and the heat load. This should be compared with a constant return temperature independent of the supply temperature, an assumption in many commercial simulation programmes.

At present DH Sim can simulate DH networks without loops and it can handle one production unit. DH Sim uses the so-called “node model” for calculating temperature dynamics in pipes, Benonysson (1991), Pálsson (1997).

DH Sim has a number of options for utilising the consumer information and in this work the programme has been improved with three new options: -d, -e and -s. In the general case DH Sim needs information on the heat exchanger size and the secondary temperatures of the heat exchanger to calculate the primary return temperature. In the new **option -s**, the flow is calculated from primary return temperatures. The introduction of this new option was necessary because information on the secondary temperatures in Roedovre was not available for all buildings.

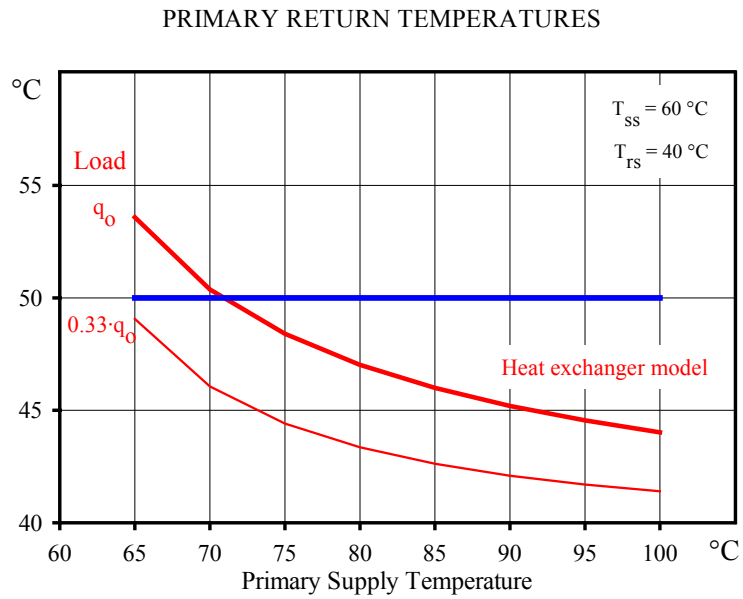

Figure 4.1. Primary return temperature from a specific heat exchanger as a function of primary supply temperature and the heat load. Secondary supply and return temperatures 60/40 ˚C, respectively.

When during the optimisation the supply temperature is changed, the primary cooling of the heat exchanger is expected to change. In **option –d**, it is first assumed that the efficiency of the heat exchanger remains the same when the supply temperature is changed (for a known heat load). Secondly, a correction is made to this cooling. Therefore the new cooling* at the new supply temperature Ts* is calculated as:

Cool_prim*(t) = Cool_prim(t) · [Ts_prim*(t) - Tr_sec] / [Ts_prim(t) - Tr_sec] · [Ts_prim(t) / Ts_prim*(t)] ˆ(a).

For the buildings in Roedovre, the secondary return temperatures were estimated from the measured primary return temperatures.

In **option –e** the new return temperature is calculated from:

Tr_prim*(t) = Tr_prim(t) + [(Ts_prim*(t) / Ts_prim(t)) ˆ(a) -1] · b,

where a and b are constants. Different values are assigned to the constant a when the new supply temperature is either above or below the measured supply temperature. In this way, the return temperature response will be similar to the response shown in Figure 4.1.

In the Roedovre case study we used: a = -1, when Ts_prim(t)* > Ts_prim(t),

a = -3, when Ts_prim(t)* <= Ts_prim(t).

b = 5.

All connected buildings will influence the return temperature at the plant, but to give an impression of the influence of supply temperature, Table 4.1 shows the return temperature at the plant as a function of different supply temperatures.

Table 4.1. Test of DH Sim option –e. Return temperature and cooling at the substation as a function of supply temperature.

ºC	R01 week 2			R01 week 13		
Supply temperature from the substation	80	90	100	80	90	100
Return temperature	56.3	54.1	53.2	51.0	49.5	48.7
Cooling	23.7	35.9	46.8	29.0	40.5	51.3

4.3.2 MATLAB

Object function and constraints

The goal in this work has been defined to find an optimum supply temperature from the plant for the coming period, for instance 48 hours.

The object function typically includes the following:

- Either production cost or heat loss cost (if DSM is not utilized, the solution is not affected)
- Pumping cost, incl. variable efficiency of the pump
- Tariff costs (penalty/bonus for cooling or for load variations)
- A terminal cost.

The constraint function typically includes:

- Capacity of the circulation pump (pumping curve)
- Maximum permissible change in supply temperature from the plant from one time step to the next
- Start and stop conditions (for the supply temperature).

Figure 4.2 shows as an example the pumping curve for Roedovre subsystem R01 Madumvej. The figure also shows actual measured data from January 2003 (6-minutes values). Although the weather was very cold, cf. Appendix B, the flow and pressure were below the design values 125 m3/h and 40 m water gauge at 1450 rpm.

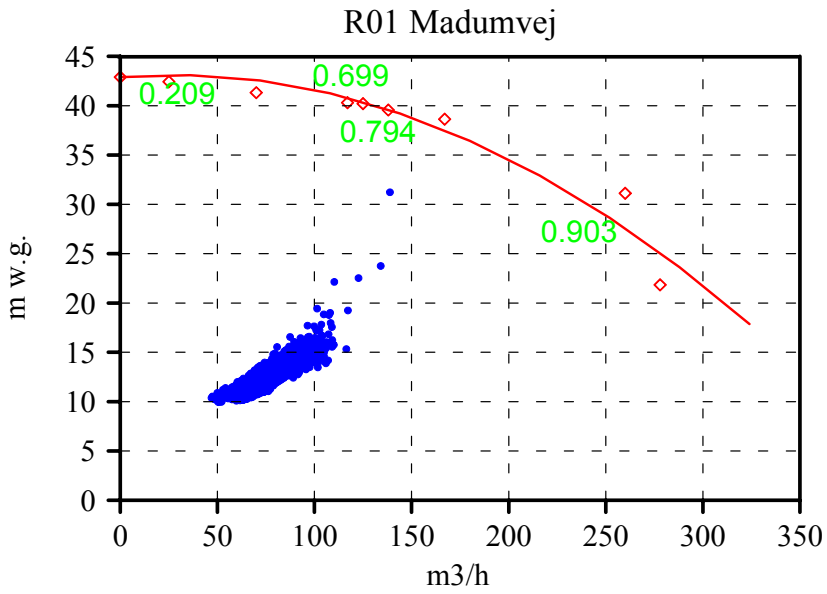

Figure 4.2. Pumping curve for R01 Madumvej at 1450 rpm. Differential pressure as a function of flow (red) with data points for 1450 rpm. inserted. Measured efficiency of the pump at 1450 rpm shown in green numbers. Actual flow in January 2003 shown in blue.

For calculating the operational costs of the pump we will apply a simple model. The efficiency of the pump will be found by placing a parabola through (0,0) and the actual flow and pressure and finding the efficiency at the intersection with the efficiency curve at 1450 rpm. In addition the efficiency of the frequency converter will be taken as 0.9. Do to some problems with the SCADA system it has not been possible to compare the model with the measured power consumption of the pumps in Roedovre in the selected periods.

Optimisation functions

In the beginning of the project, optimisations were made with aggregated pipe models based on the "element method", programmed in Matlab 4.2, and utilizing the Matlab function "constr". In Matlab 6.5, the function "constr" does not work properly, and instead the function "fmincon" had to be used. Next an interface between Matlab 6.5 and DH Sim was built enabling DH Sim simulations to be called from Matlab, using the Matlab function fmincon.

We found that the latest results differ slightly from the earlier ones, bearing in mind that two different pipe models and two different optimisation routines were used. We have noticed that the fmincon function appears to give results with a more oscillatory behavior of the optimum supply temperature than the constr function.

How to start and stop the optimisation

If we do not put any constraints or lower and upper bounds on the optimisation, the optimisation routine would like to start high and to end low. In this way we do not pay for heating up the network at the beginning and at the end we think that the world stops and there is no need for heating the following day. This is, of course, not acceptable.

After some trials it was decided to use the following assumptions:

When the optimisation starts, the supply temperature must be equal to the measured supply temperature (unless we want to analyse the effect of a different temperature level).

At the end of the optimisation horizon we can either "lock" the temperatures or we can punish the system by applying a terminal value, i.e. we must pay the cost of heating up the pipes to the initial condition if the temperature level is lower than in the beginning.

4.3.3 A test case with constant heat load (IV_1, Model P01 K05)

To better understand what is going on, we will start with a simple case, the one pipe - one consumer model. The physical parameters in the thermal network are based on the aggregated Ishoej model D_1 (P01), see Bøhm et al. (2002), but the heat load located at the plant has been removed to make the model even more simple. The pressure loss is calculated by a 5-pipe model K05.

The supply temperature must be in the range 90 – 115 ºC and it must not change more than 10 ºC per hour.

First we will consider the case of constant heat loads and a period of 48 hours. The variable costs are the pumping costs and the dynamic heat loss, defined as the heat production minus the heat load. With Pfuel = 49 kr/GJ and Ppower= 328 kr/GJ, the variable costs (excluding the buildings) of running the system for 48 hours are:

Ts = 90 ºC: 6459 DKK. Ppump = 3205 DKK, Ploss = 3254 DKK.

Ts = 105 ºC: 4428 DKK. Ppump = 889 DKK, Ploss = 3539 DKK.

Ts = 115 ºC: 4261 DKK. Ppump = 510 DKK, Ploss = 3751 DKK.

It appears that a supply temperature of 115 ºC gives the lowest costs.

The result of an optimisation is shown in Figure 4.3. It is here required that the supply temperature at the end of the period is the same as at the start. There is a terminal cost of heating up the pipe if the temperatures are lower that in the beginning included in the objective function. The variable cost is 3660 DKK.

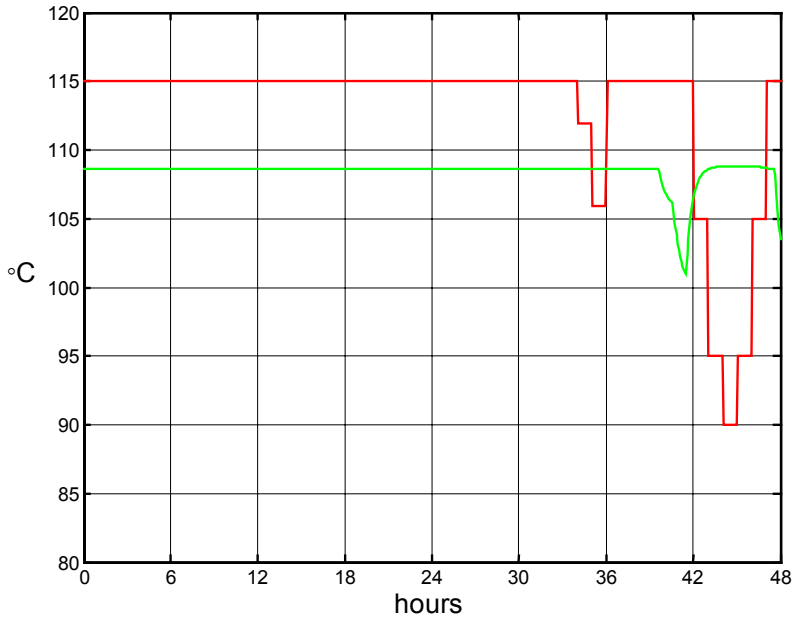

Figure 4.3. Model IV_1. Optimum supply temperature at the plant (red) and the supply temperature at the end of the pipe (green).

Figure 4.4 shows the heat production, the heat load in the buildings and the dynamic heat loss.

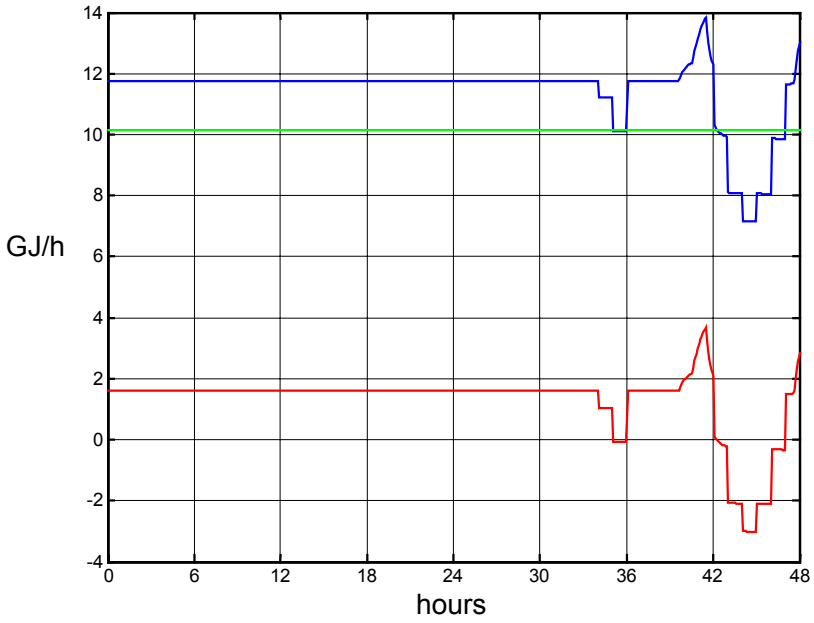

Figure 4.4. Heat production (blue), heat load (green) and the dynamic heat loss (red).

Although there is a terminal cost included, the optimisation programme benefits from lowering the supply temperature in the end of the period, because the plug of "cold" water will not reach the end of the pipe within the time period considered.

The lowering of the supply temperature at approximately 35 hours is difficult to understand, but the effect is that the supply temperature at the end of the pipe at 48 hours is higher than if the supply temperature had not been changed.

It is really not desirable that the terminal costs influence the optimum supply temperature curve. One way to avoid this is to use the optimum curve for less than the 48 hours, say for instance 30 hours, and to repeat the optimisation after for instance 24 hours.

By ensuring that the optimum supply temperature is the same at 48 hours as in the first hour, test carried out for Case 4A IV_5, cf. Section 4.4, showed that the terminal value is not important for the operational costs, and for this reason the terminal value was not included in the costs for the other Cases B-G, with many pipes to be taken into consideration.

4.4 Some optimisation results without an incentive tariff

In the following we will discuss some results from operational optimisation of different DH systems. In this section we will only consider heat loss costs and pumping costs. In the next chapter we will include an incentive tariff with respect to the return temperature level and the heat load variations. The influence of DSM measures will be discussed in Chapters 6 to 8.

Case 4A: Ishoej DH system, Dec. 19, 12:00 – Dec. 21, 12:00, 2000

Model: IV_5 (P05-K05).

The maximum permissible change of supply temperature per hour is set to be 1 ˚C (to avoid overloading the compensators in the network).

Table 4.2 shows the costs of operating the system for 48 hours for the following cases:

A constant supply temperature of 115, 105 and 90 ˚C, representing the maximum, the actual and the minimum supply temperature from the DH plant.

Furthermore the table shows the optimum temperature, and the optimum temperature when the price of electricity is zero and the pump does not violate the pump constraints (the pump curve). The latter solution is not optimal when the pumping cost is included (4204 DKK).

The optimum operational cost is 3748 DKK for the two day period, which should be compared the cost of 171,522 DKK for heating the buildings. In this winter case the dynamic heat loss is 1.8 % of the building heat load and the savings in operational cost rather small.

Table 4.2. Ishoej DH system. Operational costs for 48 hours.

	115 ºC	**OPTIMUM**	**105 ºC**	**Optimum solution for Ppower = 0 and pump constraints active**	**90 ºC constraints violated**
Dynamic Heat Storage, GJ	66.30	63.18	60.57	56.45	48.07
Pumping, GJ	1.55	2.05	2.70	4.41	9.65
Costs, DKK	3760	3748	3859	4204	5538

P fuel = 48.91 DKK/GJ, P power = 327.78 DKK/GJ, Q buildings = 3,507 GJ ≈ 171,522 DKK.

Figure 4.5 shows the optimum supply curve, the corresponding return temperature and the heat load.

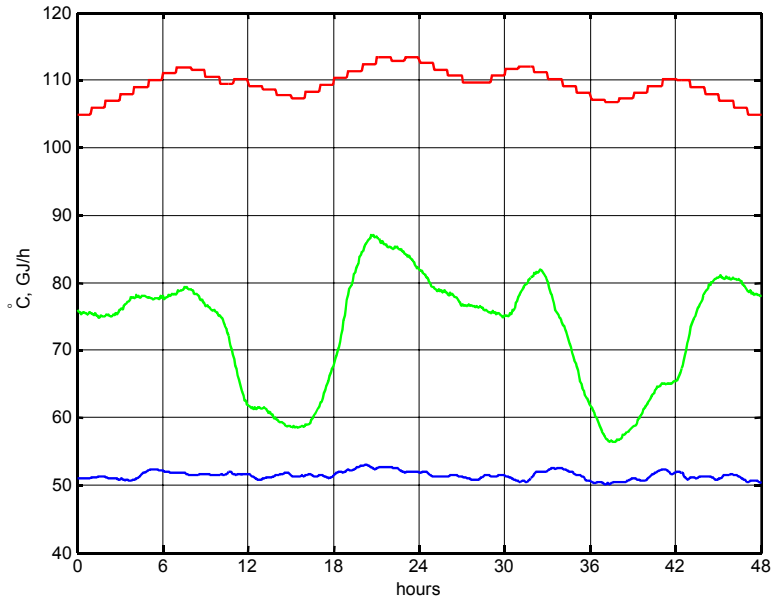

Figure 4.5. IV_5. Optimum supply temperature curve (red), the corresponding return temperature (blue) and the total heat load in the buildings (green).

Figure 4.6 shows the solution when the price of power is equal to zero and the pump curve is not violated.

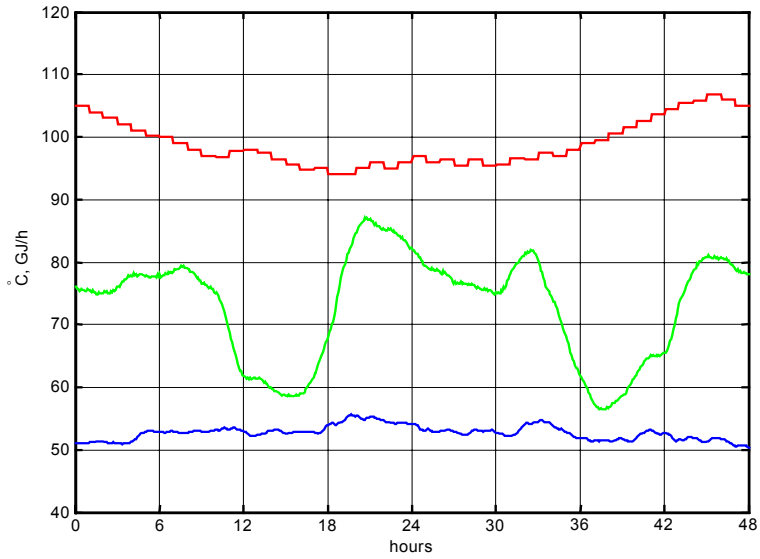

Figure 4.6. IV_5. Optimum supply temperature curve for zero electricity price (red), the corresponding return temperature (blue) and the heat load in the buildings (green).

In this case the starting point at 105 ºC and the maximum allowable change of 1 ºC/h limits the possibility to lower the supply temperature fast from the starting point. This temperature curve would be the optimum curve if the electricity price was zero, but with the actual prices of electricity and heat, the lowest possible supply temperature is NOT the optimum choice.

Case 4A shows that for a DH system like Ishoej, with a high line heat demand (low heat loss) and the actual costs of fuel and electricity, the optimum supply temperature is above 105 ºC.

Case 4B: Hvalsoe DH system, Jan. 22-23, 1998

Model: Full description. The maximum permissible change of supply temperature per hour is set to be 2 ˚C.

Table 4.3 shows the costs of operating the system for 48 hours for the following cases:

A constant supply temperature of 90, 75 and 70 ˚C, representing the maximum, the actual and the minimum supply temperature from the DH plant.

Furthermore the table shows the optimum temperature, and the optimum temperature when the price of electricity is zero and the pump does not violate the pump constraints (the pump curve).

Table 4.3. Hvalsoe DH system. Operational costs for 48 hours.

	90 ºC	OPTIMUM	75.4 ºC	Optimum solution for Ppower = 0 and pump constraints active	70 ºC constraints violated
Dynamic Heat Storage, GJ	92.94	84.04	84.99	83.59	81.85
Pumping, GJ	0.59	1.42	1.25	1.62	2.44
Costs, DKK	7783	7328	7352	7356	7483

P fuel = 81.66 DKK/GJ, P power = 327.78 DKK/GJ, Q buildings = 664 GJ ≈ 54,200 DKK.

The optimum operational cost is 7328 DKK for the two day period, which should be compared the cost of 54,200 DKK for heating the buildings. In this winter case the dynamic heat loss is 11.2 % of the heat production and the savings in operational cost rather small when compared with the cost of applying the actual temperature (75 ºC).

Figure 4.7 shows the optimum supply temperature as well as the optimum solution for zero power price and pumping constraints satisfied.

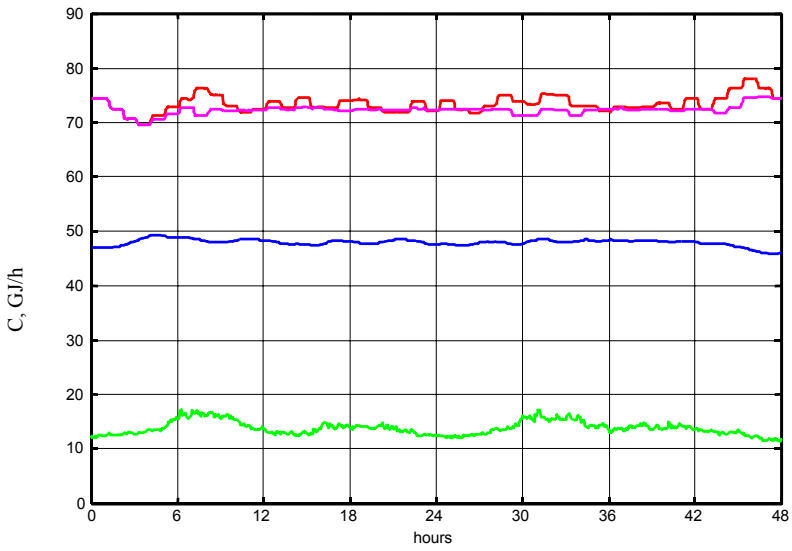

Figure 4.7. Hvalsoe. Optimum supply temperature curve (red), the corresponding return temperature (blue) and the total heat load in the buildings (green). The pink curve is the optimum solution for zero power price and pump curve not violated.

Case 4B shows that for a DH system like Hvalsoe, with a low line heat demand (relatively high heat loss) and the actual costs of fuel and electricity, the optimum supply temperature is close to the solution for zero electricity price, i.e. approximately 75ºC.

Calculation time:
In this case the heat exchanger equations are solved in every time step for the 535 consumers. Therefore one simulation takes 57 seconds, and to obtain the optimum solution (5 iterations) it takes almost 5 hours on a 2.6 GHz PC.

Case 4C: Hvalsoe DH system, Jan. 22-23, 1998

Model: Hvalsoe_12, 12 pipe model for thermal network, cf. Bøhm et al. (2002). No aggregated pressure model is available and as an approximation the pressure difference at the plant is taken as 2.23 times the calculated pressure difference at the plant in the aggregated thermal model. The maximum permissible change of supply temperature per hour is set to be 2 ˚C.

Calculation time:

In this case the heat exchanger equations are solved in every time step for 12 consumers. One simulation takes 0.26 seconds, and it takes approximately 0.3 hour on a 2.6 GHz PC to obtain the optimum solution (4 iterations). Thus the benefit of using an aggregated model of the DH system is clear.

Case 4D: Roedovre subsystem R01 Madumvej, Week 2 in January 2003

Model: Full description. The maximum permissible change of supply temperature per hour is set to be 2 ˚C.

Table 4.4 shows the costs of operating the system for 48 hours for the following cases:

A constant supply temperature of 100 and 85 ˚C, representing the maximum and the minimum supply temperature from the DH plant.

Furthermore the table shows the optimum temperature, the measured temperature (approximately 90 ºC) and the optimum temperature when the price of electricity is zero and the pump does not violate the pump constraints (the pump curve).

Table 4.4. R01 Madumvej week 2. Operational costs for 48 hours.

	100 ºC	OPTIMUM	Measured Ts	Optimum solution for Ppower = 0 and pump constraints active	85 ºC
Dynamic Heat Storage, GJ	20.75	19.84	19.12	16.03	18.11
Pumping, GJ	0.42	0.52	0.67	2.72	1.10
Costs, DKK	1154	1140	1154	1676	1244

P fuel = 48.91 DKK/GJ, P power = 327.78 DKK/GJ, Q buildings = 564 GJ ≈ 27,574 DKK.

The optimum operational cost is 1140 DKK for the two day period, which should be compared the the cost of 27,574 DKK for heating the buildings. In this winter case the dynamic heat loss is 3.4 % of the heat production and the savings in operational cost rather small unless a too low supply temperature is applied.

Figure 4.8 shows the optimum supply curve, the corresponding return temperature and the heat load as well as the actual supply temperature curve.

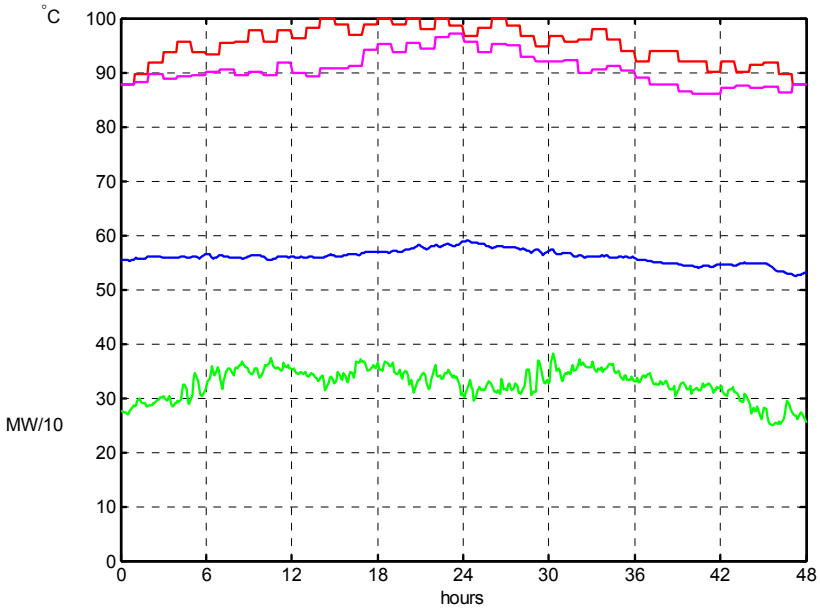

Figure 4.8. R01 Madumvej week 2. Optimum supply temperature curve (red), the corresponding return temperature (blue) and the total heat load in the buildings (green). The pink curve is the measured supply temperature.

Figure 4.9 shows the optimum solution for zero electricity price and no violation of the pump constraints, while Figure 4.10 shows the constraint function values for this case. It appears that both the constraints from the pump curve and the constraints associated with the maximum permitted change of supply temperature per hour are active during the optimisation. A further reduction of the supply temperature will violate the pumping constraint.

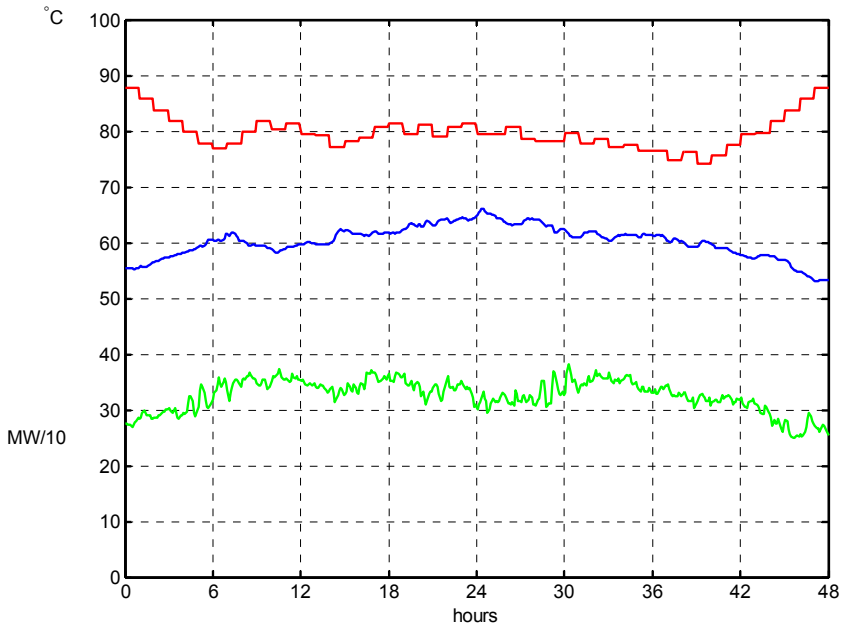

Figure 4.9. R01 Madumvej week 2. Optimum supply temperature curve for zero electricity price (red), the corresponding return temperature (blue) and the heat load in the buildings (green).

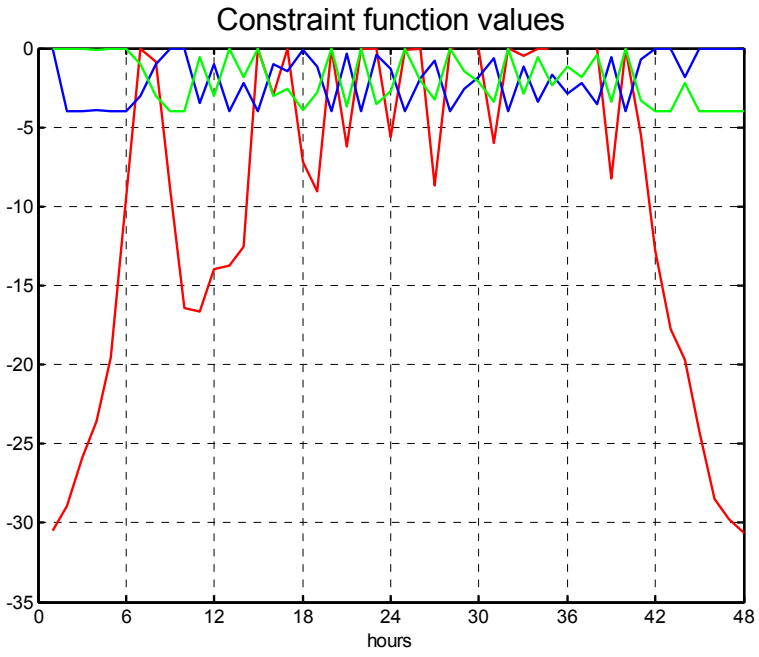

Figure 4.10. R01 Madumvej week 2. Constraint function values for the optimum solution in case of zero electricity price. Blue and green curves: Maximum change of supply temperature 2 ºC per hour. Red curve: pumping curve. This constraint value must be ≤ 0. Zero means that the constraint is active during the optimisation.

Case 4D shows that for a DH system like R01 Madumvej with a high line heat demand (low heat loss) and with the actual heat load (winter case) and costs of fuel and electricity, the optimum supply temperature is in the range 90-100 ºC.

Case 4E: Roedovre Subsystem 01, Week 13, March 2003

Model: Full description. The maximum permissible change of supply temperature per hour is set to be 2 ˚C.

Table 4.5 shows the costs of operating the system for 48 hours for the following cases:

A constant supply temperature of 100 and 80 ˚C, representing the maximum and the minimum supply temperature from the DH plant. Furthermore the table shows the optimum temperature, the measured temperature (approximately 80 ºC) and the optimum temperature when the price of electricity is zero and the pump does not violate the pump constraints (the pump curve).

Table 4.5. R01 Madumvej week 13. Operational costs for 48 hours

	100 ºC	OPTIMUM	Measured Ts	Optimum solution for Ppower = 0 and pump constraints active	80 ºC
Dynamic Heat Storage, GJ	20.88	18.19	18.81	17.40	18.31
Pumping, GJ	0.18	0.28	0.29	0.57	0.31
Costs, DKK	1079	982	1014	1039	997

P fuel = 48.91 DKK/GJ, P power = 327.78 DKK/GJ, Q buildings = 277 GJ ≈ 13,548 DKK.

The optimum operational cost is 982 DKK for the two day period, which should be compared the cost of 13,548 DKK for heating the buildings. In this spring case the dynamic heat loss is 6.2 % of the heat production and the savings in operational cost rather small.

Figure 4.11 shows the optimum supply curve, the corresponding return temperature and the heat load as well as the actual supply temperature curve.

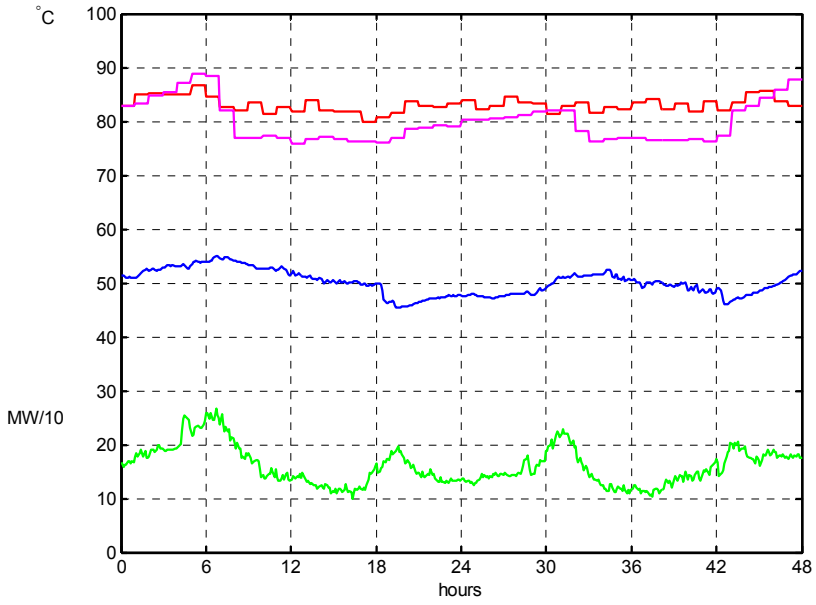

Figure 4.11. R01 Madumvej week 13. Optimum supply temperature curve (red), the corresponding return temperature (blue) and the total heat load in the buildings (green). The pink curve is the measured supply temperature.

Figure 4.12 shows the optimum solution for zero electricity price and no violation of the pump constraints.

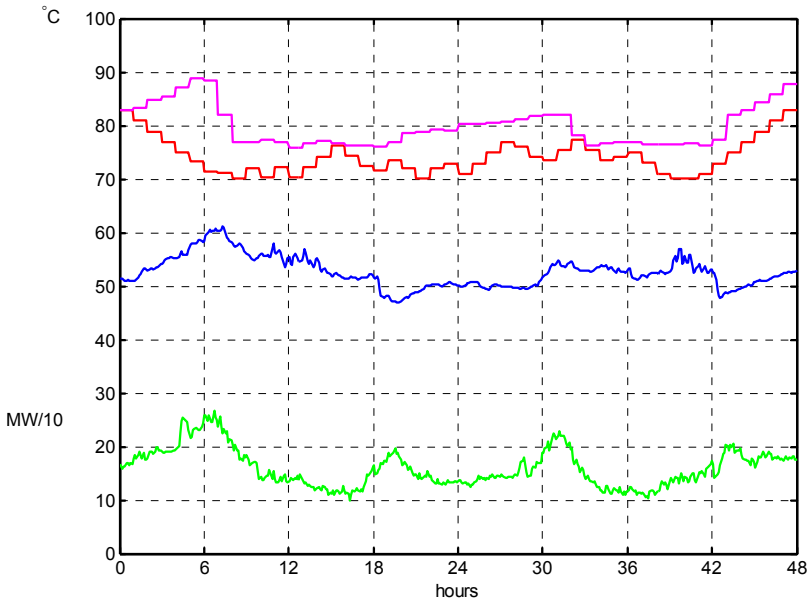

Figure 4.12. R01 Madumvej week 13. Optimum supply temperature curve for zero electricity price (red), the corresponding return temperature (blue) and the heat load in the buildings (green). Please, observe the return temperature response. Also shown is the measured supply temperature curve (pink).

Case 4E shows that for a DH system like Roedovre R01 with a high line heat demand (low heat loss) and with the actual heat load (spring situation) and costs of fuel and electricity, the optimum supply temperature is in the range 75 - 85 ºC.

Calculation time:

When option –e is applied, the heat exchanger equations are not solved in every time step.

One simulation takes 0.7 seconds, and it takes approximately 50 minutes on a 2.6 GHz PC to obtain the optimum solution (27 iterations).

Case 4F: Roedovre Subsystem 01, Week 13, March 2003

Model: Model: R011303_5 (P05-K05). Aggregated models for temperature and pressure with 5 pipes. The maximum permissible change of supply temperature per hour is set to be 2 ˚C.

Calculation time:

When option –e is applied, the heat exchanger equations are not solved. Instead of 14 consumers in the full model we now have 5 consumers in the thermal and 6 consumers in the pressure model (One of these loads is located at the DH plant). One simulation takes 0.26 seconds, and it takes approximately 7 minutes and 5 iterations on a 2.6 GHz PC to obtain the optimum solution. Thus the benefit of using an aggregated model of the DH system is smaller in this case than when the heat exchanger equations must be solved (case B).

Case 4G: Roedovre Subsystem 02, Week 33, August 2003

Model: Full description. The maximum permissible change of supply temperature per hour is set to be 2 ˚C.

Table 4.6 shows the costs of operating the system for 48 hours for the following cases:

A constant supply temperature of 100 and 70 ˚C, representing the maximum and the minimum supply temperature from the DH plant. Furthermore the table shows the optimum temperature, the measured temperature (approximately 80 – 85 ºC) and the optimum temperature when the price of electricity is zero and the pump does not violate the pump constraints (the pump curve).

Table 4.6. R02 Broparken week 33. Operational costs for 48 hours

	100 ºC	**OPTIMUM**	**Measured Ts**	**Optimum solution for Ppower = 0 and pump constraints active**	**70 ºC**
Dynamic Heat Storage, GJ	23.32	18.31	20.24	18.28	18.29
Pumping, GJ	0.16	0.20	0.17	0.20	0.21
Costs, DKK	1192	960	1046	959	962

P fuel = 48.91 DKK/GJ, P power = 327.78 DKK/GJ, Q buildings = 113 GJ ≈ 5,527 DKK.

The optimum operational cost is 960 DKK for the two day period, which should be compared the the cost of 5527 DKK for heating the buildings. The optimum solution is the same as the optimum solution obtained for zero electricity price. In this summer case the dynamic heat loss is 13.9 % of the heat production and the savings in operational cost rather small unless a too high supply temperature is used.

Figure 4.13 shows the optimum supply curve, the corresponding return temperature and the heat load as well as the actual supply temperature curve.

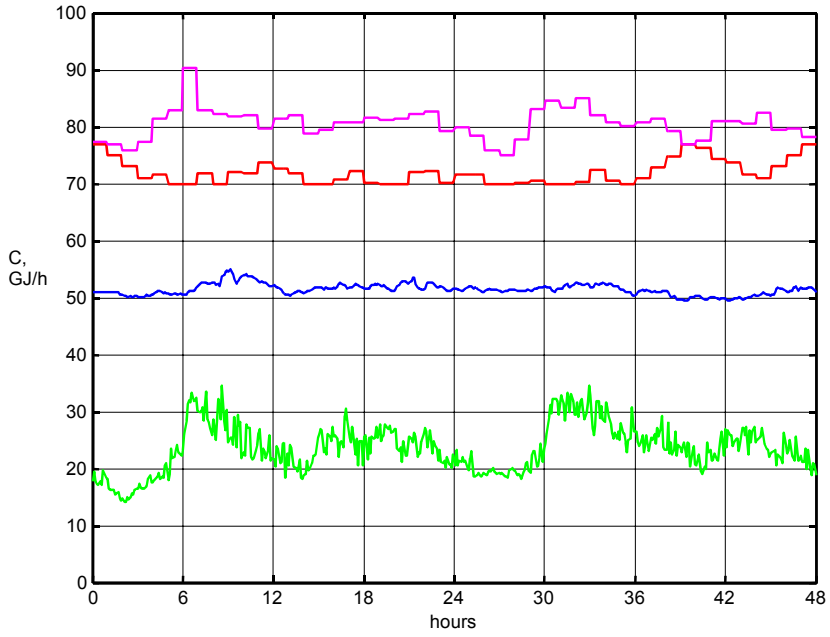

Figure 4.13. R02 Broparken week 33. Optimum supply temperature curve (red), the corresponding return temperature (blue) and the total heat load in the buildings (green) multiplied by a factor of 10. The pink curve is the measured supply temperature.

Case 4F shows that for a DH system like Roedovre R02 with a high line heat demand (low heat loss) and with the actual heat load (summer situation) and costs of fuel and electricity, the optimum supply temperature is in the range 70 -75 ºC.

Chapter 5 Operational optimisation with an incentive tariff

In this chapter we will discuss optimum operation of the selected DH systems when the incentive tariff described in chapter 4.2 is applied. Only the DH systems connected to the VEKS transmission system will be considered.

Case 5A: Ishoej DH system, Dec. 19, 12:00 – Dec. 21, 12:00, 2000

Model: IV_5 (P05-K05).

The maximum permissible change of supply temperature per hour is set to be 1 ˚C.

Table 5.1 shows the costs of operating the system for 48 hours for the following cases:

A constant supply temperature of 115, 105 and 90 ˚C, representing the maximum, the actual and the minimum supply temperature from the DH plant.

Furthermore the table shows the optimum temperature, and the optimum temperature when the price of electricity is zero and the pump does not violate the pump constraints (the pump curve). The latter solution is not optimal when the pumping cost is included.

The optimum operational cost is -327 DKK for the two day period, which should be compared the the cost of 171,522 DKK for heating the buildings. It should be remembered that the fixed cost is not included in the optimisation and the negative cost should be regarded as a reduction of the fixed cost paid to VEKS.

Table 5.1. Ishoej DH system. Operational costs for 48 hours.

	115 °C	**OPTIMUM**	**105 °C**	**Optimum solution for Ppower = 0 and pump constraints active**	**90 °C constraints violated**
Dynamic Heat Storage, GJ	66.30	58.09	60.57	57.65	48.07
Pumping, GJ	1.55	3.61	2.70	3.79	9.65
Costs, DKK	3752	4024	3847	4081	5513
f 1 **f 2**	0.9822 1.0109	0.9756 1.0012	0.9820 1.0108	0.9762 1.0017	0.9804 1.0098
Tr 1 **Tr 2**	51.25 50.91	52.58 52.11	52.09 51.67	52.64 52.21	54.86 54.17
Incentive, DKK	-3446	-4363	-2928	-4189	-1427
Adjusted costs, DKK	314	-327	931	-107	4111

P fuel = 48.91 DKK/GJ, P power = 327.78 DKK/GJ, Q buildings = 3,507 GJ ≈ 171,522 DKK.

Figure 5.1 shows the optimum supply curve, the corresponding return temperature and the heat load.

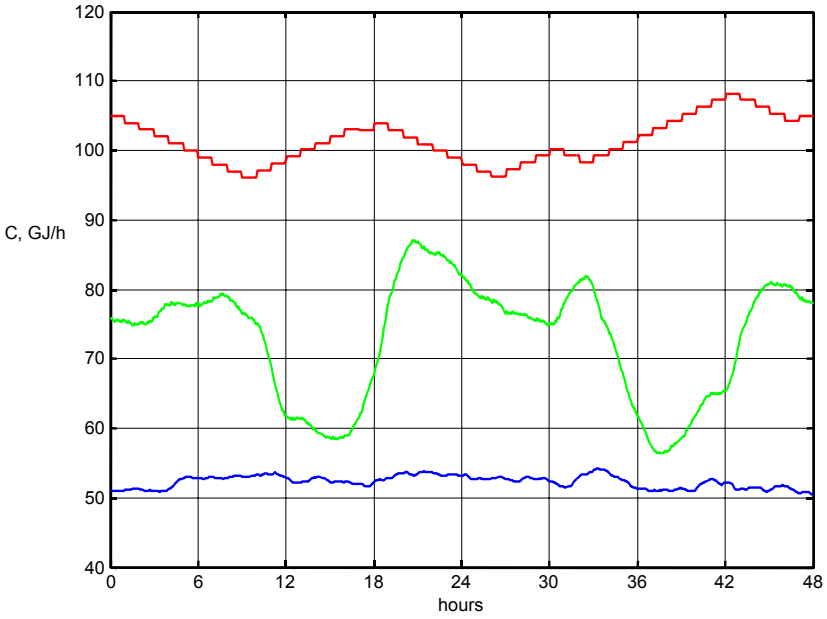

Figure 5.1. IV_5. Optimum supply temperature curve (red), the corresponding return temperature (blue) and the total heat load in the buildings (green).

The ordinary operational costs (heat loss and pumping) are bigger in the optimum solution when the penalty is included in the optimisation than when not included. However, the optimum solution seeks to reduce the load factor f and the return temperature at the plant, thus resulting in a negative operational cost. It appears from Figure 5.1 that the optimum supply temperature follows the variation in the total heat load, but starts to rise before the heat load does and vice versa.

Case 5A shows that the penalty function has a big influence compared with the heat loss and pumping costs. Even small changes (reductions) in the load factor f and the return temperature at the plant has a significant influence on the optimum solution.

Case 5D: Roedovre subsystem R01 Madumvej, week 2 in January 2003

Model: Full description. The maximum permissible change of supply temperature per hour is set to be 2 ˚C.

Table 5.2 shows the costs of operating the system for 48 hours for the following cases:

A constant supply temperature of 100 and 85 ˚C, representing the maximum and the minimum supply temperature from the DH plant.

Furthermore the table shows the optimum temperature, the measured temperature and the optimum temperature when the price of electricity is zero and the pump does not violate the pump constraints (the pump curve).

The optimum operational cost is 75 DKK for the two day period, which should be compared the the cost of 27,574 DKK for heating the buildings. It should be remembered that the fixed cost is not included in the optimisation.

Table 5.2. R01 Madumvej week 2. Operational costs for 48 hours.

	100 ºC	OPTIMUM	Measured Ts	Optimum solution for Ppower = 0 and pump constraints active	85 ºC
Dynamic Heat Storage, GJ	20.74	18.63	19.12	18.05	18.11
Pumping, GJ	0.42	0.88	0.67	1.18	1.09
Costs, DKK	1153	1201	1153	1269	1244
f 1 **f 2**	0.9446 0.9741	0.9365 0.9616	0.9471 0.9760	0.9385 0.9631	0.9454 0.9747
Tr 1 **Tr 2**	56.12 55.32	57.88 56.85	56.94 56.17	58.53 57.62	58.58 57.54
Incentive, DKK	-1033	-1126	-879	-998	-752
Adjusted costs, DKK	120	75	274	271	492

P fuel = 48.91 DKK/GJ, P power = 327.78 DKK/GJ, Q buildings = 564 GJ ≈ 27,574 DKK.

Figure 5.2 shows the optimum supply curve, the corresponding return temperature and the heat load.

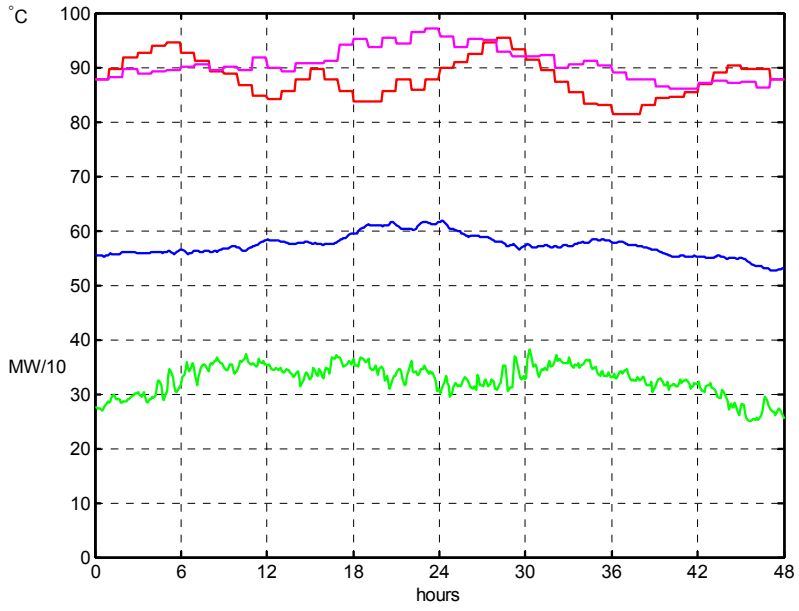

Figure 5.2. R01 Madumvej week 2. Optimum supply temperature (red), the corresponding return temperature (blue) and the total heat load in the buildings (green).
The pink curve is the measured supply temperature.

As in the Ishoej case, the ordinary operational costs (heat loss and pumping) are bigger in the optimum solution when the penalty is included in the optimisation than when not included. However, the optimum solution seeks to reduce the load factor f and the return temperature at the plant, thus reducing the operational costs considerable.

Case 5E: Roedovre subsystem R01 Madumvej, week 13, March 2003

Model: Full description. The maximum permissible change of supply temperature per hour is set to be 2 ˚C.

Table 5.3 shows the costs of operating the system for 48 hours for the following cases:

A constant supply temperature of 100 and 80 ˚C, representing the maximum and the minimum supply temperature from the DH plant.

Furthermore the table shows the optimum temperature, the measured temperature and the optimum temperature when the price of electricity is zero and the pump does not violate the pump constraints (the pump curve).

The optimum operational cost is 2070 DKK for the two day period, which should be compared the the cost of 27,574 DKK for heating the buildings. It should be remembered that the fixed cost is not included in the optimisation.

Table 5.3. R01 Madumvej week 13. Operational costs for 48 hours.

	100 ºC	**OPTIMUM**	**Measured Ts**	**Optimum solution for Ppower = 0 and pump constraints active**	**80 ºC**
Dynamic Heat Storage, GJ	20.88	19.09	18.81	19.03	18.31
Pumping, GJ	0.18	0.30	0.29	0.32	0.31
Costs, DKK	1079	1031	1013	1037	997
f 1 **f 2**	1.0994 1.1515	1.0727 1.1201	1.1033 1.1641	1.0729 1.1202	1.1011 1.1547
Tr 1 **Tr 2**	49.57 47.61	51.59 48.54	51.48 49.85	51.79 48.56	51.85 49.87
Incentive, DKK	1365	1038	1586	1046	1514
Adjusted costs, DKK	2444	2070	2599	2084	2511

P fuel = 48.91 DKK/GJ, P power = 327.78 DKK/GJ, Q buildings = 277 GJ ≈ 13,548 DKK.

Figure 5.3 shows the optimum supply curve, the corresponding return temperature and the heat load.

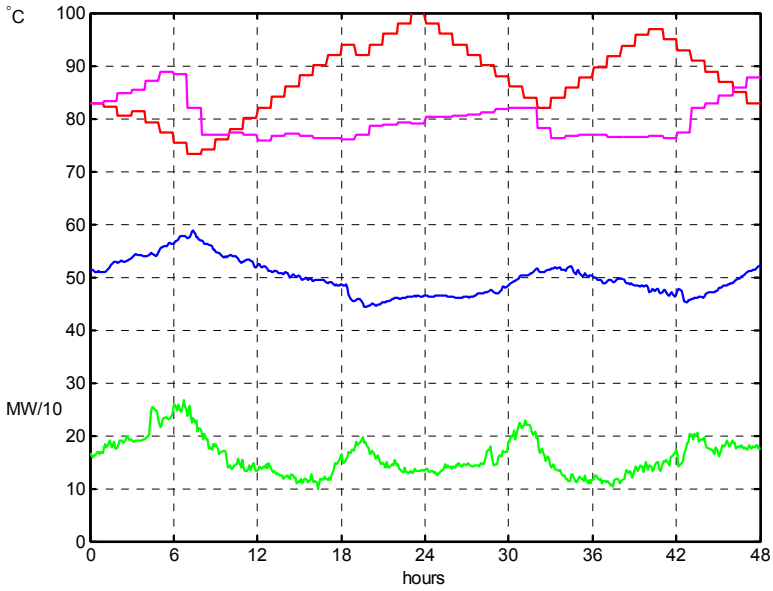

Figure 5.3. R01 Madumvej week 13. Optimum supply temperature (red), the corresponding return temperature (blue) and the total heat load in the buildings (green). The pink curve is the measured supply temperature.

In this case it is not possible to obtain a load factor below 1 due to the large variations in the heat load and consequently the adjusted costs are higher compared with the previous case. It is also not clear why the optimum supply temperature curve varies in time as it does compared with the heat load variations.

Calculation time:

When option –e is applied, the heat exchanger equations are not solved in every time step.

One simulation takes 0.7 seconds, and it takes approximately 39 minutes on a 2.6 GHz PC to obtain the optimum solution (20 iterations).

Case 5F: Roedovre Subsystem 01, Week 13, March 2003

Model: Model: R011303_5 (P05-K05). Aggregated models for temperature and pressure with 5 pipes. The maximum permissible change of supply temperature per hour is set to be 2 ˚C.

Calculation time:

When option –e is applied, the heat exchanger equations are not solved. Instead of 14 consumers in the full model we now have 5 consumers in the thermal and 6 consumers in the pressure model (One of these loads is located at the DH plant). One simulation takes 0.29 seconds, and it takes approximately 7 minutes and 5 iterations on a 2.6 GHz PC to obtain the optimum solution. The benefit of using an aggregated model of the DH system is smaller in this case than when the heat exchanger equations must be solved (case B).

Case 5G: Roedovre subsystem R02 Broparken, week 33, August 2003

Model: Full description. The maximum permissible change of supply temperature per hour is set to be 2 ˚C.

Table 5.4 shows the costs of operating the system for 48 hours for the following cases:

A constant supply temperature of 100 and 70 ˚C, representing the maximum and the minimum supply temperature from the DH plant.

Furthermore the table shows the optimum temperature, the measured temperature and the optimum temperature when the price of electricity is zero and the pump does not violate the pump constraints (the pump curve).

The optimum operational cost is 690 DKK for the two day period, which should be compared the the cost of 5527 DKK for heating the buildings. It should be remembered that the fixed cost is not included in the optimisation.

Table 5.4. R02 Broparken week 33. Operational costs for 48 hours.

	100 ºC	**OPTIMUM**	**Measured Ts**	**Optimum solution for Ppower = 0 and pump constraints active**	**70 ºC**
Dynamic Heat Storage, GJ	23.32	18.59	20.24	18.57	18.29
Pumping, GJ	0.16	0.19	0.17	0.19	0.21
Costs, DKK	1192	973	1046	972	962
f 1 **f 2**	1.0055 1.0503	0.9653 0.9713	1.0535 1.1077	0.9656 0.9712	1.0108 1.0434
Tr 1 **Tr 2**	46.57 45.98	51.54 51.11	49.01 48.13	51.57 51.12	53.02 51.88
Incentive, DKK	-50	-283	331	-282	101
Adjusted costs, DKK	1143	690	1378	690	1064

P fuel = 48.91 DKK/GJ, P power = 327.78 DKK/GJ, Q buildings = 113 GJ ≈ 5,527 DKK.

Figure 5.4 shows the optimum supply curve, the corresponding return temperature and the heat load.

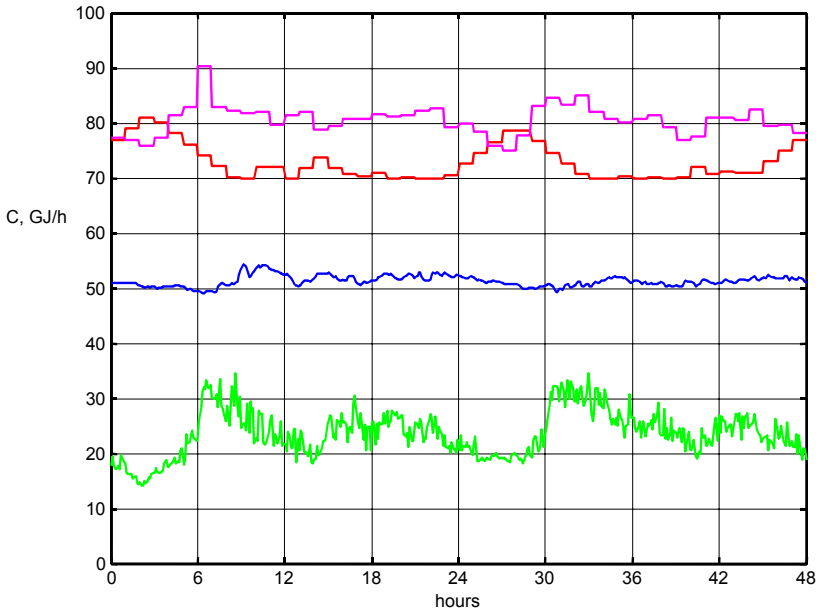

Figure 5.4. R02 Broparken week 33. Optimum supply temperature (red), the corresponding return temperature (blue) and the total heat load in the buildings (green) multiplied by a factor of 10. The pink curve is the measured supply temperature.

It is also not clear why the optimum supply temperature curve varies in time as it does compared with the heat load variations. In this summer case the penalty is not big and the optimum supply temperature curves are similar with and without the incentive tariff.

In all of the Roedovre cases 5D, 5E and 5G we see a significant influence of the incentive tariff. In the winter and spring case the incentive tariff influences the level of the optimum supply temperature curve.

The possibility to change the load factor by changing the supply temperature - and thus the flow and the heat production - is rather limited and in case 5E, it is not possible to reduce the load factor below 1.

It should be observed that the return temperature from the buildings is based on a model (option –e) that has not been verified in the real DH system.

It should also be remembered that the results from the investigated DH systems can not directly be used for other DH systems. For instance the pump constraints in Roedovre are seldom active due to the design of the pipe network (oversized pipes).

Chapter 6 Operational optimisation with DSM measures (20% peak reduction)

In this chapter we will discuss the influence of Demand Side Management applied in the buildings. First we will consider the case with 20% peak reduction in all buildings, i.e. the peaks as well as the "valleys" are even out by 20%, but the mean value of the heat load is preserved. This approach is illustrated in Figure 6.5 for one of the buildings in Roedovre. This way of changing the heat load does not take into account the control system in building and the heat capacity of the building.

Figure 6.1 is a more accurate picture of DSM and peak shaving, but it is beyond the scope of this project to model DSM measures in each building. Additional information on DSM in DH systems can be found in the following references: van der Meulen (1988), Sipilä and Kärkkäinen (2000), Wigbels et al. (2004).

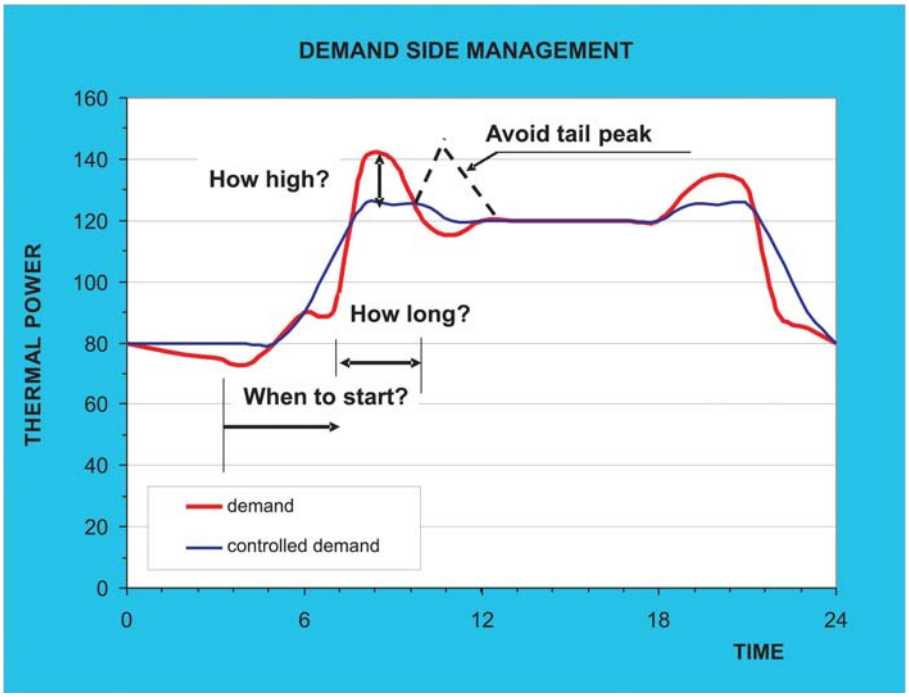

Figure 6.1. Principle of Demand Side Management. When is the heat supply to be stopped and for how long? How fast should the boosting take place, how is the DH plant affected? Bøhm et al. (2004).

In the following we will analyse the effect of a 20% reduction of the peaks for the DH systems connected to the VEKS transmission system.

Case 6A: Ishoej DH system, Dec. 19, 12:00 – Dec. 21, 12:00, 2000

Model: IV_5 (P05-K05).

The maximum permissible change of supply temperature per hour is set to be 1 ˚C. Table 6.1 shows the costs of operating the system for 48 hours. The optimum solution as well as constant supply temperature of 105 ˚C is shown.

Table 6.1. Ishoej DH system. Operational costs for 48 hours.

	OPTIMUM	**105 ºC**
Dynamic Heat Storage, GJ	57.52	60.57
Pumping, GJ	3.92	2.67
Costs, DKK	4,120	3,850
f 1 **f 2**	0.9604 0.9804	0.9655 0.9888
Tr 1 **Tr 2**	52.67 52.30	52.07 51.66
Incentive, DKK	-8,216	-7,162
Adjusted costs, DKK	-4,095	-3,312

P fuel = 48.91 DKK/GJ, P power = 327.78 DKK/GJ, Q buildings = 3,507 GJ ≈ 171,522 DKK.

The optimum opeational cost is –4,095 DKK for the two day period. Compared with case 5A we see a reduction of 3768 DKK for the two-day period. This has primarily been obtained by a reduction of the f-factor from 0.9756 to 0.9604 for day 1, and from 1.0012 to 0.9804 for day 2.

Figure 6.2 shows the optimum supply curve, the corresponding return temperature and the heat load.

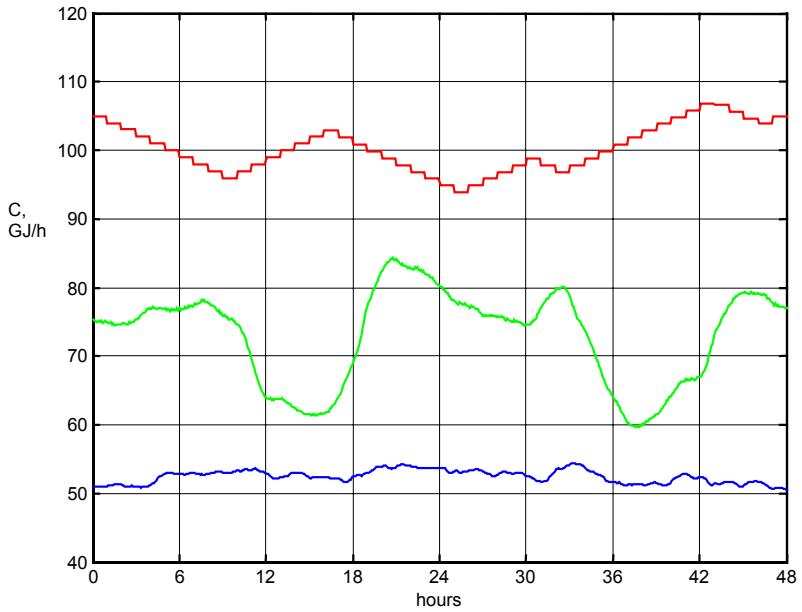

Figure 6.2. IV_5. Optimum supply temperature curve (red), the corresponding return temperature (blue) and the total heat load in the buildings (green) with 20% peak reduction.

Case 6D: Roedovre subsystem R01 Madumvej, week 2 in January 2003

Model: Full description. The maximum permissible change of supply temperature per hour is set to be 2 ˚C.

Table 6.2 shows the costs of operating the system for 48 hours. The optimum solution as well as applying the measured supply temperature is shown.

Table 6.2. R01 DH system week 2. Operational costs for 48 hours.

	OPTIMUM	**Measured Ts**
Dynamic Heat Storage, GJ	18.46	19.11
Pumping, GJ	0.97	0.67
Costs, DKK	1221	1153
f 1 **f 2**	0.9301 0.9490	0.9388 0.9616
Tr 1 **Tr 2**	58.18 57.02	56.93 56.18
Incentive, DKK	-1353	-1185
Adjusted costs, DKK	-132	-32

P fuel = 48.91 DKK/GJ, P power = 327.78 DKK/GJ, Q buildings = 564 GJ ≈ 27,574 DKK.

Figure 6.3 shows the optimum supply curve, the corresponding return temperature and the heat load.

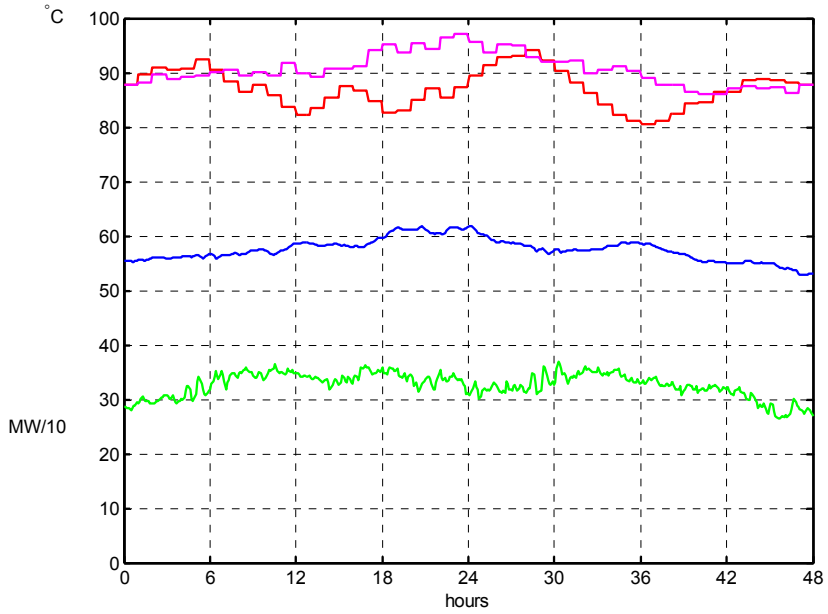

Figure 6.3. R01 Madumvej week 2. Optimum supply temperature curve (red), the corresponding return temperature (blue) and the total heat load in the buildings (green) with 20% peak reduction. The pink curve shows the measured supply temperature. Please, observe the scaling of the heat load.

Case 6E: Roedovre subsystem R01 Madumvej, week 13, March 2003

Model: Full description. The maximum permissible change of supply temperature per hour is set to be 2 ˚C.

Table 6.3 shows the costs of operating the system for 48 hours. The optimum solution as well as applying the measured supply temperature is shown.

Table 6.3. R01 Madumvej week 13. Operational costs for 48 hours

	OPTIMUM	**Measured Ts**
Dynamic Heat Storage, GJ	18.59	18.75
Pumping, GJ	0.32	0.28
Costs, DKK	1014	1010
f 1 **f 2**	1.0408 1.0783	1.0671 1.1180
Tr 1 **Tr 2**	51.87 49.01	51.43 49.90
Incentive, DKK	556	1023
Adjusted costs, DKK	1570	2033

P fuel = 48.91 DKK/GJ, P power = 327.78 DKK/GJ, Q buildings = 277 GJ ≈ 13,548 DKK.

Compared with case 5E we see a reduction of 500 DKK for the two day period. This has primarily been obtained by a reduction of the f-factor from 1.0727 to 1.0408 for day 1, and from 1.1201 to 1.0783 for day 2.

Figure 6.4 shows the optimum supply curve, the corresponding return temperature and the heat load, and Figure 6.5 shows the effect of 20% peak reduction for building L1-05.

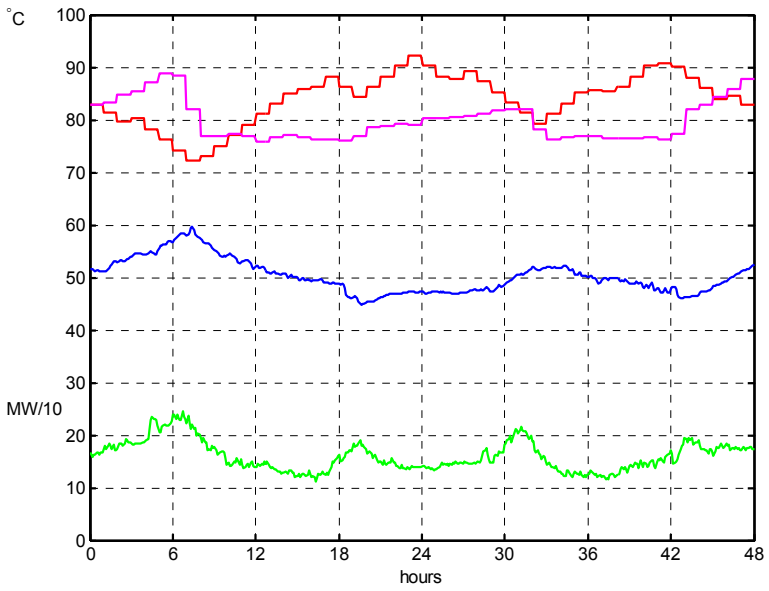

Figure 6.4. R01 Madumvej week 13. Optimum supply temperature curve (red), the corresponding return temperature (blue) and the total heat load in the buildings (green) with 20% peak reduction. The pink curve shows the measured supply temperature. Please, observe the scaling of the heat load.

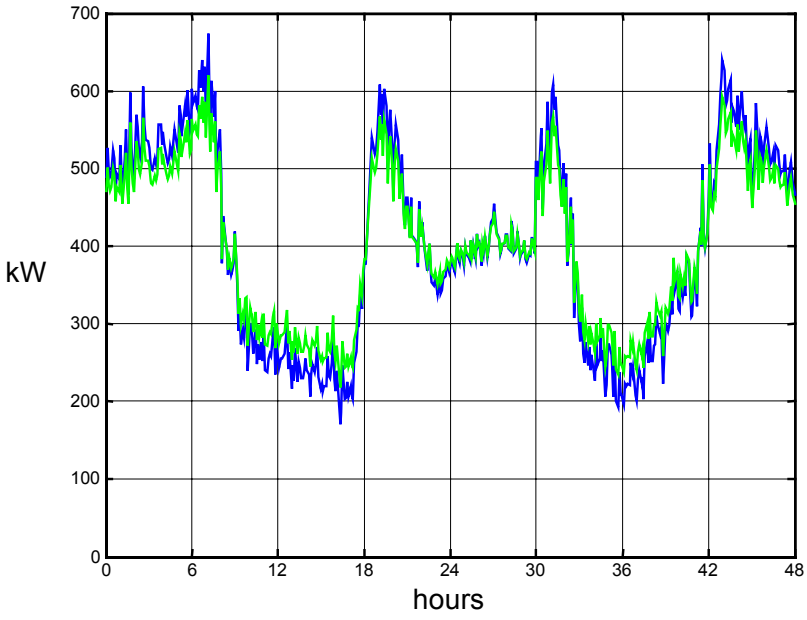

Figure 6.5. L1-05 with (green) and without (blue) 20% DSM.

Case 6G: Roedovre subsystem R02 Broparken, week 33, August 2003

Model: Full description. The maximum permissible change of supply temperature per hour is set to be 2 ˚C.

Table 6.4 shows the costs of operating the system for 48 hours. The optimum solution as well as applying the measured supply temperature is shown.

Table 6.4. R02 DH system week 33. Operational costs for 48 hours.

	OPTIMUM	**Measured Ts**
Dynamic Heat Storage, GJ	18.57	20.23
Pumping, GJ	0.20	0.17
Costs, DKK	972	1046
f 1 **f 2**	0.9461 0.9520	1.0338 1.0799
Tr 1 **Tr 2**	51.66 51.41	49.10 48.18
Incentive, DKK	-394	187
Adjusted costs, DKK	578	1233

P fuel = 48.91 DKK/GJ, P power = 327.78 DKK/GJ, Q buildings = 113 GJ ≈ 5,527 DKK.

Figure 6.6 shows the optimum supply curve, the corresponding return temperature and the heat load.

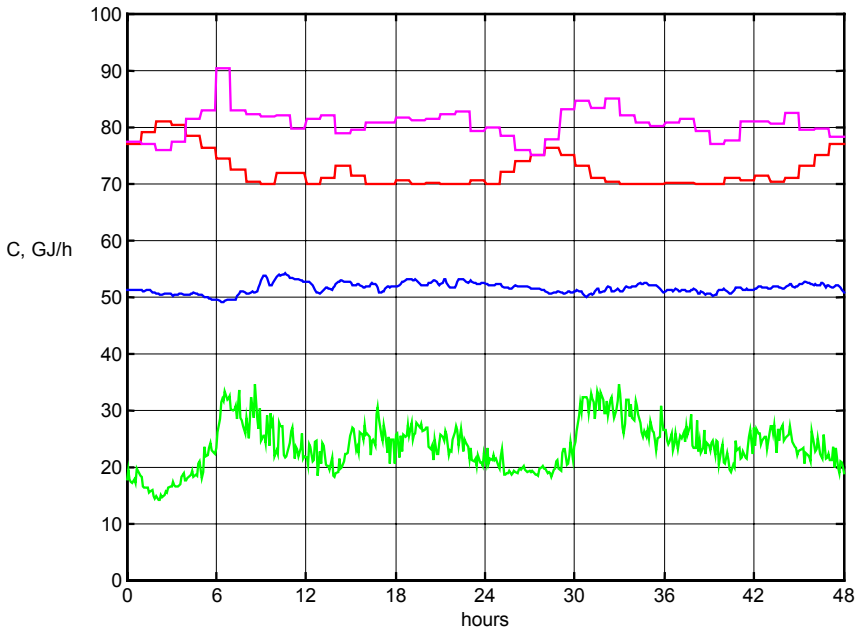

Figure 6.6. R02 Broparken week 33. Optimum supply temperature (red), the corresponding return temperature (blue) and the total heat load in the buildings (green) multiplied by a factor of 10. The pink curve is the measured supply temperature.

Chapter 7 Operational optimisation with DSM measures (50% peak reduction)

In Chapters 7 and 8 we will further investigate the effect of DSM measures. As our case study we will use R01 Madumvej week 13, where the biggest load variations occur. The effect of 50 and 80% peak reduction will be analysed.

Case 7E: Roedovre subsystem R01 Madumvej, week 13, March 2003

Model: Full description. The maximum permissible change of supply temperature per hour is set to be 2 ˚C.

Table 7.1 shows the costs of operating the system for 48 hours. The optimum solution as well as applying the measured supply temperature is shown.

Table 7.1. R01 Madumvej week 13. Operational costs for 48 hours.

	OPTIMUM	**Measured Ts**
Dynamic Heat Storage, GJ	18.46	18.65
Pumping, GJ	0.30	0.28
Costs, DKK	1003	1004
f 1 **f 2**	0.9859 1.0095	1.0133 1.0501
Tr 1 **Tr 2**	51.77 49.18	51.36 49.98
Incentive, DKK	-287	191
Adjusted costs, DKK	715	1195

P fuel = 48.91 DKK/GJ, P power = 327.78 DKK/GJ, Q buildings = 277 GJ ≈ 13,548 DKK.

Compared with case 5E we see a reduction of 1355 DKK for the two day period. This has primarily been obtained by a reduction of the f-factor from 1.0727 to 0.9859 for day 1, and from 1.1201 to 1.0095 for day 2.

Figure 7.1 shows the optimum supply curve, the corresponding return temperature and the heat load, while Figure 7.2 shows the heat demand in building L1-05 with and without 50% peak reduction.

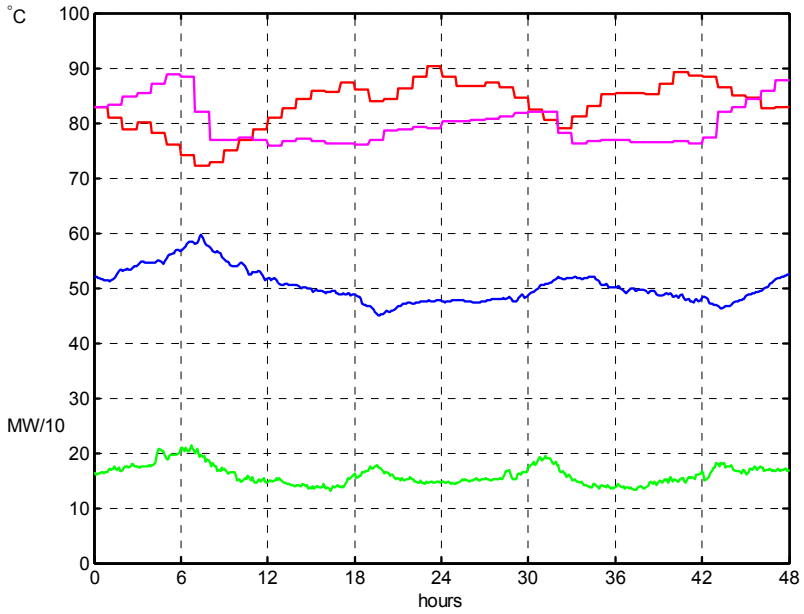

Figure 7.1. R01 Madumvej week 13. Optimum supply temperature curve (red), the corresponding return temperature (blue) and the total heat load in the buildings (green) with 50% peak reduction. The pink curve shows the measured supply temperature. Please, observe the scaling of the heat load.

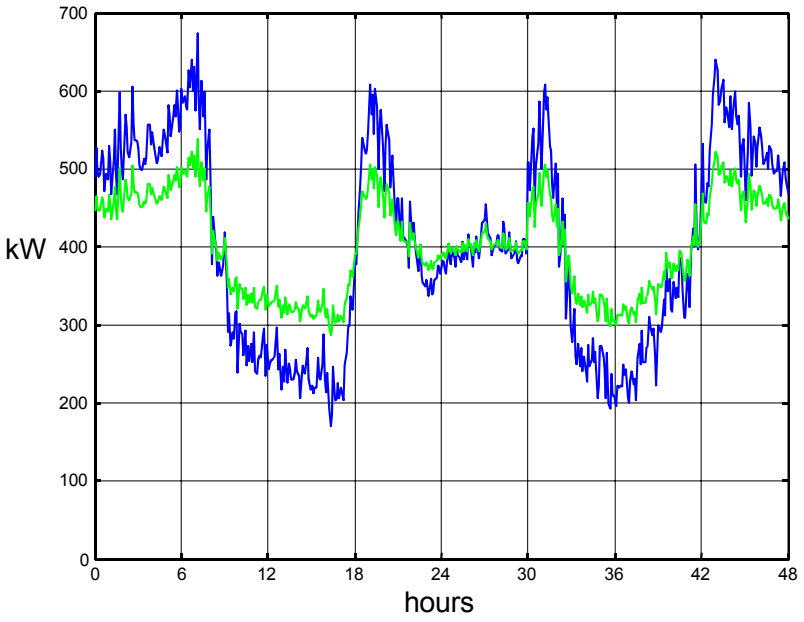

Figure 7.2. L1-05 with (green) and without (blue) 50% peak reduction.

Chapter 8 Operational optimisation with DSM measures (80% peak reduction)

Case 8E: Roedovre subsystem R01 Madumvej, week 13, March 2003

Model: Full description. The maximum permissible change of supply temperature per hour is set to be 2 ˚C.

Table 8.1 shows the costs of operating the system for 48 hours. The optimum solution as well as applying the measured supply temperature is shown.

Table 8.1. R01 Madumvej week 13. Operational costs for 48 hours.

	OPTIMUM	Measured Ts
Dynamic Heat Storage, GJ	18.28	18.53
Pumping, GJ	0.30	0.28
Costs, DKK	993	998
f 1 **f 2**	0.9330 0.9443	0.9631 0.9862
Tr 1 **Tr 2**	51.72 49.37	51.28 50.05
Incentive, DKK	-1091	-591
Adjusted costs, DKK	-98	407

P fuel = 48.91 DKK/GJ, P power = 327.78 DKK/GJ, Q buildings = 277 GJ ≈ 13,548 DKK.

Compared with case 5E we see a reduction of 2168 DKK for the two day period. This has primarily been obtained by a reduction of the f-factor from 1.0727 to 0.9330 for day 1, and from 1.1201 to 0.9443 for day 2.

Figure 8.1 shows the optimum supply curve, the corresponding return temperature and the heat load while Figure 8.2 shows the heat demand in building L1-05 with and without 80% peak reduction.

Table 8.2 summarises the effect of peak reduction by showing the adjusted operational costs for increasing peak reduction (0-80%).

Finally in Figure 8.3 it is shown how the optimum supply temperature curve is affected by the peak reduction. When the heat load variations are reduced by the peak reduction in the buildings, there is less need for changing the optimum supply temperature at the DH plant to reduce the f-factors. As a result we see a optimum supply temperature curve with less variations for 80% peak reduction compared with no peak reduction.

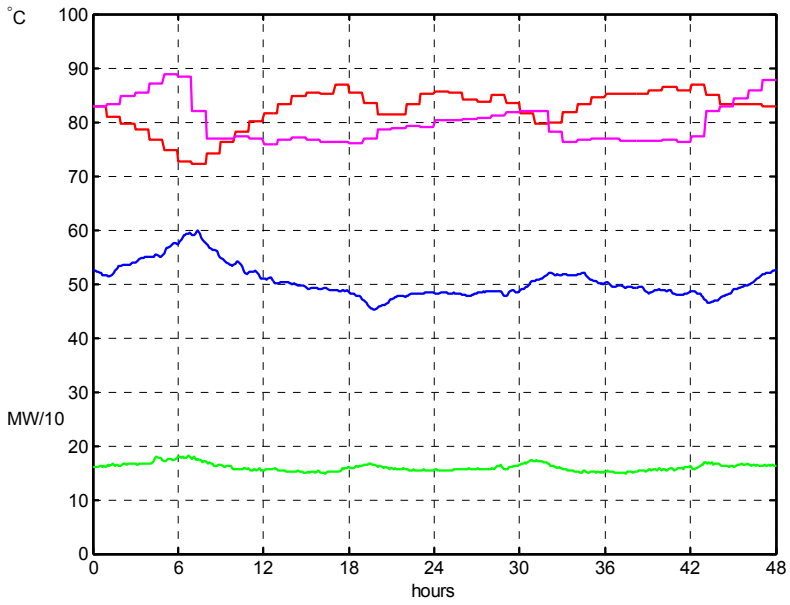

Figure 8.1. R01 Madumvej week 13. Optimum supply temperature curve (red), the corresponding return temperature (blue) and the total heat load in the buildings (green) with 80% peak reduction. The pink curve shows the measured supply temperature. Please, observe the scaling of the heat load.

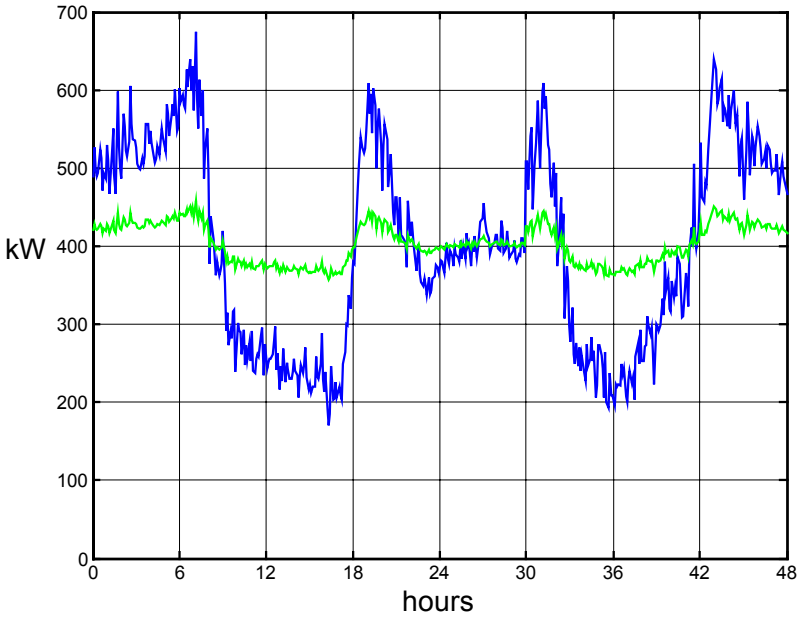

Figure 8.2. L1-05 with (green) and without (blue) 80% DSM.

Table 8.2. R01 Madumvej week 13. Adjusted operational costs for 48 hours.

	OPTIMUM	**Measured Ts**
No peak reduction	2070	2599
20 % reduction	1570	2033
50 % reduction	715	1195
80 % reduction	-98	407

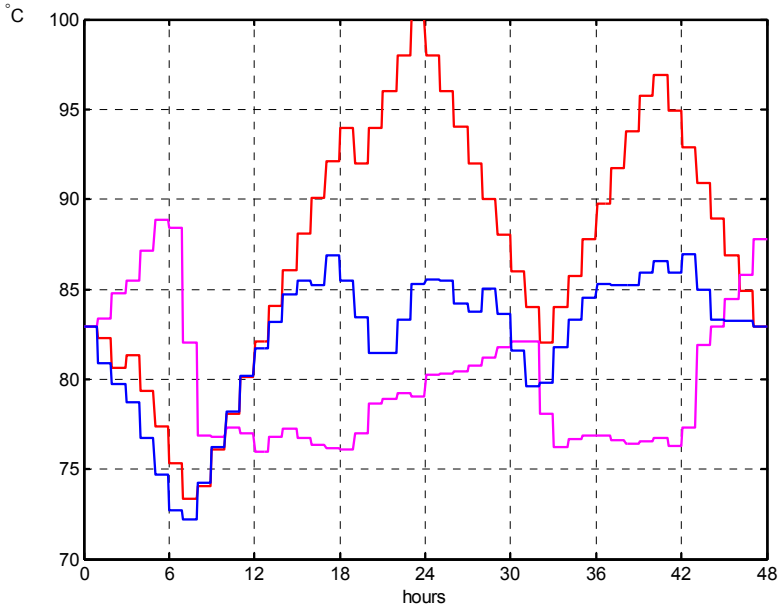

Figure 8.3. R01 Madumvej week 13. Optimum supply temperature curve for zero peak reduction (red), optimum supply temperature curve for 80 % peak reduction (blue), and the measured supply temperature (pink).

Chapter 9 A different way of finding the building heat loads, an on-line approach to operational optimisation

In Roedovre - as in some other DH systems using dataloggers in the house stations - the heat loads, flows and temperatures at the house station are transferred to the control room once every night. In order to use this information for optimisation purposes, the data must be processed and the time series in the simulation programme updated before the optimisation programme can start.

In order to avoid this rather time consuming process, discussions have taken place with Roedovre DH company to find a way of updating the simulation files in an easier way. The basic idea that was proposed was to use only the SCADA information which is allways available in the control room, and to find the heat loads at the house stations from the heat loads at the substation (DH plant).

Two preliminary tests have been carried out that will be discussed here. In the first one information from the substation as well as the house stations is utilised to find the heat load in every house station in every time step from the measured heat load at the substation. The result is a matrix with the heat load at each house station in percentage of the substation heat load. This gives a perfect match for the period considered, here week 13, 2003. The idea is then that this matrix only needs to be updated after a certain period, maybe once every month. To test the idea, the matrix for week 13 will be used for week 2, 2003 for subsystem R01 Madumvej, Case 9D.

In the second approach, it is assumed that the heat load in all house stations varies proportionally with the heat load at the substation (DH plant), Case 9E.

Case 9D: Roedovre subsystem R01 Madumvej, week 2 in January 2003

Model: Full description. The maximum permissible change of supply temperature per hour is set to be 2 ˚C.

The heat loads at the house stations are obtained from the heat load at the substation in week 2, and the load matrix from week 13. It should be noted that by this approach no correction is made for the different heat losses in percentage in week 2 and 13. The difference is about 3%. The return temperatures at the house stations are calculated by option –e, utilising the measured cooling time series for week 2.

Table 9.1 shows the result.

Table 9.1. R01 Madumvej week 2. **New heat loads.** Operational costs for 48 hours.

	Measured Ts Real heat loads	**Measured Ts** New heat loads	**OPTIMUM** Real heat loads	**OPTIMUM** New heat loads
Dynamic Heat Storage, GJ	19.12	19.25	18.63	18.96
Pumping, GJ	0.67	0.63	0.88	0.70
Costs, DKK	1153	1148	1201	1157
f 1 **f 2**	0.9471 0.9760	0.9783 1.0131	0.9365 0.9616	0.9644 0.9969
Tr 1 **Tr 2**	56.94 56.17	56.24 55.54	57.88 56.85	56.52 55.94
Incentive, DKK	-879	-37	-1126	-395
Adjusted costs, DKK	274	1112	75	762

P fuel = 48.91 DKK/GJ, P power = 327.78 DKK/GJ, Q buildings = 564 GJ ≈ 27,574 DKK (in case of the real heat loads).

It appears from Table 9.1 that by using the heat load variations from week 13 in week 2, the load variations at the plant are exaggerated and the penalty is increased compared with the original heat loads. Figure 9.1 shows the optimum supply temperature curves and the total heat loads.

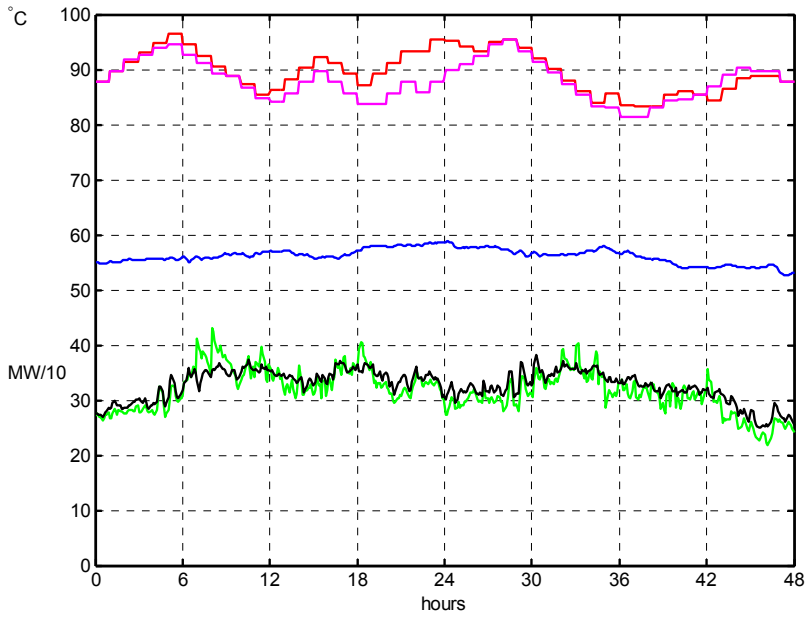

Figure 9.1. R01 Madumvej week 2. New heat loads. Optimum supply temperature (red), the corresponding return temperature (blue) and the total heat load in the buildings (green). The optimum supply temperature for the real heat loads is shown in pink and the real total heat load is shown in black.

The goal of the optimisation being the determination of the optimum supply temperature curve rather than determining the operational costs, it appears from Figure 9.1 that the two solutions (with new and real heat loads) do not differ much.

Case 9E: Roedovre subsystem R01 Madumvej, week 13, March 2003

Model: Full description. The maximum permissible change of supply temperature per hour is set to be 2 ˚C.

The heat loads at the house stations are obtained as a percentage of the heat load at the substation in week 13, with a reduction of 6.4% made for the heat loss in the network.

Table 9.2 shows the result.

Table 9.2. R01 Madumvej week 13. **New heat loads.** Operational costs for 48 hours.

	Measured Ts Real heat loads	**Measured Ts** New heat loads	**OPTIMUM** Real heat loads	**OPTIMUM** New heat loads
Dynamic Heat Storage, GJ	18.81	18.65	19.09	18.58
Pumping, GJ	0.29	0.28	0.30	0.33
Costs, DKK	1013	1005	1031	1016
f 1 **f 2**	1.1033 1.1641	1.1123 1.1831	1.0727 1.1201	1.0794 1.1343
Tr 1 **Tr 2**	51.48 49.85	51.49 50.05	51.59 48.54	51.92 49.04
Incentive, DKK	1586	1786	1038	1207
Adjusted costs, DKK	2599	2791	2070	2222

P fuel = 48.91 DKK/GJ, P power = 327.78 DKK/GJ, Q buildings = 277 GJ ≈ 13,548 DKK.

It appears from Table 9.2 that the load variations at the plant are slightly exaggerated when it is assumed at all loads in the house stations vary in the same manner. Thus the penalty is increased compared with the original heat loads. The difference is approximately 7%.

Figure 9.2 shows the optimum solution for the new heat loads in the buildings as well as the total heat loads. It appears from Figure 9.2 that the two solutions for the new and the real heat loads do not differ so much.

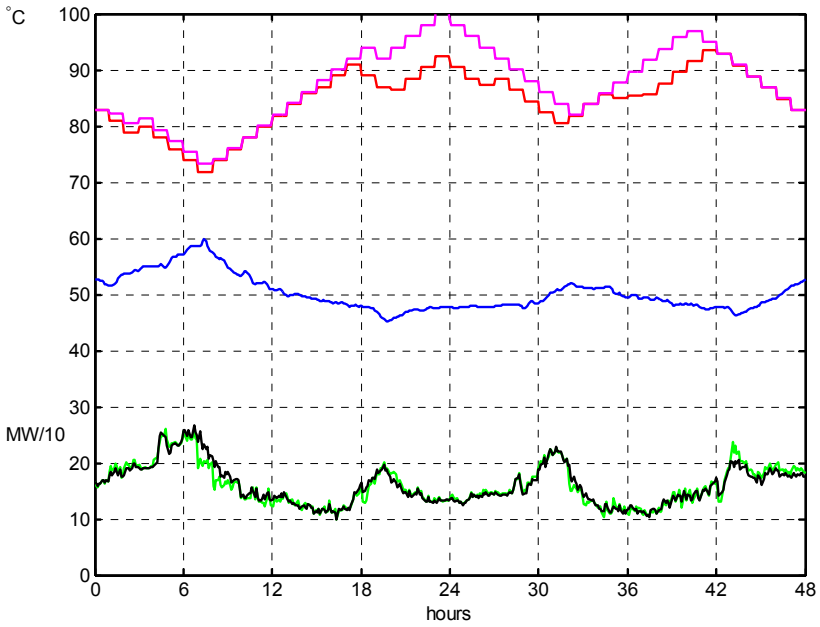

Figure 9.2. R01 Madumvej week 13. New heat loads. Optimum supply temperature (red), the corresponding return temperature (blue) and the total heat load in the buildings (green). The pink curve is the optimum solution for the real heat loads and the real total heat load is shown in black .

It appears that the results in case 9E are better than in case 9D. However, further work should be done to improve the methods of obtaining the heat loads in the buildings from the heat load at the substation (or DH plant).

References

Benonysson, A. (1991): ”Dynamic modelling and operational optimization of district heating systems”. Ph. D. dissertation. Technical University of Denmark. ISBN 87-38038-24-6.

Bøhm, B., Ha, S., Kim, W., Kim, B., Koljonen, T., Larsen, H.V., Lucht, M., Park, Y., Sipilä, K., Wigbels, M. and Wistbacka, M. (2002): “Simple models for operational optimisation”, IEA Annex VI, NOVEM, 2002. ISBN 90-5748-021-2.

Bøhm, B. and Danig, P.O. (2004): “Monitoring the energy consumption in a district heated apartment building in Copenhagen, with specific interest in the thermodynamic performance”. Energy and Buildings 36 (2004) 229-236.

Bøhm, B., Wigbels, M., Sipila, K., Hansen, B.S. and Jensen, G. (2004). ”Fup eller fakta om driftsoptimering”. Fjernvarmen 9/2004, pp. 20-22.

Larsen, H.V., Pálsson, H., Bøhm, B. and Ravn, H.F. (2002): “Aggregated dynamic simulation model of district heating networks”. Energy Conversion and Management, 43/8, pp. 995-1019.

Larsen, H.V., Bøhm, B. and Wigbels, M. (2004): “A Comparison of Aggregated Models for Simulation and Operational Optimisation of District Heating Networks”. Energy Conversion and Management (2004) 45/7-8, pp. 1119-1139.

Larsson, G (1999): “Dynamik i fjärrvärmesystem”. Dissertation, Dept. Thermo and Fluid Dynamics, Chalmers University of Technology. ISBN 91-7197-814-3.

Larsson, G (2003): “Flödesutjämnande körstrategi”. Svensk Fjärrvärme, FOU 2003:86.

Loewen, A. (2001): “Entwicklung eines Verfahrens zur Aggregation komplexer Fernwärmenetze”. Dissertation, Universität Dortmund. UMSICHT-Schriftenreihe Band 29, Fraunhofer IRB Verlag.

Loewen, A., Wigbels, M., Althaus, W., Augusiak, A., Renski, A. (2001): “Structural simplification of complex DH-networks”. Euroheat & Power 2001:46-50.

van der Meulen, S.F. (1988): “Load Management in District Heating Systems”, Energy and Buildings, 12 (1988) 179-189.

Pálsson, H. (1997): “Analysis of numerical methods for simulating temperature dynamics in district heating pipes”. Int. Symposium, Nordic Council of Ministers, Reykjavik, 1997.

Pálsson, H., Larsen, H.V., Bøhm, B., Ravn, H.F. and Zhou, J. (1999): “Equivalent models of district heating systems”. Department of Energy Engineering, Technical University of Denmark and Risoe National Laboratory, Systems Analysis Department. ISBN 87-7475-221-9, 179p.

Sipilä, K. and Kärkkäinen, S (2000): “Demand Side Management in District Heating Systems” Euroheat & Power-Fernwärme international 3/2000, pp. 36-45.

Tryggvason, G. (1999): “Modelling and operational analysis of district heating systems”. M.Sc. thesis ET-EP 99-15. Department of Energy Engineering, Technical University of Denmark.

Wigbels, M., Bøhm, B., Sipilä, K. (2004): “State of the art report”. IEA Annex VII project “Dynamic heat storage optimisation and demand side management”. Project is on-going.

Appendix A Roedovre district heating grids

This appendix gives data on outdoor temperature and average loads for the selected weeks, and data on DH grids of Madumvej and Broparken.

Average outdoor temperature in the selected weeks of 2003.

Week	Outdoor temperature
2	-4.2
13	6.6
19	13.3
23	19.7
33	21.6

Data measured at Roedovre.

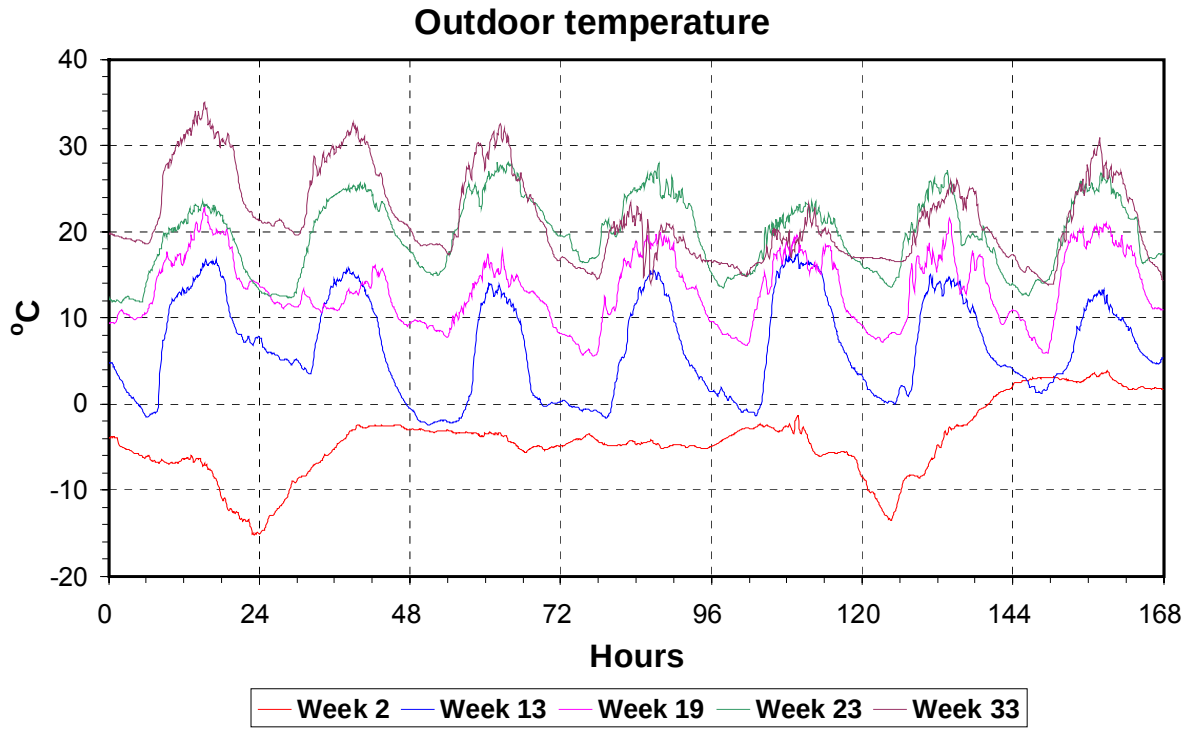

Madumvej: Average loads, MW.

Load	Week 2	Week 13	Week 23
L1-01	0.166	0.096	0.024
L1-02	0.202	0.090	0.000
L1-03	0.141	0.072	0.013
L1-04	0.319	0.187	0.026
L1-05	0.646	0.409	0.096
L1-06	0.296	0.146	0.039
L1-07	0.260	0.128	0.032
L1-08	0.390	0.228	0.063
L1-09	0.178	0.081	0.008
L1-10	0.088	0.041	0.006
L1-11	0.041	0.017	0.001
L1-12	0.115	0.051	0.004
L1-13	0.063	0.030	0.007
L1-14	0.040	0.014	0.002

Broparken: Average loads, MW.

Load	Week 2	Week 19	Week 33
L2-01	0.625	(a)	0.075
L2-02	0.209	0.062	0.028
L2-03	0.033	0.009	0.003
L2-04	0.070	0.014	0.009
L2-05	0.239	0.067	0.034
L2-06	0.223	0.071	0.034
L2-08	0.095	0.040	0.011
L2-09	0.158	0.048	0.017
L2-10	0.039	0.016	0.006
L2-11	0.069	0.017	0.002
L2-12	0.400	0.125	0.044
L2-13	0.256	0.067	0.030
L2-14	0.068	0.020	0.008
L2-16	0.161	0.015	0.005
L2-17	0.203	0.057	0.031
L2-18	0.646	0.195	0.096
L2-21	0.499	0.127	0.062
L2-22	0.112	0.030	0.012
L2-23	(b)	0.070	0.038
L2-24	(c)	0.060	0.060

(a) : Missing data.
(b) : Missing data.
(c) : New load not yet connected in week 2.

Madumvej: District heating grid and average flow.

Branch	Node A	Node B	Pipe type	Length	Flow Week 2	Flow Week 13	Flow Week 23
				m	kg/s	kg/s	kg/s
N07_N01	CENTRAL	N01	DN200	64	21.389	13.213	3.264
N01_N02	N01	N02	DN125	91	6.239	4.025	0.995
N01_N08	N01	N08	DN200	1	15.150	9.188	2.269
N02_N03	N02	N03	DN125	100	5.909	3.858	0.952
N02_N10	N02	N10	DN50	30	0.330	0.167	0.043
N08_N09	N08	N09	DN150	221	15.150	9.188	2.269
N03_N04	N03	N04	DN125	105	4.081	2.675	0.656
N03_N23	N03	N23	DN80	84	1.828	1.183	0.296
N09_N11	N09	N11	DN150	115	12.831	7.036	2.029
N09_N13	N09	N13	DN100	169	2.320	2.152	0.240
N04_N05	N04	N05	DN125	1	1.312	0.535	0.037
N04_N22	N04	N22	DN100	42	2.769	2.140	0.619
N11_N15	N11	N15	DN100	40	6.327	2.889	0.791
N05_N06	N05	N06	DN80	65	1.312	0.535	0.037
N15_N16	N15	N16	DN65	32	0.953	0.339	0.349
N15_N17	N15	N17	DN100	128	5.374	2.551	0.442
N14_N32	N11	N32	DN125	826	6.504	4.147	1.238
N17_N18	N17	N18	DN100	14	5.054	2.439	0.424
N17_N31	N17	N31	DN65	33	0.320	0.112	0.018
N32_N33	N32	N33	DN125	69	4.335	2.931	0.773
N32_N34	N32	N34	DN80	185	2.169	1.216	0.465
N18_N19	N18	N19	DN100	40	4.203	1.960	0.315
N18_N28	N18	N28	DN80	8	0.851	0.479	0.109
N19_N20	N19	N20	DN100	35	3.576	1.620	0.280
N19_N29	N19	N29	DN50	24	0.627	0.340	0.035
N20_N30	N20	N30	DN40	27	0.314	0.105	0.011
N21_N24	N20	N24	DN100	59	3.262	1.516	0.269
N24_N25	N24	N25	DN100	3	1.940	0.663	0.001
N24_N27	N24	N27	DN80	63	1.321	0.853	0.268
N25_N26	N25	N26	DN80	37	1.940	0.663	0.001

Broparken: District heating grid and average flow.

Branch	Node A	Node B	Pipe type	Length	Flow Week 2	Flow Week 19	Flow Week 33
				m	kg/s	kg/s	kg/s
CENTRAL	CENTRAL	N54+65	DN350	1	33.308	9.111	5.399
N54_N52	N54+65	N52	DN200	223	22.404	5.555	3.431
N65_N66	N54+65	N66	DN200	90	10.904	3.556	1.968
N52_N53	N52	N53	DN100	317	1.426	0.112	0.066
N66_N67	N66	N67	DN200	65	8.971	3.155	1.715
N66_N72	N66	N72	DN100	19	1.933	0.401	0.253
N67_N68	N67	N68	DN200	1	4.555	1.820	0.999
N67_N73	N67	N73	DN125	17	4.415	1.335	0.717
N56_N57	N52	N57	DN200	245	20.978		3.365
N68_N69	N68	N69	DN150	149	4.555	1.820	0.999
N57_N87	N57	N87	DN125	55	7.624		0.783
N58_N74	N57	N74	DN200	141	13.354	5.443	2.582
N60_N61	N69	N61	DN125	133	4.555	1.820	0.999
N74_N75	N74	N75	DN200	55	13.002	5.259	2.457
N74_N85	N74	N85	DN200	2	0.351	0.185	0.125
N61_N62	N61	N62	DN125	101	3.808	1.538	0.855
N61_N70	N61	N70	DN65	26	0.748	0.282	0.144
N75_N80	N75	N80	DN80	83		1.071	0.698
N85_N86	N85	N86	DN50	40	0.351	0.185	0.125
N62_N63	N62	N63	DN125	2		0.539	0.344
N62_N71	N62	N71	DN100	80	3.808	0.999	0.511
N76_N77	N75	N77	DN200	178	10.911	4.188	1.759
N80_N80A	N80	N80A	DN80	1	2.092	0.636	0.218
N80_N80B	N80	N80B	DN80	1		0.435	0.480
N63_N64	N63	N64	DN100	95		0.539	0.344
N77_N78	N77	N78	DN200	15	7.756	3.307	1.441
N77_N83	N77	N83	DN125	63	3.155	0.881	0.319
N78_N79	N78	N79	DN150	54	7.756	3.307	1.441
N79_N84	N79	N84	DN65	30	0.605	0.129	0.028
N48_N49	N79	N49	DN150	267	7.151	3.178	1.413
N49_N50	N49	N50	DN150	20	6.834	2.994	1.321
N49_N82	N49	N82	DN40	66	0.318	0.184	0.092
N50_N81	N50	N81	DN80	89	1.039	0.404	0.229
N43_N44	N50	N44	DN150	227	5.795	2.590	1.092
N44_N51	N44	N51	DN65	22	0.800	1.046	0.118
N38_N39	N44	N39	DN150	86	4.995	1.544	0.974
N39_N40	N39	N40	DN150	39	4.523	1.461	0.916
N39_N46	N39	N46	DN65	34	0.472	0.084	0.059
N40_N41	N40	N41	DN150	151	4.297	1.398	0.885
N40_N45	N40	N45	DN50	23	0.226	0.063	0.031
N41_N47	N41	N47	DN80	15	1.391	0.505	0.325
N35_N36	N41	N36	DN150	86	2.905	0.894	0.560
N36_N37	N36	N37	DN150	86	1.367	0.435	0.264
N36_N42	N36	N42	DN80	13	1.539	0.459	0.295

Pipe types.

DN	Steel pipe Inner diam.	Steel pipe Thickness	Steel pipe Surface roughness	Insulation Thickness	Mantle Thickness
	mm	mm	mm	mm	mm
DN40	43.1	2.6	0.1	28.4	2.5
DN50	54.5	2.9	0.1	29.9	2.5
DN65	70.3	2.9	0.1	29.0	3.0
DN80	82.5	3.2	0.1	32.6	3.0
DN100	107.1	3.6	0.1	39.7	3.2
DN125	132.5	3.6	0.1	39.2	3.5
DN150	160.3	4.0	0.1	37.0	3.9
DN200	210.1	4.5	0.1	43.1	4.9
DN350	344.4	5.6	0.1	65.5	6.7

Appendix B Measured time series in Roedovre

Substations (VEKS heat exchangers):

The following 6 figures show supply and return temperature (left axis) at the secondary side of the VEKS heat exchangers supplying Broparken and Madumvej. Also shown are power delivered to the DH grid and pressure head drop from the heat exchanger and out to the critical consumer (right axis). Pressure is scaled as indicated in the legend. In Madumvej the critical consumer with regard to pressure head is L1-06, and in Broparken it is L2-02.

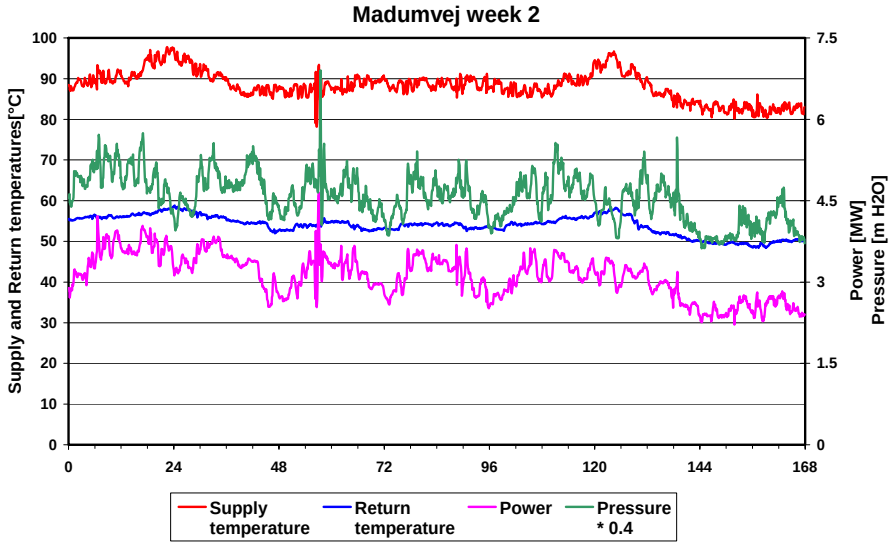

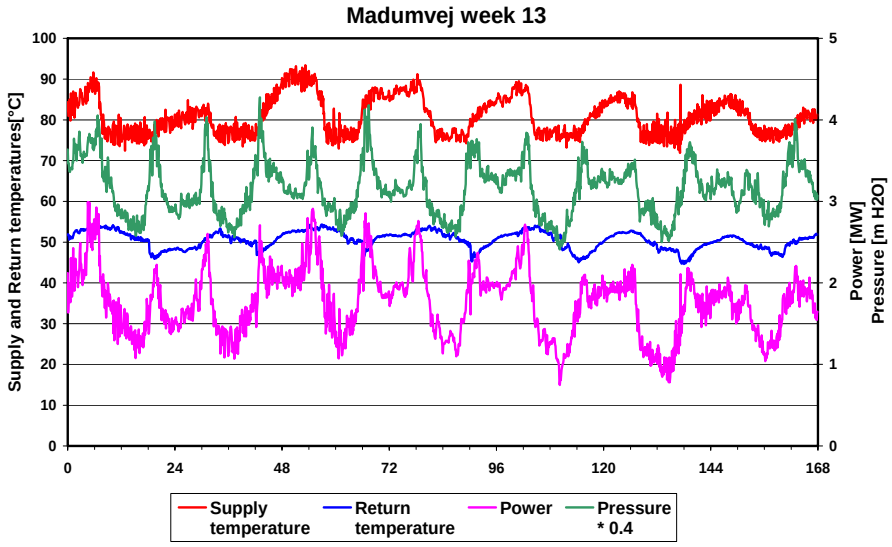

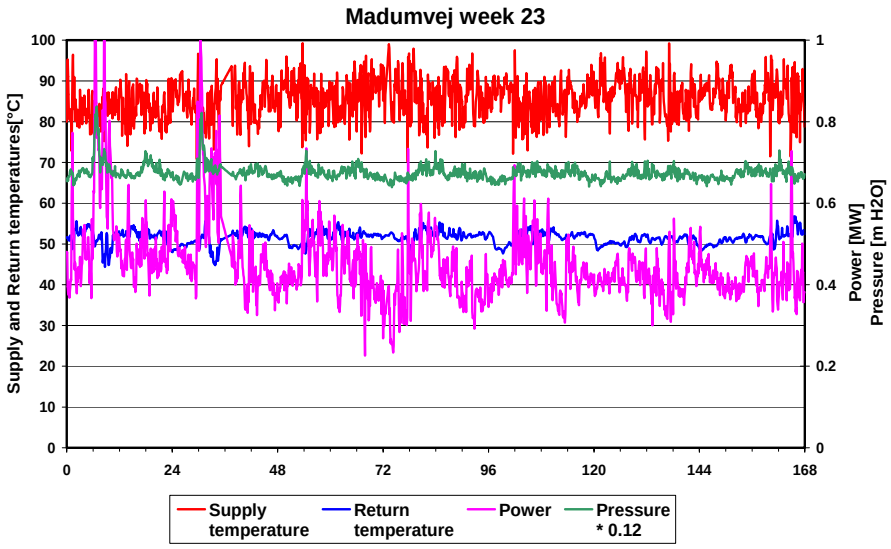
Madumvej week 23
Supply and Return temperatures[°C]
Power [MW]
Pressure [m H2O]
Supply temperature
Return temperature
Power
Pressure * 0.12

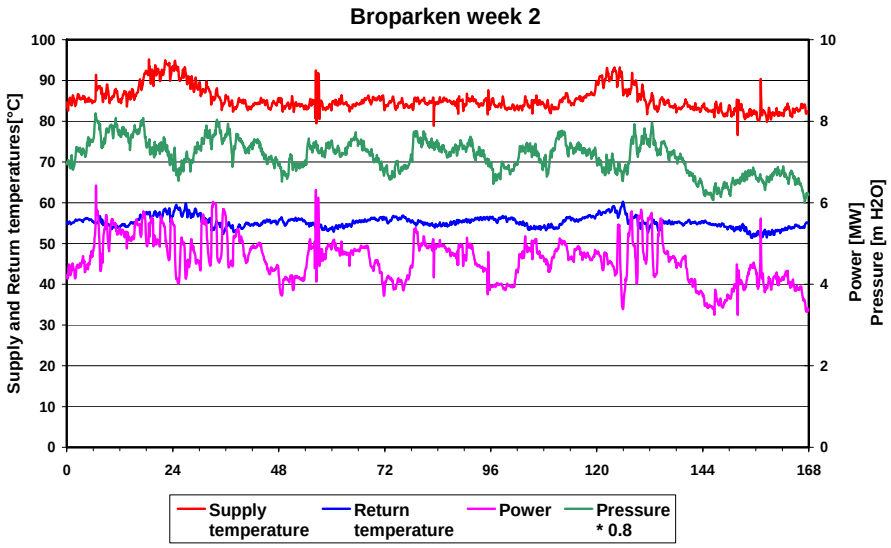
Broparken week 2
Supply and Return temperatures[°C]
Power [MW]
Pressure [m H2O]
Supply temperature
Return temperature
Power
Pressure * 0.8

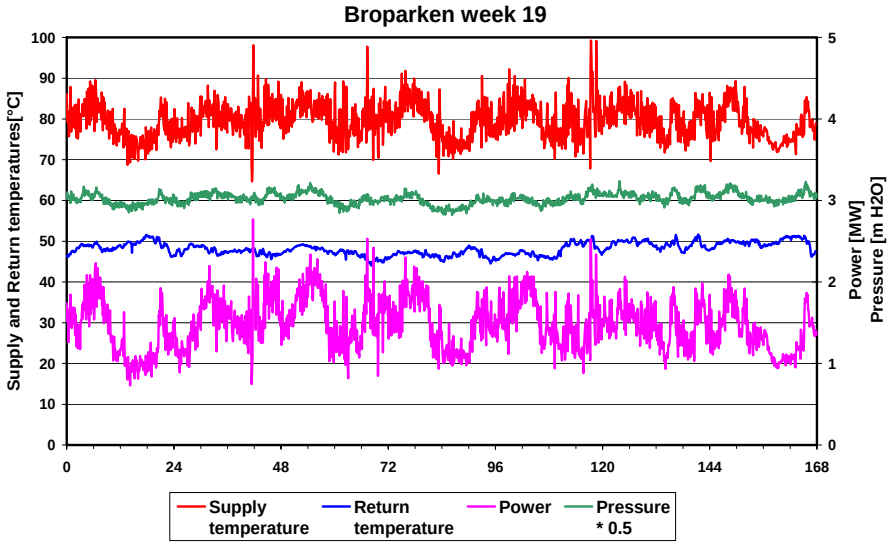
Broparken week 19
Supply and Return temperatures[°C]
Power [MW]
Pressure [m H2O]
Supply temperature
Return temperature
Power
Pressure * 0.5

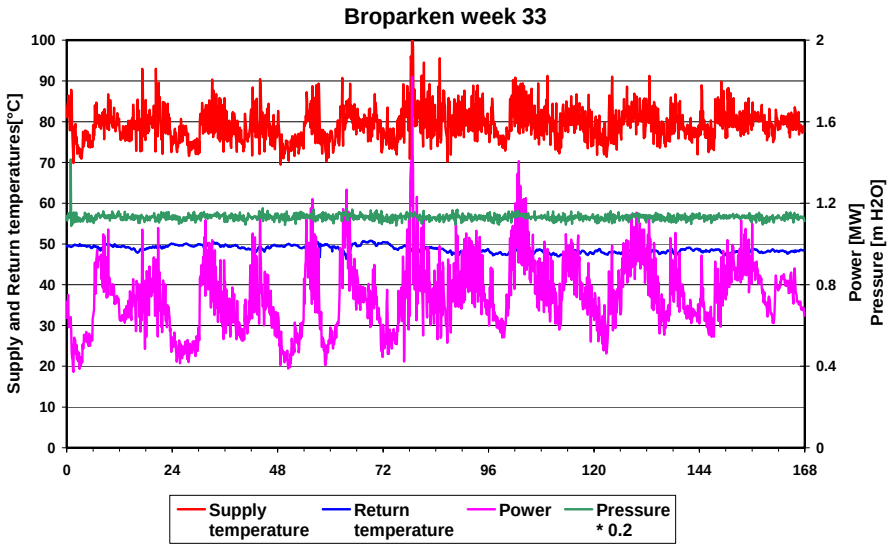
Broparken week 33
Supply and Return temperatures[°C]
Power [MW]
Pressure [m H2O]
100
90
80
70
60
50
40
30
20
10
0
2
1.6
1.2
0.8
0.4
0
0
24
48
72
96
120
144
168
Supply temperature
Return temperature
Power
Pressure * 0.2

Heat loads in R01 Madumvej:

For each of the consumers and each of the three weeks considered, measured time series for heat consumption and primary supply and return temperatures are shown in the following figures. In Madumvej there are 14 consumers.

Madumvej, week 2:

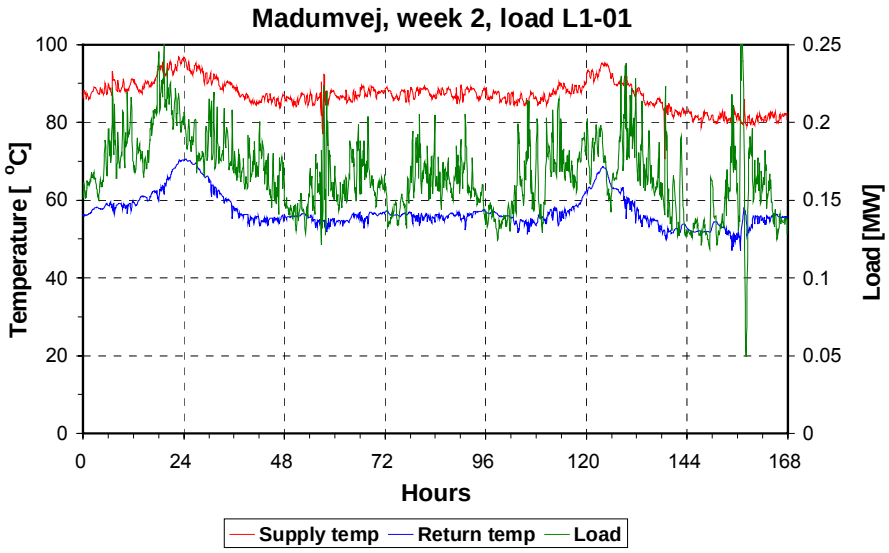

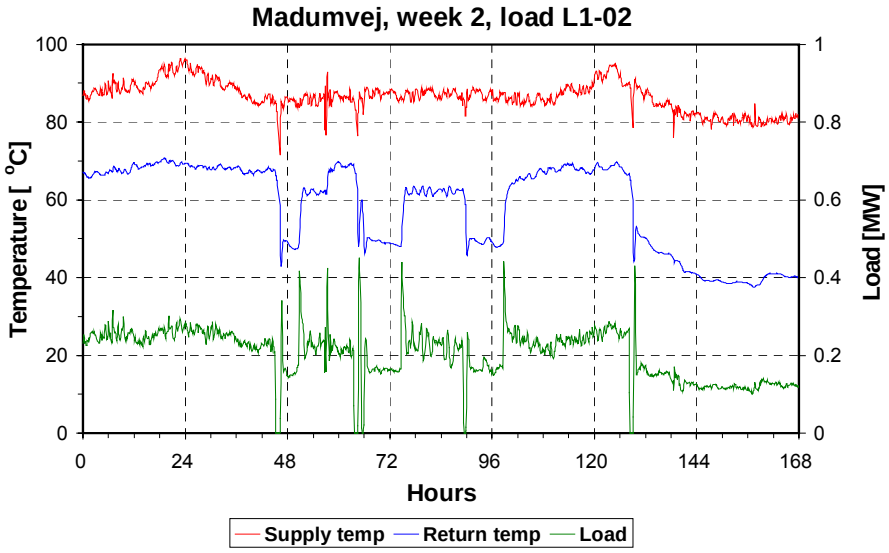

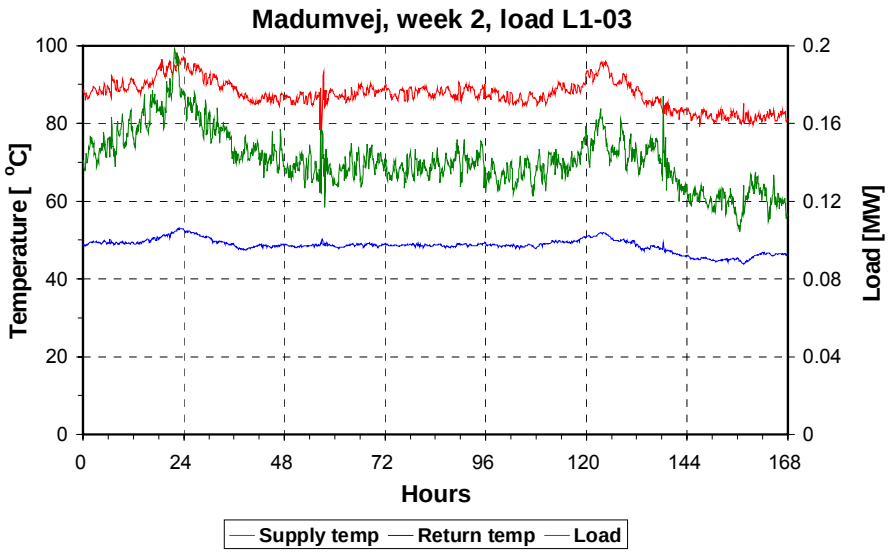
Madumvej, week 2, load L1-03
Temperature [°C]
Load [MW]
Hours
Supply temp
Return temp
Load

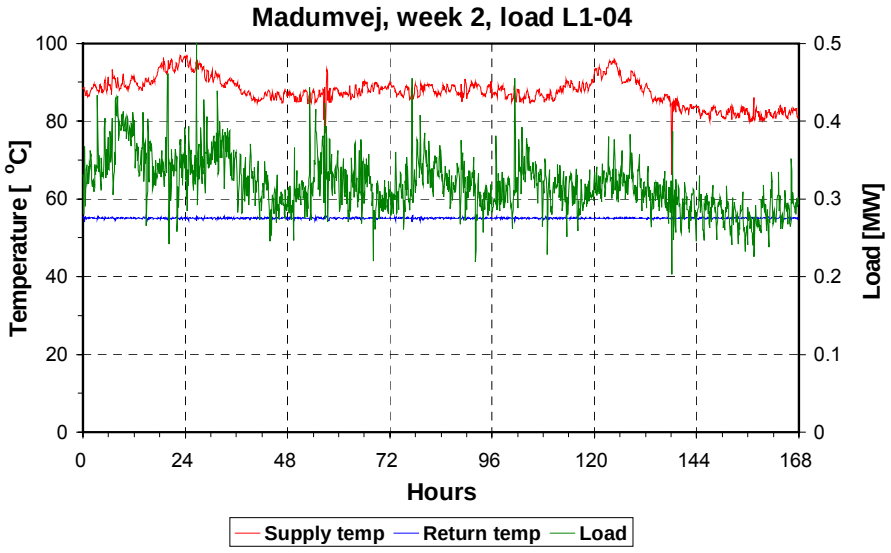
Madumvej, week 2, load L1-04
Temperature [°C]
Load [MW]
Hours
Supply temp
Return temp
Load

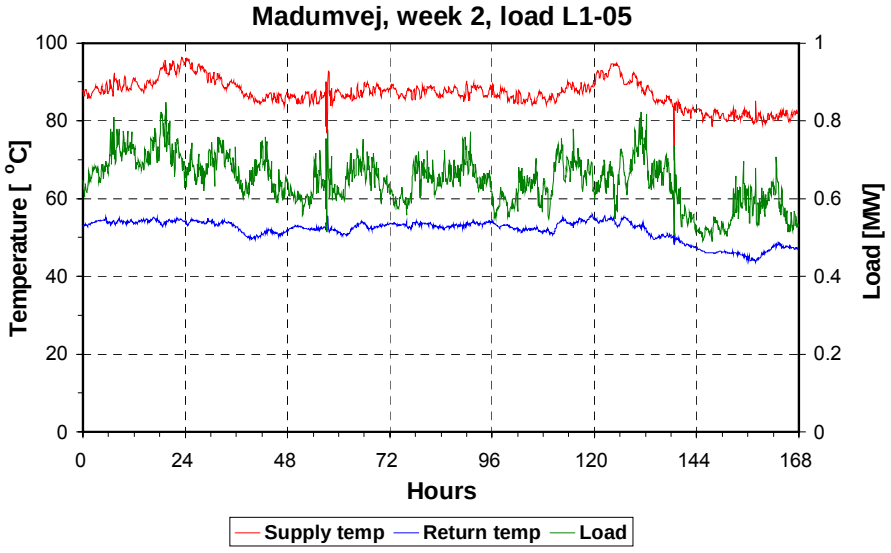
Madumvej, week 2, load L1-05
Temperature [°C]
Load [MW]
Hours
Supply temp
Return temp
Load

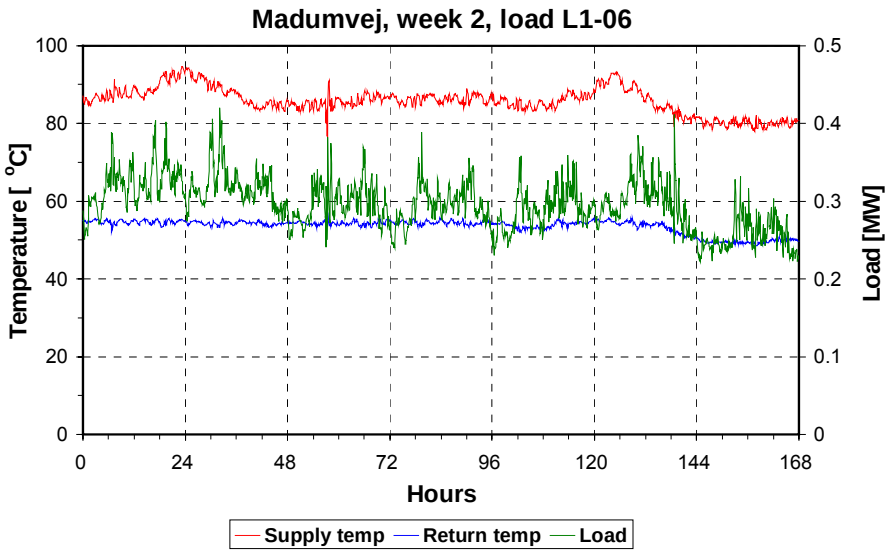
Madumvej, week 2, load L1-06
Temperature [°C]
Load [MW]
Hours
Supply temp
Return temp
Load

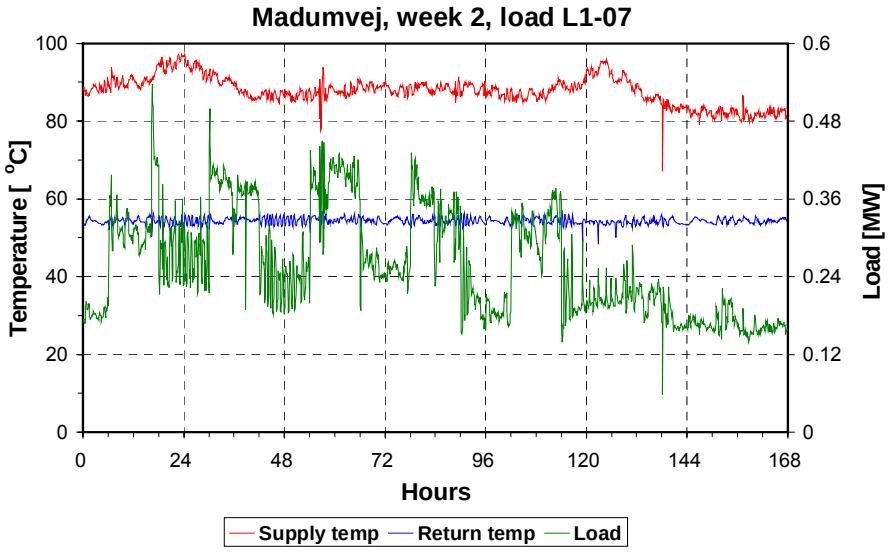
Madumvej, week 2, load L1-07
Temperature [°C]
Load [MW]
Hours
Supply temp
Return temp
Load

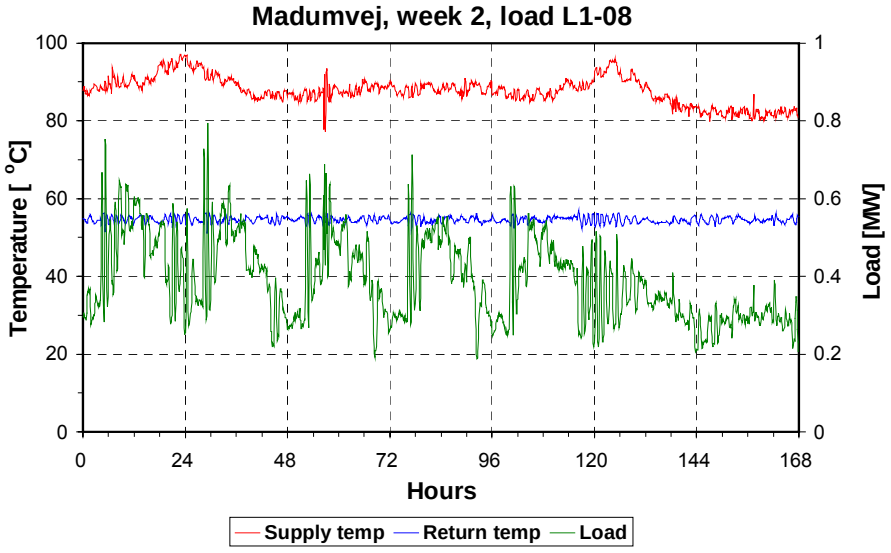
Madumvej, week 2, load L1-08
Temperature [°C]
Load [MW]
Hours
Supply temp
Return temp
Load

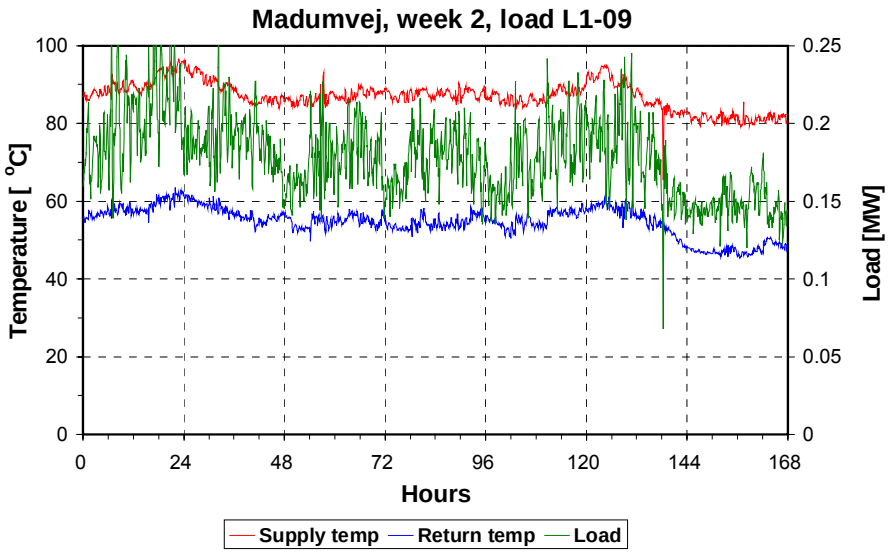
Madumvej, week 2, load L1-09
Temperature [°C]
Load [MW]
Hours
0
24
48
72
96
120
144
168
0
20
40
60
80
100
0
0.05
0.1
0.15
0.2
0.25
Supply temp
Return temp
Load

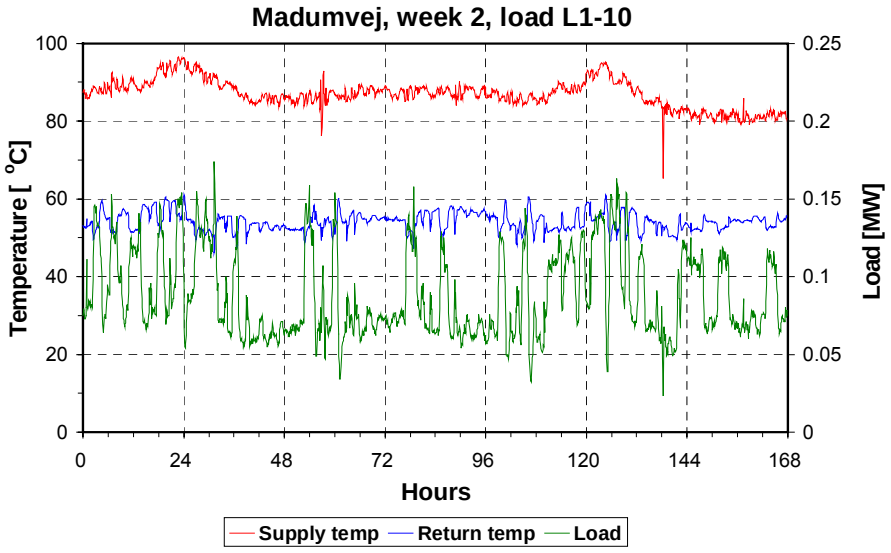
Madumvej, week 2, load L1-10
Temperature [°C]
Load [MW]
Hours
0
24
48
72
96
120
144
168
0
20
40
60
80
100
0
0.05
0.1
0.15
0.2
0.25
Supply temp
Return temp
Load

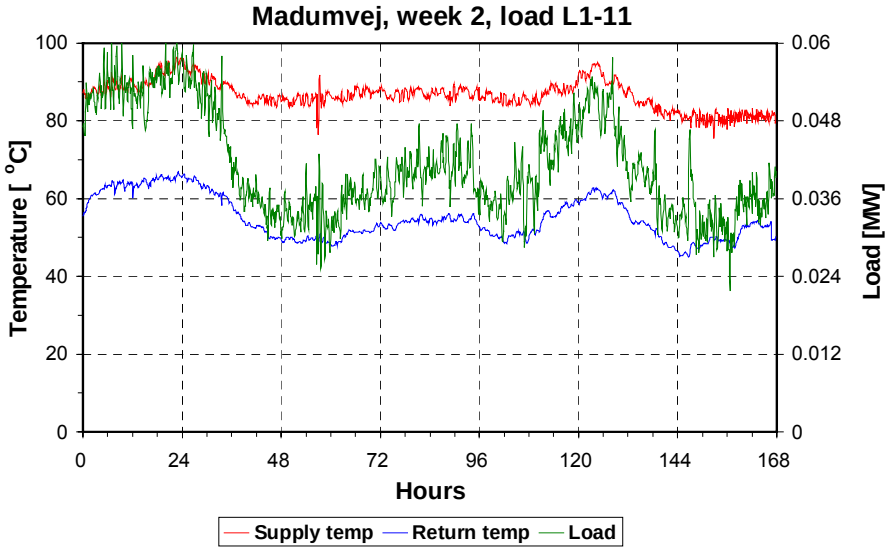
Madumvej, week 2, load L1-11
Temperature [°C]
Load [MW]
Hours
0
24
48
72
96
120
144
168
0
20
40
60
80
100
0
0.012
0.024
0.036
0.048
0.06
Supply temp
Return temp
Load

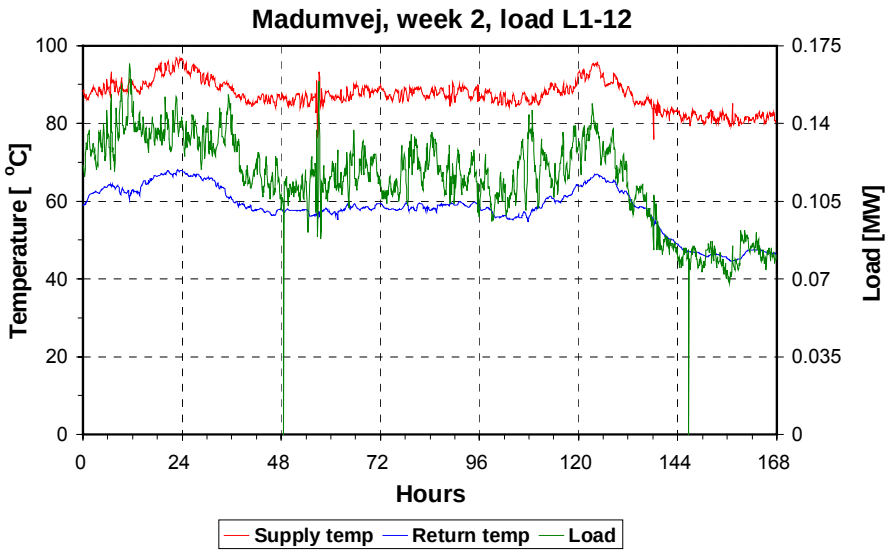

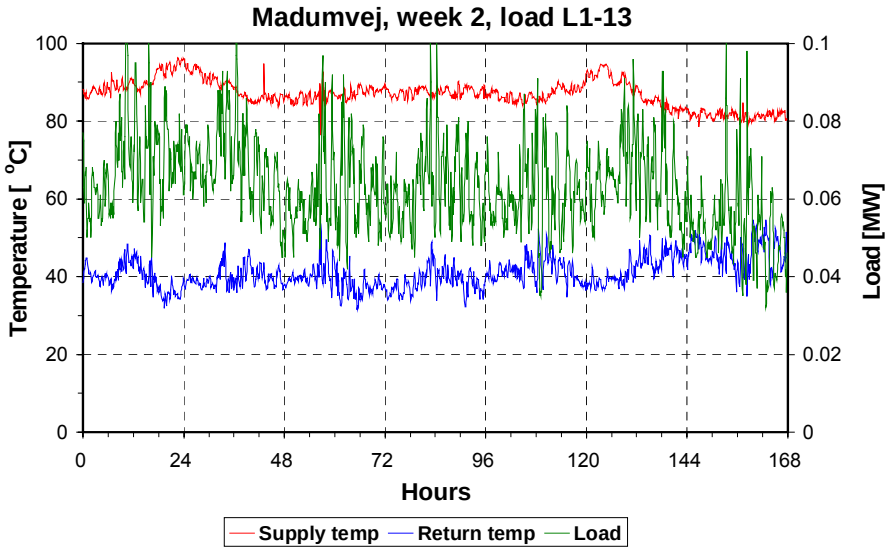

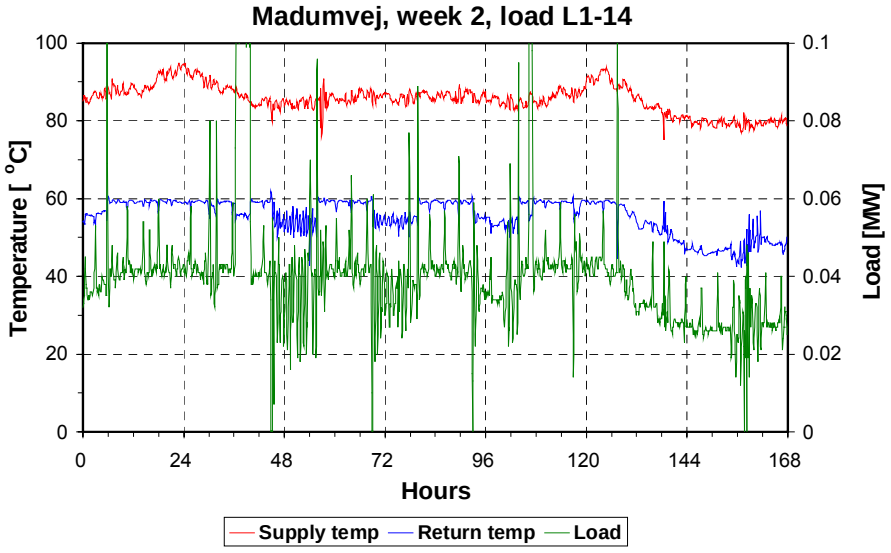

Madumvej, week 13:

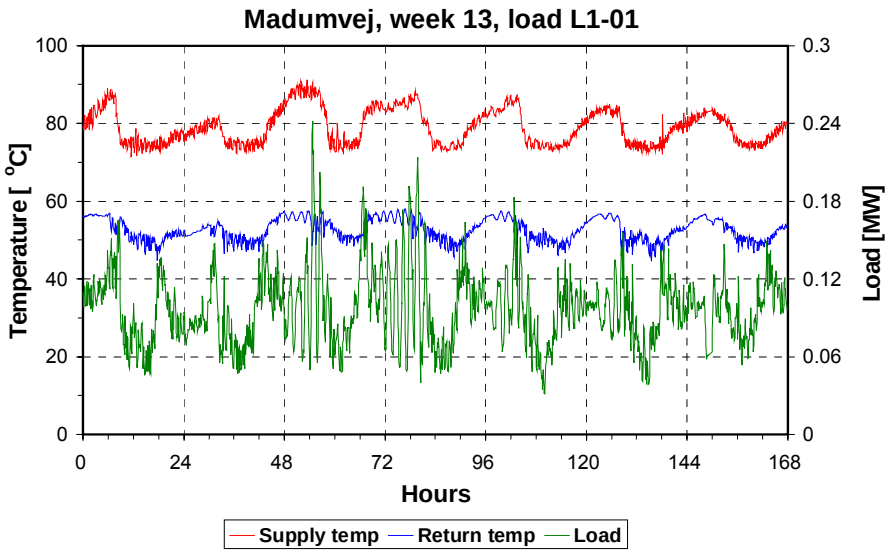
Madumvej, week 13, load L1-01
Temperature [°C]
Load [MW]
Hours
Supply temp
Return temp
Load

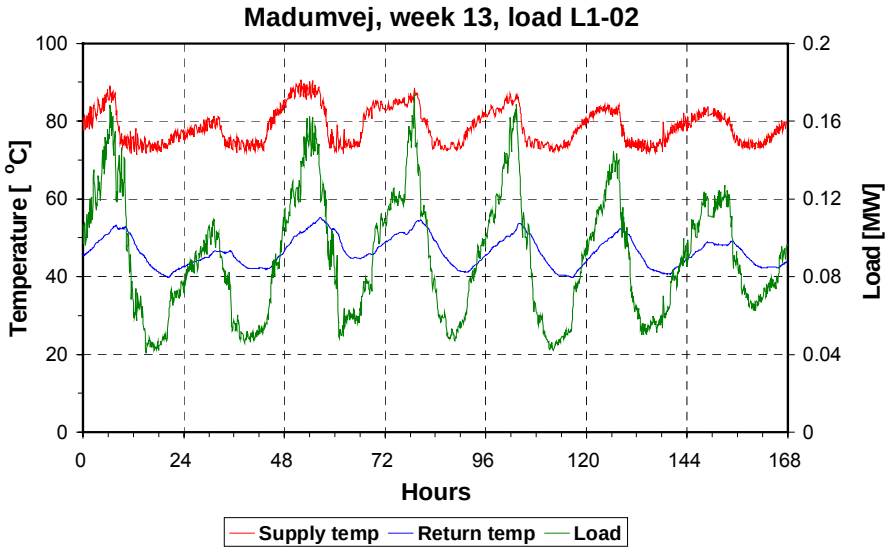
Madumvej, week 13, load L1-02
Temperature [°C]
Load [MW]
Hours
Supply temp
Return temp
Load

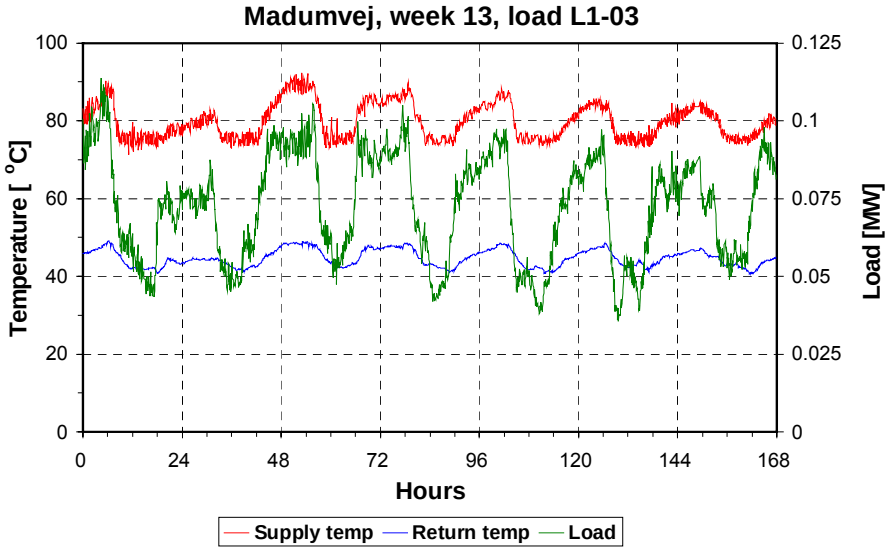
Madumvej, week 13, load L1-03
Temperature [°C]
Load [MW]
Hours
Supply temp
Return temp
Load

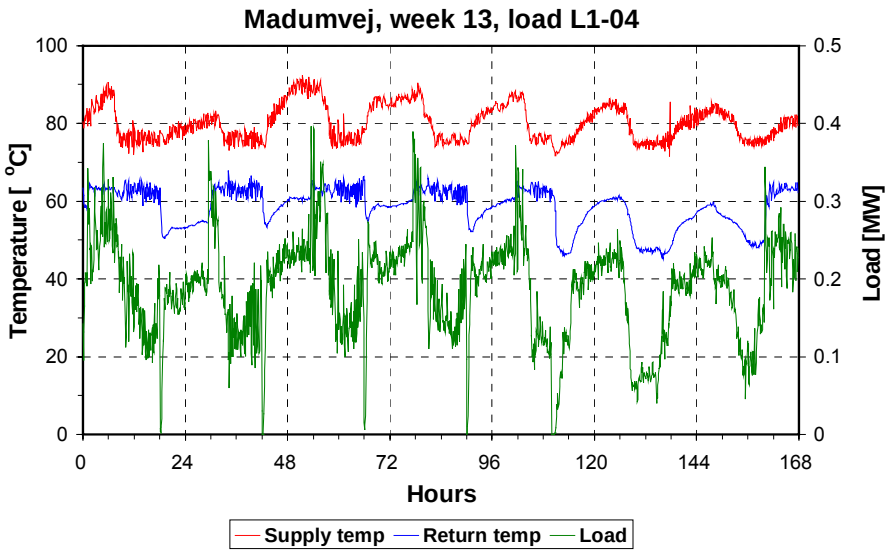
Madumvej, week 13, load L1-04
Temperature [°C]
Load [MW]
Hours
0
24
48
72
96
120
144
168
0
20
40
60
80
100
0
0.1
0.2
0.3
0.4
0.5
Supply temp
Return temp
Load

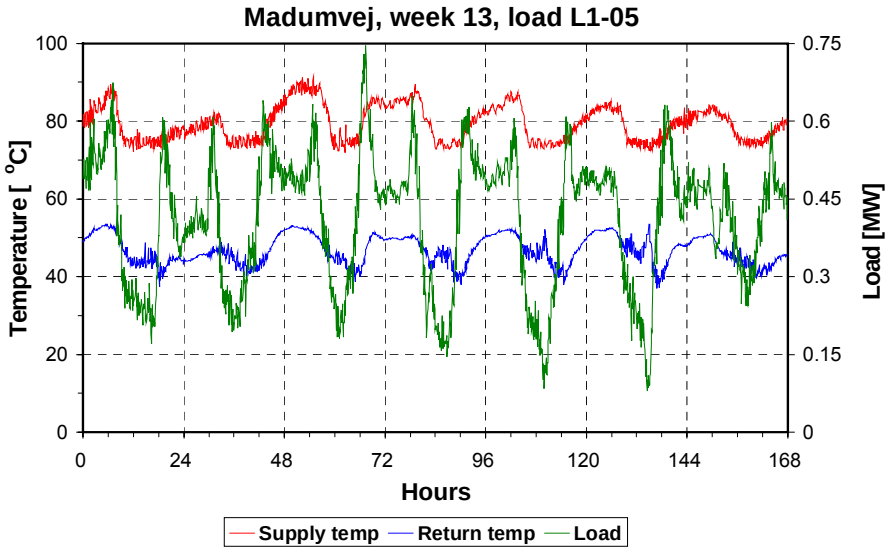
Madumvej, week 13, load L1-05
Temperature [°C]
Load [MW]
Hours
0
24
48
72
96
120
144
168
0
20
40
60
80
100
0
0.15
0.3
0.45
0.6
0.75
Supply temp
Return temp
Load

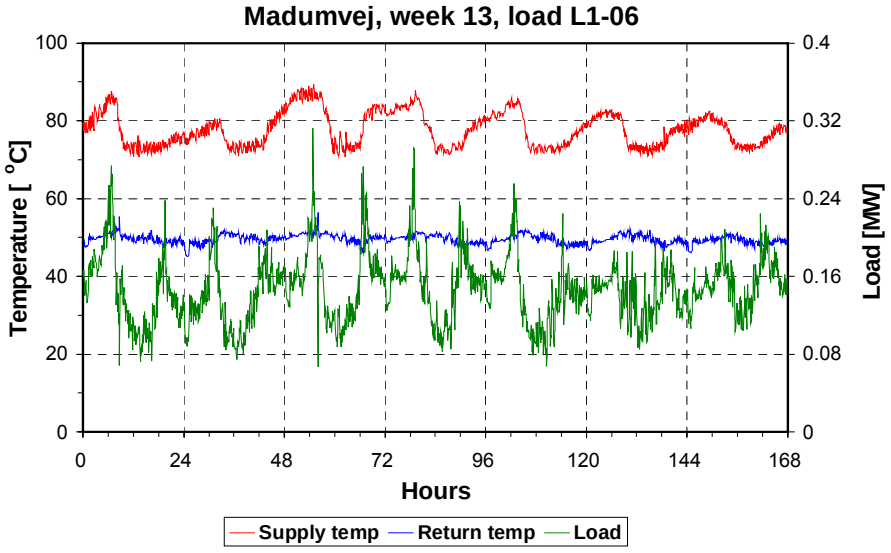
Madumvej, week 13, load L1-06
Temperature [°C]
Load [MW]
Hours
0
24
48
72
96
120
144
168
0
20
40
60
80
100
0
0.08
0.16
0.24
0.32
0.4
Supply temp
Return temp
Load

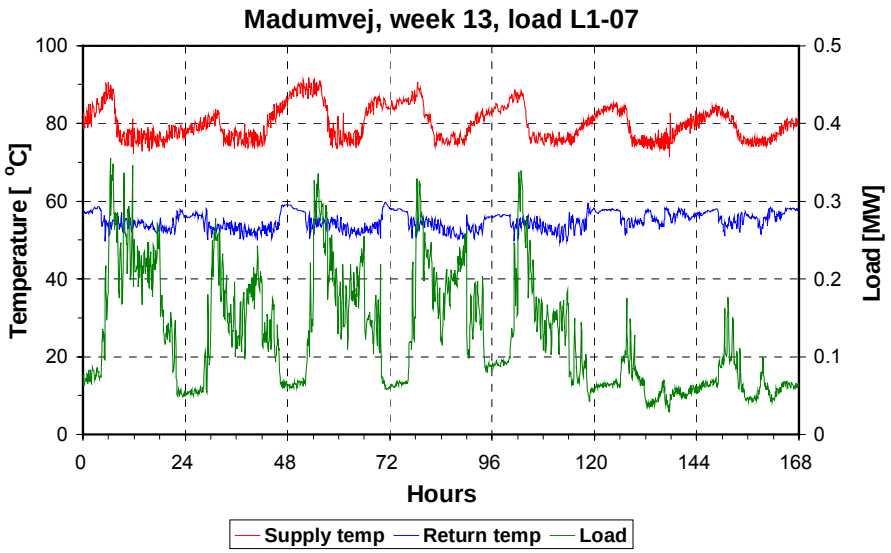
Madumvej, week 13, load L1-07
Temperature [°C]
Load [MW]
Hours
Supply temp
Return temp
Load

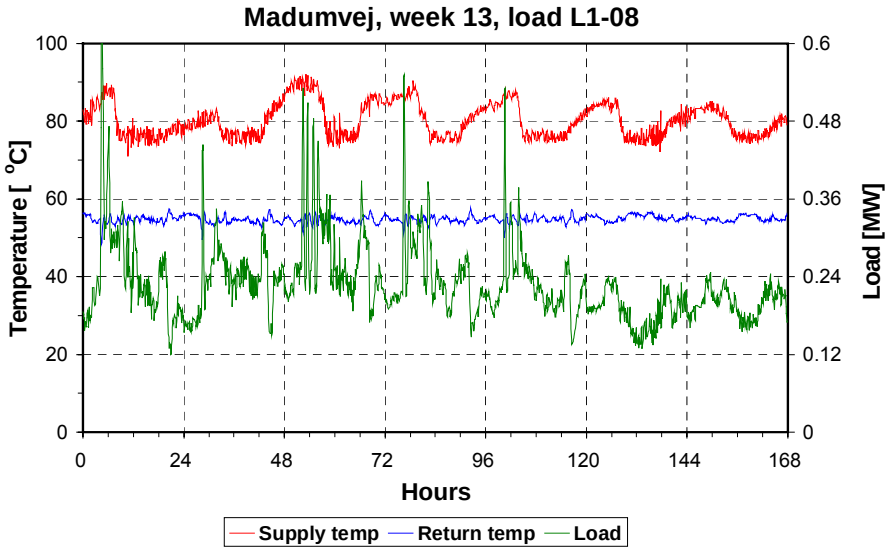
Madumvej, week 13, load L1-08
Temperature [°C]
Load [MW]
Hours
Supply temp
Return temp
Load

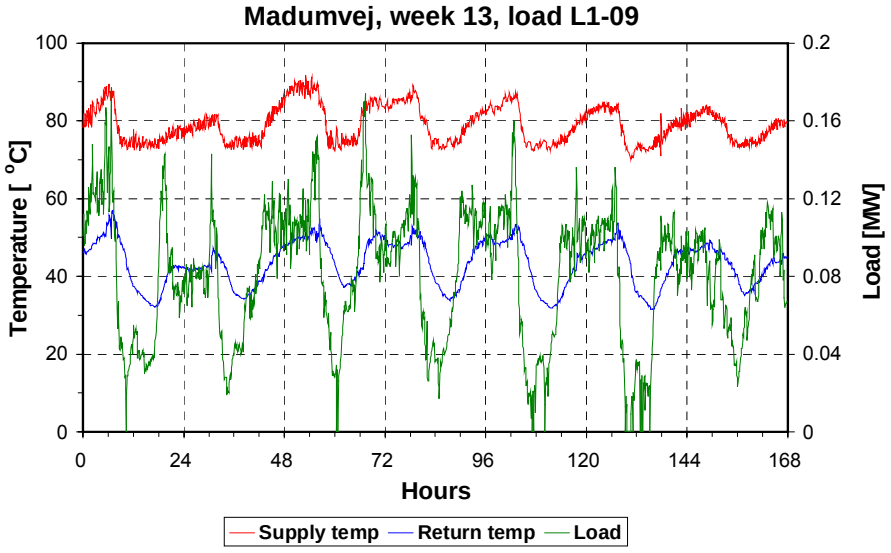
Madumvej, week 13, load L1-09
Temperature [°C]
Load [MW]
Hours
Supply temp
Return temp
Load

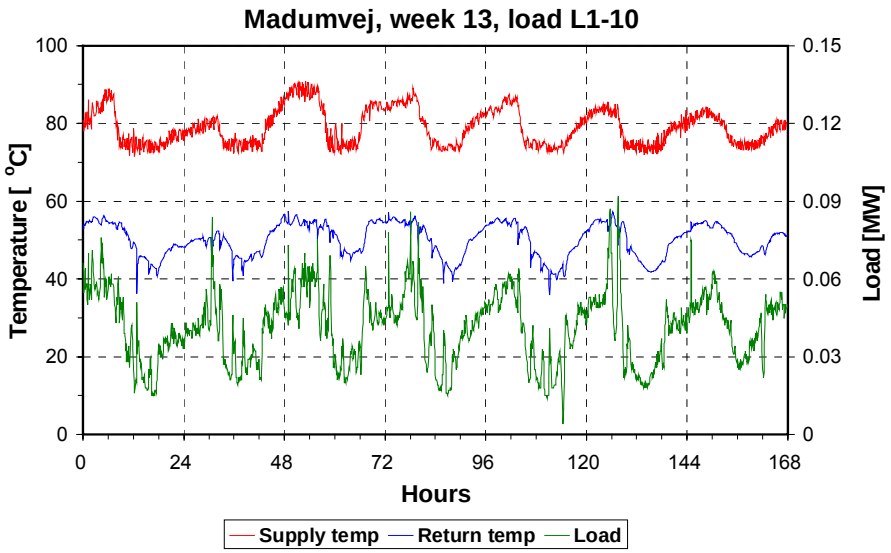
Madumvej, week 13, load L1-10
Temperature [°C]
Load [MW]
Hours
Supply temp
Return temp
Load

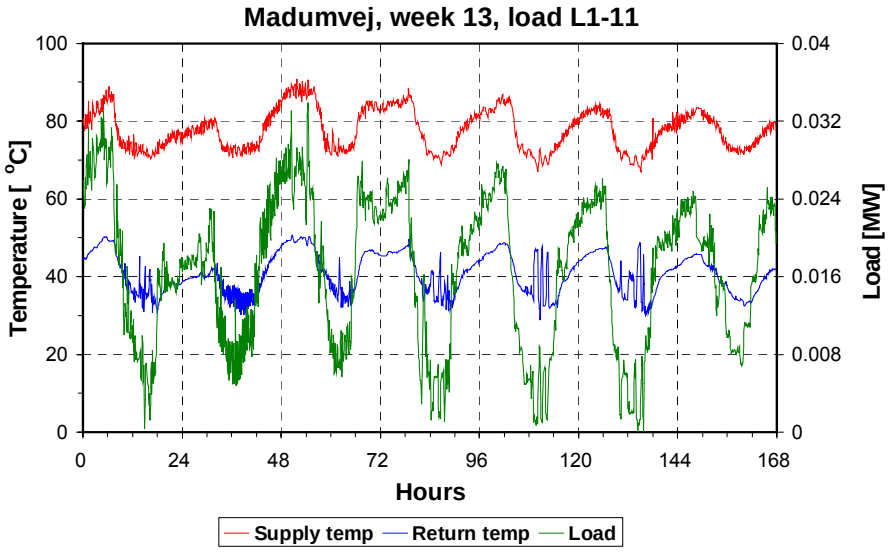
Madumvej, week 13, load L1-11
Temperature [°C]
Load [MW]
Hours
Supply temp
Return temp
Load

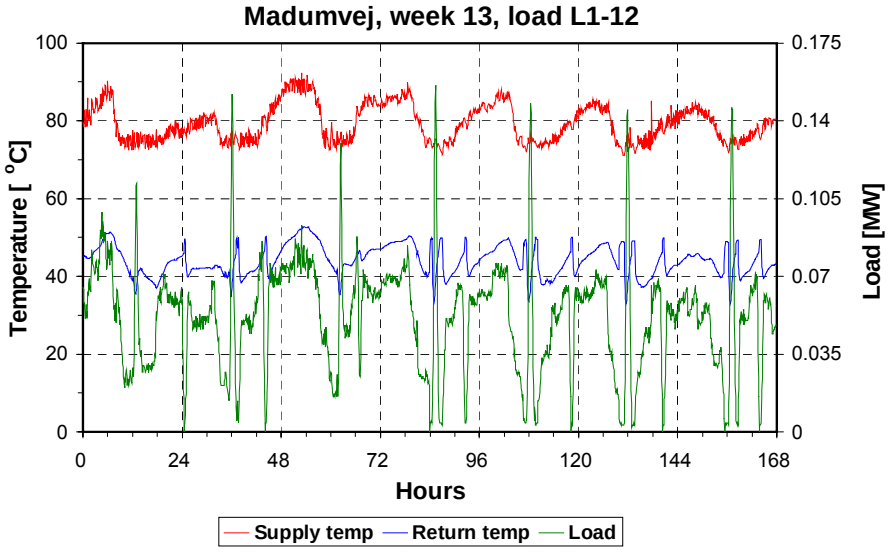
Madumvej, week 13, load L1-12
Temperature [°C]
Load [MW]
Hours
Supply temp
Return temp
Load

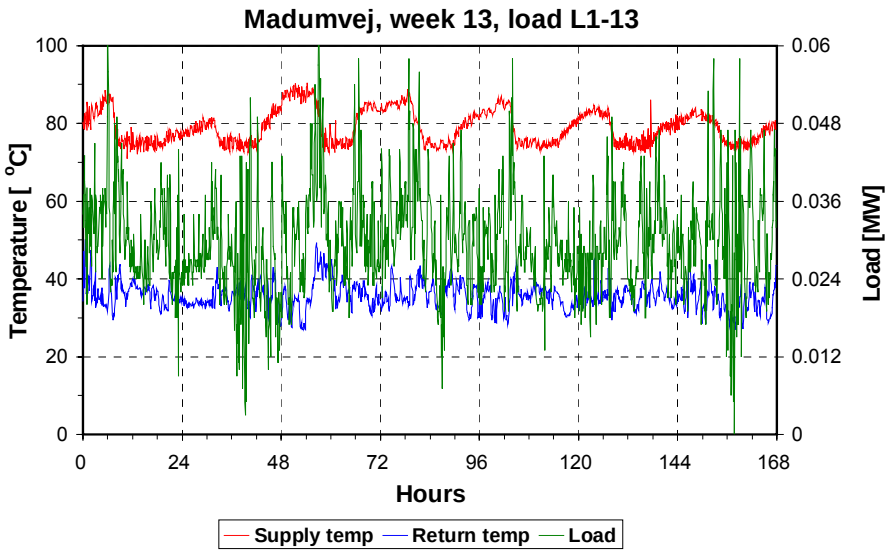
Madumvej, week 13, load L1-13
Temperature [°C]
Load [MW]
Hours
0
24
48
72
96
120
144
168
0
20
40
60
80
100
0
0.012
0.024
0.036
0.048
0.06
Supply temp
Return temp
Load

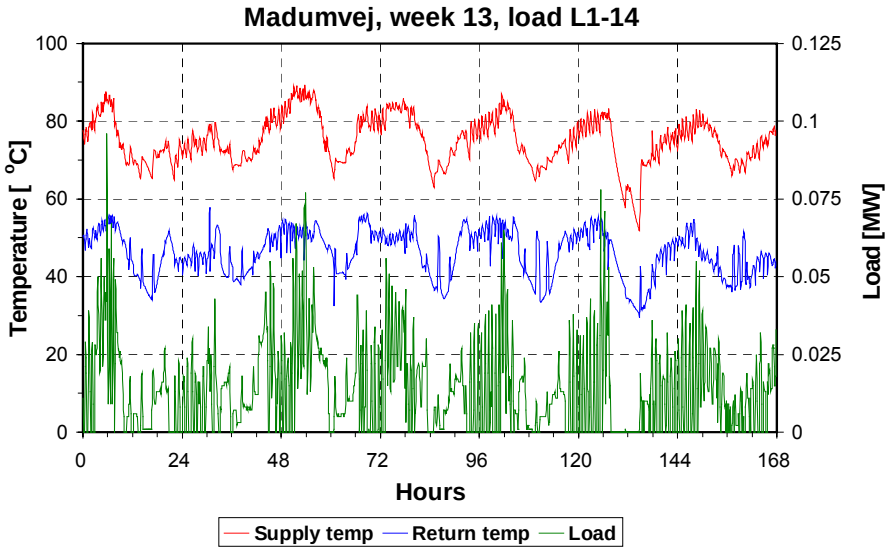
Madumvej, week 13, load L1-14
Temperature [°C]
Load [MW]
Hours
0
24
48
72
96
120
144
168
0
20
40
60
80
100
0
0.025
0.05
0.075
0.1
0.125
Supply temp
Return temp
Load

Madumvej, week 23:

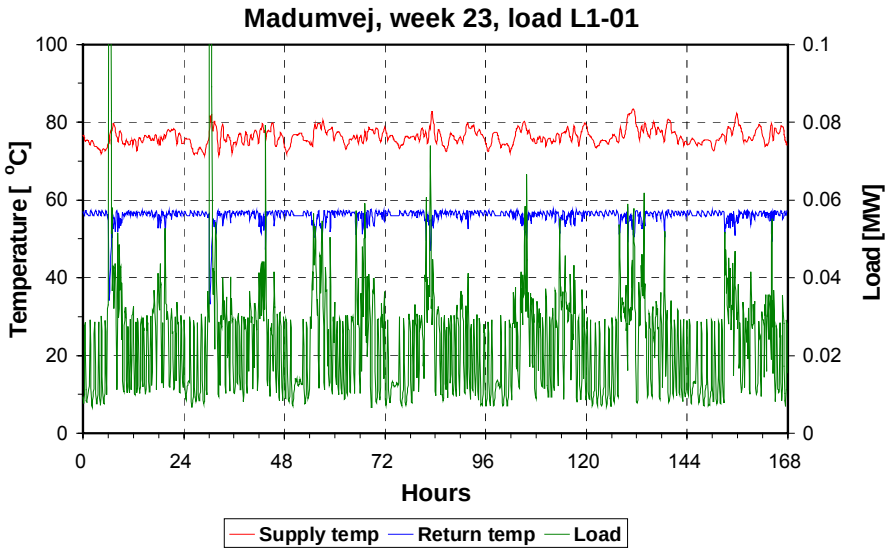

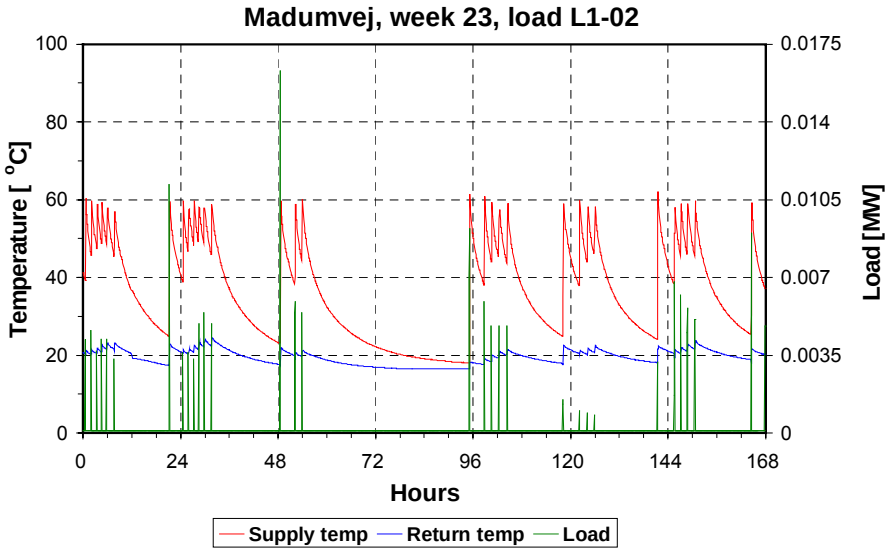

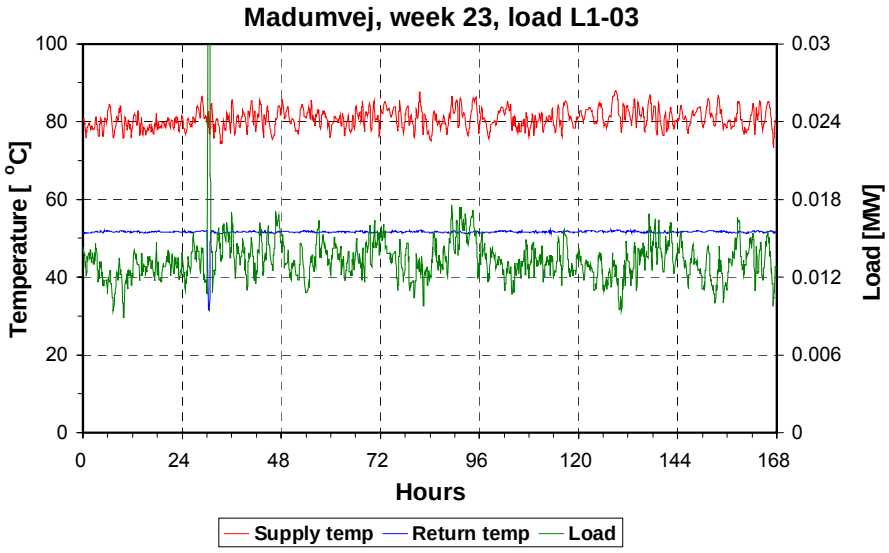

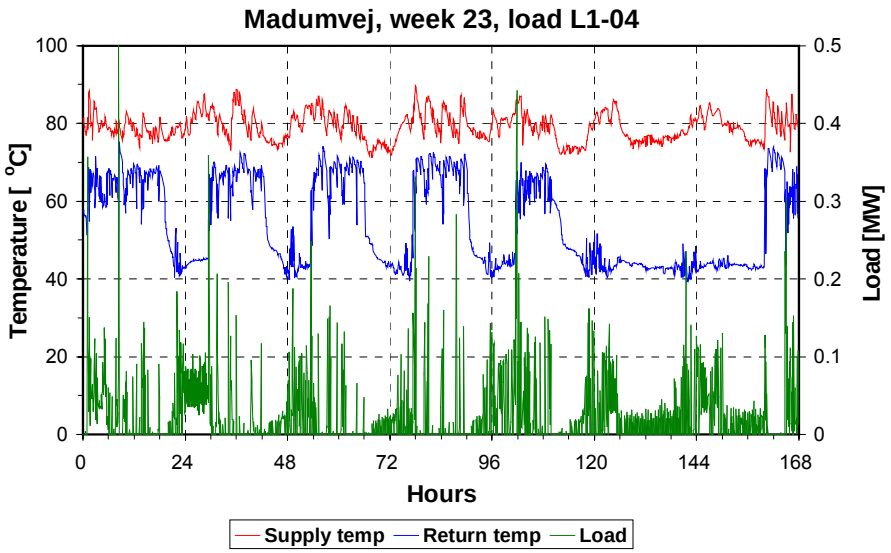
Madumvej, week 23, load L1-04
Temperature [°C]
Load [MW]
Hours
0
24
48
72
96
120
144
168
0
20
40
60
80
100
0
0.1
0.2
0.3
0.4
0.5
Supply temp
Return temp
Load

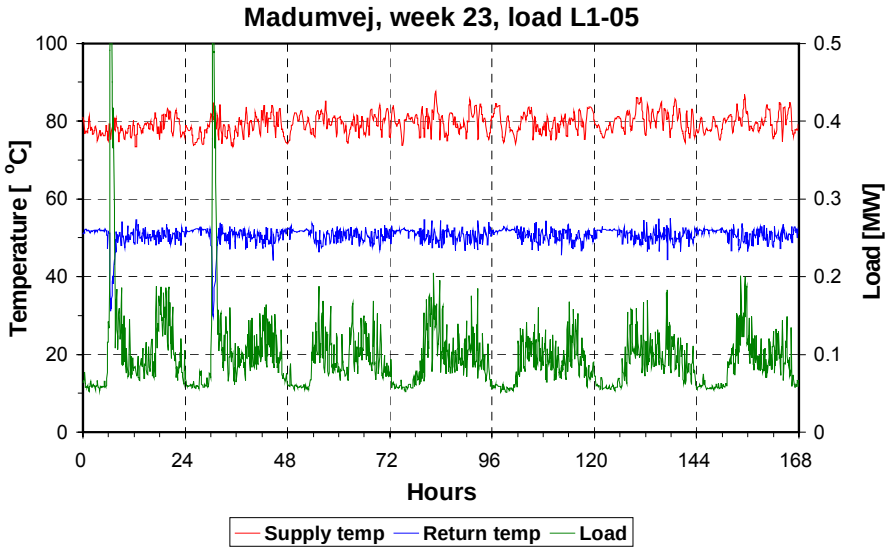
Madumvej, week 23, load L1-05
Temperature [°C]
Load [MW]
Hours
0
24
48
72
96
120
144
168
0
20
40
60
80
100
0
0.1
0.2
0.3
0.4
0.5
Supply temp
Return temp
Load

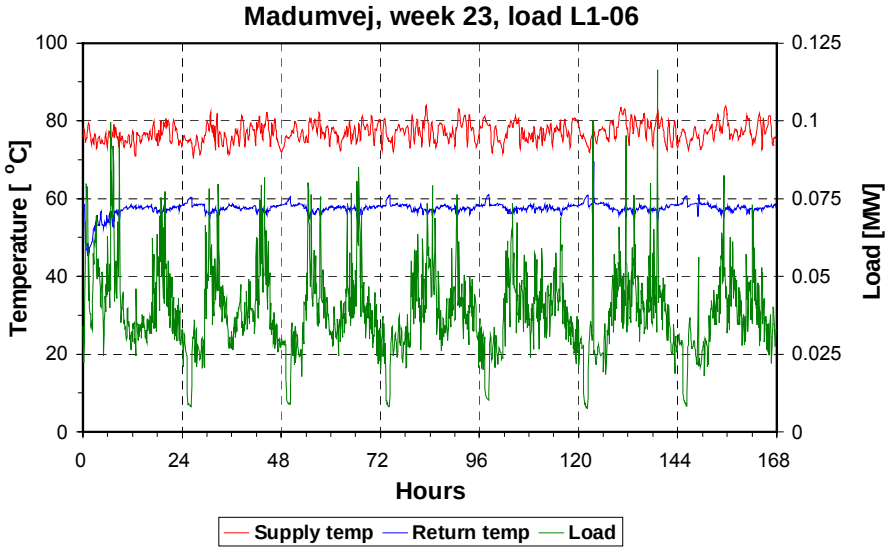
Madumvej, week 23, load L1-06
Temperature [°C]
Load [MW]
Hours
0
24
48
72
96
120
144
168
0
20
40
60
80
100
0
0.025
0.05
0.075
0.1
0.125
Supply temp
Return temp
Load

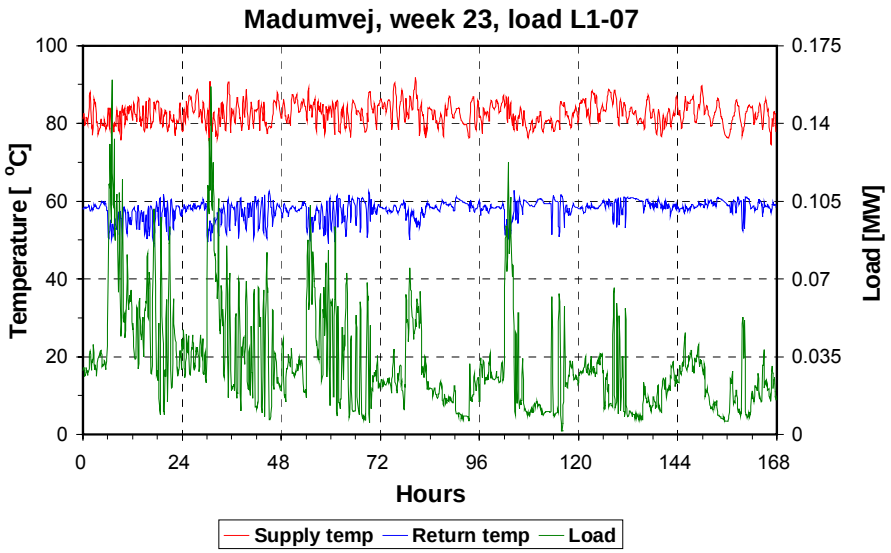
Madumvej, week 23, load L1-07
Temperature [°C]
Load [MW]
Hours
Supply temp
Return temp
Load

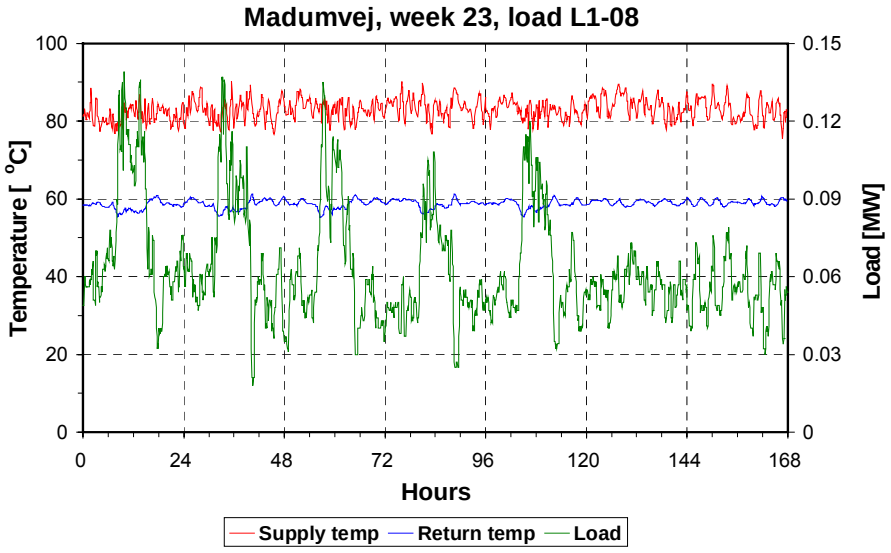
Madumvej, week 23, load L1-08
Temperature [°C]
Load [MW]
Hours
Supply temp
Return temp
Load

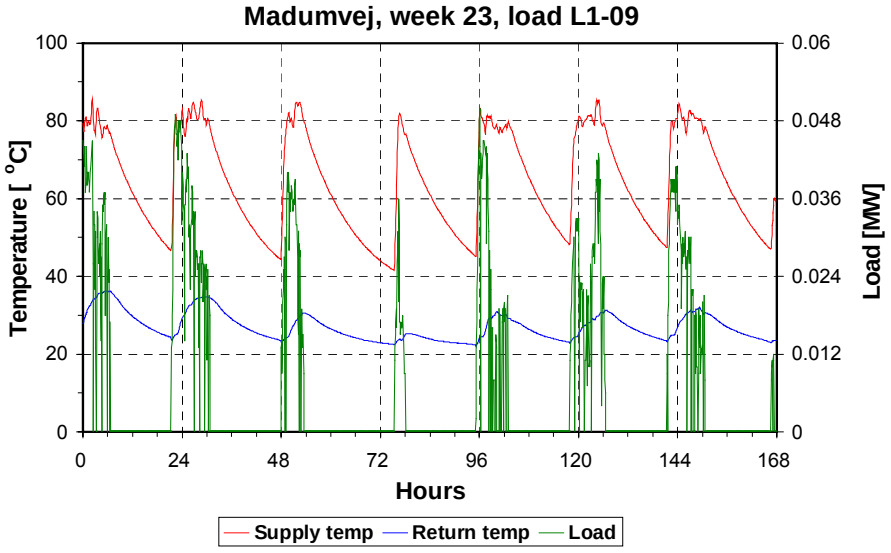
Madumvej, week 23, load L1-09
Temperature [°C]
Load [MW]
Hours
Supply temp
Return temp
Load

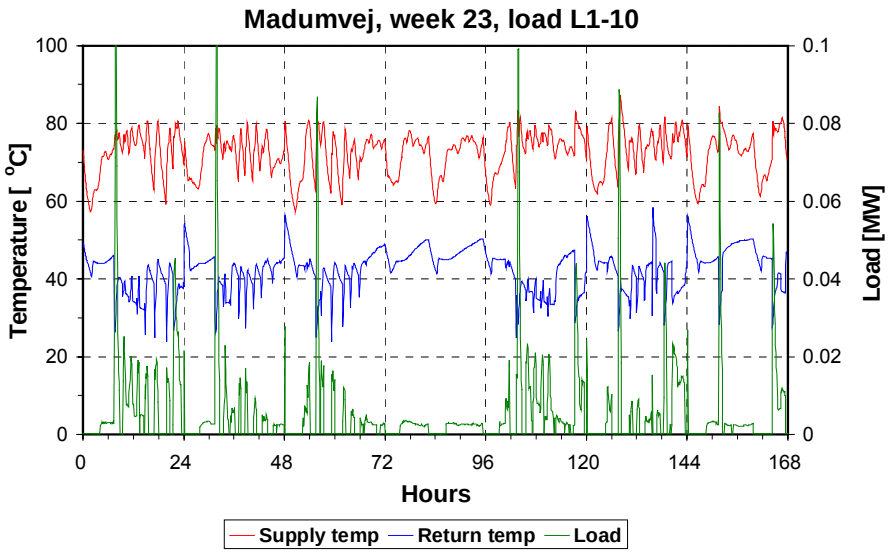
Madumvej, week 23, load L1-10
Temperature [°C]
Load [MW]
Hours
Supply temp
Return temp
Load

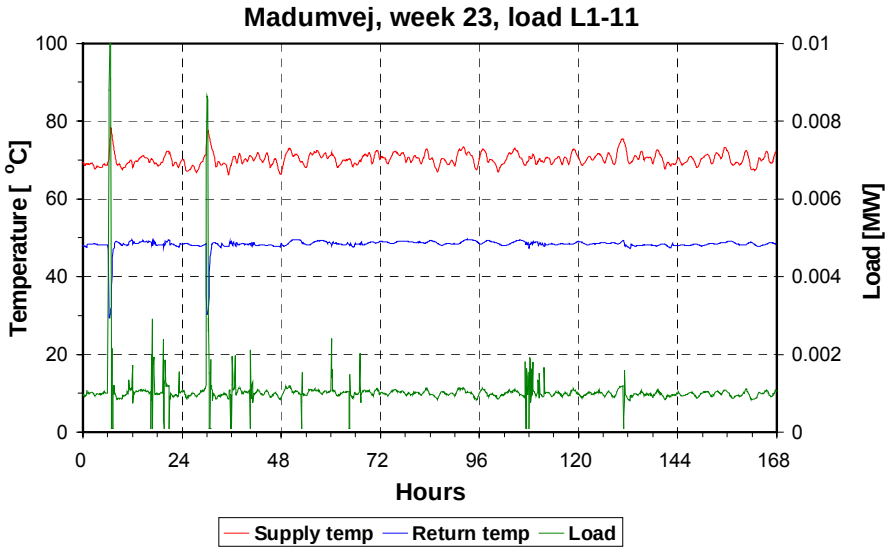
Madumvej, week 23, load L1-11
Temperature [°C]
Load [MW]
Hours
Supply temp
Return temp
Load

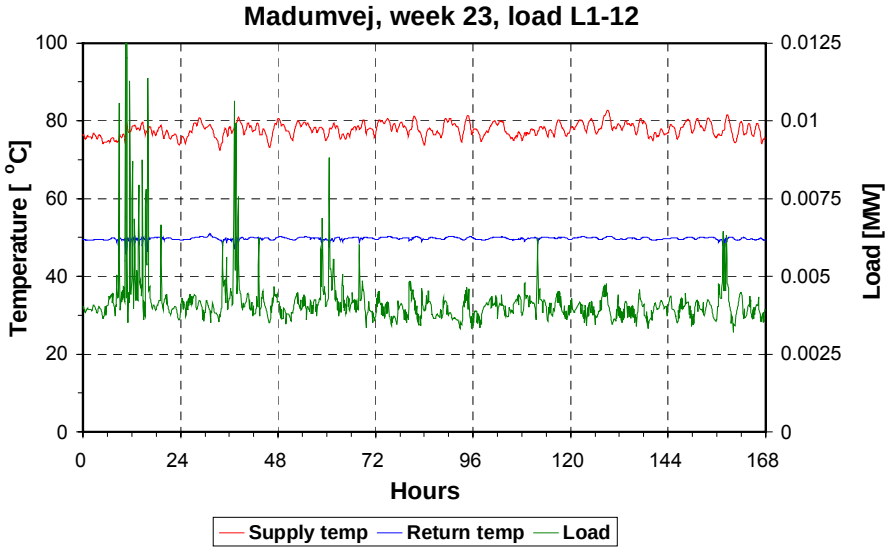
Madumvej, week 23, load L1-12
Temperature [°C]
Load [MW]
Hours
Supply temp
Return temp
Load

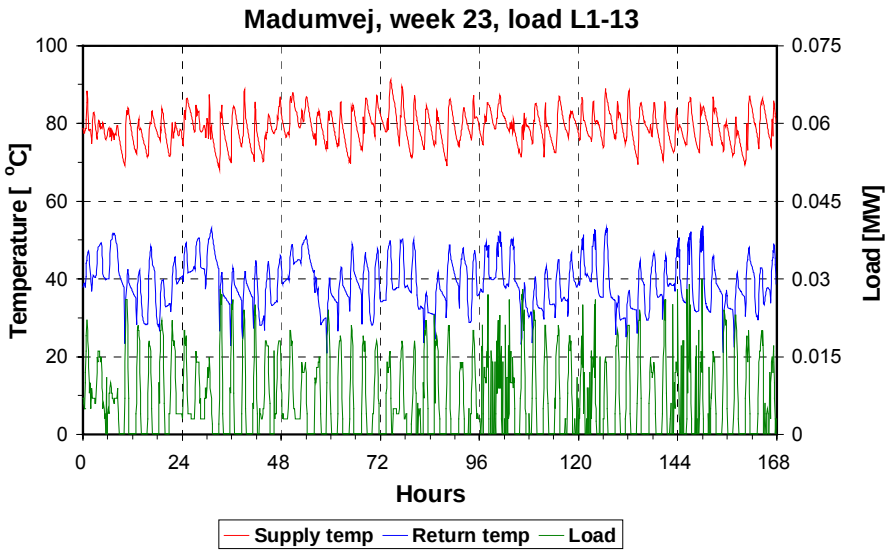
Madumvej, week 23, load L1-13
Temperature [°C]
Load [MW]
Hours
0
24
48
72
96
120
144
168
0
20
40
60
80
100
0
0.015
0.03
0.045
0.06
0.075
Supply temp
Return temp
Load

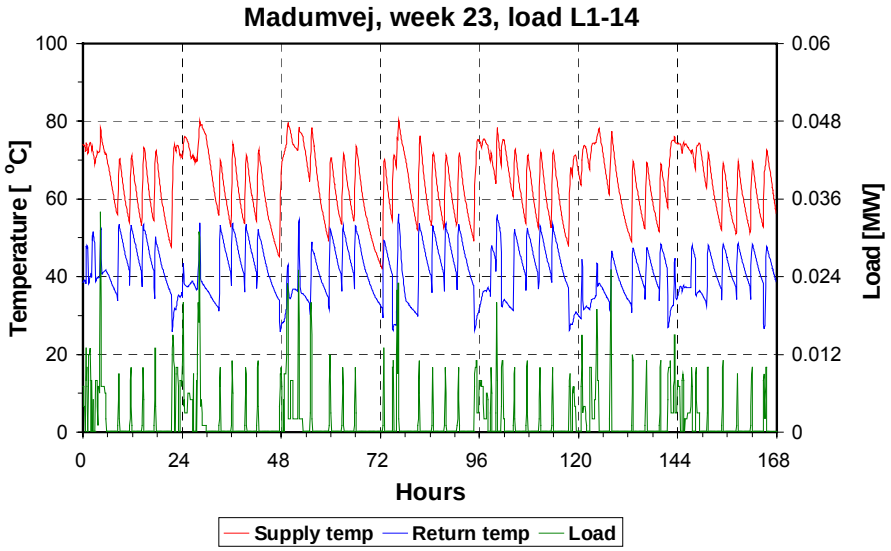
Madumvej, week 23, load L1-14
Temperature [°C]
Load [MW]
Hours
0
24
48
72
96
120
144
168
0
20
40
60
80
100
0
0.012
0.024
0.036
0.048
0.06
Supply temp
Return temp
Load

Heat loads in R02 Broparken:

For each of the consumers and each of the three weeks considered, measured time series for heat consumption and primary supply and return temperatures are shown in the following figures. In Broparken there are 18, 19 or 20 consumers depending on the week.

Broparken, week 2:

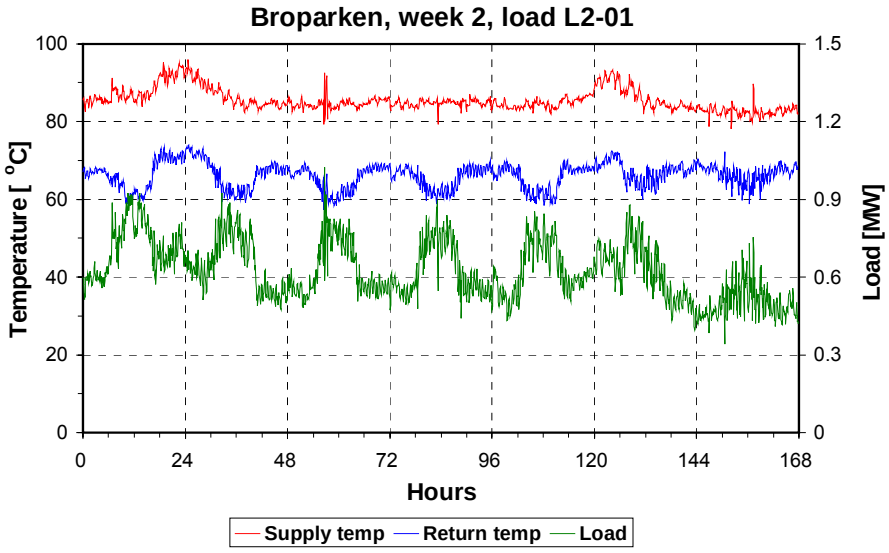

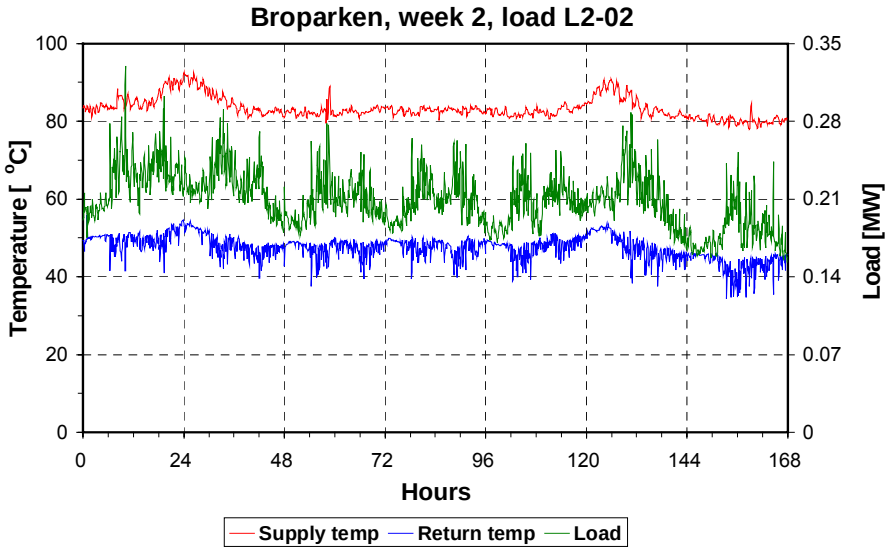

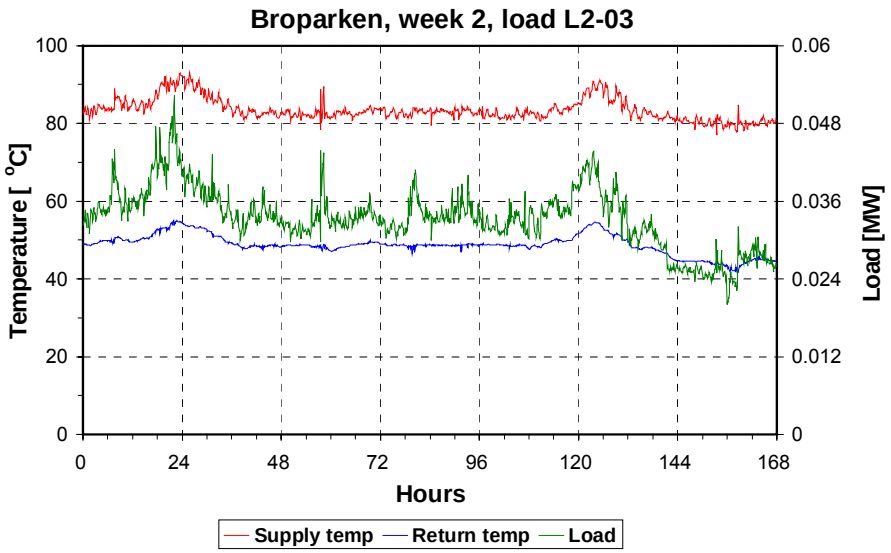
Broparken, week 2, load L2-03
Temperature [°C]
Load [MW]
Hours
0
24
48
72
96
120
144
168
0
20
40
60
80
100
0
0.012
0.024
0.036
0.048
0.06
Supply temp
Return temp
Load

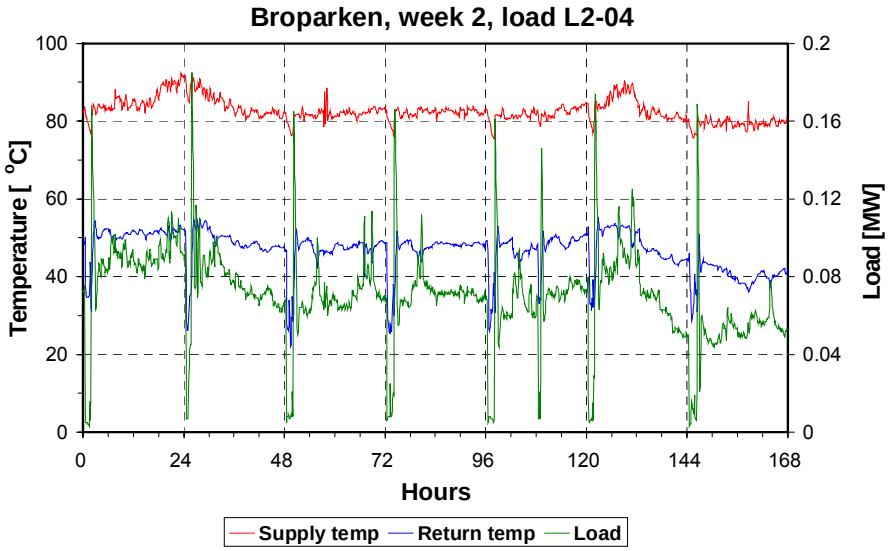
Broparken, week 2, load L2-04
Temperature [°C]
Load [MW]
Hours
0
24
48
72
96
120
144
168
0
20
40
60
80
100
0
0.04
0.08
0.12
0.16
0.2
Supply temp
Return temp
Load

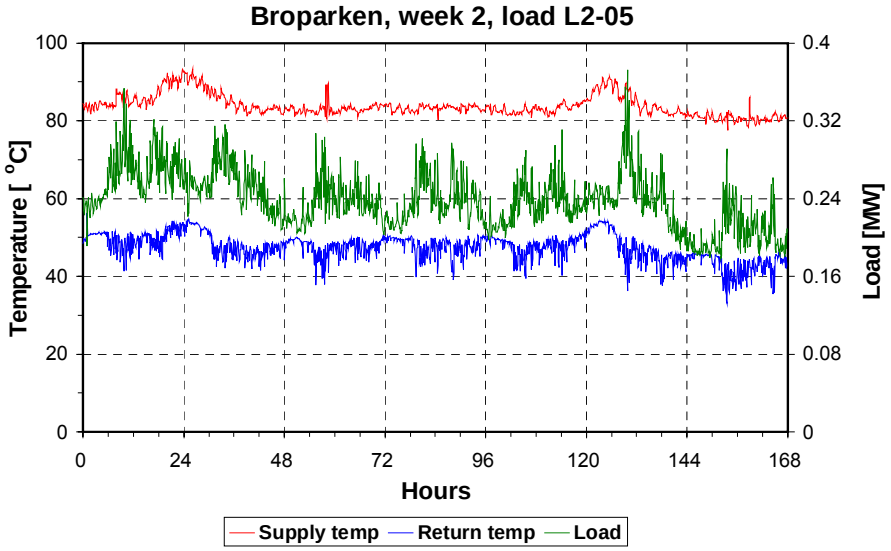
Broparken, week 2, load L2-05
Temperature [°C]
Load [MW]
Hours
0
24
48
72
96
120
144
168
0
20
40
60
80
100
0
0.08
0.16
0.24
0.32
0.4
Supply temp
Return temp
Load

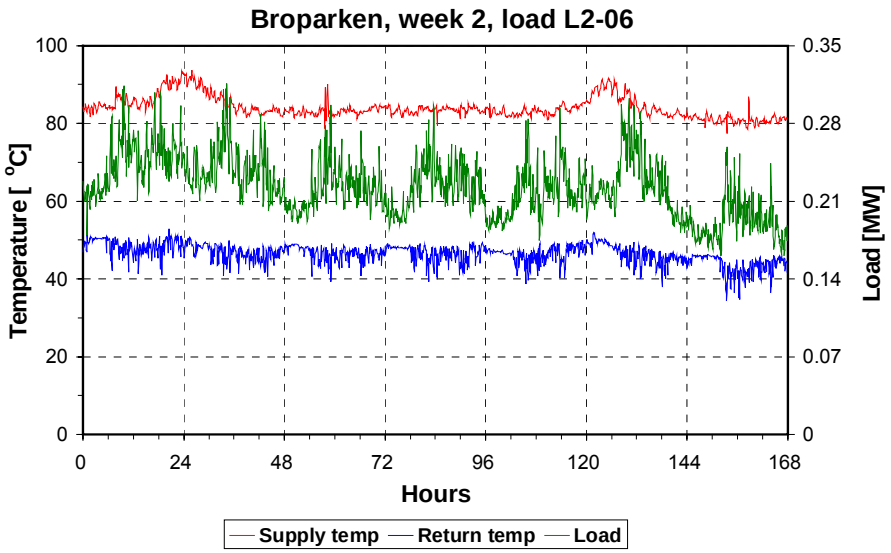
Broparken, week 2, load L2-06
Temperature [°C]
Load [MW]
Hours
0
24
48
72
96
120
144
168
0
20
40
60
80
100
0
0.07
0.14
0.21
0.28
0.35
Supply temp
Return temp
Load

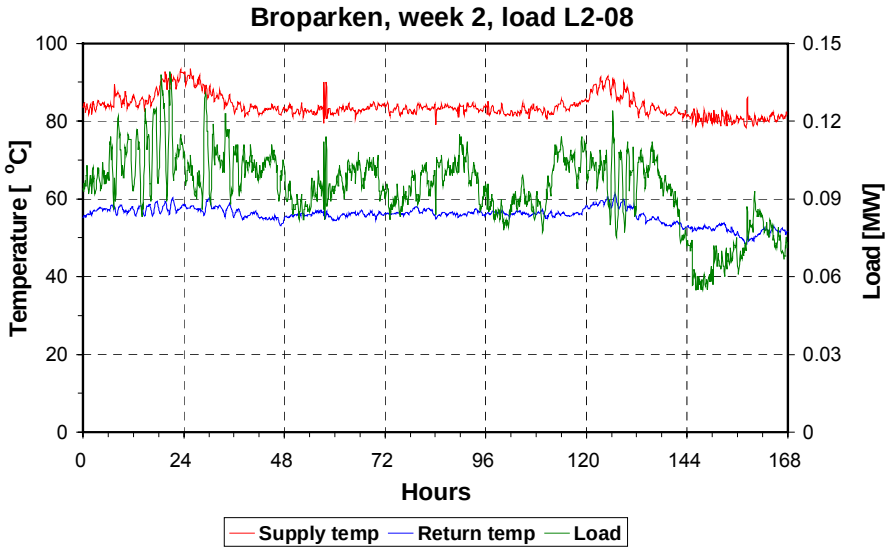
Broparken, week 2, load L2-08
Temperature [°C]
Load [MW]
Hours
0
24
48
72
96
120
144
168
0
20
40
60
80
100
0
0.03
0.06
0.09
0.12
0.15
Supply temp
Return temp
Load

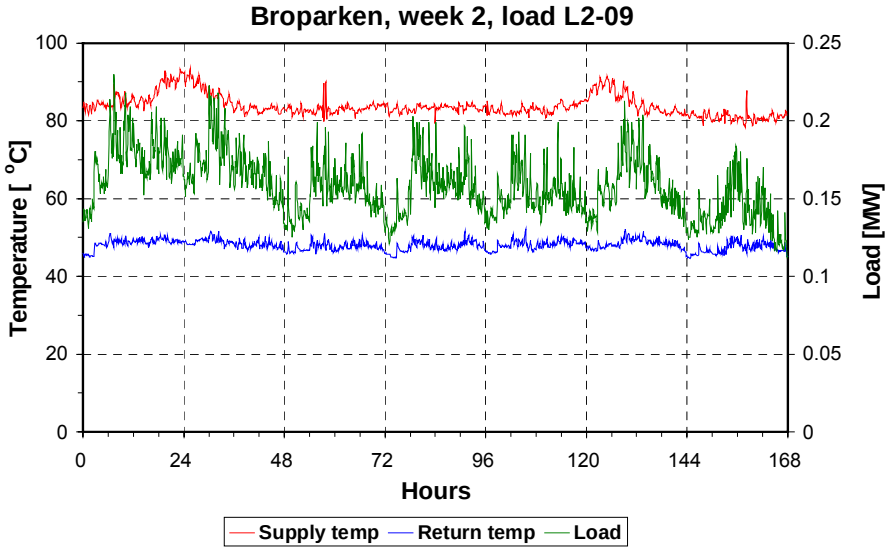
Broparken, week 2, load L2-09
Temperature [°C]
Load [MW]
Hours
0
24
48
72
96
120
144
168
0
20
40
60
80
100
0
0.05
0.1
0.15
0.2
0.25
Supply temp
Return temp
Load

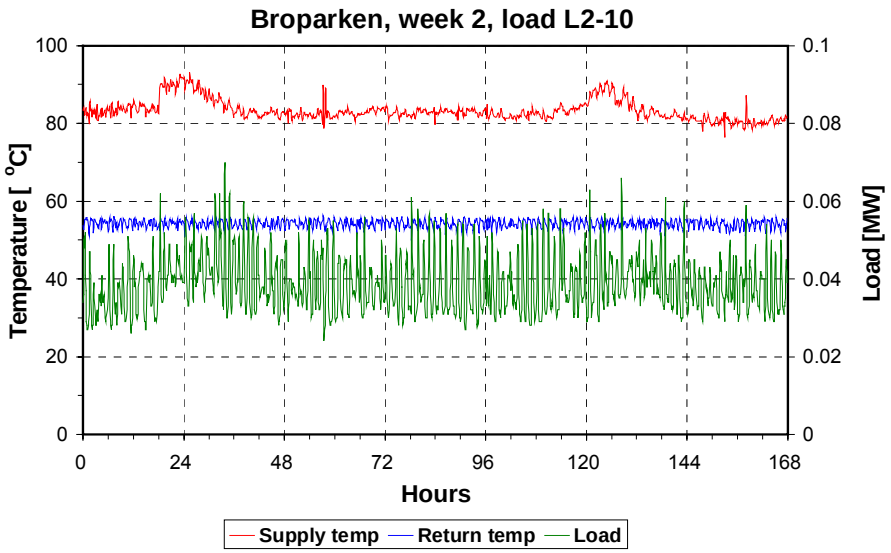
Broparken, week 2, load L2-10
Temperature [°C]
Load [MW]
Hours
0
24
48
72
96
120
144
168
0
20
40
60
80
100
0
0.02
0.04
0.06
0.08
0.1
Supply temp
Return temp
Load

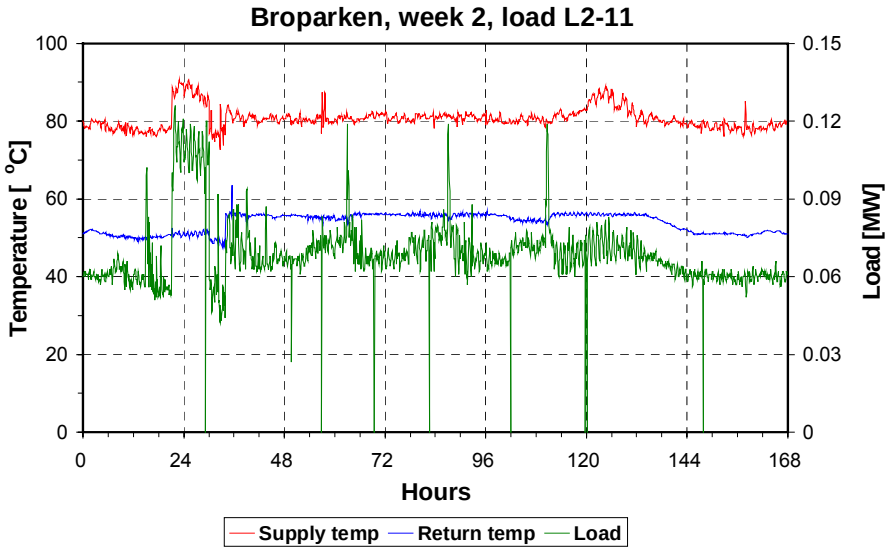
Broparken, week 2, load L2-11
Temperature [°C]
Load [MW]
Hours
0
24
48
72
96
120
144
168
0
20
40
60
80
100
0
0.03
0.06
0.09
0.12
0.15
Supply temp
Return temp
Load

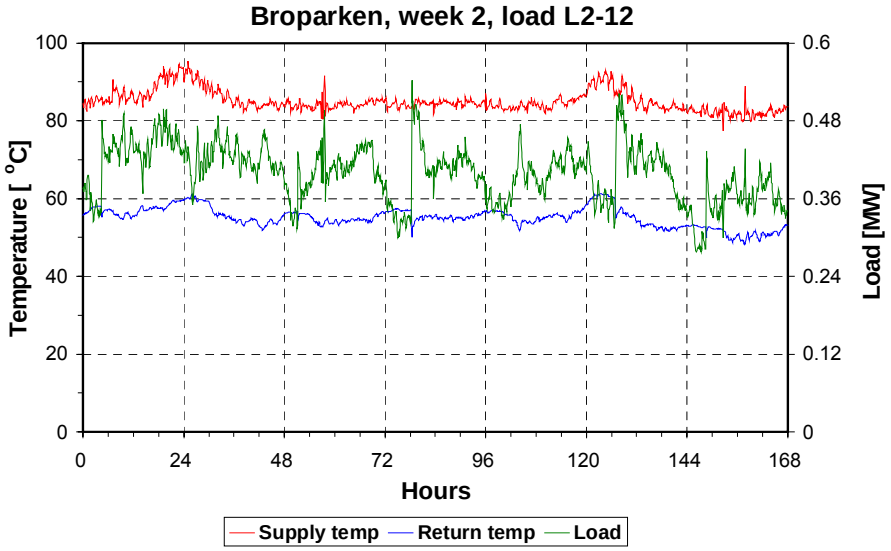
Broparken, week 2, load L2-12
Temperature [°C]
Load [MW]
Hours
0
24
48
72
96
120
144
168
0
20
40
60
80
100
0
0.12
0.24
0.36
0.48
0.6
Supply temp
Return temp
Load

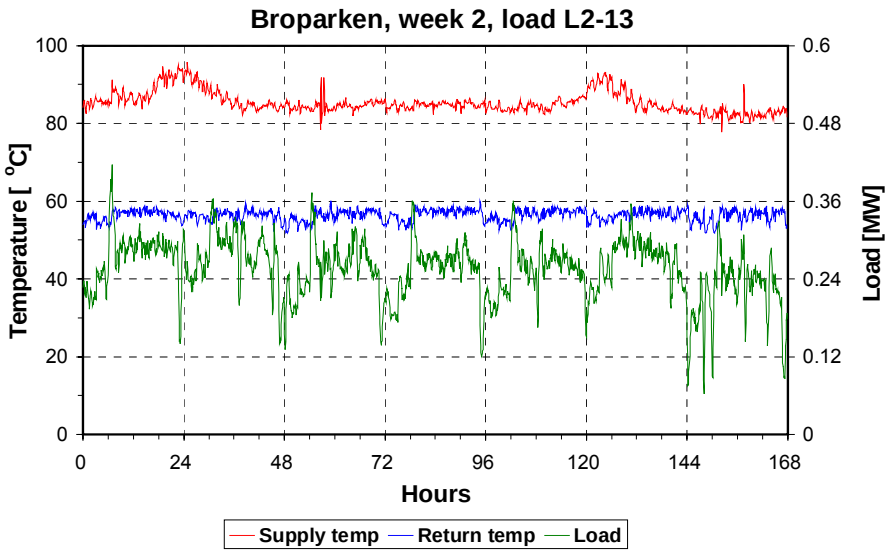
Broparken, week 2, load L2-13
Temperature [°C]
Load [MW]
Hours
0
24
48
72
96
120
144
168
0
20
40
60
80
100
0
0.12
0.24
0.36
0.48
0.6
Supply temp
Return temp
Load

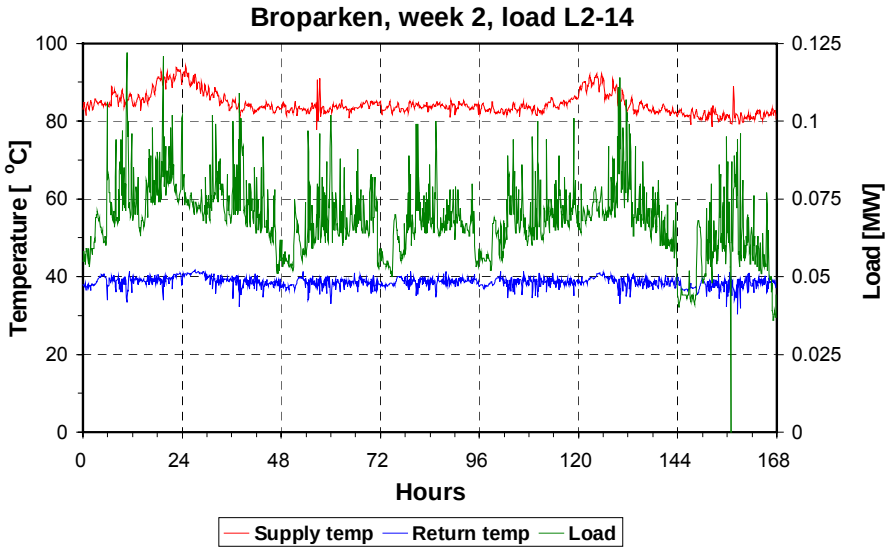
Broparken, week 2, load L2-14
Temperature [°C]
Load [MW]
Hours
0
24
48
72
96
120
144
168
0
20
40
60
80
100
0
0.025
0.05
0.075
0.1
0.125
Supply temp
Return temp
Load

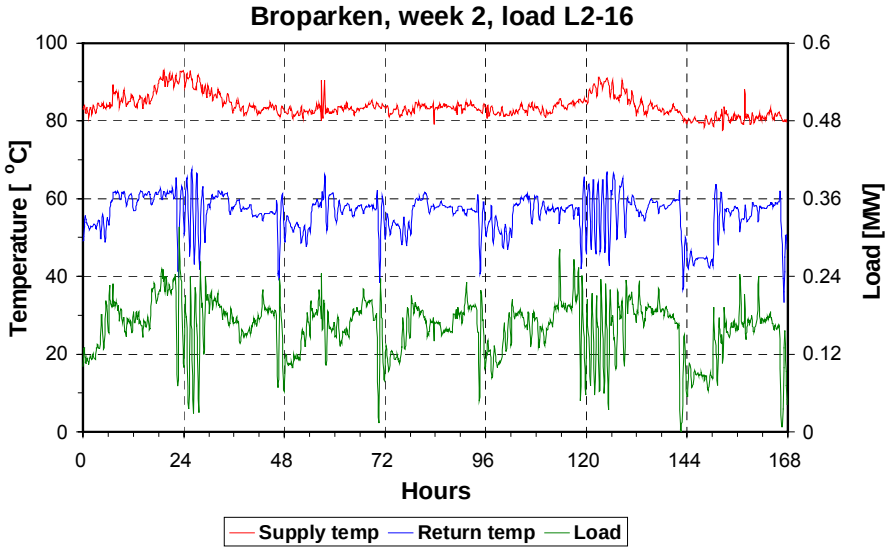
Broparken, week 2, load L2-16
Temperature [°C]
Load [MW]
Hours
0
24
48
72
96
120
144
168
0
20
40
60
80
100
0
0.12
0.24
0.36
0.48
0.6
Supply temp
Return temp
Load

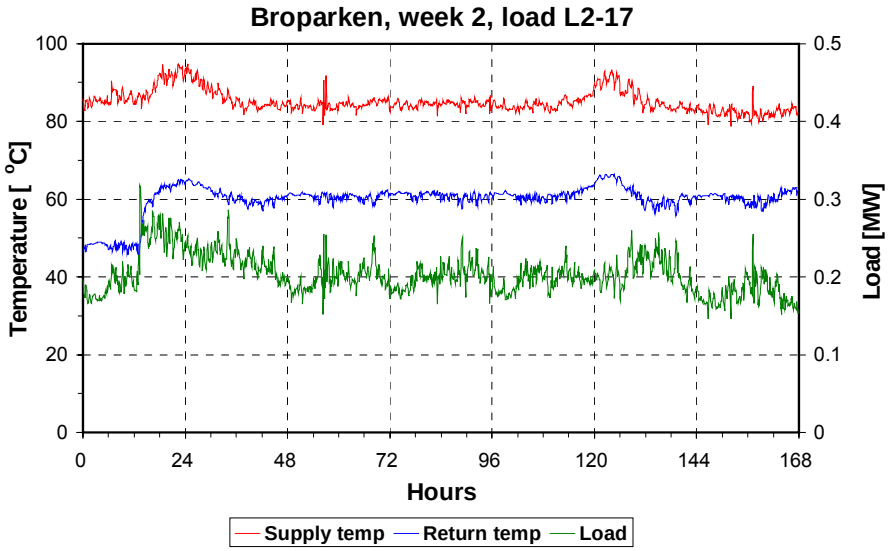
Broparken, week 2, load L2-17
Temperature [°C]
Load [MW]
Hours
0
24
48
72
96
120
144
168
0
20
40
60
80
100
0
0.1
0.2
0.3
0.4
0.5
Supply temp
Return temp
Load

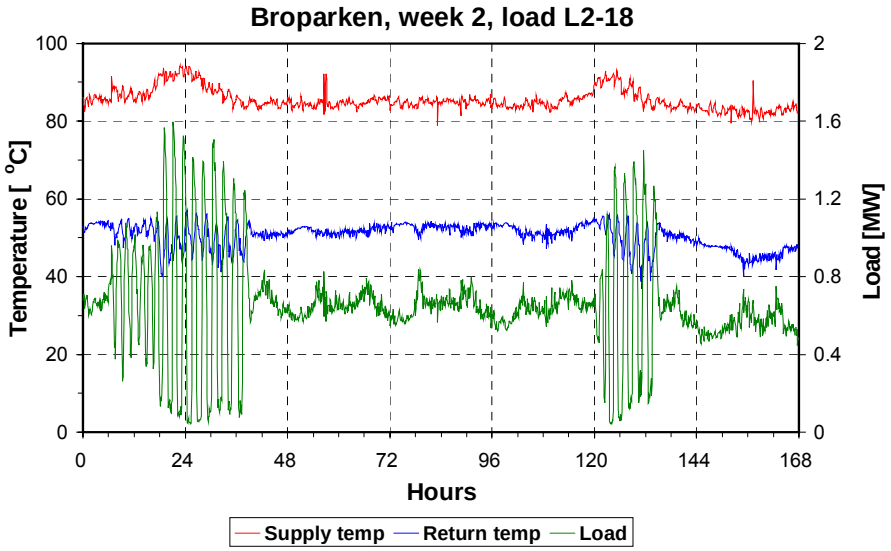
Broparken, week 2, load L2-18
Temperature [°C]
Load [MW]
Hours
0
24
48
72
96
120
144
168
0
20
40
60
80
100
0
0.4
0.8
1.2
1.6
2
Supply temp
Return temp
Load

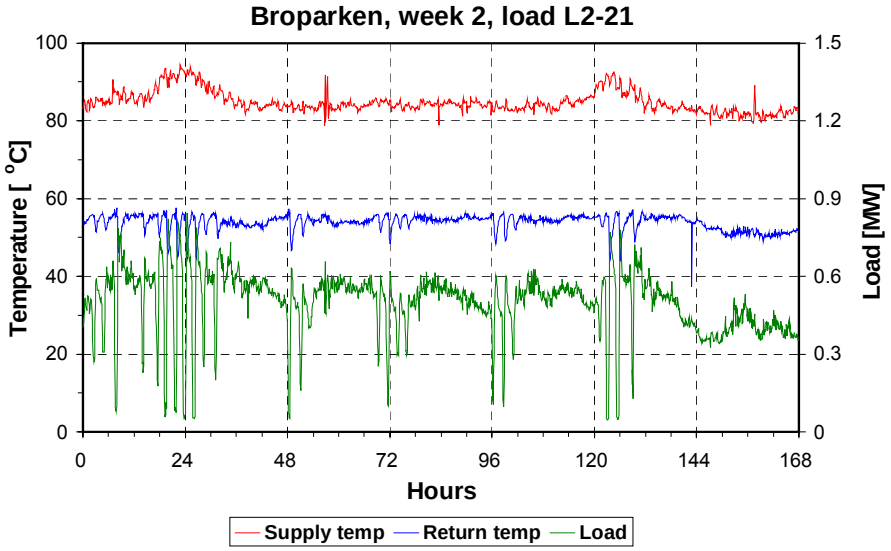
Broparken, week 2, load L2-21
Temperature [°C]
Load [MW]
Hours
0
24
48
72
96
120
144
168
0
20
40
60
80
100
0
0.3
0.6
0.9
1.2
1.5
Supply temp
Return temp
Load

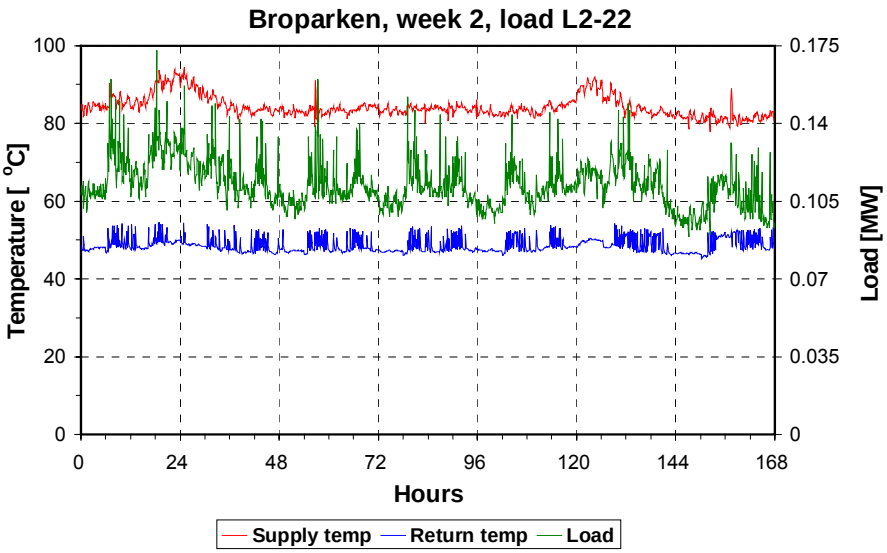
Broparken, week 2, load L2-22
Temperature [°C]
Load [MW]
Hours
0
20
40
60
80
100
0
0.035
0.07
0.105
0.14
0.175
0
24
48
72
96
120
144
168
Supply temp
Return temp
Load

Broparken, week 19:

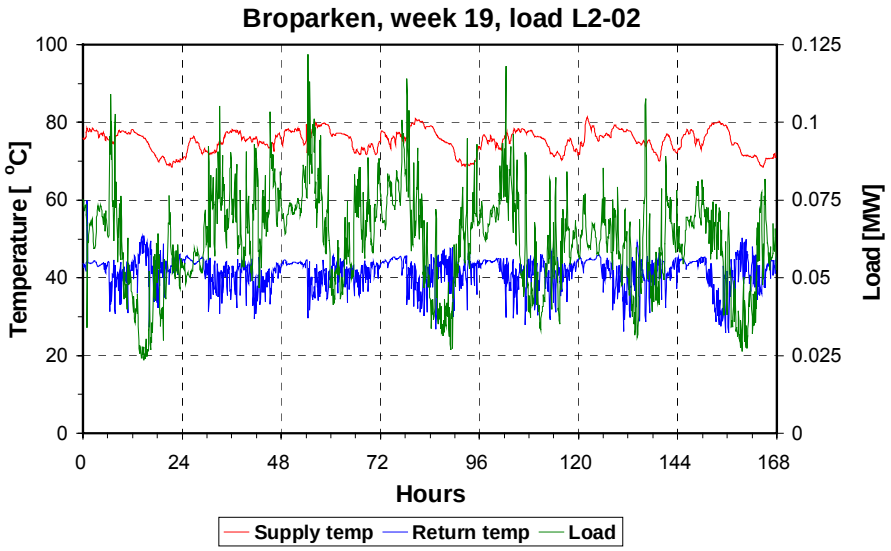

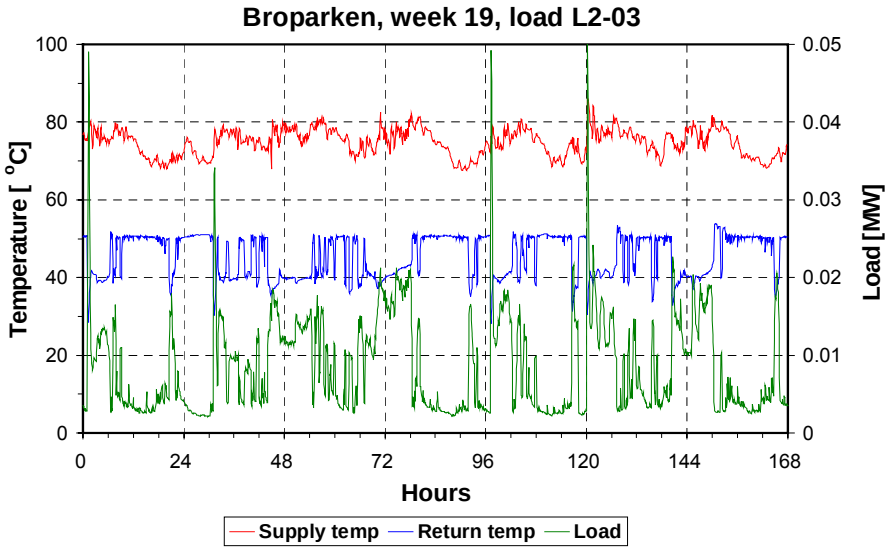

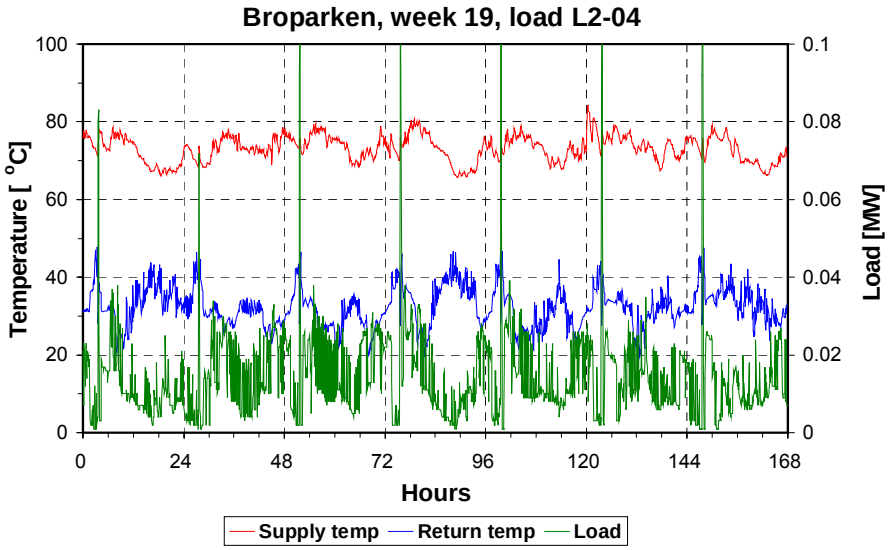

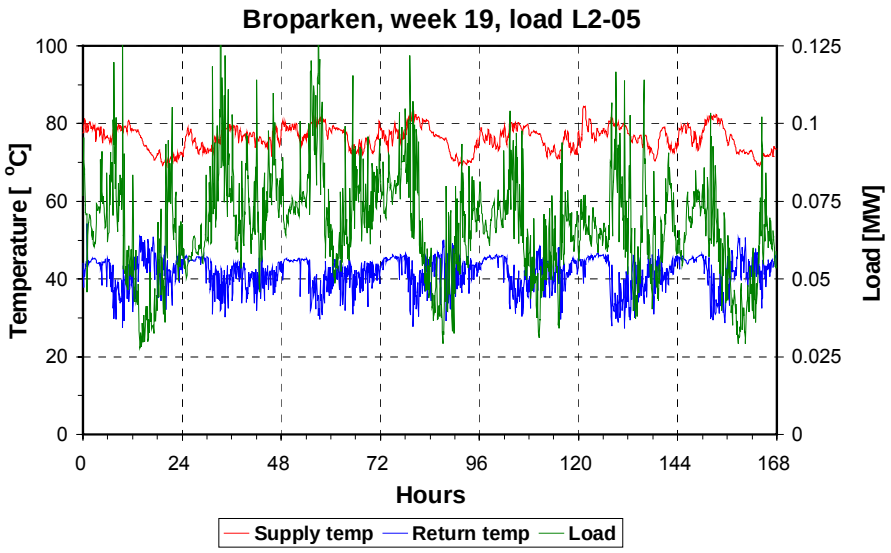
Broparken, week 19, load L2-05
Temperature [°C]
Load [MW]
Hours
0
24
48
72
96
120
144
168
0
20
40
60
80
100
0
0.025
0.05
0.075
0.1
0.125
Supply temp
Return temp
Load

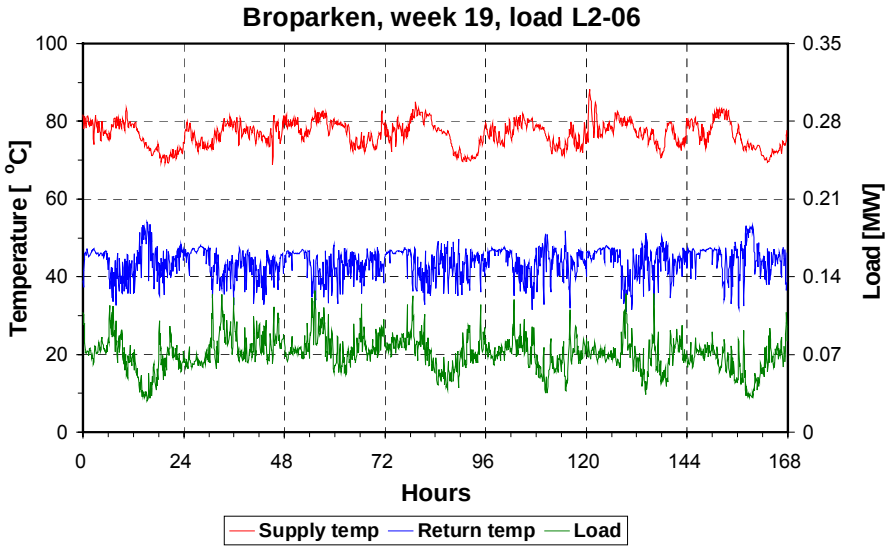
Broparken, week 19, load L2-06
Temperature [°C]
Load [MW]
Hours
0
24
48
72
96
120
144
168
0
20
40
60
80
100
0
0.07
0.14
0.21
0.28
0.35
Supply temp
Return temp
Load

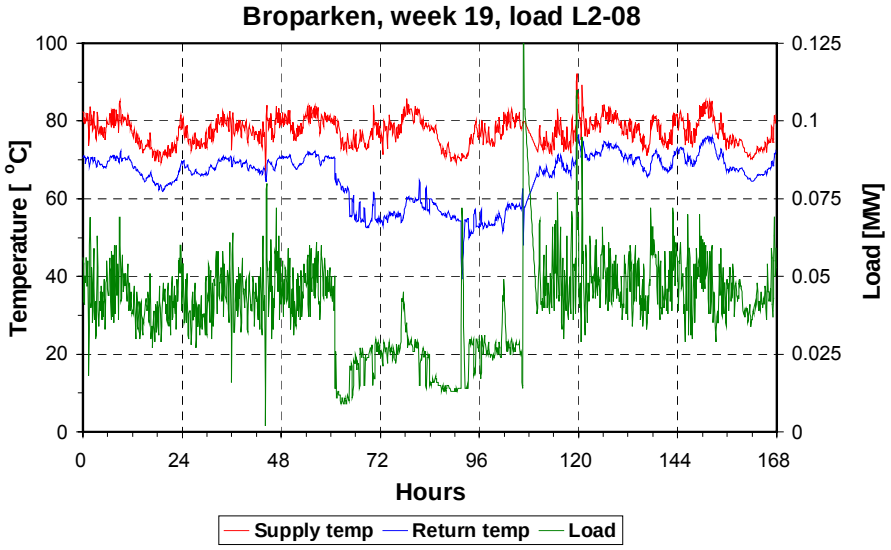
Broparken, week 19, load L2-08
Temperature [°C]
Load [MW]
Hours
0
24
48
72
96
120
144
168
0
20
40
60
80
100
0
0.025
0.05
0.075
0.1
0.125
Supply temp
Return temp
Load

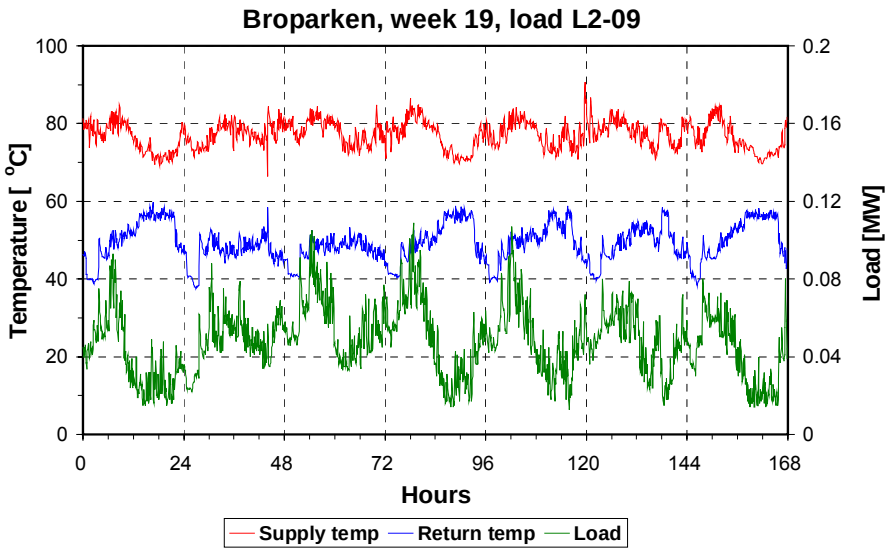
Broparken, week 19, load L2-09
Temperature [°C]
Load [MW]
Hours
0
24
48
72
96
120
144
168
0
20
40
60
80
100
0
0.04
0.08
0.12
0.16
0.2
Supply temp
Return temp
Load

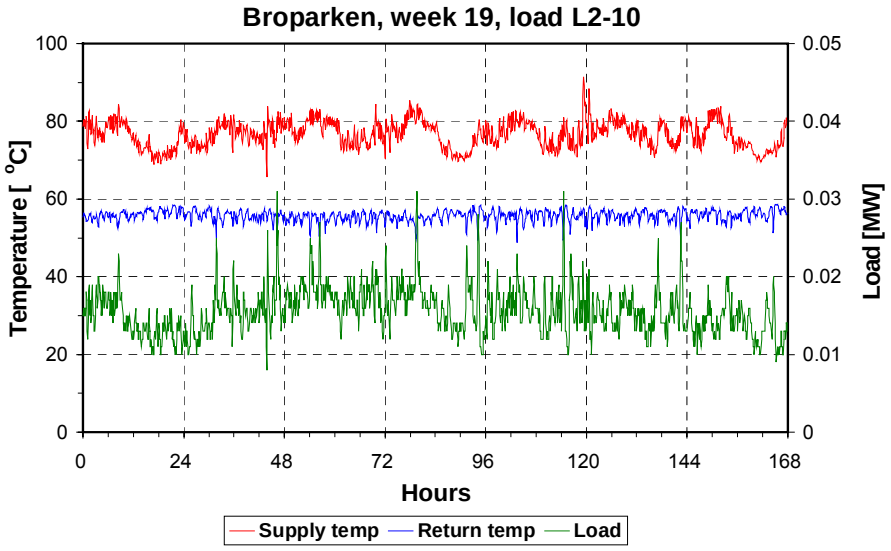
Broparken, week 19, load L2-10
Temperature [°C]
Load [MW]
Hours
0
24
48
72
96
120
144
168
0
20
40
60
80
100
0
0.01
0.02
0.03
0.04
0.05
Supply temp
Return temp
Load

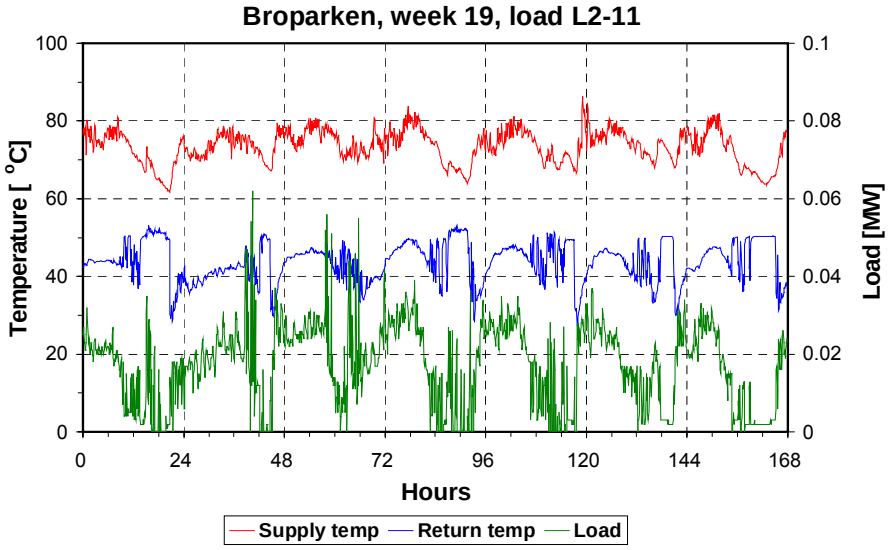
Broparken, week 19, load L2-11
Temperature [°C]
Load [MW]
Hours
0
24
48
72
96
120
144
168
0
20
40
60
80
100
0
0.02
0.04
0.06
0.08
0.1
Supply temp
Return temp
Load

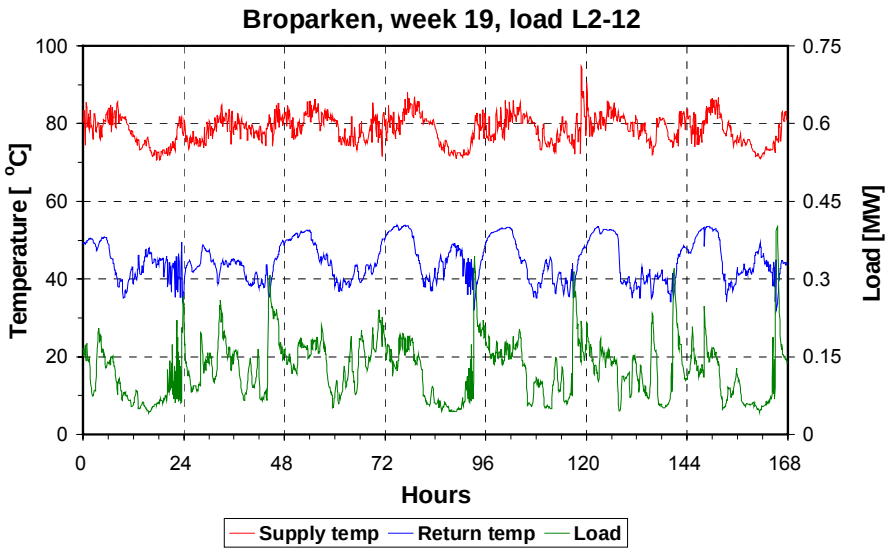
Broparken, week 19, load L2-12
Temperature [°C]
Load [MW]
Hours
Supply temp
Return temp
Load

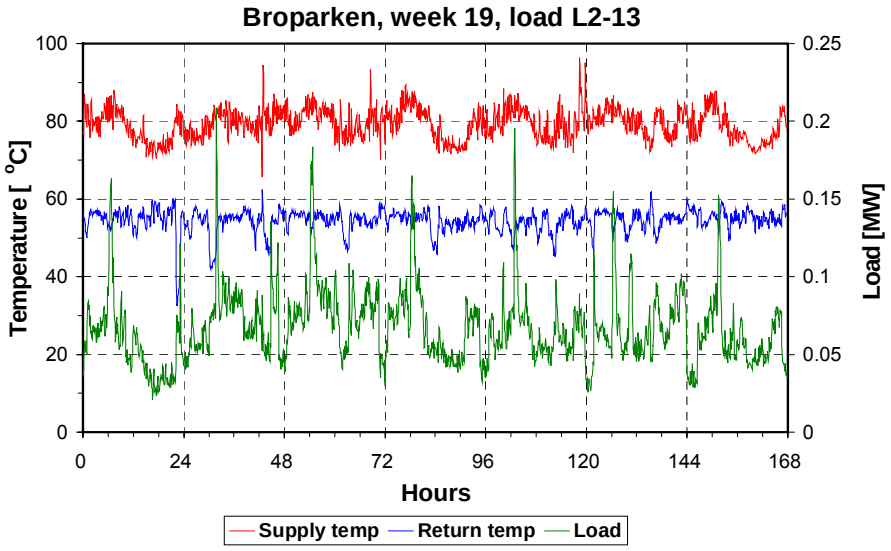
Broparken, week 19, load L2-13
Temperature [°C]
Load [MW]
Hours
Supply temp
Return temp
Load

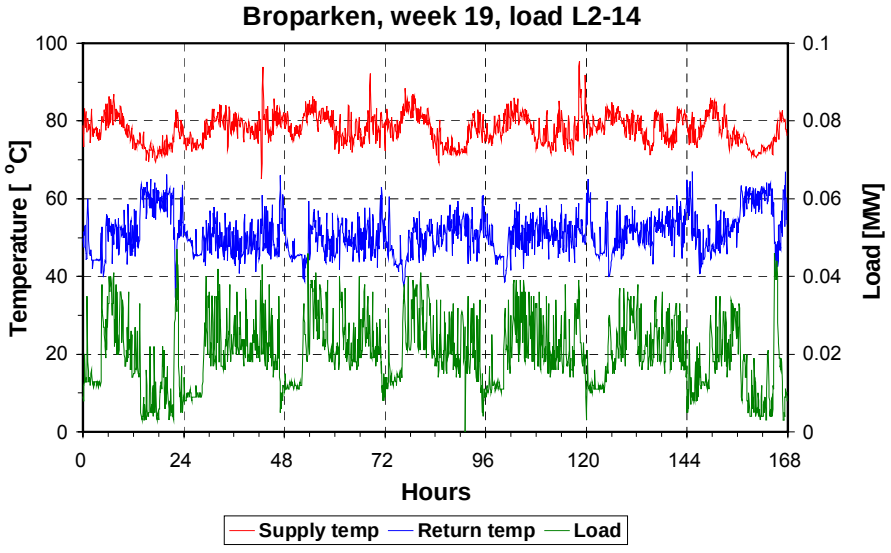
Broparken, week 19, load L2-14
Temperature [°C]
Load [MW]
Hours
Supply temp
Return temp
Load

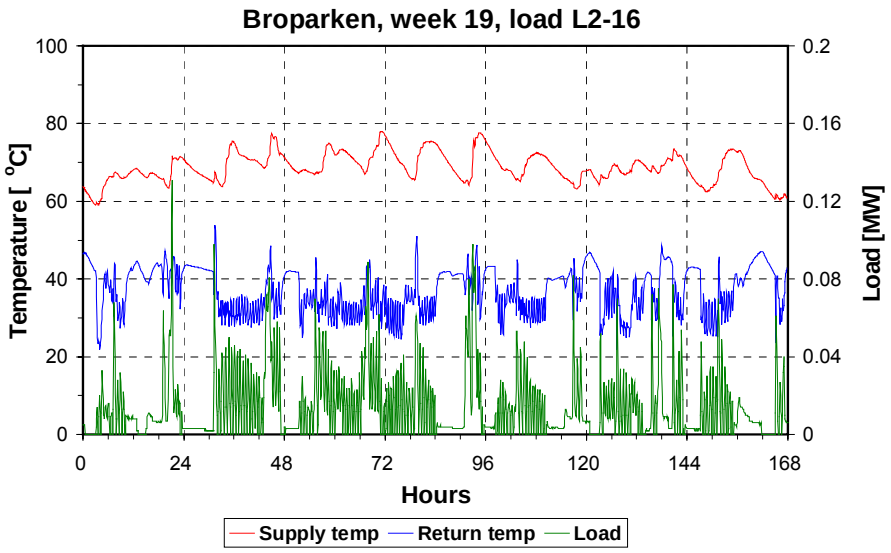
Broparken, week 19, load L2-16
Temperature [°C]
Load [MW]
Hours
Supply temp
Return temp
Load

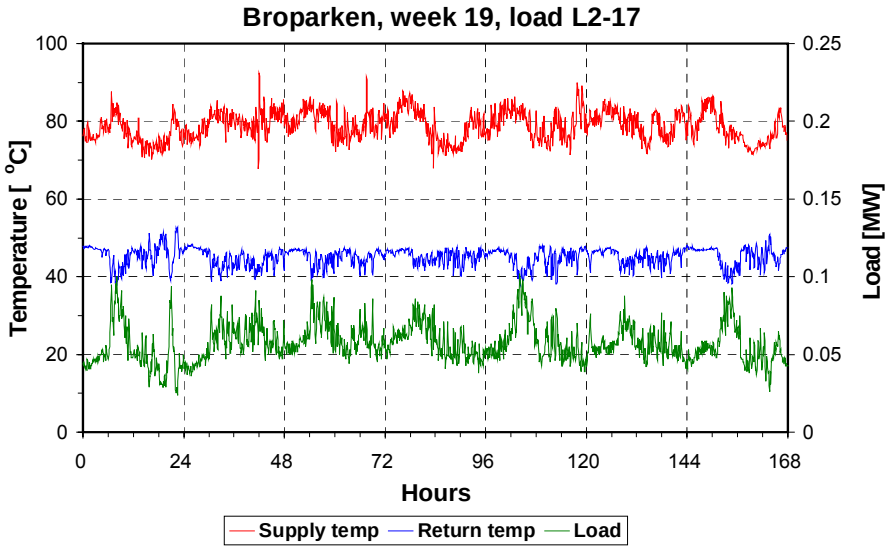
Broparken, week 19, load L2-17
Temperature [°C]
Load [MW]
Hours
Supply temp
Return temp
Load

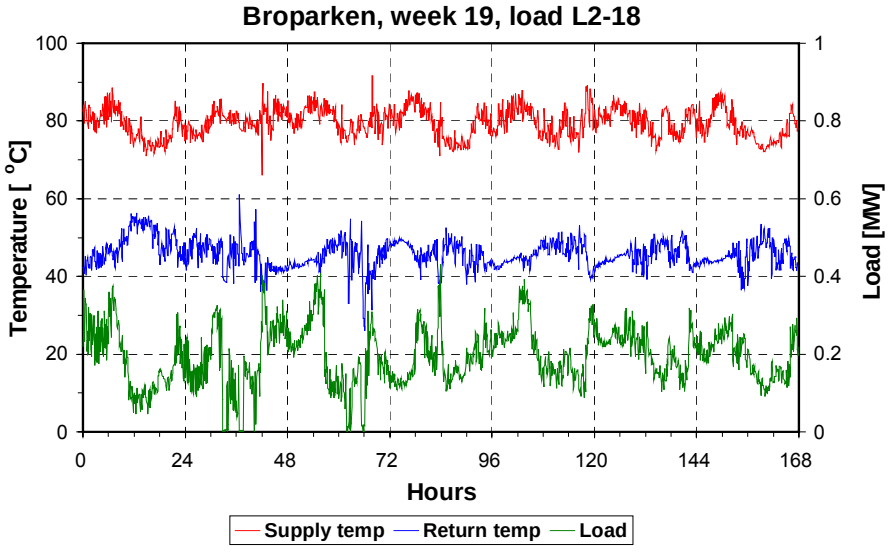
Broparken, week 19, load L2-18
Temperature [°C]
Load [MW]
Hours
Supply temp
Return temp
Load

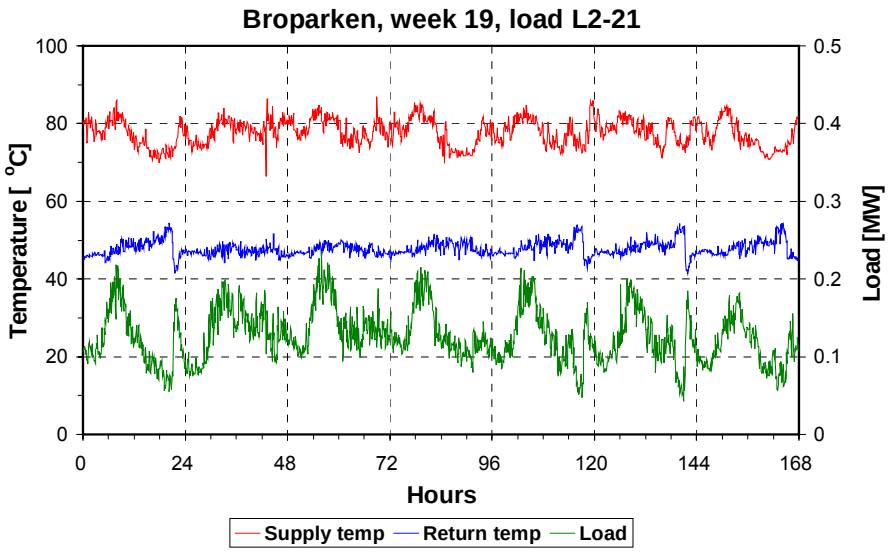
Broparken, week 19, load L2-21
Temperature [°C]
Load [MW]
Hours
Supply temp
Return temp
Load

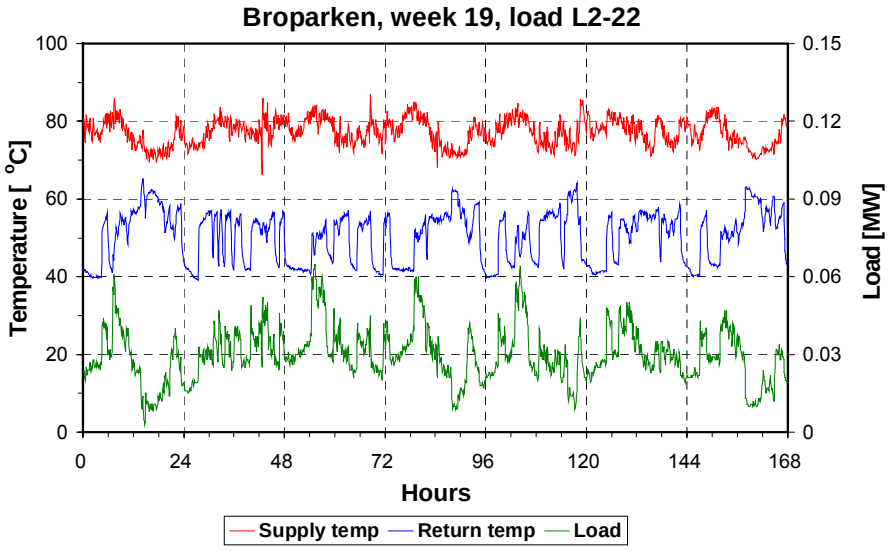
Broparken, week 19, load L2-22
Temperature [°C]
Load [MW]
Hours
Supply temp
Return temp
Load

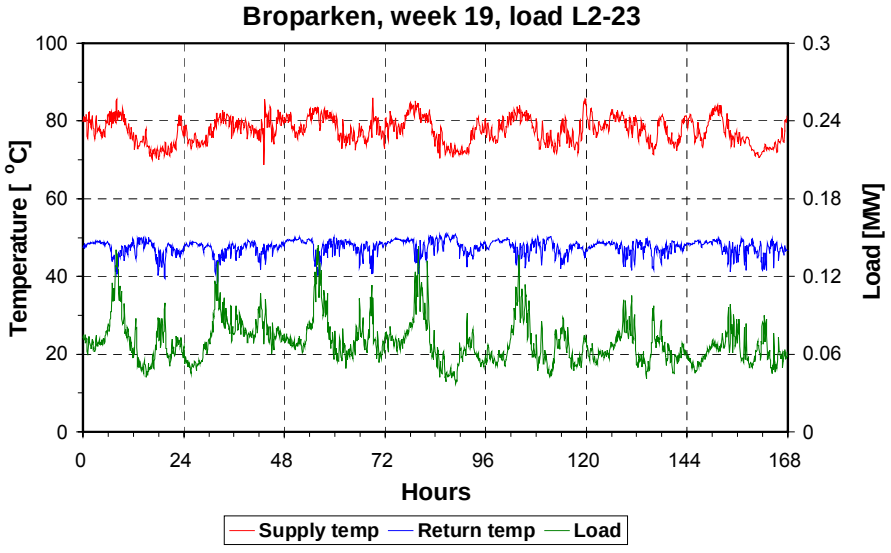
Broparken, week 19, load L2-23
Temperature [°C]
Load [MW]
Hours
Supply temp
Return temp
Load

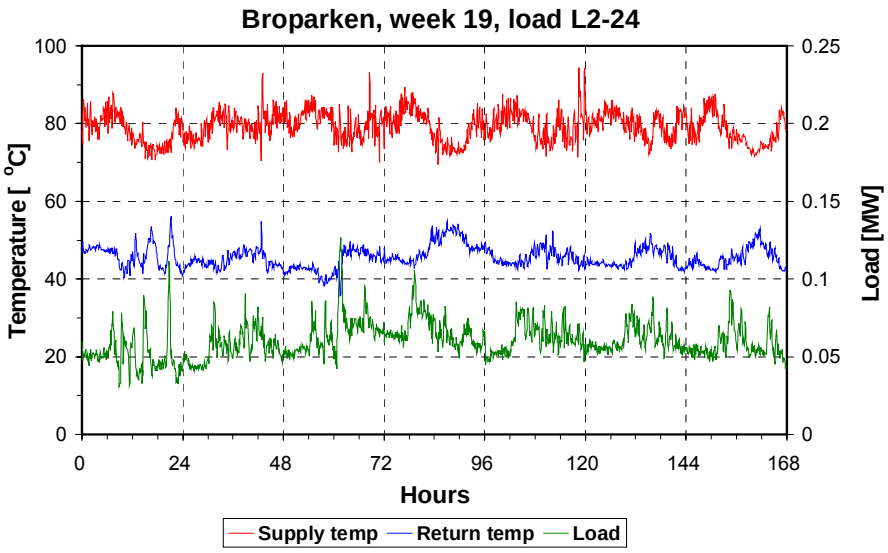
Broparken, week 19, load L2-24
Temperature [°C]
Load [MW]
Hours
0
20
40
60
80
100
0
0.05
0.1
0.15
0.2
0.25
0
24
48
72
96
120
144
168
Supply temp
Return temp
Load

Broparken, week 33:

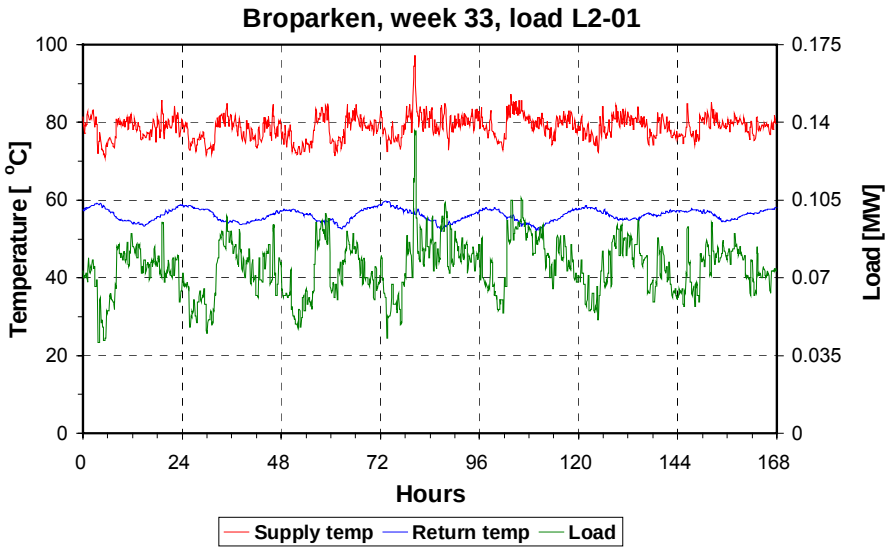

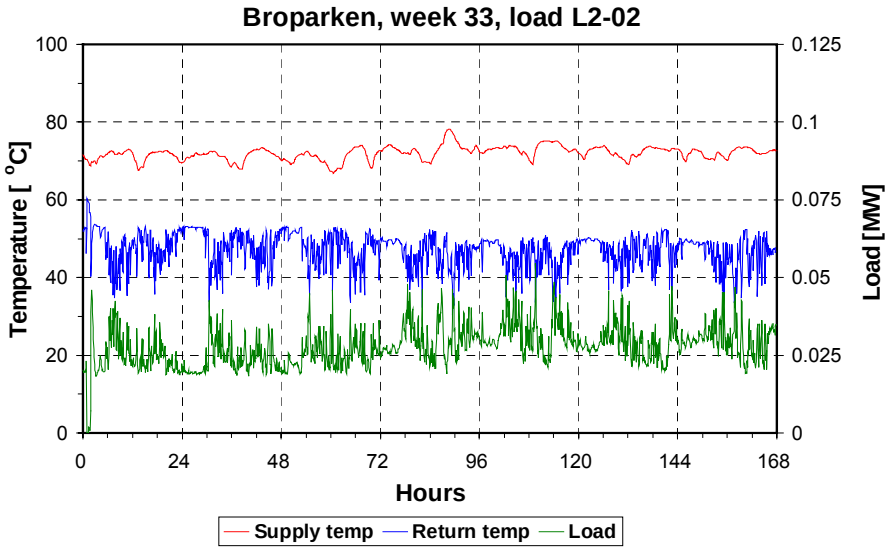

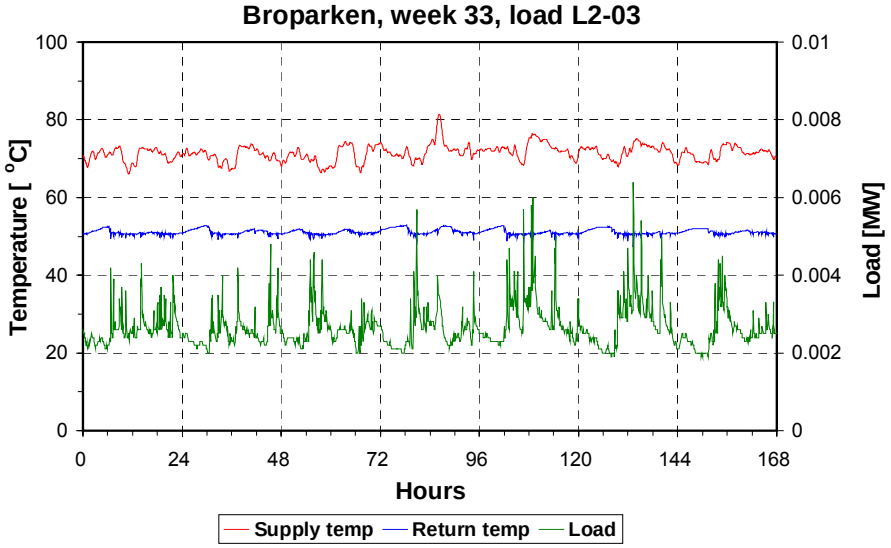

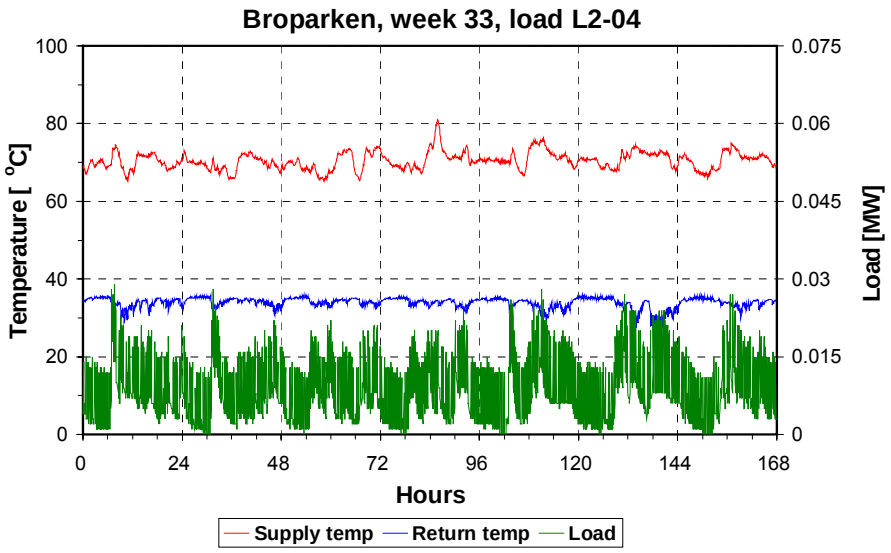
Broparken, week 33, load L2-04
Temperature [°C]
Load [MW]
Hours
0
24
48
72
96
120
144
168
0
20
40
60
80
100
0
0.015
0.03
0.045
0.06
0.075
Supply temp
Return temp
Load

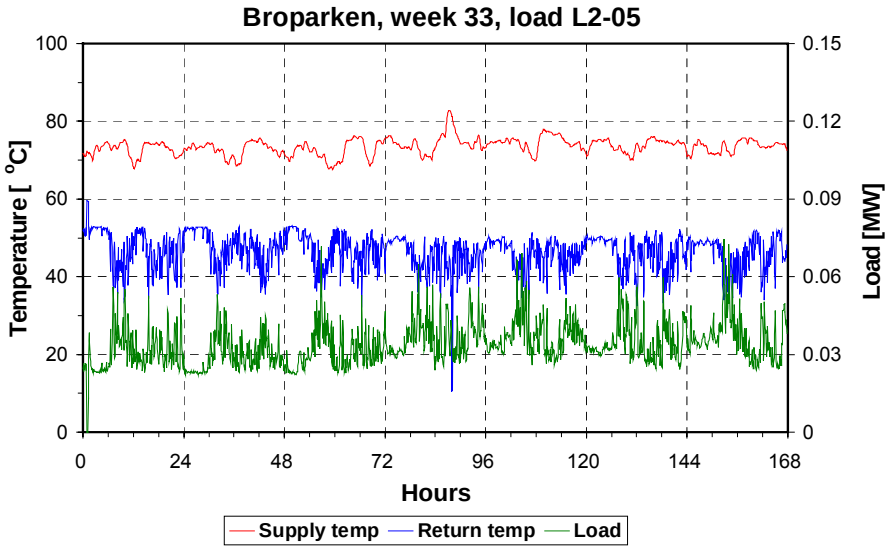
Broparken, week 33, load L2-05
Temperature [°C]
Load [MW]
Hours
0
24
48
72
96
120
144
168
0
20
40
60
80
100
0
0.03
0.06
0.09
0.12
0.15
Supply temp
Return temp
Load

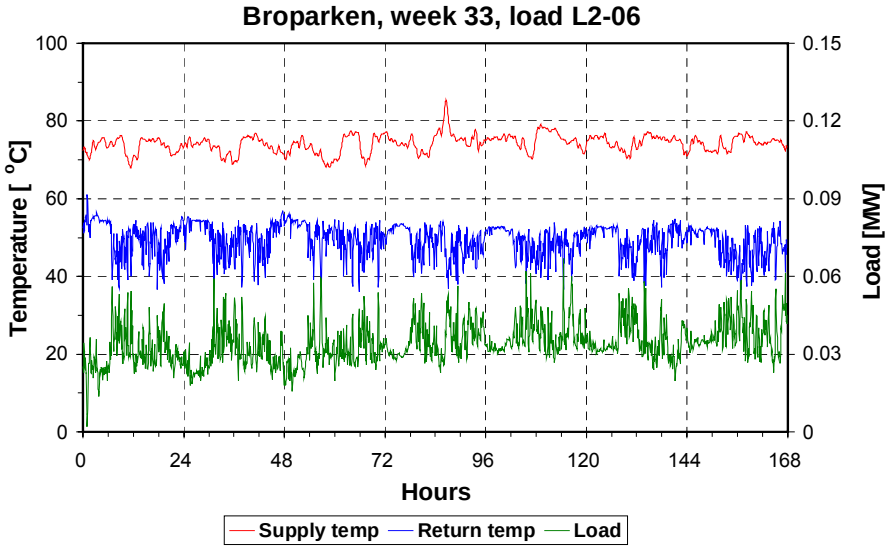
Broparken, week 33, load L2-06
Temperature [°C]
Load [MW]
Hours
0
24
48
72
96
120
144
168
0
20
40
60
80
100
0
0.03
0.06
0.09
0.12
0.15
Supply temp
Return temp
Load

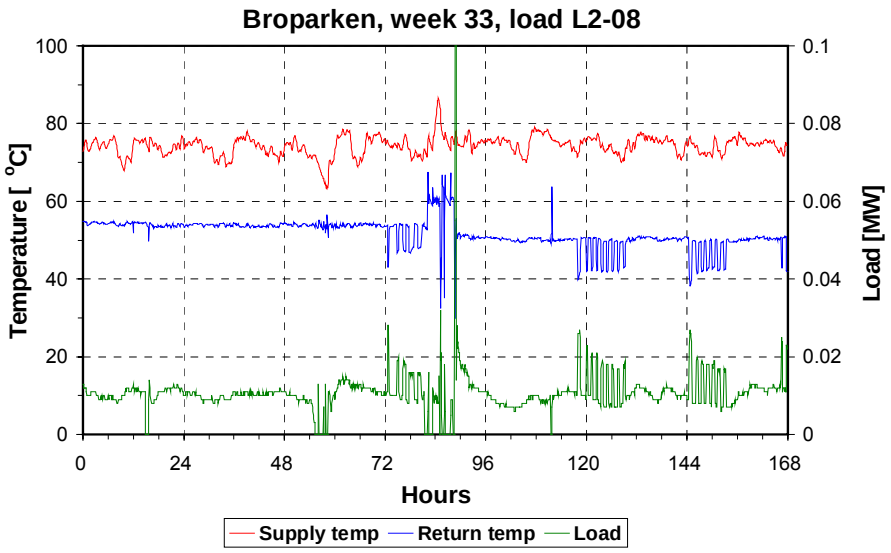
Broparken, week 33, load L2-08
Temperature [°C]
Load [MW]
Hours
Supply temp
Return temp
Load

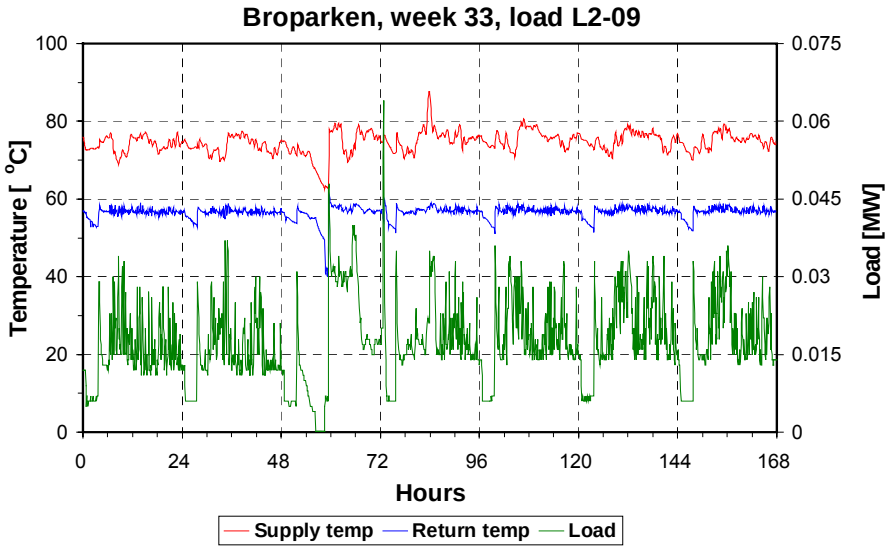
Broparken, week 33, load L2-09
Temperature [°C]
Load [MW]
Hours
Supply temp
Return temp
Load

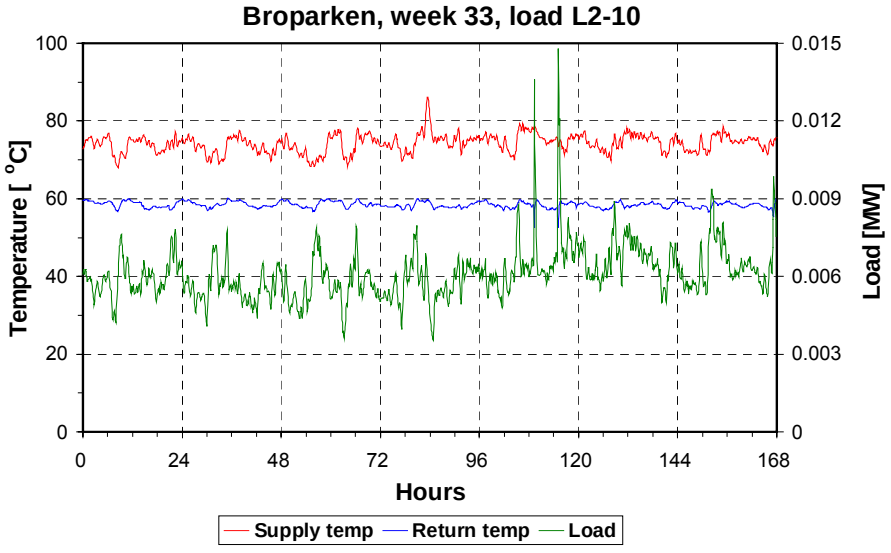
Broparken, week 33, load L2-10
Temperature [°C]
Load [MW]
Hours
Supply temp
Return temp
Load

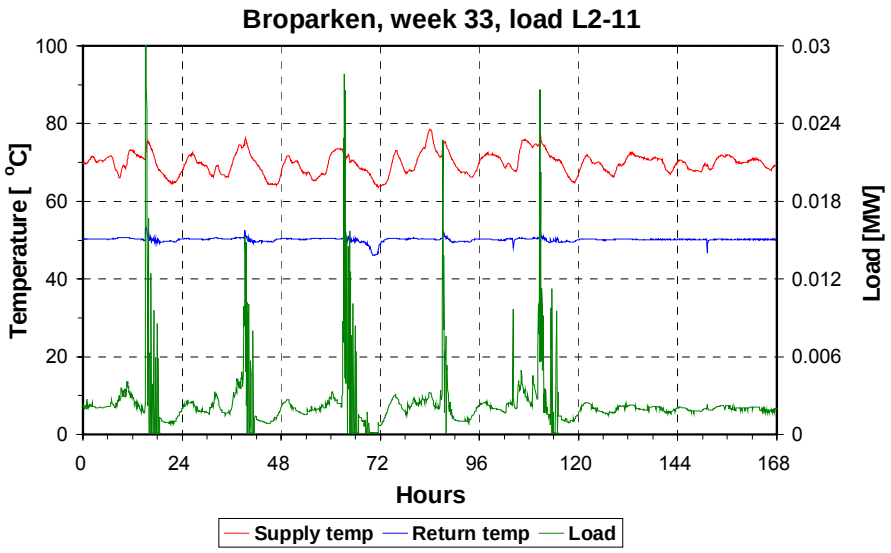
Broparken, week 33, load L2-11
Temperature [°C]
Load [MW]
Hours
0
24
48
72
96
120
144
168
0
20
40
60
80
100
0
0.006
0.012
0.018
0.024
0.03
Supply temp
Return temp
Load

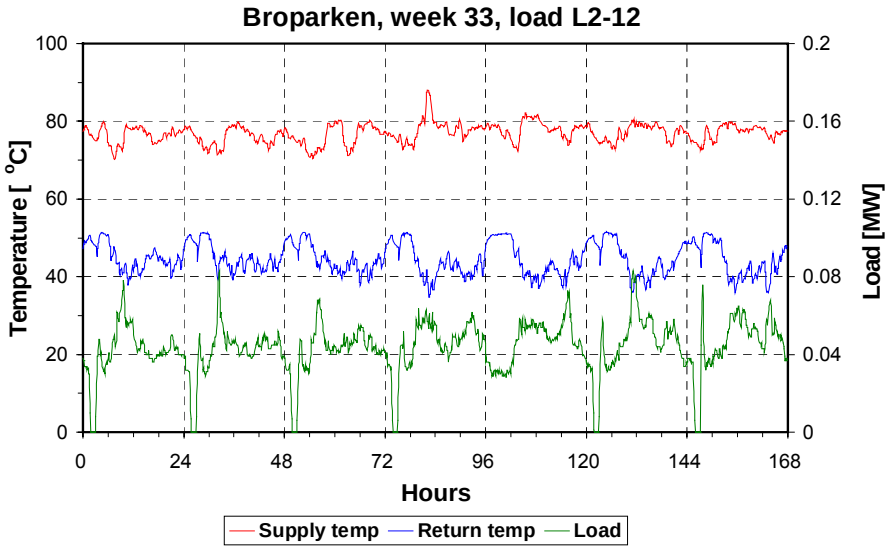
Broparken, week 33, load L2-12
Temperature [°C]
Load [MW]
Hours
0
24
48
72
96
120
144
168
0
20
40
60
80
100
0
0.04
0.08
0.12
0.16
0.2
Supply temp
Return temp
Load

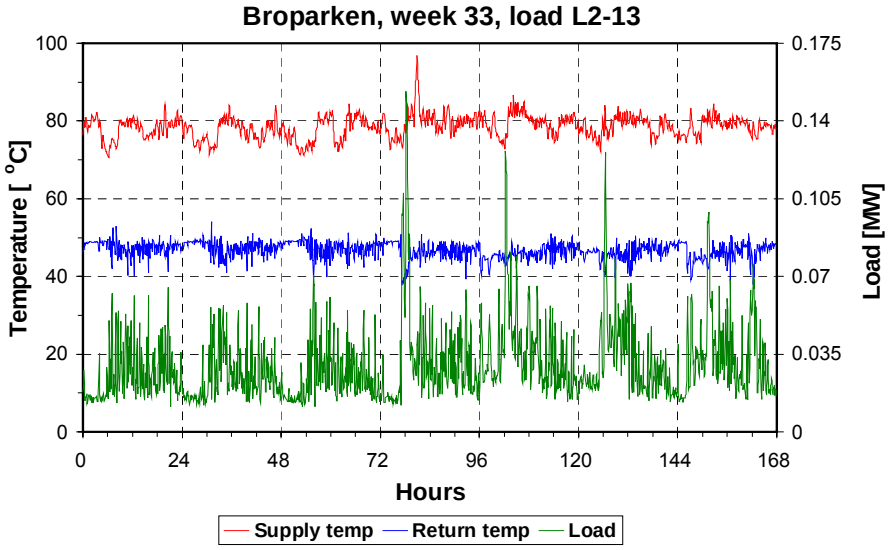
Broparken, week 33, load L2-13
Temperature [°C]
Load [MW]
Hours
0
24
48
72
96
120
144
168
0
20
40
60
80
100
0
0.035
0.07
0.105
0.14
0.175
Supply temp
Return temp
Load

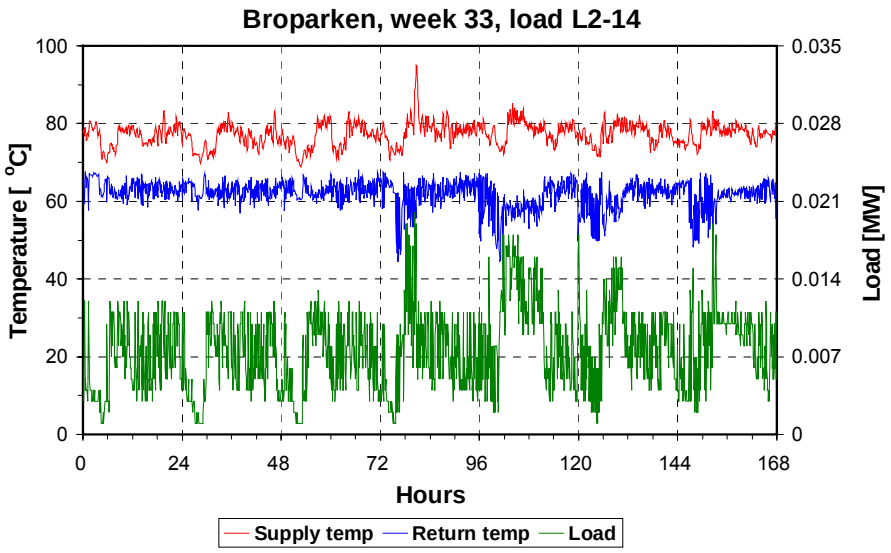
Broparken, week 33, load L2-14
Temperature [°C]
Load [MW]
Hours
0
24
48
72
96
120
144
168
0
20
40
60
80
100
0
0.007
0.014
0.021
0.028
0.035
Supply temp
Return temp
Load

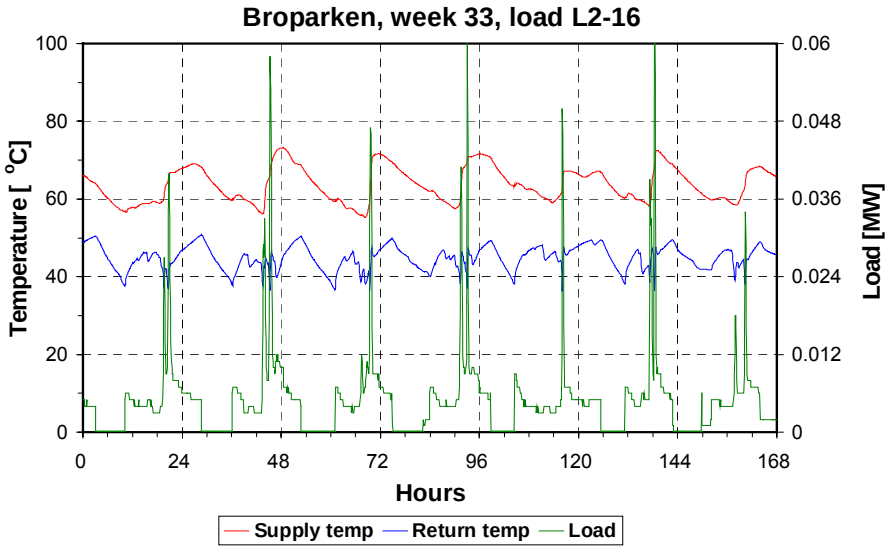
Broparken, week 33, load L2-16
Temperature [°C]
Load [MW]
Hours
0
24
48
72
96
120
144
168
0
20
40
60
80
100
0
0.012
0.024
0.036
0.048
0.06
Supply temp
Return temp
Load

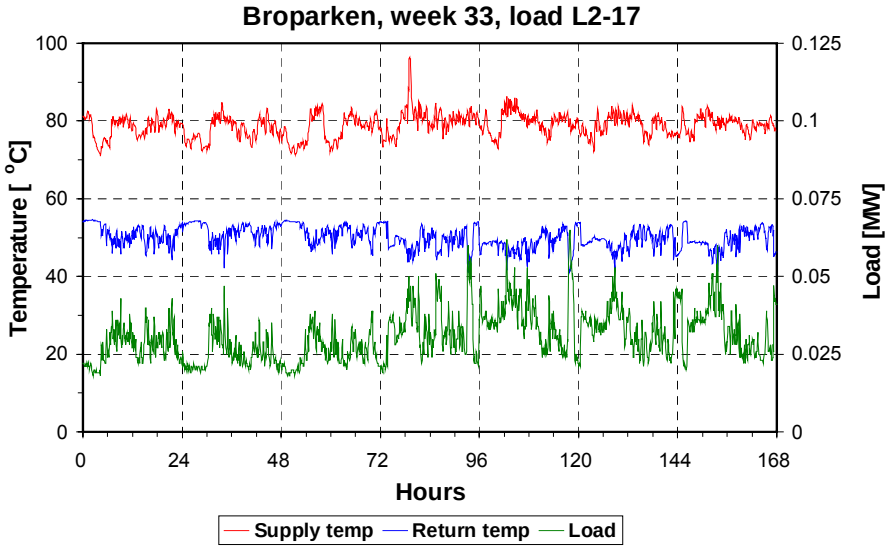
Broparken, week 33, load L2-17
Temperature [°C]
Load [MW]
Hours
0
24
48
72
96
120
144
168
0
20
40
60
80
100
0
0.025
0.05
0.075
0.1
0.125
Supply temp
Return temp
Load

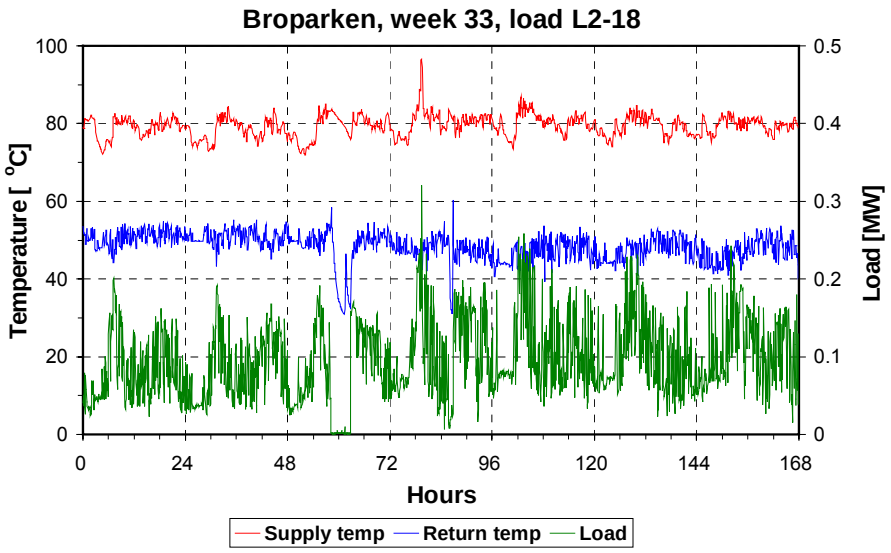
Broparken, week 33, load L2-18
Temperature [°C]
Load [MW]
Hours
Supply temp
Return temp
Load

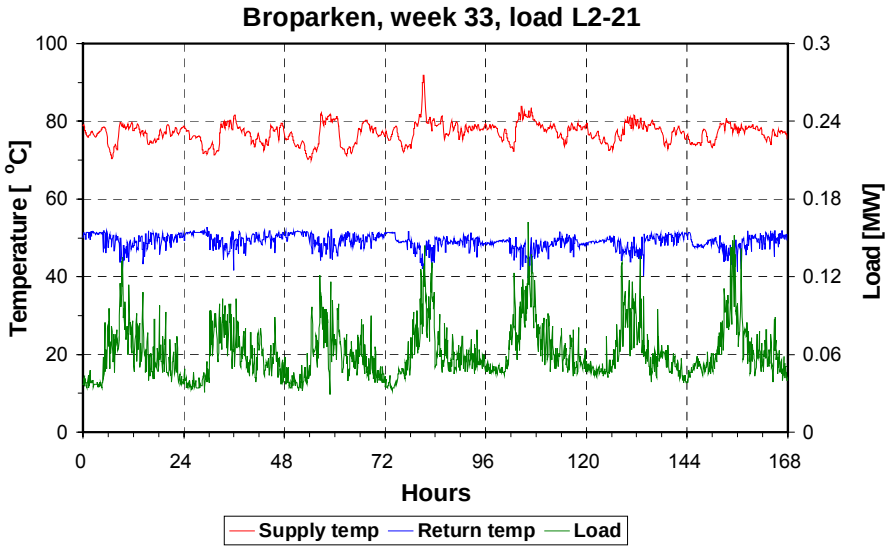
Broparken, week 33, load L2-21
Temperature [°C]
Load [MW]
Hours
Supply temp
Return temp
Load

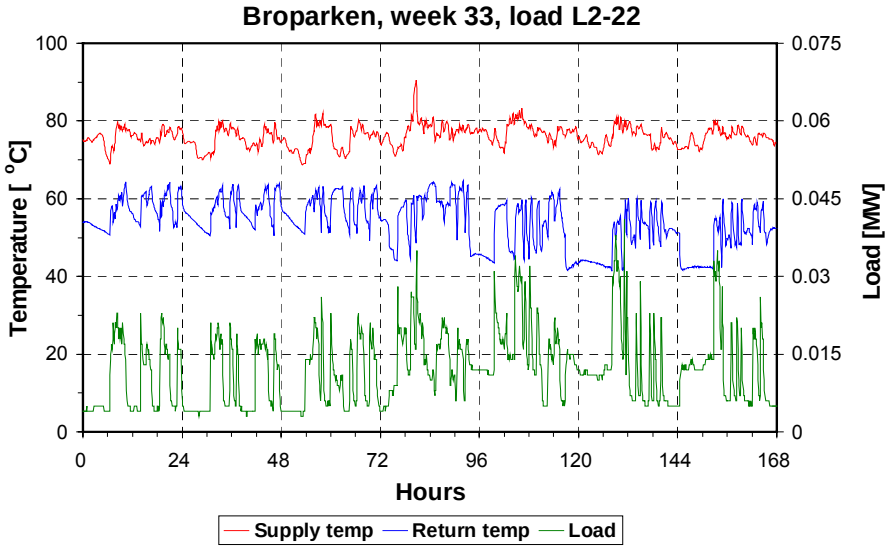
Broparken, week 33, load L2-22
Temperature [°C]
Load [MW]
Hours
Supply temp
Return temp
Load

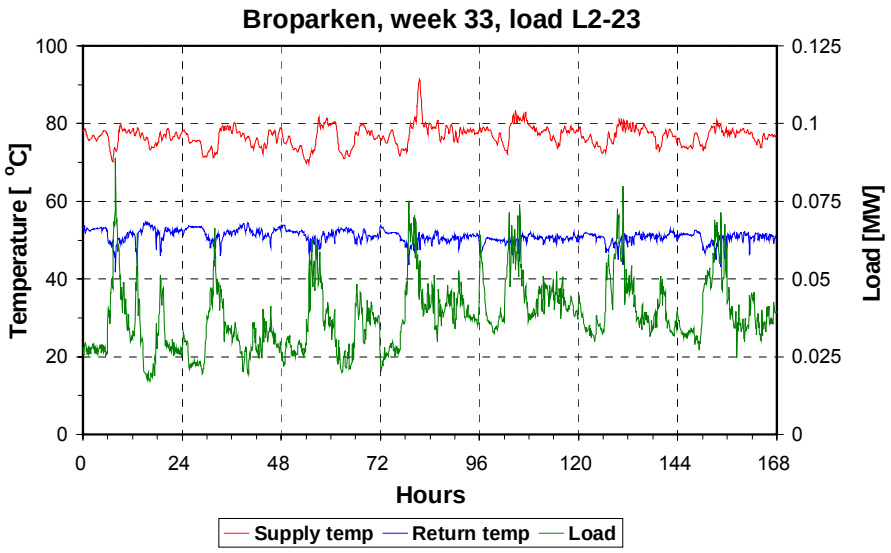
Broparken, week 33, load L2-23
Temperature [°C]
Load [MW]
Hours
0
24
48
72
96
120
144
168
0
20
40
60
80
100
0
0.025
0.05
0.075
0.1
0.125
Supply temp
Return temp
Load

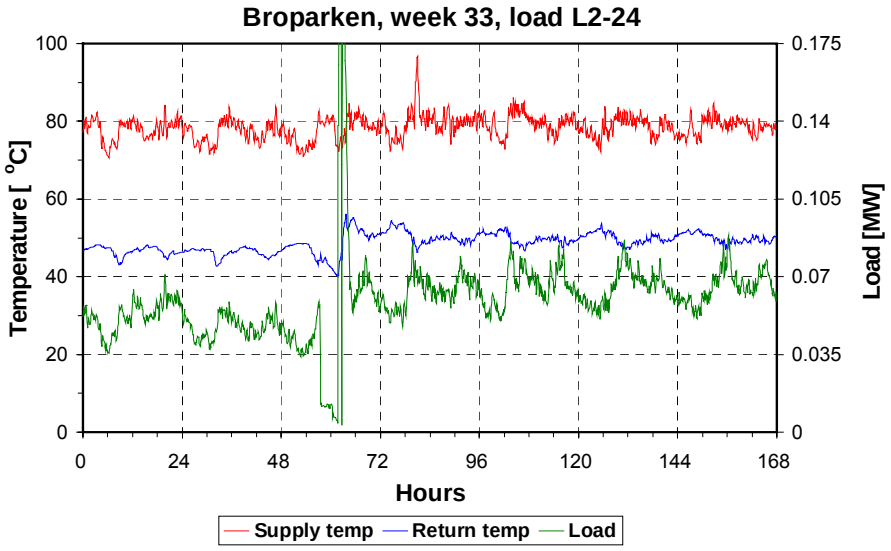
Broparken, week 33, load L2-24
Temperature [°C]
Load [MW]
Hours
0
24
48
72
96
120
144
168
0
20
40
60
80
100
0
0.035
0.07
0.105
0.14
0.175
Supply temp
Return temp
Load

Appendix C Ishoej district heating grid

Physical system:

Branch	Node A	Node B	Length	Steel pipe	Heat loss coefficient	
				Inner diam.	Supply pipe	Return pipe
			m	m	W/(m·°C)	W/(m·°C)
Plant-K1	Plant	K1	71.8	0.3444	0.5364	0.4864
K1-K2	K1	K2	605.8	0.3127	0.5519	0.4964
K1-V39	K1	V39	395.3	0.1603	0.2915	0.2742
K2-K11	K2	K11	235.2	0.3127	0.5519	0.4964
K11-V03	K11	V03	13.9	0.3127	0.5519	0.4964
K11-K12	K11	K12	840.7	0.1847	0.3703	0.3421
K12-V01	K12	V01	97.7	0.1847	0.3703	0.3421
K2-K3	K2	K3	602.4	0.3127	0.5519	0.4964
K3-K21	K3	K21	150.5	0.3127	0.5519	0.4964
K3-K4	K3	K4	47.8	0.2630	0.4749	0.4321
K4-K31	K4	K31	139.8	0.1847	0.3703	0.3421
K31-K32	K31	K32	154.4	0.1603	0.3548	0.3279
K32-K33	K32	K33	116.0	0.1325	0.3107	0.2894
K33-K34	K33	K34	103.1	0.1325	0.3107	0.2894
K34-K35	K34	K35	34.3	0.1008	0.2472	0.2334
K36-I13	K36	I13	6.5	0.0428	0.1911	0.1815
K35-K36	K35	K36	44.3	0.0702	0.2440	0.2291
K35-K37	K35	K37	150.0	0.1008	0.2472	0.2334
K37-V20	K37	V20	129.1	0.0826	0.2573	0.2413
K4-K5	K4	K5	227.6	0.2630	0.4749	0.4321
K5-K41	K5	K41	56.5	0.1847	0.3703	0.3421
K41-V08	K41	V08	16.7	0.1847	0.3703	0.3421
K41-K42	K41	K42	319.7	0.1847	0.3703	0.3421
K42-V07	K42	V07	14.9	0.1847	0.3703	0.3421
K5-K6	K5	K6	110.8	0.1258	0.2876	0.2694
K6-K7	K6	K7	216.5	0.1258	0.2876	0.2694
K6-I79	K6	I79	78.1	0.0826	0.2247	0.2129
K7-K8	K7	K8	154.6	0.1008	0.2472	0.2334
K7-V13	K7	V13	16.8	0.0826	0.2247	0.2129
K8-K9	K8	K9	323.0	0.0702	0.2960	0.2732
K9-V11	K9	V11	15.1	0.0702	0.2960	0.2732
K9-V11A	K9	V11A	170.1	0.0702	0.2960	0.2732
K21-V02	K21	V02	82.8	0.2101	0.3771	0.3492
K12-V04	K12	V04	592.0	0.1847	0.3703	0.3421
K42-V09	K42	V09	437.1	0.0826	0.2247	0.2129
K36-V10	K36	V10	26.4	0.0702	0.2440	0.2291
K34-V12	K34	V12	27.7	0.1008	0.2472	0.2334
K37-V14	K37	V14	64.3	0.1008	0.2472	0.2334
K12-V15	K12	V15	382.1	0.1008	0.2472	0.2334
K33-V17	K33	V17	440.7	0.1325	0.3745	0.3421
K21-V18	K21	V18	322.9	0.1068	0.2668	0.2506
K32-V61	K32	V61	39.8	0.1603	0.3548	0.3279
K31-V62	K31	V62	134.1	0.1068	0.2668	0.2506
K8-V05	K8	V05	72.0	0.1008	0.2472	0.2334

Aggregated systems:

The following table lists the aggregated models. The model in a specific row of the table is made from the model in the preceding row by a further aggregation. The physical grid is shown in the top of the table.

Model	Number of branches	Number of loads	Description
Phys	44	23	The physical system.
D_44	44	23	All branches in-line. The number of branches is not reduced.
D_23	23	23	All branches with no load in-between are collapsed to one branch.
D_20	20	20	Short branches are removed.
D_15	15	15	Short branches are removed.
D_10	10	10	Short branches are removed.
D_5	5	5	Short branches are removed.
D_4	4	4	Short branches are removed.
D_3	3	3	Short branches are removed.
D_2	2	2	Short branches are removed.
D_1	1	2	Short branches are removed. There is also a load at the plant.

Appendix D Measured time series in Ishoej

All time series in this appendix are measured values covering the simulated period, i.e. from December 19, 2000 12:00 until December 24, 2000 24:00.

The first chart shows the supply and return temperatures from the DH plant and the power delivered to the DH grid.

The following charts show measured time series for primary and secondary supply and return temperatures as well as for the load for each of the 23 consumers in Ishoej.

For those substations where no data was available, a heat load series was constructed from other substations with data, taking into account the type of building (block of flats, school, etc.) and the heat consumption according to Table 1.3. To distinguish between these two kinds of substations, substations with real measurements are called Vxx or Ixx, while substations with simulated time series are called Sxx. Despite the uncertainty associated with this way of generating the missing data, the result is quite good as is shown in Figure 1.4 where the measured heat production at the Ishoej plant is compared with the sum of the heat loads in the house stations.

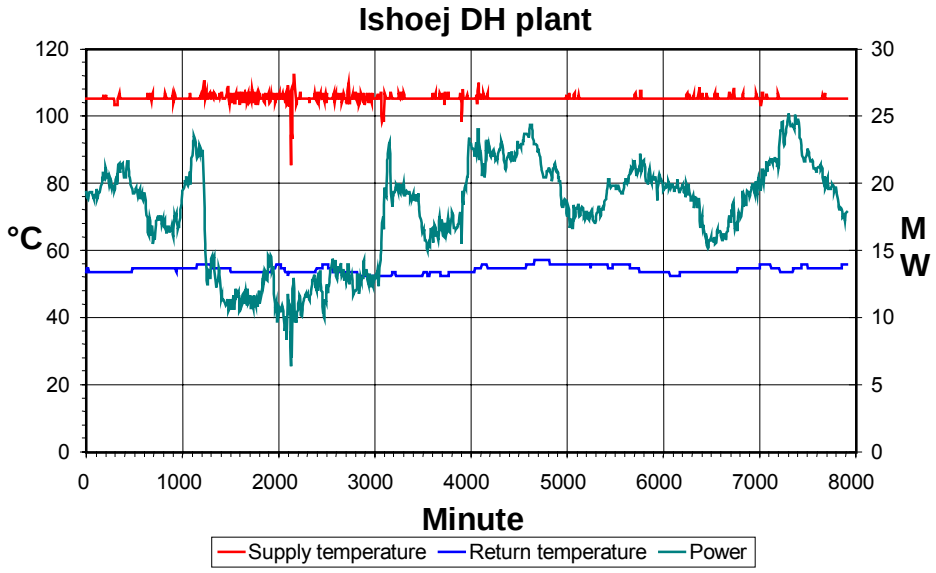

Temperatures and load at each consumer:

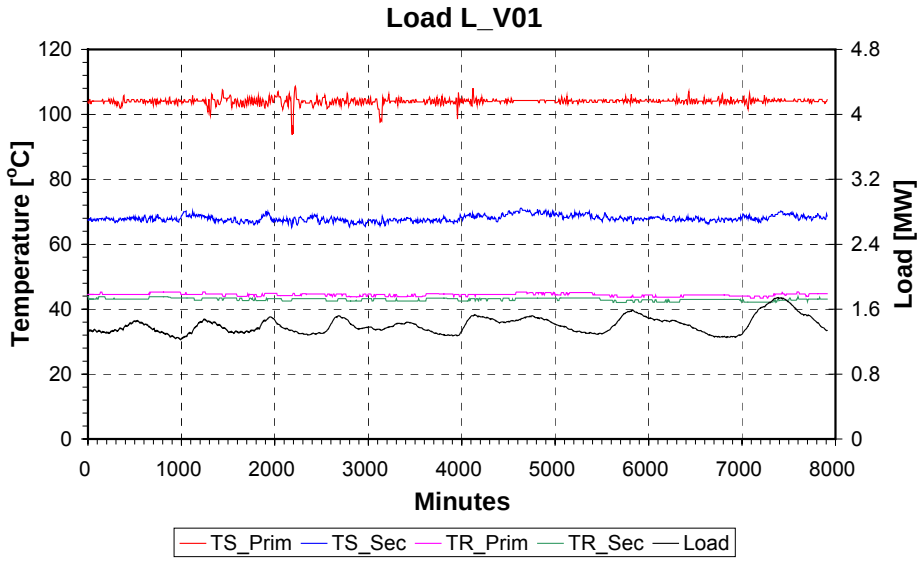

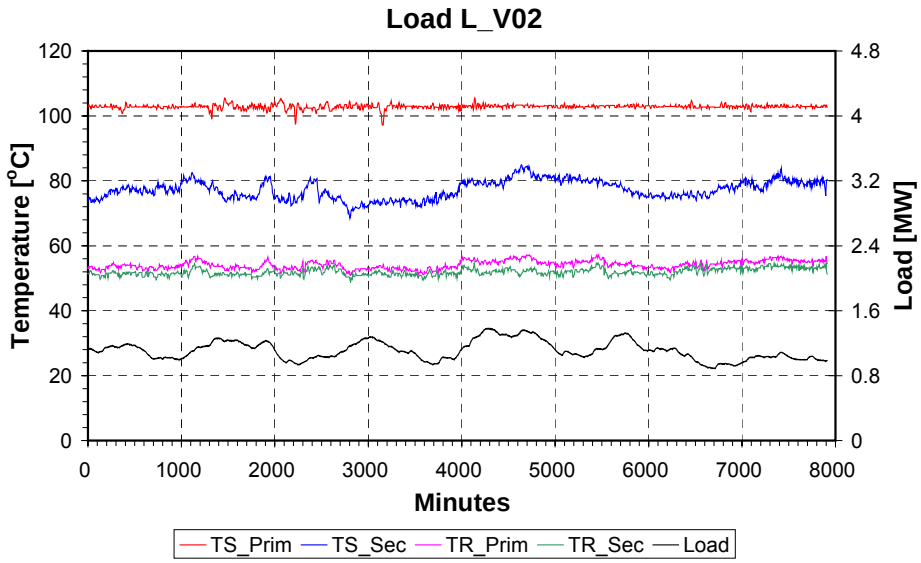

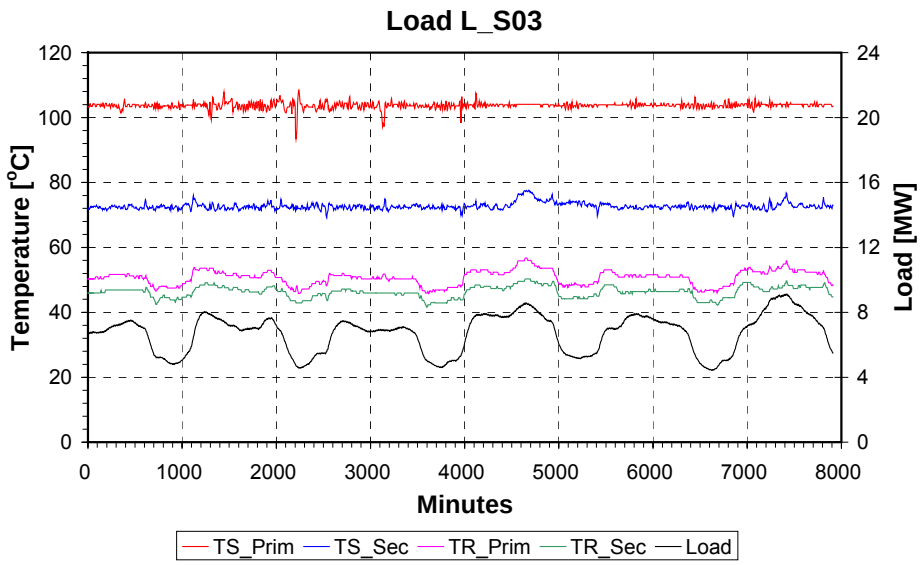
Load L_S03
Temperature [°C]
Load [MW]
Minutes
TS_Prim
TS_Sec
TR_Prim
TR_Sec
Load

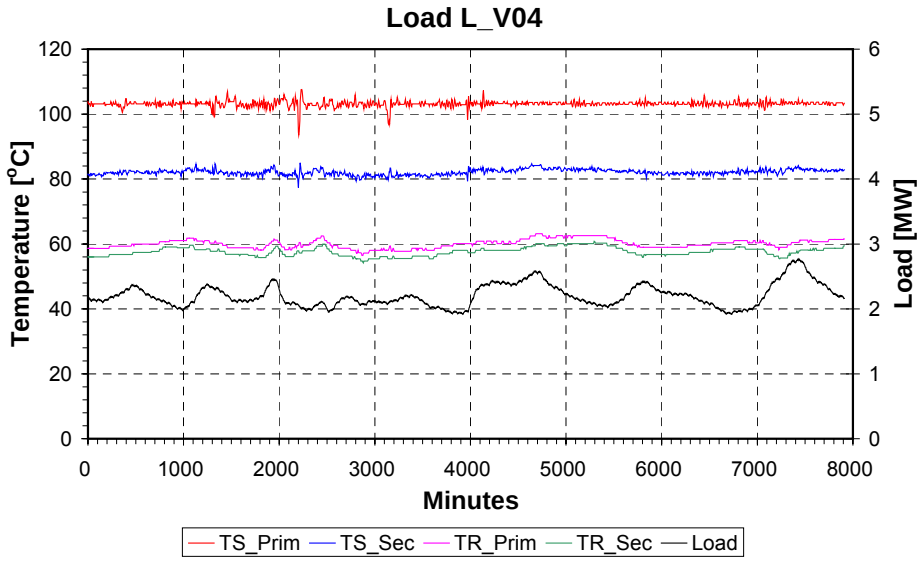
Load L_V04
Temperature [°C]
Load [MW]
Minutes
TS_Prim
TS_Sec
TR_Prim
TR_Sec
Load

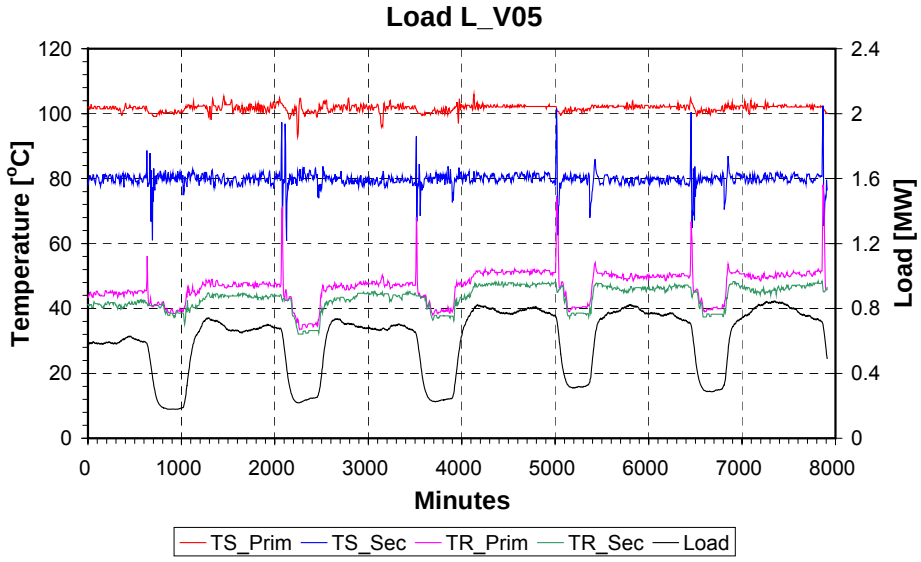
Load L_V05
Temperature [°C]
Load [MW]
Minutes
TS_Prim
TS_Sec
TR_Prim
TR_Sec
Load

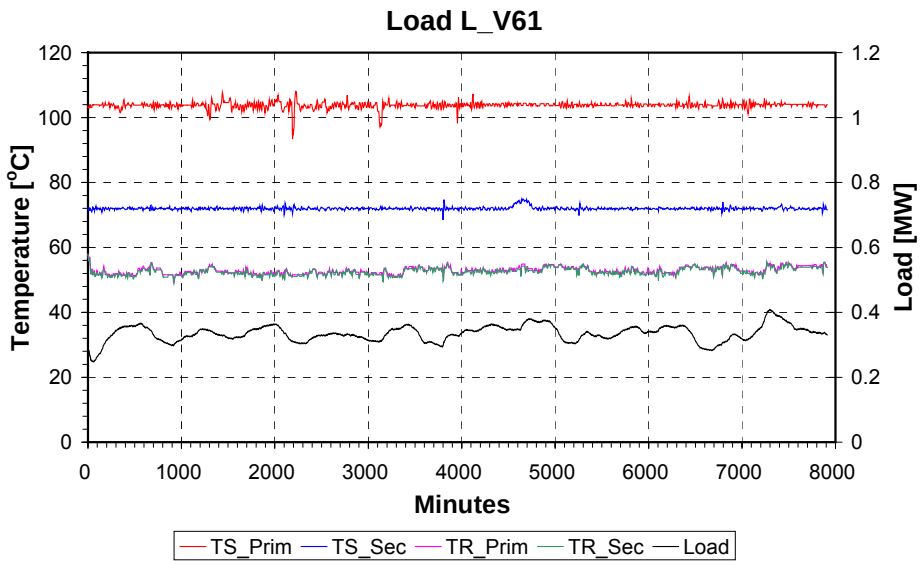
Load L_V61
Temperature [°C]
Load [MW]
Minutes
TS_Prim
TS_Sec
TR_Prim
TR_Sec
Load

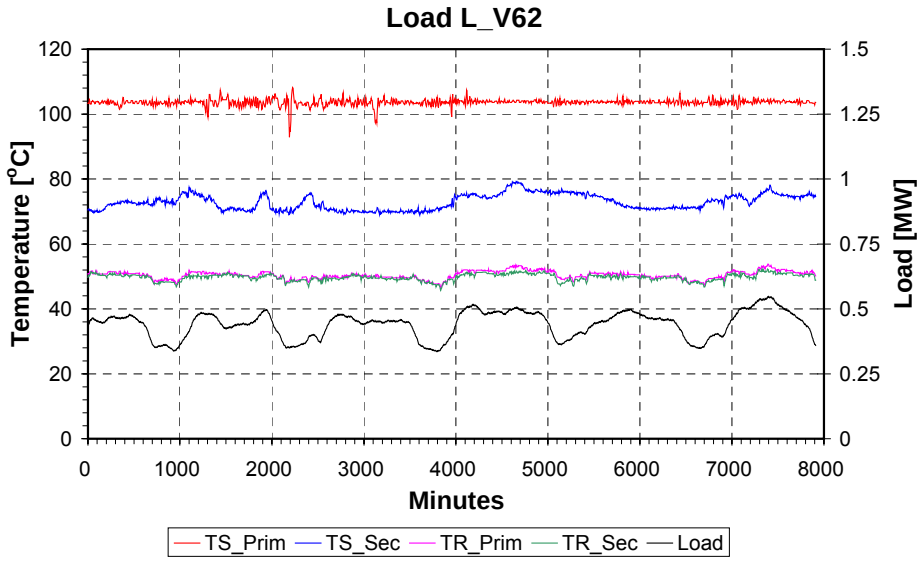
Load L_V62
Temperature [°C]
Load [MW]
Minutes
TS_Prim
TS_Sec
TR_Prim
TR_Sec
Load

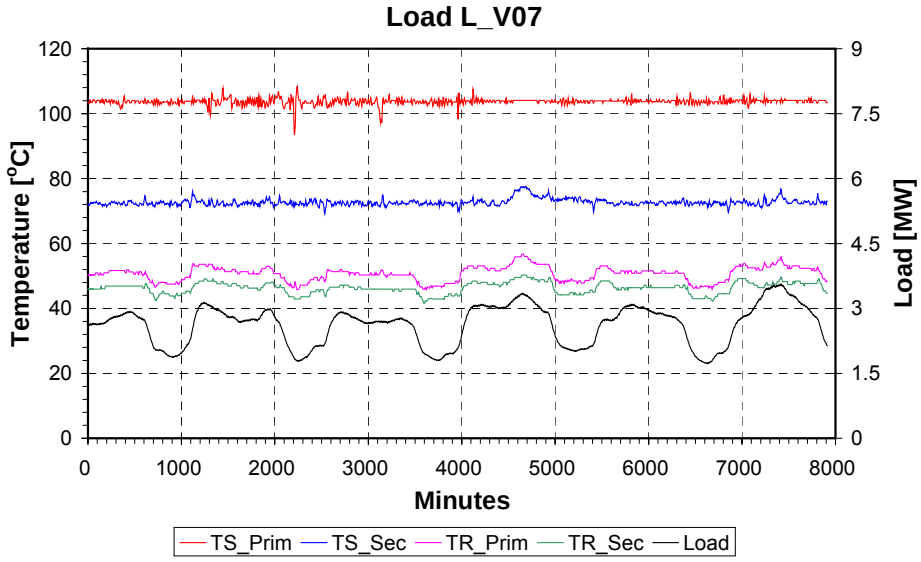
Load L_V07
Temperature [°C]
Load [MW]
Minutes
TS_Prim
TS_Sec
TR_Prim
TR_Sec
Load

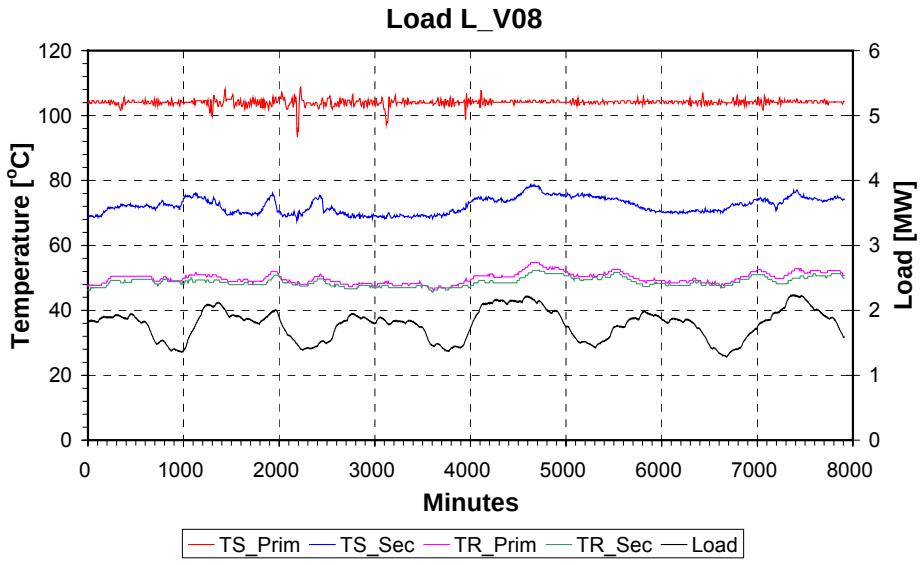
Load L_V08
Temperature [°C]
Load [MW]
Minutes
TS_Prim
TS_Sec
TR_Prim
TR_Sec
Load

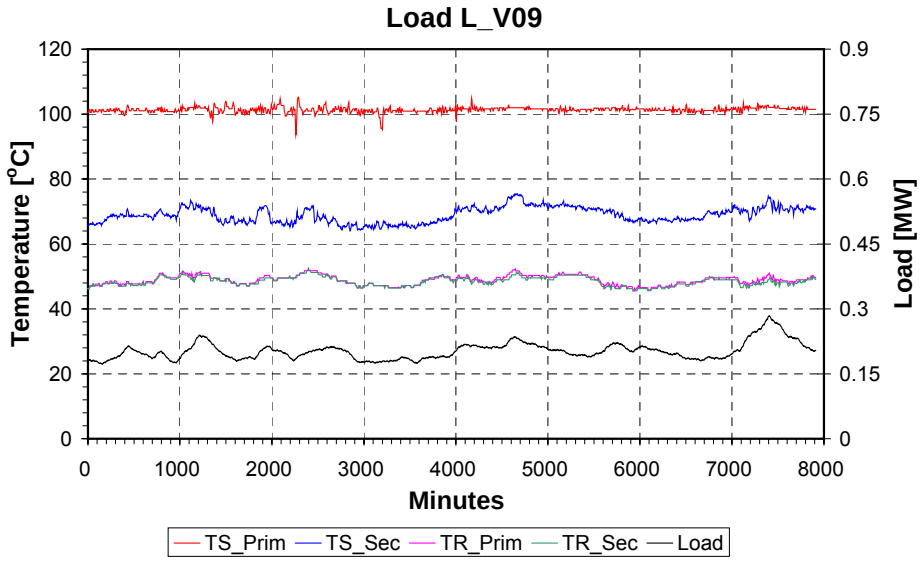
Load L_V09
Temperature [°C]
Load [MW]
Minutes
TS_Prim
TS_Sec
TR_Prim
TR_Sec
Load

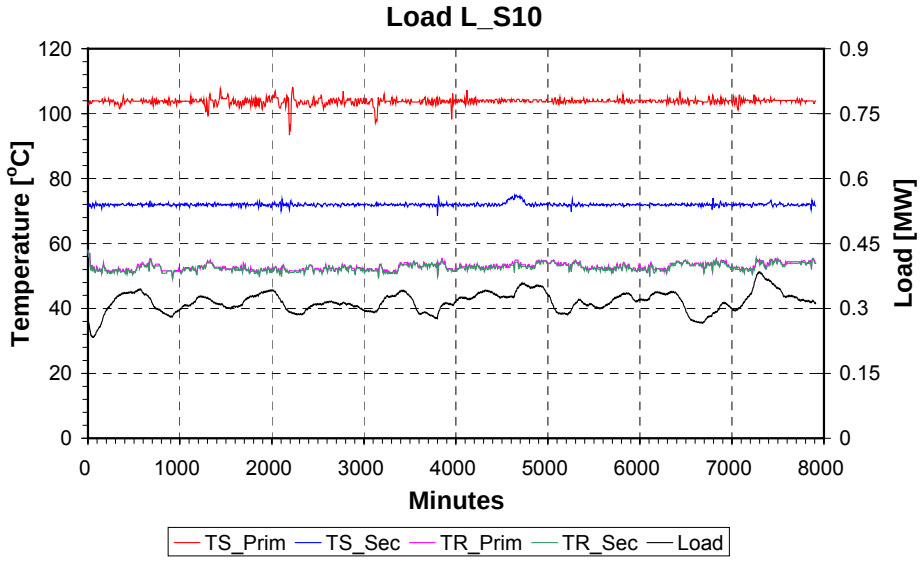
Load L_S10
Temperature [°C]
Load [MW]
Minutes
TS_Prim
TS_Sec
TR_Prim
TR_Sec
Load

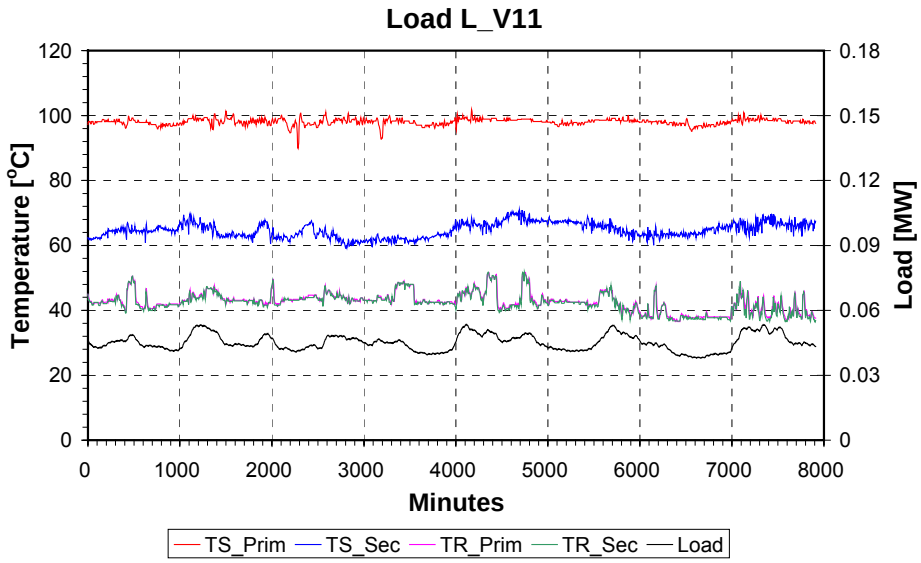
Load L_V11
Temperature [°C]
Load [MW]
Minutes
TS_Prim
TS_Sec
TR_Prim
TR_Sec
Load

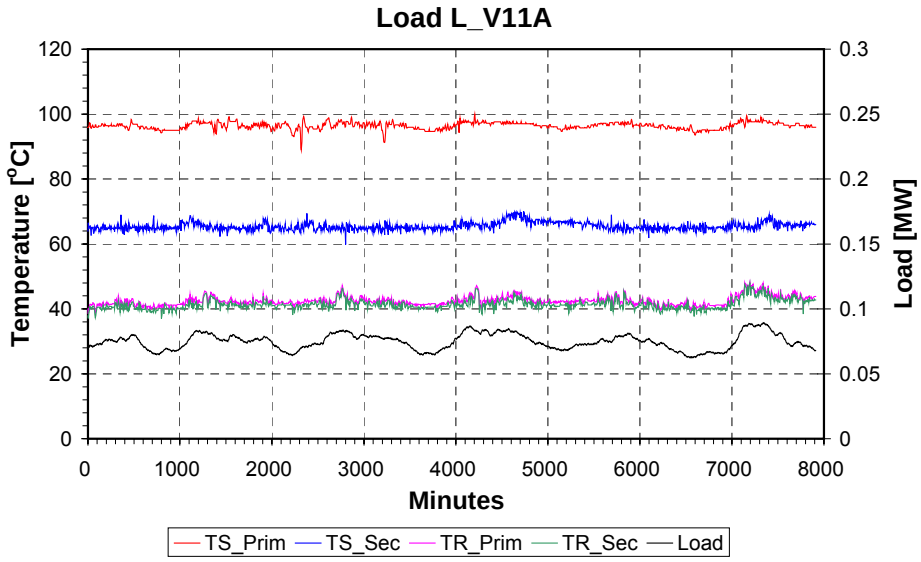
Load L_V11A
Temperature [°C]
Load [MW]
Minutes
TS_Prim
TS_Sec
TR_Prim
TR_Sec
Load

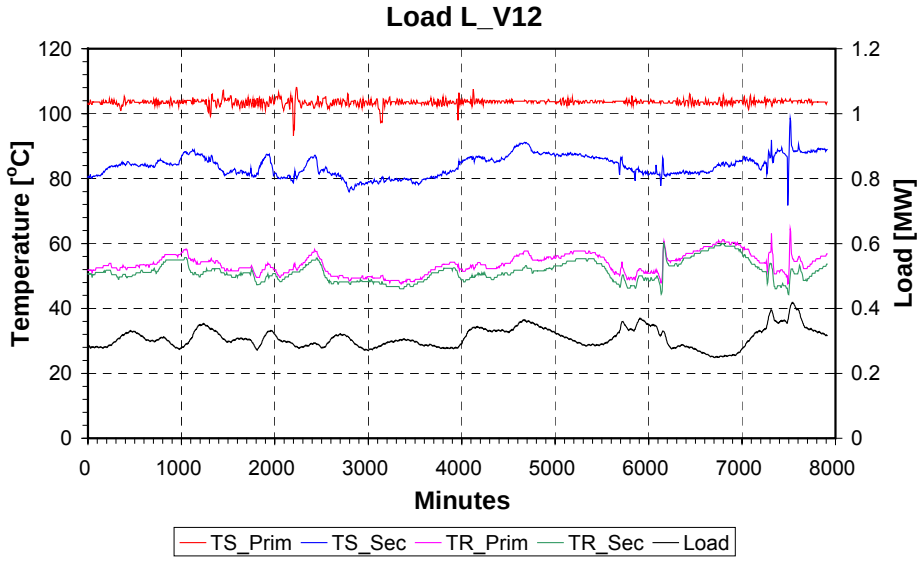
Load L_V12
Temperature [°C]
Load [MW]
Minutes
TS_Prim
TS_Sec
TR_Prim
TR_Sec
Load

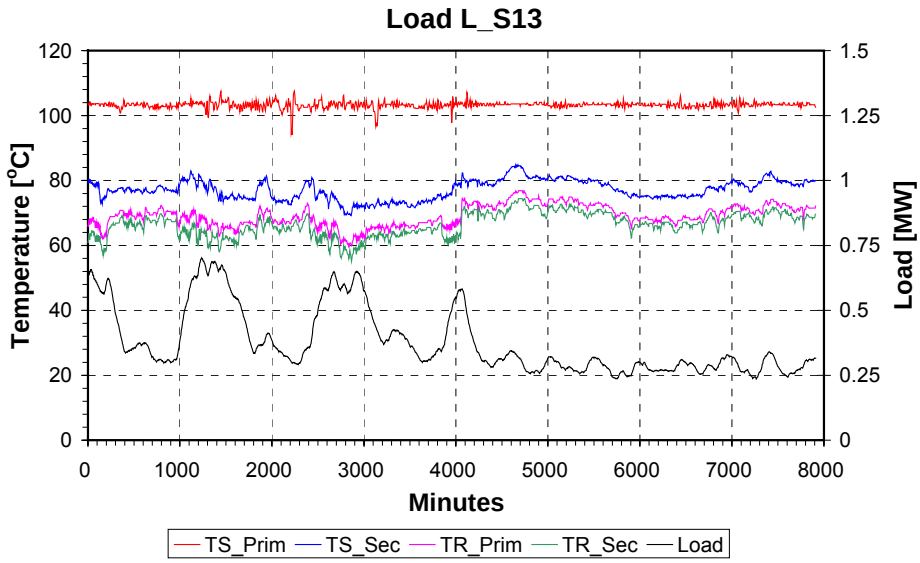
Load L_S13
Temperature [°C]
Load [MW]
Minutes
TS_Prim
TS_Sec
TR_Prim
TR_Sec
Load

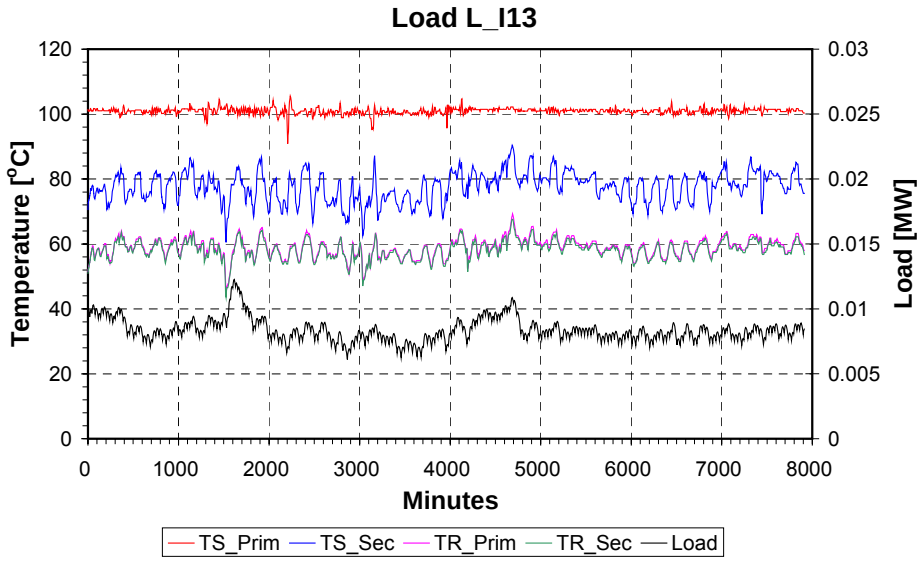
Load L_I13
Temperature [°C]
Load [MW]
Minutes
TS_Prim
TS_Sec
TR_Prim
TR_Sec
Load

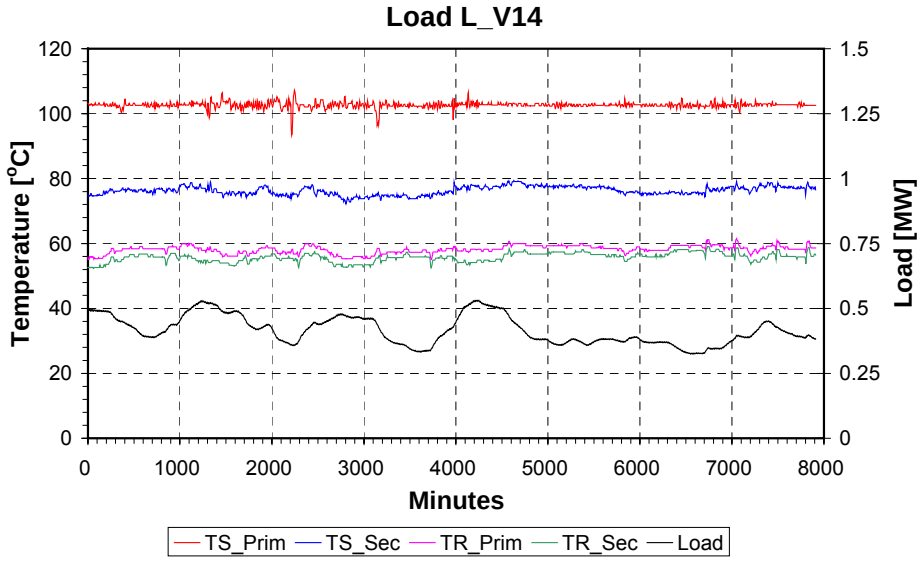
Load L_V14
Temperature [°C]
Load [MW]
Minutes
TS_Prim
TS_Sec
TR_Prim
TR_Sec
Load

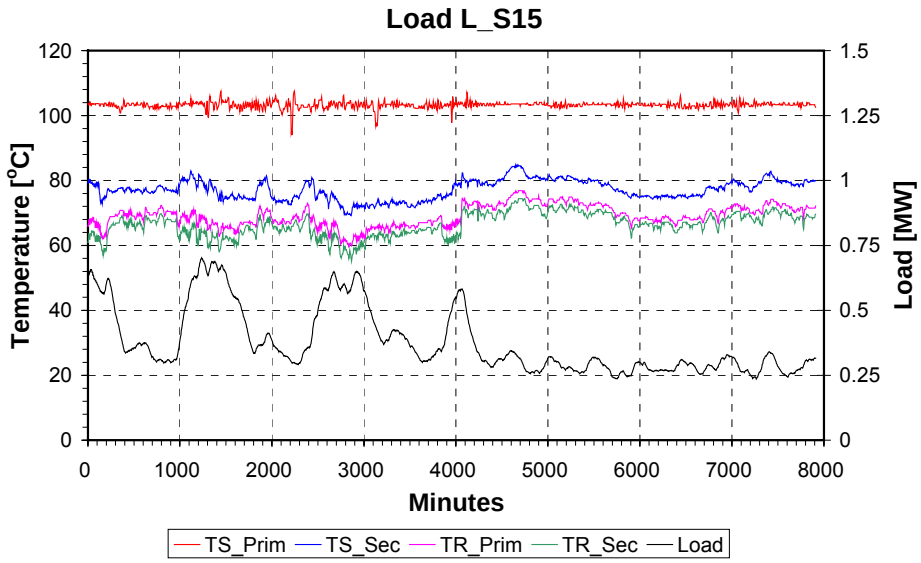
Load L_S15
Temperature [°C]
Load [MW]
Minutes
TS_Prim
TS_Sec
TR_Prim
TR_Sec
Load

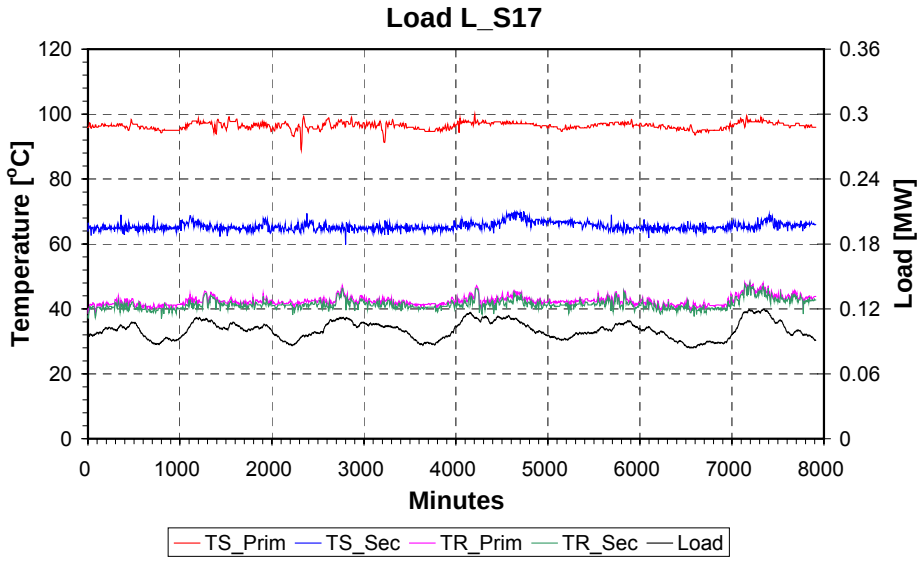
Load L_S17
Temperature [°C]
Load [MW]
Minutes
TS_Prim
TS_Sec
TR_Prim
TR_Sec
Load

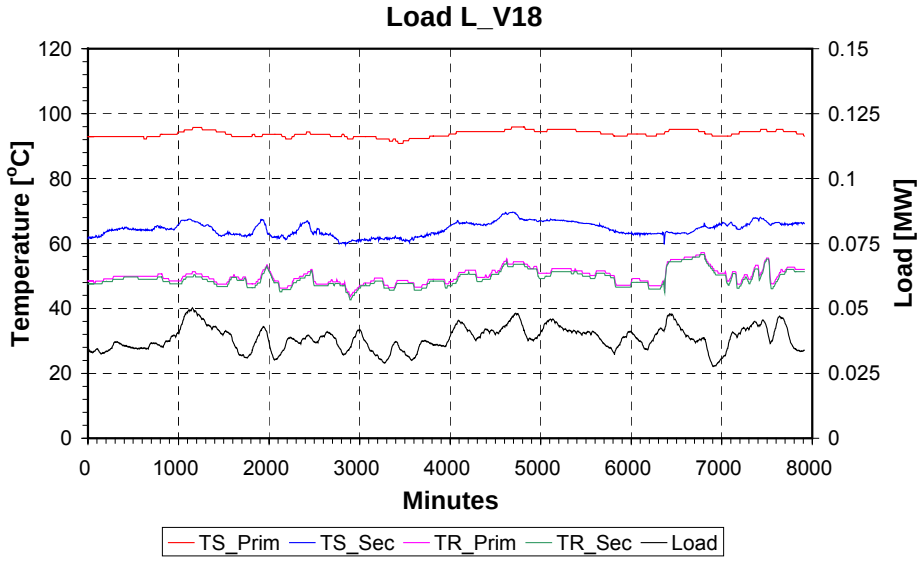
Load L_V18
Temperature [°C]
Load [MW]
Minutes
TS_Prim
TS_Sec
TR_Prim
TR_Sec
Load

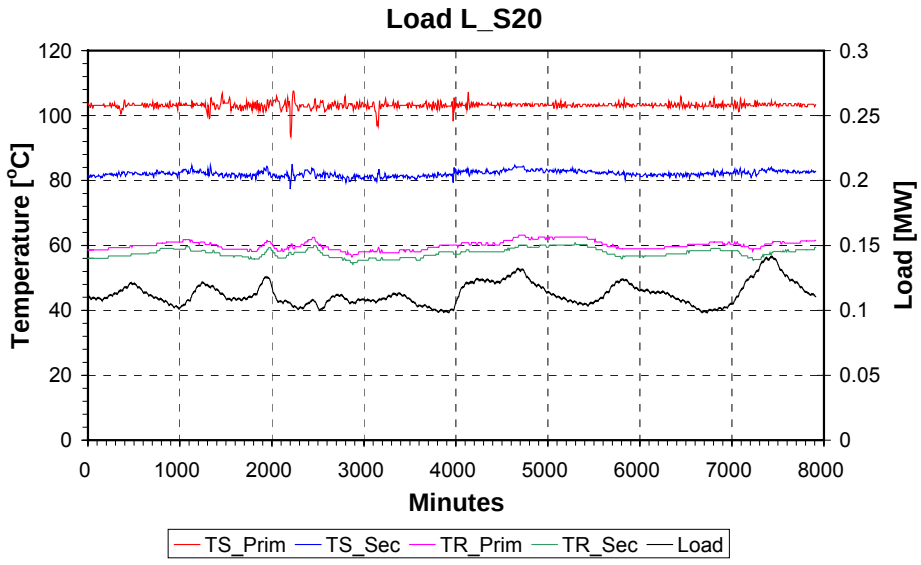
Load L_S20
Temperature [°C]
Load [MW]
Minutes
TS_Prim
TS_Sec
TR_Prim
TR_Sec
Load

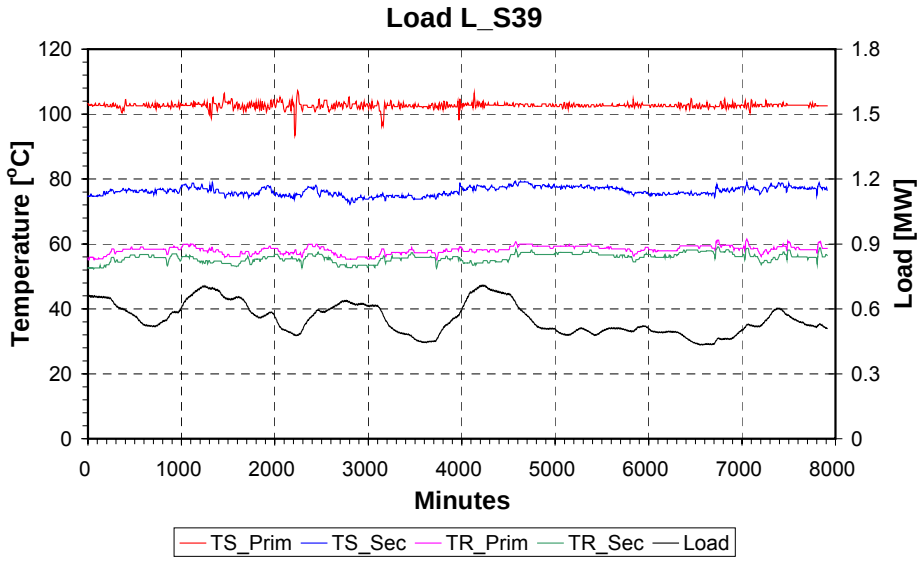
Load L_S39
Temperature [°C]
Load [MW]
Minutes
TS_Prim
TS_Sec
TR_Prim
TR_Sec
Load

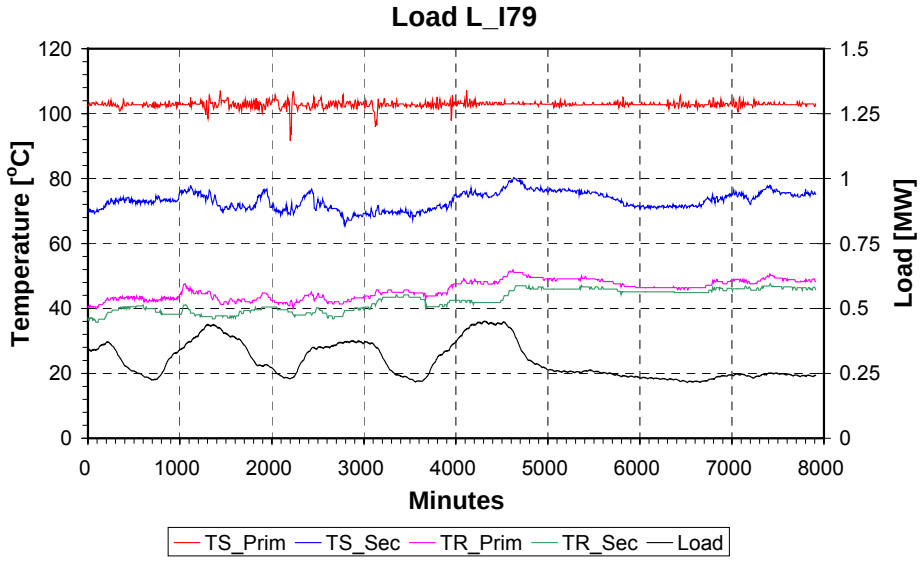
Load L_I79
Temperature [°C]
Load [MW]
Minutes
TS_Prim
TS_Sec
TR_Prim
TR_Sec
Load